School of Life Sciences
Technische Universität München

In situ characterization of non-degraded and brown rot colonized cell wall of furfuryl alcohol modified wood

Gabriele Gunhilde Ehmcke

Vollständiger Abdruck der von der TUM School of Life Sciences der Technischen Universität München zur Erlangung des akademischen Grades einer Doktorin der Naturwissenschaften genehmigten Dissertation.

Vorsitzender: Prof. Dr.-Ing. Jan Willem van de Kuilen

Prüfende der Dissertation:

1. Prof. Dr. rer. nat. Klaus Richter
2. Prof. Dr. rer. silv. habil. Cordt Zollfrank
3. Priv.-Doz. Dr. rer. nat. Gerald Koch (Universität Hamburg)

Die Dissertation wurde am 15.02.2021 bei der Technischen Universität München eingereicht und durch die TUM School of Life Sciences am 28.10.2021 angenommen.

Eidesstattliche Erklärung

Ich erkläre an Eides statt, dass ich die bei der promotionsführenden Einrichtung
TUM School of Life Sciences

der TUM zur Promotionsprüfung vorgelegte Arbeit mit dem Titel:

In situ characterization of non-degraded and brown rot colonized cell wall of furfuryl alcohol modifeid wood

in Lehrtstuhl für Holzwissenschaft
Fakultät, Institut, Lehrstuhl, Klinik, Krankenhaus, Abteilung

unter der Anleitung und Betreuung durch: Prof. Dr. rer. nat. Klaus Richter (TUM-SoLS) ohne sonstige Hilfe erstellt und bei der Abfassung nur die gemäß § 6 Ab. 6 und 7 Satz 2 angebotenen Hilfsmittel benutzt habe.

☒ Ich habe keine Organisation eingeschaltet, die gegen Entgelt Betreuerinnen und Betreuer für die Anfertigung von Dissertationen sucht, oder die mir obliegenden Pflichten hinsichtlich der Prüfungsleistungen für mich ganz oder teilweise erledigt.

☒ Ich habe die Dissertation in dieser oder ähnlicher Form in keinem anderen Prüfungsverfahren als Prüfungsleistung vorgelegt.

☐ Die vollständige Dissertation wurde in _____ veröffentlicht. Die promotionsführende Einrichtung

_____

hat der Veröffentlichung zugestimmt.

☒ Ich habe den angestrebten Doktorgrad noch nicht erworben und bin nicht in einem früheren Promotionsverfahren für den angestrebten Doktorgrad endgültig gescheitert.

☐ Ich habe bereits am _____ bei der Fakultät für _____

_____

der Hochschule _____
unter Vorlage einer Dissertation mit dem Thema _____

_____

die Zulassung zur Promotion beantragt mit dem Ergebnis: _____

_____

Die öffentlich zugängliche Promotionsordnung der TUM ist mir bekannt, insbesondere habe ich die Bedeutung von § 28 (Nichtigkeit der Promotion) und § 29 (Entzug des Doktorgrades) zur Kenntnis genommen. Ich bin mir der Konsequenzen einer falschen Eidesstattlichen Erklärung bewusst.

Mit der Aufnahme meiner personenbezogenen Daten in die Alumni-Datei bei der TUM bin ich

☒ einverstanden, ☐ nicht einverstanden.

Ammersbek, 09.02.2021, Unterschrift

Acknowledgements

The work underlying this thesis was carried out at the Chair of Wood Science, at the Technical University of Munich, and at the Thünen Institute of Wood Research. Several people contributed in many ways during my work on this thesis, and I am very grateful to all of them.

I am very thankful to my head supervisor, Professor Dr. Klaus Richter, at the Chair of Wood Science for the supervision of my thesis, his trust in my work and the opportunity to find my own way. He significantly contributed with his ideas, critical and valuable feedback and input to this thesis.

A special thanks to PD Dr. habil. Gerald Koch at the Thünen Institute of Wood Research for the scientific basis for this work, the possibility to use technical equipment at his institute and being cordially welcomed in his working group during all of my stays in Hamburg.

I am very thankful to the technical staff at the Thünen Institute who contributed with their excellent technical expertise and their valuable support during my work at their institute.

My thanks go to Dr. Annica Pilgård for guiding me through my PhD project, for her scientific and personal support and for being my friend. She showed me what it means to be a PhD student and how to become a scientist.

Thanks to all my colleagues at the Wood Research Institute in Munich for their (technical) support in many ways, especially in the laboratory, with media design and proofreading of my papers. In addition, many thanks for the inspiring coffee breaks we had together.

Thanks as well to master students Michael Algeier, who did the major part of the pre-decay test of my first paper, and Anton Wadenspanner, who enthusiastically plunged into the Raman investigations.

Finally, I would like to give my warmest thanks to my whole family for unconditionally standing by me during the entire time, for helping out babysitting, for proofreading and for all the big and small invaluable means of support. Thank you so much. A very special thanks to Matthies for his unconditional love, his patience and support and for jokingly reminding me that “there is no shame in finishing…”. Loving thanks to my kids for being such wonderful kids; you are a gift from heaven.

Summary

Wood, as an essential part of the natural carbon cycle, stores the largest amount of aboveground terrestrial carbon compared to other plants. The performance of wood and wood-based applications in building and construction is limited due to its natural degradability. Varying environmental conditions, diverse constructional designs and a permanent presence of microbial organisms are currently initiating degradation processes. The limited performance of bio-based building materials require effective wood protection solutions and information on service life predictions. With regard to increasing environmental concerns, the finiteness of resources and, consequently, the long-term strategic vision for a climate neutral European Union economy by 2050, the improved utilization of bio-based resources is necessary and indispensable. As a result, there is an increasing demand for sustainable building materials.

To delay or even prevent biodegradation processes and the risk of organism attack, there are three options: 1) application of effective constructional designs, 2) use of suitable (natural durable) wood species or 3) protection of nondurable wood material according to standard DIN 68800-3:2020-03. Option 1: Here, the responsibility lies with architects and building designers to apply constructive wood protection. Option 2: The ongoing deforestation of especially tropical and sub-tropical forests and, thus, the legal production of durable timber demand a responsible use of natural durable wood. Option 3: The increased introduction of restrictive, governmental regulations reduces the use of toxic wood preservatives, which lead to changes in the traditional wood protection sector. Consequently, the governmental restrictions power the development of environmentally benign treatments and a grown interest in the development of wood modification processes.

Wood modification (permanent bulking and/or alteration of the molecular structure of the wood cell wall polymers) improve the wood properties, i.e. durability, stability and performance of wood in use, without the use of toxic chemicals. Wood modification with furfuryl alcohol (FA) is one of the available modification processes that has been widely investigated throughout the last decades. FA modified wood is well established on the market as an environmentally friendly product which is produced by the company Kebony AS (Norway). However, it is still not clear how the enhanced durability is exactly achieved and how the FA molecule interacts with the wood cell wall. Since wood cell wall lignin presents a natural barrier to wood decay, it would be of great interest to investigate if FA binds to the cell wall lignin and thereby supports or improves its properties.

Therefore, the main objective of this PhD-thesis was to spectroscopically examine FA modified hard- and softwood on a (sub)cellular level, aiming for a better understanding of the mode of action of FA modified wood. *In situ* characterization on a cellular level was addressed and initial decay patterns by *Rhodonia placenta* were investigated in a high timely and spatial resolution.

The results show that cellular UV microspectrophotometry (UMSP), with its high resolution (0,25 µm x 0,25 µm) of the UV-spectroscopic scanning tool and the UV-spectroscopic point

measurements (1 μm²), is a well-suited method to topochemically studying furfurylated wood. The modified wood is characterized by very high UV absorbance (overflow) of the condensed phenolic/aromatic compounds in the modified tissue, which require individual threshold adaption of the UV intensities to a min. of 1.00% and a max. of 67.50%. The absorbance increment at 280 nm/278 nm of non-degraded furfurylated Radiata pine (*Pinus radiata*) and maple (*Acer* sp.) can be interpreted as a manifestation of the preferred deposition of condensed UV-active FA compounds at places of high lignin concentration in the cell wall *in situ*.

For the first time, UMSP area scans and selective line scans of an individual cell wall region have provided detailed insights into non-enzymatic oxidative lignin modification. Non-enzymatic oxidative degradation at the initial decay stage of FA modified Radiata pine is visualized *in situ*. The UMSP results of the analyzed degraded furfurylated and untreated Radiata pine samples reveal comparable decay pattern in untreated and furfurylated Radiata pine, which underlines the nontoxic properties of the modified wood. Degradation patterns in the form of modified lignin do not only occur in the area of the outermost S2 layer, but also on local spots over the entire wood cell wall, especially at the interfaces of the cell wall layers of the analyzed untreated and FA-modified samples. The ingenious system of the interfaces between the cell wall layers and the linkages between cellulose fibrils, hemicelluloses and lignin seem to be seriously affected by the initial decay damage of brown rot, which could explain the enormous loss of strength in this decay phase.

The data from the light microscopic evaluation of the degraded samples are not sufficient for a conclusive answer to the question of what is more important for the biological resistance of furfurylated wood: filled lumens or cell wall penetration. It can be assumed that a combination of both parameters impede brown rot degradation by giving a physical barrier for the hyphal expanse and, perhaps, an improved cell wall lignin by FA modification that is hard to for outside influences to attack.

With respect to the role of the solvent in the FA modification process, a test was carried out as to whether the formed polymer itself of treatment A (water based solvent) and C (alcohol based solvent) showed any difference between these two treatments in the obtained infrared spectra using IR micro-spectroscopy. The obtained infrared spectra of the investigated individual cell lumina and cell walls of process A and C show the same pattern, with a difference between cell wall and filled lumen. Independently of the treatment, the polymers formed are the same for the same anatomical location within the wood tissue. On the other hand, the polymer formed in the lumen and the polymer formed within the cell wall are not the same. The light microscopic quantification of the number of tracheids with lumina filled with FA polymer vs. the number of tracheids without any visible filling showed that there was a significant difference between the analyzed treatments A and C. This strengthens the hypothesis that the distribution within the wood tissue seems to be affected by the solvent used.

To elucidate the kind of chemical bond between FA and the cell wall lignin, the modified wood was subjected to Raman spectroscopy. Unfortunately, it was not possible to analyze FA modified wood using the available Raman laboratory equipment.

To conclude, the results of this study reveal that FA modified wood behaves similar to untreated wood with respect to the decay pattern of *R. placenta*, which underlines the nontoxic mode of action of furfurylated wood. Furthermore, this study shows that FA modified cell wall lignin influences the fungal degradation process, and therefore, presents another possible reason for the enhanced brown rot resistance of furfurylated wood. However, the role it plays is yet not sufficiently understood. Studies on FA modified cell wall lignin and on the visualization of non-enzymatic oxidative degradation pattern need to be further investigated. Therefore, further topochemical, cytochemical, and immunolabeling studies could be advantageous. For a climate neutral European Union economy by 2050, wood modification with FA can contribute to an increase in the sustainable use of wood and could mobilize currently unused nondurable wood materials, thereby contribute to satisfy the growing demand for wood. In this context, issues of sustainability and carbon sequestration meet in the search for new ‘green’ technologies.

Zusammenfassung

Holz, als wesentlicher Bestandteil des natürlichen Kohlenstoffkreislaufs, speichert die größte Menge an oberirdischem terrestrischem Kohlenstoff. Die Lebensdauer von Holzbau- und Konstruktionsmaterial ist auf Grund seiner natürlichen Abbaubarkeit begrenzt. Wechselnde Umgebungsbedingungen, unterschiedliche Bauweisen und die ständige Präsenz mikrobieller Organismen führen zu unerwünschten Abbauprozessen am und im Holz. Die dadurch einhergehende begrenzte Nutzbarkeit biobasierter Baumaterialien erfordert effektive (Holz)Schutzlösungen und belastbare Informationen zur voraussichtlichen Nutzungsdauer. In Bezug auf das wachsende Umweltbewusstsein, der Endlichkeit der Ressourcen und der langfristigen strategischen Vision einer klimaneutralen Wirtschaft in der Europäischen Union bis 2050 machen eine optimierte Nutzung biobasierter Ressourcen notwendig und unerlässlich.

Infolgedessen treiben die staatlichen Restriktionen die Entwicklung umweltfreundlicher Behandlungen voran und führen zu einem wachsenden Interesse an der Entwicklung von nachhaltigen Baumaterialien. Um biologische Abbauprozesse und das Risiko eines mikrobiellen Befalls hinauszuzögern oder gar zu verhindern, gibt es drei Möglichkeiten, 1) Anwendung eines wirksamen baulichen (konstruktiven) Holzschutzes, 2) Verwendung geeigneter (natürlich dauerhafter) Holzarten oder 3) Schutz von nicht dauerhaften Holzarten mit geeigneten Verfahren nach DIN 68800-3:2020-03. Bei der 1. Möglichkeit liegt die Verantwortung bei den Architekten und Bauplanern, konstruktiven Holzschutz anzuwenden. Bei der 2. Möglichkeit verlangt der fortschreitende Waldflächenrückgang, insbesondere der tropischen und subtropischen Primärwälder und die dadurch zurückgehende legale Produktion von natürlich dauerhaften Hölzern, einen sehr verantwortungsbewussten Umgang mit diesen. Möglichkeit 3 ist durch die zunehmende Einführung restriktiver, staatlicher Vorschriften hinsichtlich der Verwendung von toxischen Holzschutzmitteln eingeschränkt, was ein Umdenken im traditionellen Holzschutzmittelsektor erfordert. Die aus Umweltschutz- und Vorsorgegründen erlassenen Beschränkungen und Verbote fördern infolgedessen die Entwicklung eines umweltfreundlichen Holzschutzes und damit auch das Interesse an der Entwicklung von Verfahren zur Holzmodifizierung.

Die Holzmodifizierung im Allgemeinen verändert das Zellwandvolumen und/oder die molekularen Strukturen der Zellwandpolymere des Holzes. Sie umfasst Vergütungsverfahren, welche zu dauerhaft verbesserten Holzeigenschaften wie Dauerhaftigkeit, Dimensionsstabilität und Gebrauchseigenschaften führt.

Die Behandlung von Holz mit Furfuryl Alkohol (FA) ist als Modifizierungsverfahren industriell etabliert und wird von der Firma Kebony AS (Norwegen) kommerziell durchgeführt. Die Prozesssteuerung und die Holzeigenschaftsänderungen wurden in den letzten Jahrzehnten weitgehend untersucht.

Dennoch sind die wissenschaftlichen Mechanismen, die zu der verbesserten Dauerhaftigkeit beitragen, bisher nicht vollständig geklärt. Insbesondere ist unklar, ob es eine Interaktion zwischen den FA-Molekülen und den Holzzellwandmolekülen gibt. Da das Lignin der

Holzzellwand eine natürliche Barriere gegen pilzlichen Abbau darstellt, wäre es von großem Interesse zu untersuchen, ob sich FA an das Zellwandlignin bindet und dadurch dessen Eigenschaften unterstützt oder verbessert. Diese Doktorarbeit setzt subzelluläre Untersuchungen ein, um den Wirkmechanismus der FA-Modifizierung aufzuklären. Das Hauptziel der Arbeit war die spektroskopische Begutachtung von mit FA-modifizierten Laub- und Nadelholz mit dem Ziel, ein besseres Verständnis der Wirkungsweise von FA im modifiziertem Holz zu erlangen. Es wurde sowohl eine *In situ*-Charakterisierung auf zellulärer Ebene vorgenommen als auch erste Anzeichen pilzlichen Abbaus durch *Rhodonia placenta* in hoher zeitlicher und räumlicher Auflösung untersucht. Die Ergebnisse zeigen, dass die zelluläre UV-Mikrospektrophotometrie (UMSP) mit ihrem hochauflösenden, zellulären UV-spektroskopischen Scanning-Verfahren (Ortsauflösung von 0,25 µm x 0,25 µm) und der UV-spektroskopischen Punktmessung (Ortsauflösung von 1 µm²) eine gut geeignete Methode zur topochemischen Untersuchung von furfuryliertem Holz ist.

Das modifizierte Holz zeichnet sich durch sehr hohe Absorptionswerte (Overflow) der kondensierten phenolischen/aromatischen Verbindung im Holzgewebe aus, die eine individuelle Anpassung der Schwellenwerte für die Auswertung auf min 1.00% und max 67.50% erfordern. Der Absorptionsanstieg bei 280 nm/278 nm von nicht abgebauter furfurylierter Radiata Kiefer (*Pinus radiata*) und Ahorn (*Acer* sp.) kann als Erklärung für die bevorzugte Anlagerung von kondensierten UV-aktiven FA Verbindungen an ligninreichen Stellen der Holzzellwand *in situ* interpretiert werden.

Zum ersten Mal haben UMSP Flächenscans und ausgewählte Linienscans einzelner Zellwandregionen detaillierte Einblicke in die nicht-enzymatische oxidative Ligninmodifikation durch pilzlichen Abbau ermöglicht, für die bisher noch keine grundlegenden Ergebnisse vorliegen. Der nicht-enzymatische oxidative Abbau in der frühen Abbauphase von mit FA-modifizierter Radiata Kiefer wird *in situ* sichtbar gemacht.

Die UMSP Ergebnisse der untersuchten abgebauten furfurylierten und nicht modifizierte Radiata Kiefer zeigen ein ähnelndes Abbaumuster, was die ungiftigen Eigenschaften des mit FA-modifizierten Holzes unterstreicht. Abbaumuster in Form von modifiziertem Lignin treten nicht nur in äußeren Bereichen der S2 Schicht auf, sondern lokal in der gesamte Zellwand, insbesondere an den Grenzflächen der einzelnen Zellwandschichten der untersuchten unbehandelten und FA-modifizierten Proben. Das ausgeklügelte System der Grenzflächen zwischen den Zellwandschichten und die Vernetzungen von Zellulosefibrillen, Hemizellulosen und Lignin scheinen durch die im Anfangsstadium des Braunfäuleabbaus auftretenden Aktionen stark beeinträchtigt zu sein, was den enormen Festigkeitsverlust in dieser Phase erklären könnte. Die Daten aus der lichtmikroskopischen Auswertung der abgebauten Proben reichen nicht aus, um die Frage abschließend zu beantworten, was für die biologische Resistenz von furfuryliertem Holz wichtiger ist: mit FA-Polymer gefüllte Lumina oder eine intensive Zellwandmodifizierung. Es ist davon auszugehen, dass eine Kombination beider Parameter den Braunfäuleabbau erschwert, zum einen durch eine physische Barriere für die Hyphenausbreitung und zum anderen durch ein möglicherweise verbessertes Zellwandlignin, das von äußeren Einflüssen nur schwer angegriffen werden kann.

Mit Hilfe der IR-Mikrospektroskopie wurde die Rolle des Lösungsmittels (A – auf Wasserbasis; C – auf Alkoholbasis) auf das gebildete Polymer im FA-Modifikationsprozess

dahingehend untersucht, ob die Infrarotspektren einen Unterschied zwischen diesen beiden Behandlungen aufweisen. Die erhaltenen Infrarotspektren der untersuchten Zelllumina und Zellwände von Verfahren A und C zeigen das gleiche Muster, wobei ein Unterschied zwischen Zellwand und gefülltem Lumen besteht. Unabhängig von der Behandlung sind somit die gebildeten Polymere an der gleichen anatomischen Stelle im Holzgewebe gleich. Das im Lumen gebildete Polymer und das in der Zellwand gebildete Polymer sind jedoch nicht identisch. Die lichtmikroskopische Quantifizierung der Anzahl der Tracheiden mit FA-Polymer gefüllten Lumina im Vergleich zur Anzahl der Tracheiden ohne sichtbare Füllung zeigte, dass es einen signifikanten Unterschied zwischen den analysierten Behandlungen der A und C gab. Dies untermauert die Hypothese, dass die Verteilung innerhalb des Holzgewebes durch das verwendete Lösungsmittel beeinflusst zu werden scheint.

Um die Art der chemischen Bindung zwischen FA und dem Zellwandlignin aufzuklären, wurde das modifizierte Holz einer Raman-Spektroskopie unterzogen. Leider war es nicht möglich, FA-modifiziertes Holz mit den verfügbaren Raman-Laborgeräten zu analysieren.

Zusammenfassend zeigen die Ergebnisse dieser Doktorarbeit, dass sich FA-modifiziertes Holz in Hinblick auf das Fäulnismuster von *R. placenta* ähnlich verhält wie unbehandeltes Holz. Dies unterstreicht die ungiftige Wirkungsweise von furfuryliertem Holz. Darüber hinaus zeigt diese Studie, dass FA-modifiziertes Zellwandlignin den pilzlichen Abbauprozess beeinflusst und somit eine weitere Möglichkeit für die verbesserte Braunfäuleresistenz von furfuryliertem Holz darstellt. Welche Rolle es dabei spielt, ist jedoch noch nicht ausreichend geklärt. Studien über FA-modifiziertes Zellwandlignin und über die Visualisierung nicht-enzymatischer oxidativer Abbauprozesses müssen weiter vorangebracht werden. Daher könnten weiterführende topochemische-, zytochemische-Studien und Imunolabeling-Studien den Erkenntnisgewinn fördern. Im Hinblick auf eine klimaneutrale Wirtschaft in der Europäischen Union bis 2050 kann die Modifizierung von Holz mit FA dazu beitragen, die nachhaltige Nutzung von Holz zu steigern, sowie derzeit ungenutzte, nicht dauerhafte Holzmaterialien zu mobilisieren und damit einen wertvollen Beitrag zur Deckung der wachsenden Nachfrage nach Holz leisten. In diesem Zusammenhang treffen Fragen der Nachhaltigkeit und der Kohlenstoffbindung bei der Suche nach neuen "grünen" Technologien aufeinander und führen zu neuen Synergien.

Table of Contents

Index of Figures

Index of Tables

Index of Equations

Index of Abbreviations

A	Absorbance
AFM	Atomic force microscopy
ATR-FTIR	Attenuated total reflection - Fourier transform infrared
APAMOS	Automatic Photometric Analysis of Microscopic Objects
CC	Cell wall corner
CCA	Copper-chromium-arsenic
CML	Compound middle lamella
CWS	Cell wall saturation
EMC	Equilibrium moisture content
F	Furfural
FA	Furfuryl alcohol
FT-IR	Fourier Transform Infrared Spectroscopy
GA	Glutaraldehyde
I	Intensity of the transmitted radiation
I_0	Intensity of the incident radiation
IPA	Isopropyl alcohol
LM	Light microscopy
MC	Moisture content
MCR-ALS	Multivariate curve resolution-alternating least squares
ML	Mass loss
MLcc	Middle lamella cell corner
MOE	Modulus of elasticity
MOR	Modulus of rupture
n	Number
NMR	Nuclear magnetic resonance
PA	Paraformaldehyde
PARAFAC	Parallel factor analysis
PNRD	*Pinus radiata*
PNSY	*Pinus sylvestris*
PW	Primary cell wall layer

RH	Relative humidity
RP	Ray parenchyma
SANS	Small angle neutron scattering
S1	First secondary cell wall layer
S2	Second secondary cell wall layer
S3	Third secondary cell wall layer
SEM	Scanning electron microscopy
SNV	Standard normal variate
SYP	Southern yellow pine
STD	Standard deviation
TEM	Transmission electron microscopy
UMSP	Universal-Microscope-Spectrophotometer
UV	Ultraviolet
WPG	Weight percent gain

Earnest is each Research, and deep;
And where it is its Fate to err,
Honest its Error, and Sincere.
Evan Lloyd

1 Introduction

Wood has been used as a treasured and versatile building material for thousands of years, always with the aim of keeping it in service for as long as possible (Rowell 2005b). Today, wood is much more commonly seen as a valuable renewable resource with a high potential relating to the mitigation of climate change in certain aspects. Important aspects for the use of wood are, for instance, 1) the potential to function as a carbon pool, 2) the potential for cascading and 3) the potential to substitute products with energy-intensive resources (Höglmeier et al. 2017; Hill 2019). The performance of bio-based building materials is limited by discoloration by stain and mold fungi, as well as fungal, bacterial, and insecticidal decay (Jones et al. 2019). This is because wood and bio-based applications in building and construction are faced with varying environmental conditions, diverse constructional designs and a permanent presence of microbial organisms, which demands effective wood protection solutions and information on its service life prediction. The latter can be achieved by applying available decay models (Brischke and Meyer-Veltrup 2016), whereas the first aspect is regulated in wood protection standard DIN EN 68800:2019.

There is increasing legislative pressure driven by environmental considerations regarding traditional wood protection systems with their biocide and toxic agents that have negative effects on human health and the environment. This demands for more environmentally benign treatments, for a general rethinking of traditional preservatives and for requirements to accomplish and/or substitute them by ecological wood protection systems or modified wood (Ibach 2005; Hill 2006). Innovative processes like wood modification (chemical, thermal, impregnation) are currently being adopted in the wood protection sector (Jones et al. 2019). Commercial interest will support the utilization of modified wood, which will become more and more important and will probably increase over the next couple of decades (Gérardin, 2016). Therefore, a comprehensive understanding of the mode of action of modified wood, e.g., modification with furfuryl alcohol (FA), is mandatory to further improve environmentally friendly modification processes (Skrede et al. 2019).

Wood modification means a permanent bulking and/or alteration of the molecular structure of wood cell wall polymers (cellulose, hemicelluloses and lignin) (Homan and Jorissen 2004). The treatments involve an action of a chemical, biological or physical agent upon the material and leads to a prolonged service life linked by a non-biocide mode of action (Hill 2006). Wood modification with FA has been widely investigated throughout the last few decades (Goldstein and Dreher 1960; Stamm 1977; Schneider 1995; Westin 2003) and the resulting material is well established on the market as an environmentally friendly product (Gérardin 2016, “Swan” ecological label (license number 2086 0001) for the furfurylation process adopted by Kebony ASA in Norway). Nevertheless, the studies published by Goldstein and Dreher (1960), Stamm (1977) and Schneider (1995) do not reveal how the enhanced durability properties are exactly achieved.

Improved resistance against microbial degradation was tested under different conditions resulting from different applications (saltwater contact, ground contact under environmental and laboratory conditions in several studies, e.g., Lande et al. 2004; Westin et al. 2016; Treu

et al. 2019). Furthermore, the toxic hazard of FA modified wood was analyzed, for instance, by ecotoxicity studies of the leachates (Lande et al. 2004; Pilgård et al. 2010). Another study of the gene expression pattern of a decaying fungus, for example, found no enrichment of genetic functions directly related to defense mechanisms in the modified wood compared to unmodified wood, which supports the assumption that FA modified wood is nontoxic to the fungus, as well (Skrede et al. 2019).

However, the distribution of polymerized FA over the wood tissue and the homogenously impregnated wood cell walls have a major impact on the wood protection efficacy. Therefore, the individual treatability properties of the used wood species have to be considered (Lande et al. 2010; Zimmer et al. 2014). Thygesen et al. (2009) applied fluorescence and confocal laser scanning microscopy on furfurylated wood and revealed that FA polymerization takes place in the microscopic cell cavities, and studies on the impact of the used solvent revealed differences in filled early- and latewood tracheids (Thygesen et al. 2020). Rowell et al. (2012) and Larsson Brelid (2013) questioned whether the properties of the furfurylated material appear from a reacted cell wall. However, previous studies using infrared (Venås and Rinnan 2008) and fluorescence microscopy (Thygesen et al. 2010) on furfurylated wood have shown that FA polymerization takes place within the wood tissue. Recent nanoindentation studies by Li et al. (2016) found indications that there is an indirect connection of improved indentation modulus and hardness of furfurylated wood cells that strongly demonstrates that the FA penetrates wood cell walls during the modification process. However, it has still not been definitively demonstrated how the furfurylation takes place in the wood cell wall with the cell wall compounds (Beck et al. 2019). Earlier studies on nuclear magnetic resonance (NMR) spectra of early stages of FA polymerization demonstrated that lignin model compounds form covalent bonds in a liquid-phase system with the FA polymer (Nordstierna et al. 2008). Since wood cell wall lignin presents the most significant barrier to wood decay and influences the degradation modes (Schwarze 2007), it would be of great interest to see if FA binds to the cell wall lignin and thereby supports or improves these properties. If the linkage according to Nordstierna et al. (2008) were to take place within the wood cell wall, the protection properties against fungal attack of cell wall lignin could be altered, and the resistance to brown rot degradation of furfurylated wood could be enhanced.

Other ideas regarding possible reasons for the enhanced brown rot resistance of furfurylated wood were reviewed by Ringman et al. (2014). Important modes of action of modified wood against brown rot decay fungi were revealed and they concluded that moisture exclusion might play an important role with high impact on the modes of action. The current established understanding of wood moisture relation concerning fungal decay was questioned (Brischke and Alfredsen 2020). Literature analyses of studies of water relations in untreated and modified wood under brown-rot and white-rot decay by Thybring (2017), a critical discussion of moisture for brown rot degradation in modified wood by Ringman et al. (2019) and findings by Skrede et al. (2019), support this conclusion. The latter further assumed that the furfurylation functions as both a physical barrier and a factor that lead to a less-hydrated environment for the fungus. The analysis by Thybring (2017) showed, inter alia, that changes in water relations during decay can be partly assigned by changes in chemical composition and void volume in untreated and modified wood. Ringman et al. (2019) discussed the idea of

inhibited diffusion that could arise as a key aspect, whereas no evidence was found that support the enzyme non-recognition hypothesis (Skrede et al. 2019). Another aspect that is highlighted by current research is the determination of the accessibility of hydroxyl groups in furfurylated wood during brown rot decay (Beck et al. 2019). The results showed, inter alia, that, according to the OH accessibility, a significant increase of accessible OH groups were determined, which they attributed to the opening of crystalline cellulose regions and the formation of new OH groups in lignin and the furfural polymer due to oxidative alteration. Finally, there will be a combination of different theories that play more or less of a role in brown rot degradation of FA modified wood (Ringman et al. 2019). No conclusive experimental evidence has so far been provided that gives a comprehensive explanation on the mode of action of modified wood. There are still questions as to what exactly influences the enhanced resistance of furfurylated wood to brown rot degradation.

With regard to the long-term strategic vision for a climate neutral European Union economy by 2050 (European Commission 2018), the improved utilization of biobased resources will be necessary. Timber can advance to be the material of choice for the 21st century with timber-based solutions, preferably in ways susceptible to discoloring and degrading organisms (Jones et al. 2019). One aspect that can support this overall goal is to promote environmentally friendly wood products like FA modified wood. To close the above listed knowledge gaps, the main objective of this PhD-thesis was to topochemically examine furfuryl alcohol (FA) modified wood on a (sub) cellular level, aiming for a better understanding of the mode of action of furfuryl alcohol modified wood. *In situ* characterization on a cellular level was addressed and initial decay patterns by a brown rot fungus were investigated in a high timely and spatial resolution.

2 Wood

2.1 Wood cell wall chemistry

The term *wood* describes the (secondary) xylem that is produced by the cambium as the inner tissue of a tree. Wood tissue is highly organized in several hierarchic levels – from the macro to the nano level (Henriksson et al. 2009) – and can be regarded as a three dimensional biopolymer composite (Rowell et al. 2012). The striking wood properties are directly linked to this specialized hierarchical structure. On a microscopic scale, wood tissue is formed out of tube-like cells that are mainly longitudinally oriented and differ, evolutionarily induced, between softwoods and hardwoods (Figure 1). The latter, evolutionarily younger, have more specialized cells with different functions, whereas softwood tissue mainly consists of tracheids (Table 1).

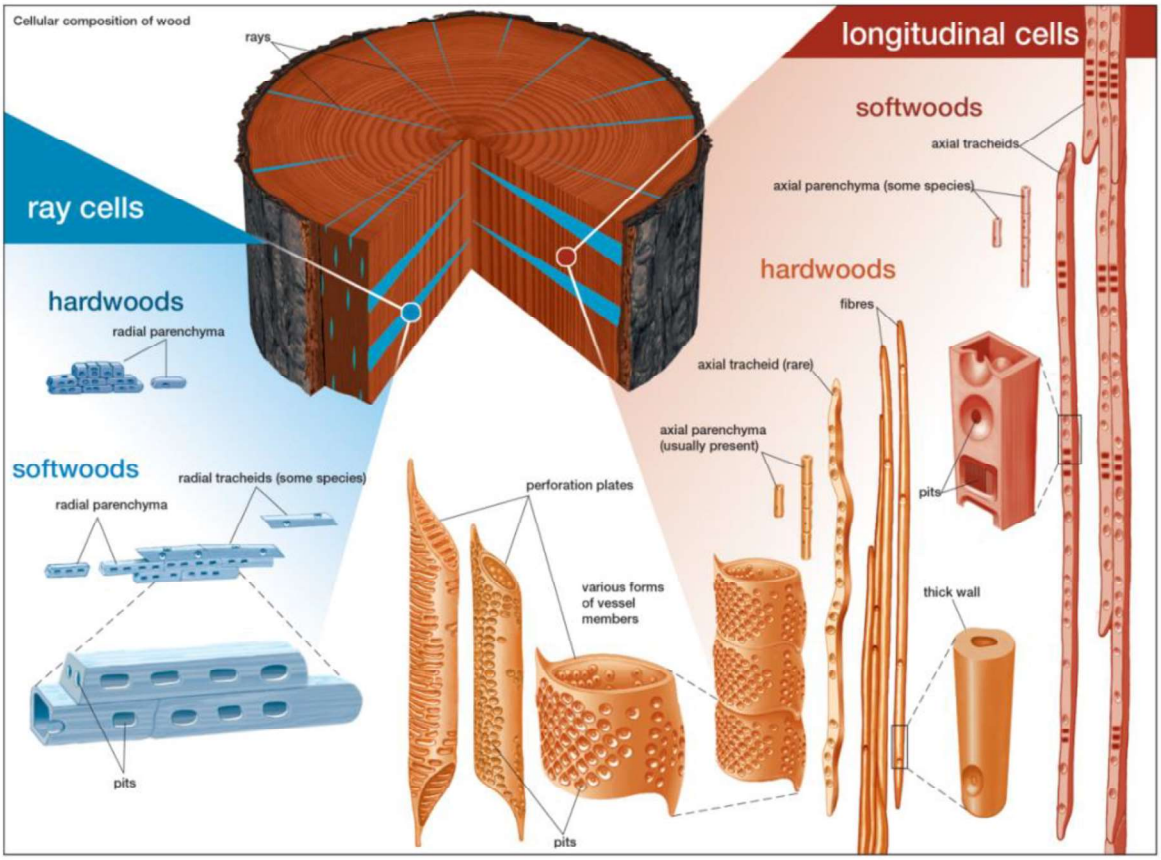

Figure 1: Wood cells of hardwoods and softwoods. Retrieved from: *Encyclopædia Britannica, Inc.* https://www.britannica.com/science/wood-plant-tissue/Microstructure

Table 1 Wood cell types and their function (according to Fengel and Wegener 1984).

	Softwood	Hardwood
Support	Longitudinal **tracheids** - Latewood	**Fibers** Libriform fibers Fiber tracheids
Conduction	Longitudinal **tracheids** – Earlywood Ray tracheids	**Vessels** Vascular tracheids Vasicentric tracheids
Storage	**Parenchyma** Ray parenchyma Longitudinal parenchyma	**Parenchyma** Ray parenchyma Longitudinal parenchyma
Secretory structures	Epithel parenchyma – resin	parenchymatous idioblast – oil, mucilage Epithel parenchyma – resins, gums

Seen from the next hierarchic level, the cell walls are formed out of cell wall layers (Figure 2a). The cells are connected via the middle lamella with adjacent cells. Species depending, different forms of the inner layer can be observed, for instance, a wart layer (*Pinus sylvestris*, vessel of *Fagus* spp.) or helical thickenings (*Taxus* spp., vessels of *Acer* spp.). One hierarchic level further, the main structural cell wall components are cellulose (~ 50%), hemicelluloses (~24-40%) and lignin (23-35% softwoods, 16-25% hardwoods). Cellulose is the most frequently occurring organic compound consisting of β-1,4- linked glucose anhydride units. These units are polymerized to β-1,4 glucan chains of varying length by the degree of polymerization. Highly oriented and unbranched cellulose chains are connected by intermolecular forces (intra- and intermolecular hydrogen bonds) to larger crystalline units, the elementary fibrils (Schmidt 2006b). These are bundled up to microfibrils (Figure 2b) to build the structural backbone of the wood cell walls (Fernandes et al. 2011; Terashima et al. 2009). A review of wood cell wall ultra-structure showed that it is currently assumed that the molecular structure of cellulose microfibrils consists of 18 cellulose chains (Donaldson 2019). The wood cell wall contains crystalline and amorphous forms of cellulose. The crystalline nature of cellulose can be displayed by using polarized light. With transvers section of Radiata pine and red beech, Donaldson (2019) showed that cell walls are birefringent due to crystalline cellulose and that different layers of the cell wall show differences in birefringence related to the orientation of cellulose microfibrils (Donaldson 2019). The partly crystalline nature of cellulose makes it recalcitrant to wood degrading fungi and bacteria, whereas amorphous cellulose is hydrolyzed much faster (Eriksson et al. 1990; Schmidt 2006c).

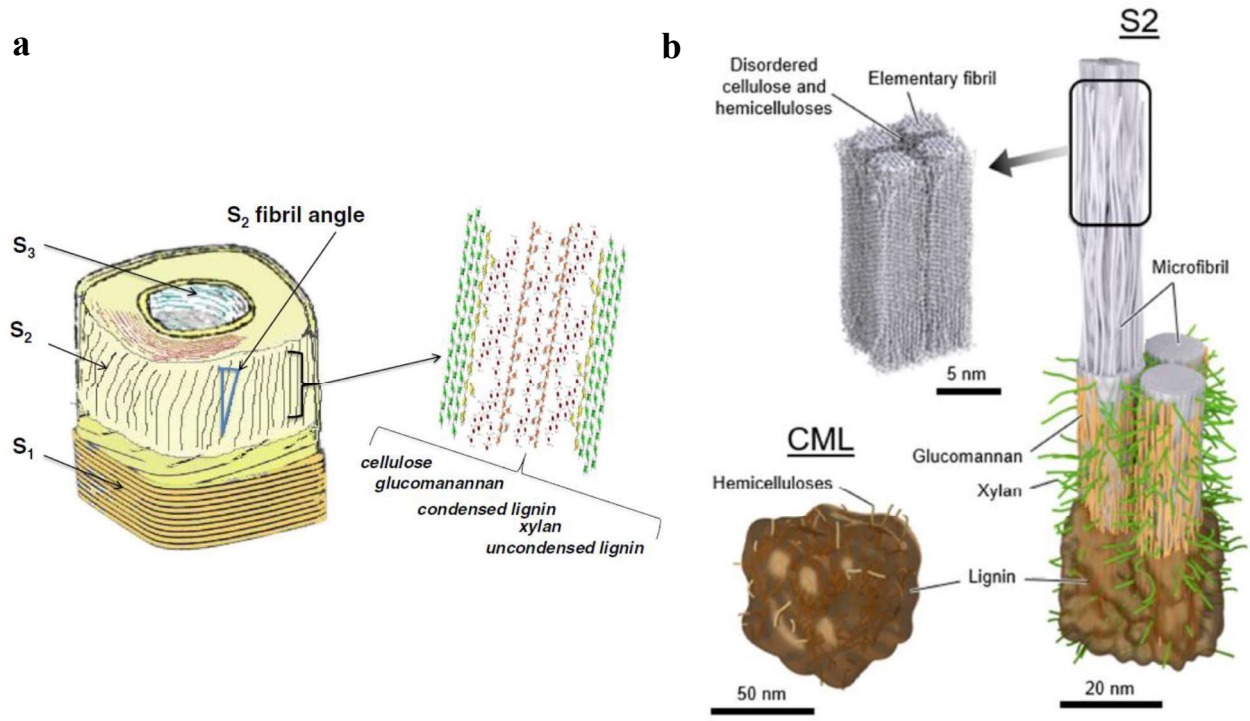

Figure 2a: Schematic illustration of the wood cell wall layers (S1, S2, S3) with a fibril angle of the S2 layer for representation of interrelations with the assumed composition of cellulose, glucomannan, xylan, and condensed and uncondensed lignin (Salmén 2015). 2b: A proposed relationship within the secondary cell wall (S2) and the compound middle lamella (CML) nanostructure (Jakes et al. 2019).

(Donaldson 2019) also reviewed that non-cellulosic carbohydrates (hemicelluloses, pectin) function as connection between cellulose and the cell wall matrix and therefore play an important role in the wood cell wall (Bergander and Salmén 2002; Salmén 2004). Pectins occur in the primary wall and ML, as well as in pit membranes (Maschek et al. 2013, Pereira et al. 2018). Hemicelluloses belong to the group of polysaccharides, consisting of a complex combination of anhydrohexoses (glucose, mannose and galactose) and anhydropentoses (xylose and arabinose) with acetyl and uranic side groups. The hemicelluloses surround the cellulose chains, and it is proposed that the nano structural organization includes a coating of the microfibrils with glucomannan (Salmén and Burgert 2009). The hemicelluloses form hydrogen bonds to cellulose fibrils and covalent links with lignin, as well (Schmidt 2006d). Hemicelluloses have more accessible OH-groups and, therefore, the hydrophilicity is about 1.6 times higher than the hydrophilicity of cellulose. Hemicelluloses are accessible and function as carbon source for many micro-organisms.

Lignin is a complex amorphous and heterogeneous aromatic polymer that is, next to cellulose and hemicelluloses, the most abundant polymeric organic substance (Fengel and Wegener 1983; Donaldson 2001; Schmidt 2006c). It is three dimensionally cross-linked, and together with the hemicelluloses, the space filling substance between the microfibrils. Lignin functions as an embedding and encrusting material in the wood cell wall. In contrast to the hemicelluloses, lignin has a higher hydrophobicity that limits the sportive water uptake of the cell wall. Furthermore, lignin presents the most significant barrier to wood decay influencing

the degradation modes (Schwarze 2007) and pathogens (Lee et al. 2019). In the case of involved lignin removal during wood decay, the degree of lignification of the secondary cell wall (S2) limits the accessibility of carbohydrates to hydrolytic enzymes.

The lignification process described below was reviewed comprehensively by Donaldson (2001). The lignin distribution across the wood cell wall is induced from where lignification starts – at the cell corners and the middle lamella (ML) (Terashima and Fukushima 1988). The lignification extended from middle lamella between pit borders, into the initial pit borders and cell corners, and then into the secondary wall as basically described for *Abies balsamea,* and similar patterns have been observed for *Pinus radiata*. Furthermore, it was stated that, in pine species, lignification proceed in three stages (Terashima and Fukushima 1988), (i) lignification of the cell corner and middle lamella after the first secondary cell wall layer (S1) formation, (ii) slow lignification during S2 formation, and (iii) main lignification after the third secondary cell wall layer (S3) formation. Based on the difference in the volume of the ML to the second secondary cell wall layer (S2), about 70% of the lignin is located in the S2, whereas the ML has the highest local lignin concentration. Donaldson (2019) recently reviewed the wood cell wall ultra-structure and summarized that the highly lignified ML leads to the concept of lignin as the glue, which binds tracheids and fibers together.

Lignin has a wide structural variation. It is linked by either (C-O-C) and carbon to carbon (C-C) linkages and consists of a complex arrangement of substituted phenolic units. The three basic building blocks of wood lignin are guaiacyl, syringyl and *p*-hydroxyphenyl moieties. Softwood lignin is mainly composed of guaiacylpropane moieties whereas hardwood lignin is composed of a varying amount of guaiacylpropane and syringylpropane moieties.

On the molecular level, lignin belongs to the group of aromatic compounds. It is rich in easy stimulating π–electrons, and this property can be used for spectroscopic assays of lignin in the wood cell wall. Carbohydrates have fewer π–electrons and are inactive in the UV range. Therefore, the absorbance bands of the lignified cell walls can be recorded in a characteristic wavelength range of 240–400 nm given in Figure 3 (Koch & Kleist, 2001). The maximum UV absorbance (A_{max}) for softwood lignin is located at λ280 nm and, for hardwood, in a range of λ272 nm to λ278 nm (Fergus and Goring 1970a, 1970b; Musha and Goring 1975; Takabe et al. 1992). This difference in A_{max} is caused by the varying ratios of the monomers between individual cell types and cell wall layers and show lower UV absorbance at an increasing OCH_3/C_9 ratio (Musha and Goring 1975).

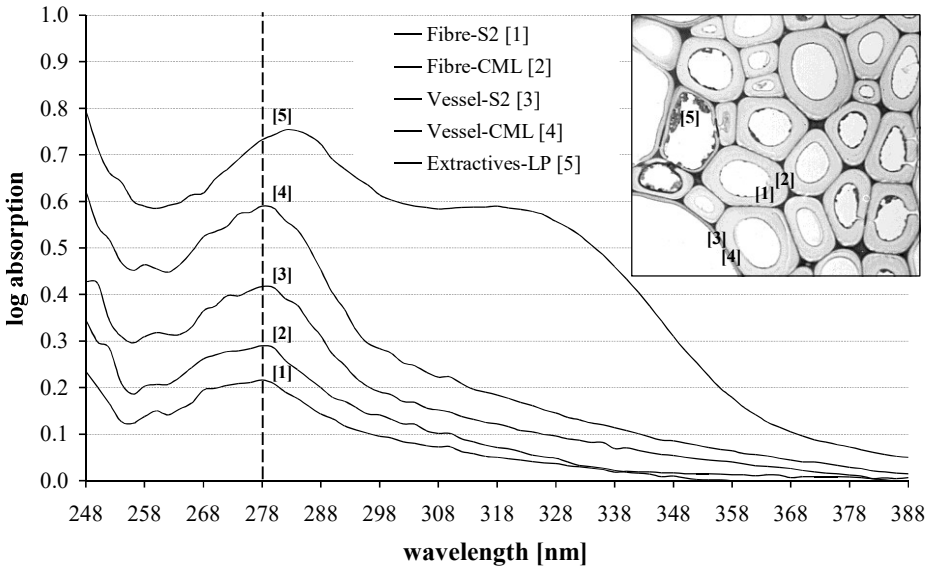

Figure 3: Representative UV absorbance spectra of individual cell wall layers and cell lumen deposited phenolic compounds in the wood tissue of *Fagus sylvatica* (S2-secondary wall, CML-compound middle lamella, L-longitudinal parenchyma). With kind permission from Koch, G.; (Koch and Grünwald 2004)

Extractives represent a complex group of accessory components that mainly consist of fats, fatty acids, fatty alcohols, phenols, terpenes, waxes, tannins and many other organic compounds (Rowell, Pettersen and Tshabalala 2012). The amount and composition of the extractives depend on the wood species and vary within the wood species, within parts of the tree and within wood tissue. Depending on where the extractives are localized, in the cell lumen or impregnated into the cell wall, they influence specific characteristics and properties such as color (lumen localized), natural durability (impregnated in the cell wall) and odor. Wood extractives are chemically extractable from wood with various neutral solvents. Depending on the solvent used and the extraction procedure, the share of accessory wood components – only a few percentiles of the wood – varies in yield and composition by having an enormous effect of the natural durability of the wood species.

The number of natural durable wood species belonging to durability classes (DC) 1/2 (DIN-EN 350:2016, very durable, durable) is relatively low compared to the total number of commercial wood species listed in the standard (DIN-EN 350:2016).

Softwood total number: 31	DC 1: 1; DC 1-2: 2
	DC 2: 6; whereas the traded assortments of softwood (e.g., spruce and fir) are not better classified than DC 3, 3-4 or 4.
Hardwood total number: 134	DC 1: 41; DC 1-2: 6; DC 2: 19

The first preference, regarding the issues of sustainability and carbon sequestration and storage, is to use a long lasting natural wood product. Natural durable tropical wood species of DC 1, 1-2 provide excellent properties for exterior applications like cladding, decking, fencing or harboring facilities. A significant demand on environmentally friendly substitutes for natural durable wood species is driven by very limited availability of higher value

assortments of naturally durable wood. This is mainly affected by illegal logging, increased worldwide environmental concerns regarding relentless development of deforestation (still 3.3 mill ha/year, 2010-2015, Garzuglia 2018) and the recognition of the valuable resources of natural durable tropical wood species as part of protected forests to conserve nature and biodiversity (13% of the global forest, Garzuglia 2018). By enhancing wood properties (in particular durability against biodegradation and dimensional stability) of nondurable wood through a nontoxic modification process, a well suited and environmentally friendly product can be designed that is able to function as an excellent substitute for durable tropical timber species. Technology meant to increase the service life of nondurable wood species without the use of toxic chemicals are being sought out (Militz, 1991; Hill 2006, 2011; Rowell 2005a; Rowell et al. 2009; Rowell 2012; Gérardin 2016). Many aspects of wood modification are known up to now; nevertheless, the fundamental influence of the process on product performance, the environment, and end-of-life scenarios remains unknown (Sandberg et al. 2017) and is part of current research.

2.2 Wood species

The composition and amount of the previously described cell wall macromolecules, cellulose, hemicelluloses and lignin, as well as extractives, depend on individual wood species, cell types and single cell wall layers (Fengel & Wegener, 1983). In general, wood is an extremely versatile material with inherent variability in its cellular, hygroscopic, anisotropic and viscoelastic properties. These properties are all directly linked to the individual species. (Durability of wood and wood-based products. Natural durability of solid wood. Part 1: General, 2016)

The selection of the wood species used in this thesis was made by the Norwegian project PolyWood (Kebony) in consideration of availability, economical aspects and treatability properties. The treatability properties of wood species are important when it comes to the penetration of the treating solution into wood tissue. The production process of Kebony SA is designed for the treatment of coniferous sapwood and hardwood species with comparable treatability properties. The sapwood, of all wood species, is classified in natural durability class 5 (DIN-EN 350:2016-12, not durable), hence providing good treatability properties at the same time. The treatability property of wood is described by the ease with which the wood is penetrated by a liquid, e.g., a wood preservative solution (DIN EN 350:2016-12). The grade/quality of liquid penetration of the three-dimensional capillary system of cells depends mainly on the connection to openings, or pits. Pits are decisive for the liquid transport in sapwood due to their size, structure, aspiration state and number (Comstock and Côté 1968; Liese and Bauch 1967; Stamm 1967). The permeability is also influenced by the interplay of flow along the axial and radial resin canals, as observed for *Pinus radiata* (Booker, 1990). The fungal activity in the decay tests was tested by the degradation rate on *Pinus sylvestris* sapwood.

2.2.1 Radiata pine (*Pinus radiata*)

The coniferous tree Radiata pine, also known as Monterey-Pine, (*Pinus radiata* D. Don; PNRD DIN EN 13556:2003-06) has its native habitat around Monterey, California (Wagenführ 2007; Mead 2013). However, Radiata pine is an economically significant tree species due to their fast-growth, representing one of the most widely cultivated timber species in the world (Mead 2013). There are large Radiata pine plantations in New Zealand (1,545 million ha, 2011), Chile (1,478 million ha, 2009), Australia (773,000 ha, 2010) and Spain (287,000 ha, 2006) (Mead 2013).

Radiata pine trees generally have wide growth rings, and their cross section is characterized by a wide, paler, yellowish-white sapwood area that can be clearly distinguished from the light brown heartwood (Wagenführ 2007). The growth rings include early- and latewood areas with varying cell wall thicknesses (1,78 µm - to 5,7 µm) and lumen diameter (10 µm - 40 µm) (Wagenführ 2007). The density at 12% moisture content varies between 0.42-0.50 g/cm³ (DIN EN 350:2016). Large resin canals are visible to the naked eye – mainly in the latewood zone. According to DIN-EN 350:2016, the heartwood is classified in natural durability class 4-5 and sapwood in class 5, not durable. When processing Radiata pine, a certain amount of sapwood is produced as a buy-product, and therefore, readily available on the market with the opportunity to supply a value-added process. The treatability of Radiata pine sapwood is classified in class 1 according to the standard DIN EN 350:2016-12.

2.2.2 Southern Yellow Pine

Southern yellow pine (SYP) comprises five major species: *Pinus caribaea, P. echinata*, *P. elliottii*, *P. palustris* and *P. taeda*. These species are almost indistinguishable and, therefore, grouped by density as so called “hard pines.” The density at 12% moisture content varies between 0.61-0.68 g/cm³. Some minor “hard pine” species are *P. glabra*, *P. rigida* and *P. serotina,* which have lower densities and are less frequently used in wood construction. Overall, the different pine trees have been introduced into many countries for timber production and are cultivated worldwide. They commonalities include a broad sapwood area, which is classified in treatability class 1 (DIN EN 350:2016). In this study, sapwood was used exclusively for sample preparation. According to DIN-EN 350:2016, sapwood is classified in durability class 5, not durable.

2.2.3 Maple (*Acer* sp.)

As one hardwood species, maple (*Acer* sp.) was included into this study. *Acer* is a species-rich genus belonging to the family of *Sapindaceae*. Maple species are found in North America, Europe and Asia. The wood structure is, to some extent, distinguishable – macroscopically (color and texture) and microscopically via wood rays (Grosser 1977, Kroeger 2004). Similar to SYP, maple species are grouped for trading by their density – into hard maple (0.61-0.67 g/m³) and soft maple (0.50-0.56 g/m³). The density of sycamore (*Acer pseudoplatanus*), at 12% moisture content, lies between 0.61-0.68 g/cm³ and the natural durability of heart- and sapwood is classified into class 5, not durable (DIN EN 350:2016). The treatability of maple is classified in class 1 according to the standard DIN EN 350:2016.

3 Biotic wood degradation

Degradation of wood is an essential part of the natural carbon cycle. Wood stores the largest amount of above-ground terrestrial carbon compared to other plant-based organisms. It is subjected to weathering and attacks by various degrading organisms for living and breeding or as nutrition source.

Long-term, unnoticed degradation processes lead to bacterial degradation. Bacteria are able to colonize and slowly degrade wood as primary or secondary colonizers and cause various decay combined with discoloration, dependent on soil conditions and wood species and wood quality (Klaassen and van Overeem 2012; Schmidt 2006a; Singh et al. 2016). The infected wood is situated in low aeration or under almost anaerobe conditions (e.g., soil contact) combined with high moisture conditions up to fiber situation range (Eaton and Hale 1983; Ibach 2005). Bacteria are omnipresent in humid soil and aqueous environments (Schmidt 2006a). Bacterial attacks above ground occurs in wood that is subjected to cycles of drying and wetting (Eaton and Hale 1983; Ibach 2005). Bacteria are divided according the evoked micromorphological decay pattern in the wood cell wall: tunneling-, erosion- and, more seldom described, cavitation bacteria (reviewed in Singh and Butcher 1991; Daniel and Nilsson 1998). This classification does not represent any form of taxonomic classification. Whereas erosion bacteria degrade the S3 and S2 layers by leaving the CML region almost intact (Kim and Singh 2000), tunneling bacteria degrade all cell wall layers (Daniel and Nilsson 1998). Electron microscopic methods are well suited to analyze bacterial degradation patterns in wood cell walls (Singh et al. 2016), as well as the microbial slime that can bind heavy metals during degradation of CCA-treated wood (Singh and Singh 2014). Singh et al. (2016) concluded that both tunneling- and erosion bacteria evolved remarkable strategies for avoiding direct competition with, e.g., wood degrading fungi: tunneling bacteria can tolerate wood preservatives and heartwood extractives; erosion bacteria can also function under conditions with extremely low levels of oxygen (Singh et al. 2016). Harbor foundation piles have been recovered in relatively good conditions even after 50-80 years of exposure, revealing unmodified and modified lignin as shown by topochemical and electron microscopic studies of cell walls degraded by bacteria (Rehbein et al. 2013).

Besides bacteria, marine organisms and insect fungi are key players in the carbon cycle (Zhang et al. 2016). Fungi in the context of wood can be divided into two groups: wood-inhabitant fungi that cause wood discoloration without losses in mechanical properties and wood degrading fungi that attack the main cell wall components, causing serious damage to the wood's structural integrity. Blue stain and mold belong to the wood-inhabitant fungi and belong to the phylum Ascomycota of the kingdom fungi. Both cause blue, grey or black discoloration; blue stain infects the entire sapwood, whereby mold only occurs on the wood surface to a depth of a few millimeters (DIN EN 68800-1:2019-06). No substantial strength loss can be expected – but rather losses in economic value. Microscopic observations revealed that the discoloration of blue stain is mainly due to pigmented hyphae growing inside the parenchyma cells of the wood rays and adjacent cell lumina. Blue stain and mold fungi require moisture conditions in the substrate above fiber saturation range (>30%) and obtain

their nutrients from the content (carbohydrates) of the parenchyma cells. Molds colonize and damage various materials. Molds cause health problems through mycotoxins, on the one hand, and serve as a basis for antibiotics or refinement of food products on the other hand. Gradeci et al. (2017) recently reviewed mold models that are applicable to wood-based materials, providing useful facts for practical means. However, wood decaying fungi cause great losses in functionality of wooden components (timber in-service), as well as economical losses. The physical/chemical limiting factors for fungal activity are nutrients, water, oxygen, pH-value, light, force of gravity, temperature and air circulation (Schmidt, 2006c). Water, as one essential key component for wood decay, is therefore dedicated to and a topic of active research (Hunt et al. 2018, Meyer and Brischke 2015; Ringman et al. 2014, 2019; Thybring 2013, 2017; Thybring et al. 2018; Zelinka et al. 2016; Zelinka et al. 2020). The studies aim to achieve knowledge to elucidate the relationship between water and the decay of wood to prevent fungal attacks. The studies focus on water inside the cell walls and the decay of wood, as well as relations of the decayed material with water during and after decay. The studies were performed with untreated and modified wood undergoing both brown-rot and white-rot decay. The papers mentioned in the section 'wood decaying fungi' agree on the essential role of water in fungal degradation of wood and that the reduction of cell wall moisture content by modification can effectively improve the resistance against wood decaying fungi. The complexity of elucidating wood-water relations and difficulties during test design and performance are shown in studies by Zelinka et al. (2020). They confirm earlier results that the moisture content at the end of the test is linearly related to the amount of mass loss. They also found that an independent control of wood moisture content is not possible, since the fungus actively controls the moisture in the wood during wood decay.

Wood colonizing and degrading fungi belong to the division of Basidiomycota and Ascomycota (Spatafora et al. 2017). They are commonly classified by the evoked kinds of wood rot: brown rot, white rot and soft rot (Schmidt 2006e). However, this way of fungal classification has been questioned since it was studies that the decay mechanisms of wood decaying fungi are much more complex than previously thought. Riley et al. (2014) suggested a more nuanced categorization of rot types that is based on an improved understanding of the genomics and biochemistry of wood decay. The common classification of the wood decaying fungi as stated in the review (Schwarze 2007) was used in this thesis with reference to relevant studies and current standards.

3.1 Brown rot

The fungal hyphae enter the wood preferably via the wood rays and spread from there into the adjacent cells (Schmidt, 2006e). The hyphae move from cell to cell by growing through pits or by direct penetration of the cell walls as reviewed by Liese (1970). Under the microscope, alterations in birefringence can be observed in the early stages of decay, whereas microscopic damaged cell walls are otherwise subtle until advanced stages (Wilcox 1993).

The established theory of the biodegradation process of brown rot organisms describes two phases: non-enzymatic oxidative degradation and enzymatic degradation (Arantes et al. 2012; Zhang et al. 2016). The non-enzymatic mechanism deconstructs the lignocellulose framework

by catalytically modifying lignin (Yelle et al. 2008, 2011; Arantes et al. 2011; Martínez et al. 2011). The rapid depolymerization through non-enzymatic oxidative degradation processes results in losses of essential engineering properties (e.g., bending strength) even before any mass loss can be detected (Schultze-Dewitz 1966; Bariska et al. 1983; Winandy and Morrell 1993; Curling et al. 2002; Witomski et al. 2016). The oxidative decay phase is followed by a second phase where hydrolyzing enzymes are secreted by the fungus (Arantes et al. 2012; Arantes and Goodell, 2014). The transition from oxidative to enzymatic degradation is initiated by the presence of solubilized sugars during non-enzymatic oxidative decay (Zhang et al. 2016). However, the non-enzymatic oxidative degradation mechanism, the chelator-mediated Fenton (CMF) system (Arantes and Goodell 2014), is not fully elucidated. Goodell et al. (1997), Eastwood et al. (2011) and Arantes et al. (2012) suggested the current theory that describes the brown-rot fungi secreting oxalic acid that functions as a chelator to sequester Fe3+ in the cell lumen. The reductants (hydroquinones) then reduce Fe3+ to Fe2+, and it is assumed that hydrogen peroxide (H_2O_2) is produced by the brown rot fungi through a reaction of hydroquinones and oxygen (Jensen et al. 2001). Hydroxyl radicals were then produced through the reaction of Fe2+ and H_2O_2 via the Fenton reaction (Fenton 1894). Hydroxyl radicals depolymerize the polysaccharide components to solubilize sugars that can diffuse through the cell walls into the lumen, to become accessible for the brown rot fungi enzymes (cellulases and hemicellulases) (Martínez et al. 2005; Goodell et al. 2017). This depolymerization process also effects lignin (Yelle et al. 2008, 2011; Arantes et al. 2011; Martínez et al. 2011). To reveal more details about the decay mechanisms, efforts are being made that aim for different aspects to accomplish the whole picture as stated in a current review about wood-water relationships regarding fungal decay by Brischke and Alfredsen (2020). In general, considerable efforts have been undertaken, e.g., by Goodell et al. (2017) to understand the interactions between enzymatic and non-enzymatic mechanisms and gene regulation and expression, e.g., by Zhang and Schilling (2017), Kölle et al. (2019) and Zhu et al. (2020).

3.2 White rot

White rot fungi prefer deciduous trees – predominantly hardwoods – degrade all major cell wall components and are capable of efficient lignin degradation. White rot fungi are the second common fungi, besides brown rot, that occur in building and construction areas (Huckfeldt and Schmidt 2015). Compared to brown rot fungi, the losses in strength are less drastic, since, at the same mass loss, lesser cellulose is degraded (Schmidt 2006e). Two main types of white rot decay can by distinguished by microscopic and ultra-structural evaluation: simultaneous white rot and successive white rot (Liese 1970). For the latter, lignin and hemicelluloses degradation happens faster – at least at the initial decay stage. Defibration by dissolution of the middle lamella is the most remarkable anatomical effect of this type of rot (Worrall et al. 1997). Simultaneous white rot is characterized by degrading carbohydrates and lignin at the same time with a similar degrading rate. In this case, erosion of the cell wall from the lumen surface is a prominent anatomical feature (Worrall et al. 1997). For both types, powerful oxidative and hydrolytic enzymes are involved (Eaton and Hale 1983). Lignin is completely mineralized, leaving bleached (white cellulose) and spongy wood behind (Ibach

2005; Schmidt 2006e; Riley et al. 2014). One individual fungus may cause these two forms of decay pattern that can be found in different portions of one wood specimen (Wilcox 1993). To enhance biorefinery profitability, white-rot decay and the enzymes involved are the focus of ongoing studies, as stated in a review by Brischke and Alfredsen (2020).

3.3 Soft rot

Soft rot fungi belong to the Ascomycetes that attack wood, where the growth of Basidiomycetes fungi is impaired (Eaton and Hale 1983; Schmidt 2006e; Schwarze 2007). High moisture content, low aeration or elevated temperatures are no limiting growth factors. Soft rot fungi spread slowly from the outside to the inner parts of the wood. Surprisingly, the wood is sound beneath the degraded surface (Eaton and Hale 1983). Infected wood is dark in color and softened in a wet stage, from which is where the name is derived (Schwarze 2007). Dried wood shows a partly spongy texture with a finely cracked, charcoal-like surface and short-fibrous splintering. Sometimes, discoloration and cracking patterns like that of brown-rot fungi are detectable (Eaton and Hale 1983). Under the microscope, a specific form of decay can be observed that produces chains of rhombus-shaped cavities parallel to the orientation of the cellulose microfibrils in the S2 layer (observed in longitudinal sections, soft rot type 1) or an erosion of the cell wall by degrading cellulose and hemicelluloses (observed in cross section, soft rot type 2). Lignin is not (or not vey often) attacked at the initial stage (Schmidt 2006e). With only 5% loss of mass, soft rot, similar to brown rot, already produces 50% loss of impact bending strength. (Schmidt 2006e).

3.4 Insects and wood borers

Basically, a distinction is made between marine and terrestrial wood destroying organisms. Wood tissue functions as a growing medium, for shelter, for breeding or as substrate for their fungus culture.

Marine organisms that live in seawater, like crustaceans and mollusks, can cause extensive damage to wood by surface attacks or by boring networks of tunnels, respectively. Gribble (*Limnoria lignorum,* Rathke) and Shipworm (*Teredo navalis*) are distributed within the temperate and boreal Northern Hemisphere, and the latter has been found worldwide. The damage caused by *L. lignorum* (diameter hole: 1.5 to 2 mm) is most pronounced near the low tide level and typically occurs at depths of 0–30 m of seawater. In a relatively short period of time, a vast amount of damage can be caused due to the possibility of rapid population increase. *T. navalis* also destroys wooden structures that are immersed in seawater very quickly due to its boring activity (diameter holes up to 1 cm). Piers, docks and wooden ships are attacked at almost the same water depths as *L. lignorum*. The deterioration of wood by marine organisms is a matter of considerable economic importance in coastal areas.

Wood degrading insects can technically be seen from an economical perspective as wood destroying organisms. From an ecological point of few, insects are valuable and essential for the natural carbon cycle and are, in most cases, secondary colonizers. However, significant wood damage is caused by larvae and adult forms of insects (Ibach 2013). Insects can be

grouped by the moisture conditions of the wood that is being attacked: freshwood (living trees or harvested round wood), drywood and rewetted wood. A re-infestation by freshwood insects can occur after processing the wood. In contrast, drywood insects are territorial until the wood has been completely degraded (re- and new infestation).

Termites or white ants belong to the most harmful wood destroying organisms in warmer climates of the world (Eaton and Hale 1983; Ibach 2013). In these regions, constructional timber is particularly threatened by termites. Comparable to wood degrading insects, termites are also grouped by the moisture conditions of the wood and the environment: subterranean, dampwood and drywood termites (Eaton and Hale 1983).

4 Wood protection and preservation

Wood applications in building and construction projects are faced with and influenced by varying environmental conditions and a permanent presence of microbial organisms. To delay or even prevent biodegradation processes and the risk of attack by these kinds of organisms, the wood material has to be protected. According to the standard DIN 68800-1:2019-06, the term *wood protection* includes every procedure that avoids depreciation or degradation by fungus, insects or marine organism to ensure a prolonged and predictable service life of the wooden building components.
Preventive wood protection tasks can be divided into five groups.

1) Natural wood protection – use of natural durable wood species;
2) Constructive wood protection – meeting the requirements of wood (cellular, hygroscopic, anisotropic and viscoelastic properties) in design; avoiding conditions that enable the attack of wood destroying organism by applying constructional approaches;
3) Physical wood protection – reduction of wood moisture in use by coating or hydrophobic impregnation;
4) Chemical wood protection – wood impregnation with biocide agents;
5) Wood protection through wood cell wall modification;

Depending on the wood application, the resulting use class (DIN 68800-1:2019-06, DIN EN 335:2013-06, DIN EN 460:2018-12) and the natural durability of the used wood species (DIN EN 350:201612) require wood protection systems in design (DIN 68800-2:2012-02) and wood protection agents (DIN 68800-3:2020-03).

Research activities in the field of wood protection and wood preservation concentrate on a wide range of aspects: surface modification, further development of existing modification processes without the use of biocides and further development of physical/mechanical/chemical test methods. This not only involves wood, but also wood- and bio-based composites. The efforts in this field were, e.g., reviewed by Winandy and Morrell (2017) regarding the improvement of the durability of wood- and bio-based composites, or in studies on beech wood modified in a paraffin-thermal process (Reinprecht and Repák 2019) and on tensile and impact bending properties (Bollmus et al. 2020). Corrosion properties of chemically and thermally modified wood, for instance, were investigated by Zelinka et al. (2020) and gene expression analyses of *Rhodonia placenta* in acetylated wood were performed by Kölle et al. (2019). Aspects of chemical modification with native impregnation agents (e.g., robina extracts) were analyzed by the group Rademacher et al. (2017) within the context of a European project of wood research from native wood to engineered materials (COST FP1407) to understand the mode of action of 1) cell wall stability, 2) cell wall penetrability and 3) cell wall impregnation.

In the following subchapter, a description of traditional wood protection and established wood modification techniques such as thermal modification, acetylation and furfurylation will be presented.

4.1 Traditional wood preservatives

Wood preservation is the chemical protection of wood and wood composites against the attack of wood destroying organisms. Traditionally, wood preservatives that use toxic preservative systems that are based on a combination of biocides and additives have negative side effects, as they harm human health and the environment. The impregnated chemicals are either fungistatic or fungitoxic and inhibit fungal growth (Zelinka et al. 2019). These systems can be classified by their chemical composition into: creosotes, water-soluble/water-based preservatives, solvent-borne preservatives and emulsions. The application of wood preservatives for preventive wood protection is regulated by the standard DIN 68800-3:2020-03. The penetration process can generally be distinguished between pressure and non-pressure processes (Eaton and Hale 1983; DIN 68800-3:2020-03). The pressure process is the most commonly used process, whereby the wood is impregnated via a full-cell (Bethell process), empty cell (Rüping process, Lowry process) or oscillation pressure method (EN 1001-2:2005-10). There are also many non-pressure processes, such as vacuum treatment or surface application preservatives by brushing. These processes can be distinguished by the penetration depth and retention of preservative (Eaton and Hale 1983; DIN 68800-3:2020-03). A special demand on wood preservatives comes from wood railway sleepers and wood poles for overhead lines. The latter are treated with wood preservatives according to use class 4 (DIN EN 14229:2011-02), whereas the wooden railway sleepers are treated with creosotes (coal- and tar-based oil) (DIN EN 68811:2007-01).

To protect wood from fungal decay and to increase its resistance to decay caused by insect attack, micro-organisms and damage caused by marine wood-boring animals, copper- based preservative treatments are often prescribed (Hunt et al. 2018). Copper chrome arsenates (CCA) have been used extensively for over 60 years (Hingston et al. 2001). The amount of CCA chemicals involved in North America alone by the year 2000 amounted to 70,000-85,000 tons of active oxide (Preston 2000). Their availability depends on regulations and maintaining their registration with environmental regulators (Lebow 2004). Biocides and pesticides are registered and regulated in The European Union's regulatory frame work Biocidal Product Regulation (BPR) (528/2012) and reviewed under the Biocidal Products Directive (BPD) (98/8/EC).

The growing concerns and the knowledge gained regarding its hazardousness to human health and the environment (Townsend et al. 2005; Kim et al. 2019) have banned it, and the use of creosotes is restricted. This being said, wood preserving industry is an important industry in Europe and North America, with annual gross sales in the USA of around $\$4.5*10^9$ in 2007 (Vlosky 2009). This industrial sector is required to carry out considerable research and development programs to generate improved biocides (Hingston et al. 2001) and is struggling with difficulties in developing effective protective systems. Several novel biocides are based on copper (Cu) due to its antifungal properties, with chrome and arsenate being replaced by a triazole biocide in copper azole, or a quaternary ammonium biocide in ammoniacal copper quaternary (Hingston et al. 2001).

Table 2 Preservative formulations standardized for applications typical for residential construction (retrieved from to Lebow 2004)

Preservative formulation as listed in AWPA standards	Proportion of preservative component		Retention kg/m³	
			Above ground	Ground contact
Acid copper chromate (ACC)	31% CuO	68% CrO_3	4.0	6.4
Alkaline copper quat (ACQ-B, D)	67% CuO	33% DDAC[a]	4.0	6.4
Alkaline copper quat (ACQ-C)	67% CuO	33% BAC[b]	4.0	6.4
Copper azole (CA-B)	96% Cu	4% azole[c]	1.7	3.3
Copper azole (CBAAB)	49% cu	2% alzole[c] 49% H_3BO_3	3.3	6.5
Copper citrate (CC)	62% CuO	38% citric acid	4.0	6.4
Copper bis dimethyldithio-carbamate (CDDC)	17% - 29% CuO	71% - 83% SDDC[d]	1.6	3.2
Copper HDO (CX-A) (pending EPA registration)	61.5% CuO	14% CuHDO[e] 24.5% H_3BO_3	2.4	NA[f]

[a]Didecylthyl ammonium chloride.
[b]Alkylbenzyldimethyl ammonium chloride.
[c]Tebuconazole.
[d]Sodium dimethyldithio-carbamate.
[e]Bis-(N-cyclohexyl-diazenium dioxy)copper.
[f]Not in standards yet.

Problems occur when it comes to copper tolerant fungi. For instance, studies on micronized copper wood preservatives aim to investigate if it is more effective than standard Cu compounds against wood degrading fungi due to specific nano formulations (Civardi et al. 2015). In this context, they also assessed the impact of a co-biocide tebuconazole (TBA). One theory was that, in Cu-tolerant brown rot fungi, the threshold for Cu-nanoparticels might be lower than the threshold for Cu^{2+} ions, due to nano formulations. In the presence of small amounts of micronized copper, the fungi may not be able to trigger Cu tolerance mechanisms (Civardi et al. 2015). They assumed further that, i.e., free hydroxyl radical production via Fenton reaction of brown rot fungi may be impaired. Civardi et al. (2015) found that the treated wood will still be degradable by Cu-tolerant fungi and concluded that the nanoparticles in the micronized copper azole formulations assessed in this study did not provide additional protection against *R. placenta,* and the main effectiveness has to be attributed to TBA. Another assessment study performed by Künniger et al. (2014) of the functionality of metallic silver nanoparticles (Ag-NP) as an alternative biocide in coatings merely showed that, under the tested conditions, Ag-NP did not protect the façades against fungal decay – and its use is questionable.

There is also a pressing need to replace synthetic and inorganic compounds with organic biocides, as presented by Singh and Singh (2012). Their comprehensive review on natural products as wood preservatives showed the enormous potential of the various approaches and the limitations in the development of effective environmentally sustainable wood protection systems. For instance, Singh and Singh (2012) reviewed several studies that provided promising results regarding the effectiveness against wood decaying fungi and termites that were obtained by extracts from cinnamon leaves, which could potentially be developed into excellent organic preservatives.

4.2 Wood modification

There has been a growing interest in the development of new modification processes since the ongoing deforestation of sub-tropical forests in particular, the declining production of durable timber, the increasing demand for sustainable building materials and the increased amount of restrictive regulations implemented by the government that reduce the use of toxic wood preservatives; this interest can be observed worldwide (Candelier et al. 2016; Jones et al. 2019). New technologies have been developed to improve durability, stability, and performance of wood without the use of toxic chemicals (Rowell 1983; Militz 1991; Hill, 2006; Rowell et al. 2009; 2012; Gérardin 2016). Furthermore, issues of sustainability and carbon sequestration come together in this search for new 'green' technologies (Rowell 2016).

One type of wood treatment, whereby the molecular structure of the cell wall polymers (cellulose, hemicelluloses and lignin) are permanently altered, is named 'wood modification' (Homan and Jorissen 2004). This treatment involves the action of a chemical, biological or physical agent upon the material (Hill 2006). Wood modification technologies are aiming, on the one hand, for enhanced wood properties such as improved decay resistance facilitating a prolonged service life and, on the other hand, for easy disposal at the end of life (Hill 2006). The modified wood-based material is non-toxic in service and at the end of the product's life cycle, as well, when it is disposed of (Jones et al. 2019). According to the type of process (chemical, thermo-hydro-mechanical and physical) used to achieve the enhanced wood properties, modified wood can be classified into three groups (Figure 4), as presented by Jones et al. (2019). Processes with potential future prospects are listed under "other processes" and will not be further described.

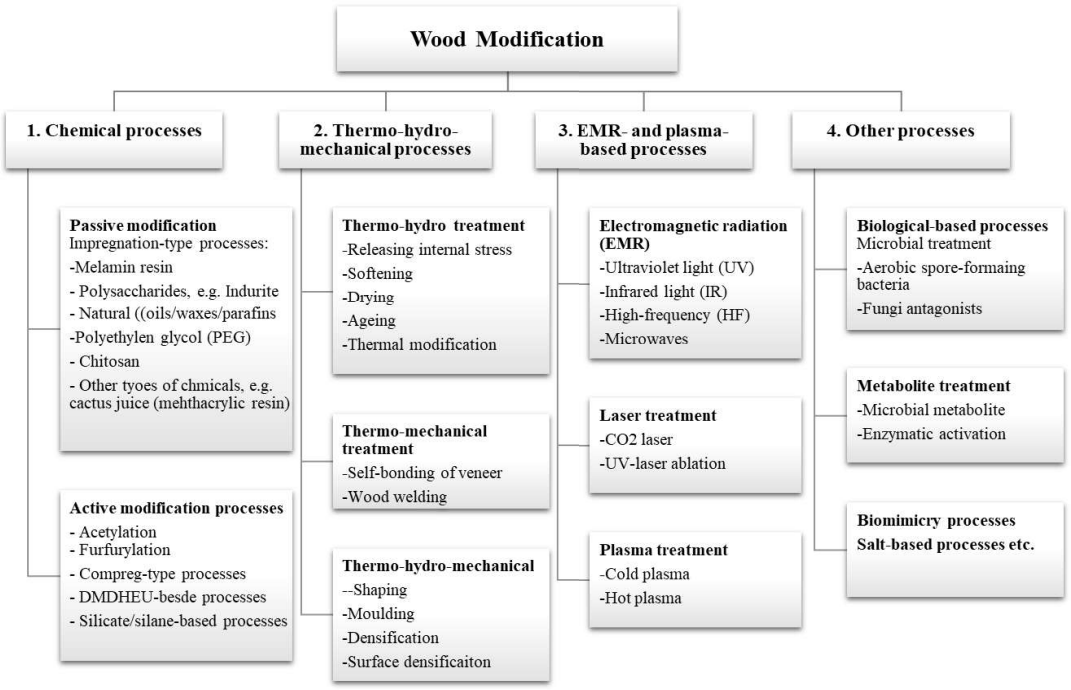

Figure 4: A diagram of the various wood modification processes at this point in time, retrieved from Jones et al. (2019)

Wood is subjected to a constant moisture exchange with the environment directly aiming for wood moisture equilibrium. Wood moisture not only influences the degradability of the wood, but its dimensional stability and mechanical properties, as well (bending strength, MOE, MOR). However, wood moisture is therefore a crucial point that should be addressed by wood modification. For instance, thermally modified, acetylated and furfurylated wood are more recently available on the market (Jones et al. 2019). The modified wood coming from these processes provides significant improved decay resistance by effecting the equilibrium moisture content (EMC) (Thybring 2013). Correlations between EMC, the treatment level and decay resistance of the modified wood were found for these three modifications (Epmeier et al. 2004; Lande et al. 2008; Rowell et al. 2009). Regarding the importance of moisture and diffusion for the decay resistance of untreated and modified wood and wood-water relationships, the latest research followed up with this topic and comprehensive reviews are available (e.g., Thybring et al. 2018, Fredriksson 2019; Ringman et al. 2019; Brischke and Alfredsen 2020; Zelinka et al. 2020). For instance, Ringman et al. (2019) pointed out three potential mechanisms for diffusion inhibition in modified wood that were discussed: i) nanopore blocking; ii) capillary condensation in nanopores; and iii) plasticization of hemicelluloses. The wood-water relationships at very humid climatic conditions were reviewed by Thybring et al. (2018), as well as the mechanisms behind moisture sorption in the over-hygroscopic range and methods that can be used for water determination by Fredriksson (2019). All in all, the complex interrelationships of wood-water relationships are not yet fully understood (Brischke and Alfredsen 2020).

The annual production volumes for the nearest coming year (Table 3) have been estimated by Jones et al. (2019) on the basis of COST FP1407. Wood modifications, like thermo-hydro (TH) and thermo-hydro-mechanical (THM) methods are not included within data compiled in Table 3.

Table 3: Estimated production volumes of modified wood in Europe for the nearest coming years (Jones et al. 2019)

Wood modification	Estimated annual production [m³]
Thermally modified timber incl. aged timber	535,000
Acetylated timber incl. production under development in the UK	120,000
Furfurylated timber incl. production under development in Belgium	45,000
Other chemical methods	35,000

4.2.1 Thermal modification of wood

Wood properties can be changed by thermal treatment (>160°C) due to heat induced chemical degradation of wood polymers under reduced oxygen conditions (DIN EN 68800-1:2019-06). This modification technique has been known and applied for a long time (Stamm et al. 1946). It is an environmentally acceptable modification method (van Eetvelde et al. 1998) that is mainly based on chemical degradation of wood polymer by heat transfer (Candelier et al. 2016). Free hydroxyl-groups will decrease in number during heat treatment, which results in

decreased hygroscopicity. Different heat treatment technologies, like mild pyrolysis, can be applied – resulting in a darker coloration of the treated wood (Militz 2002). In a recent review, a revived interest during the last three decades was documented regarding methods of controlling the thermal treatment, the effects on wood decay resistance and potential industrial use (Candelier et al. 2016). This modification process improves – without additional chemical products – the decay resistance (Tjeerdsma et al. 1998; Homan and Tjeerdsma 2000) and dimensional stability of the treated material, merely at the expense of a weakening of mechanical properties (Militz 2002). With increasing treatment temperature, the resistance against biodegradation increases, whereas the strength properties decrease (DIN CEN/TS 15679:2008-03). It is assumed that this phenomenon of strength loss cannot be explained solely by a decomposition of the hemicelluloses associated with the cellulose in the wood; a decrease of the thermal stability of the cellulose has to be considered (Kollmann and Fengel 1965). This decrease in strength properties has to be accounted for the application of thermally modified wood, as well as the energy consumption to produce thermally modified wood.

Different commercial treatments have emerged, for instance, TermoWood® (Finland), Plato® (Netherlands), Rectification® and Bois- Perdure® (France), OHT® (Germany), Denmark (WTT) and Austria (Huber Holz) (Candelier and Dibdiakova 2020). Some of these processes are in development and others are already in full production. Several wood species are used, with different process conditions, depending on the species and the final use of the product. All of the processes use sawn wood and treatment temperatures between 160ºC and 260ºC, but they differ in terms of process conditions, such as the presence of a shielding gas such as nitrogen or steam, humid or dry processes, use of oils, etc. (Militz 2002).

It is complicated to conduct a comparative study of various industrially based methods of thermal modification of wood (Scheiding et al. 2005; Welzbacher and Rapp 2002). A Portuguese life-cycle assessment study (Ferreira et al. 2016, ISO 14040/44) of thermally modified pine timber (TermoWood® method) revealed that the energy consumption needed for the production of 1 m^3 TermoWood® required about 3,900-4,720 kWh of cumulative energy with a share of non-renewable energy between 280 kWh and 560 kWh. Candelier and Dibdiakova (2020) provide a comprehensive review on the existing knowledge about life-cycle assessments of thermally modified wood and give information about the share of energy consumption: about 80% of the heat energy used is mainly needed for the preliminary drying step (Thermowood 2003). Overall, compared to traditional timber drying processes, Candelier and Dibdiakova (2020) outlined that the total energy demand for thermal modification is about 25% higher.

The current world market situation of thermally modified wood was presented by Candelier (2018) at the RACEWOOD Technical Conferences in Gabon and summed up by Jones et al. (2019).

4.2.2 Acetylation

Acetylation of wood with acetic anhydride goes back to the late twenties of the last century, according to the review presented by Rowell et al. (2009). This modification method is currently the most widely studied – and it is finding commercial success (Hill 2006; Mantanis

2017). From a chemical perspective, acetylation of wood is an esterification process, whereby acetic anhydride reacts with accessible hydroxyl groups in the wood cell wall, forming ester bonds (Rowell et al. 1994; Rowell 2005a). Since acetylation is a single-addition reaction, which means that one acetyl group is bound to one hydroxyl group with no polymerization (Rowell 2016; Mantanis 2017), the amount of blocked hydroxyl groups is directly linked to weight gain in acetyl (Rowell 2005a; Rowell et al. 2009; Rowell 2016). According to Hunt et al. (2018), the effectiveness of the treatment depends on the extent of modification, which can be quantified using weight percentage gain (WPG), defined as the mass change resulting from the modification divided by the original wood mass before modification. Furthermore, Rowell et al. (2009) assumed that 100% of the hemicelluloses hydroxyl groups are substituted, as opposed to no cellulose hydroxyl groups. The by-product acetic acid, formed in this process, has to be removed, as it potentially leads to hydrolysis of the wood carbohydrates (Hill 2006) and because of the odor of acetic acid (Rowell et al. 2009). Acetylated wood is characterized by higher dimensional stability due to a reduction in hygroscopicity of the wood material by acetyl bulking of the wood cell wall and blocking of hydroxyl groups (Militz 1991). The mechanical properties (strength and modulus of elasticity) changed very little (Militz 1991) and the acetylated wood shows low environmental impact (van Eetvelde et al. 1998). Acetylated wood displays improved biological resistance (Larsson Brelid et al. 2000), whereas fungal resistance increased linearly with increasing WPG (Hosseinpourpia & Mai, 2016). WPG in the range of 17-20% is required to protect the wood from damage by brown rot fungi (Hill 2006; Thybring 2013). The material property changes caused by acetylation that lead to the improved decay resistance are not completely understood and continue to be part of current research (Ringman et al. 2014; Alfredsen et al. 2015; Hosseinpourpia and Mai 2016; Thybring 2017; Hunt et al. 2018). Several explanations for the mechanisms behind the improved decay resistance have been proposed. For instance, Hunt et al. (2018) recommended determining the degree of modification of hemicelluloses as a parameter for the effectiveness of modification – if hemicelluloses are identified to be responsible for diffusion and decay instate of the parameter WPG – to quantify decay resistance. A further idea mentioned by Hunt et al. (2018) is, which is being pushed forward today by analyzing experimental data from literature by Thybring (2013), that, limiting the moisture and the accompanying free volume inside the cell wall may be the key to inhibiting diffusion and decay. The decreases in the wood EMC inhibit diffusion within the cell wall; this is concluded to be the most likely explanation for the enhanced decay properties of acetylated wood (Zelinka et al. 2016). A study on the resistance of acetylated wood to Fenton's reagent by Hosseinpourpia and Mai (2016) showed that an increasing WPG due to acetylation gradually reduces the tensile strength loss and mass loss during exposure. They assumed that a reduction in penetration of Fe ions into the wood cell wall is caused by the bulking effect of acetylation. Furthermore, they concluded that the reduced accessibility might explain the resistance to brown rot fungi, which uses the Fenton reaction to initiate wood decay.

In the report 'Wood modification in Europe', Jones et al. (2019) detailed another method of wood modification that has gained scientific interest: the use of vinyl acetate (Jebrane and Sèbe 2007). One advantage comparing this method to acetylation is that it can be attempted to avoid secondary processing for the removal of odorous components.

A short overview of the industrial development of the acetylation of wood was presented by Rowell (2016). Accsys Technologies in Arnhem, The Netherlands, now sells acetylated wood. It is sold under the commercial name of Accoya® and is available for several species of wood in Europe, North America and Asia. The current market situation, based on a personal notice, was presented by Mantanis (2017): approximately 40,000 m^3 of acetylated timber was produced annually by Accsys in 2017, while the company increased its capacity to 60,000 m^3 in the year 2018.

4.2.3 Furfurylation

Furfurylation of wood is also an extensively investigated chemical wood modification system (Goldstein and Dreher 1960; Stamm 1977), whereby the organic monomer furfuryl alcohol (FA) is the key agent. The process is basically described as the polymerization of FA that accrues during hydrolyzed biomass waste as a by-product. It is based on FA molecules penetrating, due to their polarity, into the lumens and the wood cell walls, polymerizing *in situ* and creating a permanent swelling of the wood cell walls (Goldstein and Dreher 1960; Stamm 1977). UV absorption bands at λ228 nm and λ286 nm (Ünver and Öktem 2013) characterize the polymerized FA. Furfurylated wood is darker than the heartwood of native European wood species and has an aesthetic appeal similar to that of natural durable (and dark) tropical timbers like teak, ipé or azobé. Studies on fungal degradation of furfurylated wood revealed a delayed fungal wood decay compared to untreated wood (Lande, Westin et al. 2004a; Venås 2008; Esteves et al. 2011; Li et al. 2015; Ringman et al. 2017; Sejati et al. 2017; Skrede et al. 2019). The decay resistance increases with higher WPG as well as with increasing EMC (Eikenes et al. 2004; Lande et al. 2004b, 200 4a; Esteves et al. 2011). Furfurylated wood fulfills the requirements for hazard classes 3 and 4 applications according to DIN EN 335:2013-06. The biological durability of wood can be upgraded to DC 1 (Gérardin, 2016). Furfurylated southern yellow pine and Radiata pine have been admitted as "proven" for window frames to the German market (VFF-Merkblatt HO.06-4 2016) as a result of a series of extensive quality tests in the context of the "Winfur" project (Bollmus et al. 2012).

The polymerization of FA itself is a complicated process. FA can be polymerized by several organic, mineral and Lewis acids and is currently understood to take place in three steps (Choura et al. 1996): In the liquid system, (1) linear FA chains are formed as well as (2) conjugated FA oligomers; (3) linear oligomers cross-link via Diels-Alder cycloadditions, forming a branched structure which causes the emergence of a rubbery state. If this third process step is allowed to progress sufficiently, a hard, stiff and glassy polymer is obtained. Mantanis (2017) recently reviewed these developments in chemical modifications, presenting a five-step industrial process production of wood furfurylation according to Lande et al. (2004):

1) Storage and mixing of chemicals
2) Vacuum pressure impregnation with the treatment solution of a full-cell process
3) Reaction/curing: *In situ* polymerization of the chemicals and grafting reactions occur
4) Drying in a kiln dryer
5) Cleaning: by cleaning the ventilated gases.

Furthermore, Mantanis (2017) presented the production figures of the company Kebony AS (Norway), which lie at approximately 22,000 m^3 annually (as in 2017); this is expected to increase.

Mechanical properties of the final polymer can be affected by furan ring openings that may occur as a side reaction during the polymerization process (Venås and Rinnan 2008). Whether this process also occurs in the wood cell wall is unclear. Schneider et al. (2000) showed that the FA solution filled the cell lumen completely or partially and penetrated the cell walls to some extent. FA polymerization taking place within the wood cell wall has been proven on furfurylated wood by infrared microscopy (Venås and Rinnan 2008) and fluorescence microscopy studies (Thygesen et al. 2010). The work carried out by Li et al. (2016) demonstrated the improved modulus and hardness of furfurylated wood cells through nanoindentation studies, indicating that furfuryl alcohol indeed penetrated wood cells during the modification process. The investigations revealed concordantly higher (poly)FA concentrations in lignin-rich parts of the wood, mainly in the cell wall corner regions (CC) and the compound middle lamella (CML). Nordstierna et al. (2008) examined the possibility of a covalent bond formation to lignin during the FA polymerization process. Nuclear magnetic resonance (NMR) spectra of a liquid-phase system of a lignin model compound and FA were studied. The results showed the formation of covalent bonds in the early stages of FA polymerization. A combined theoretical and FTIR spectroscopy study of a hybrid poly(FA)–lignin material (Barsberg and Thygesen 2017) support these findings. Possible cross-products of the simple lignin G model with FA were presented, including the definition of condensation position, e.g., at the aliphatic Ca-position. Furthermore, Barsberg and Thygesen (2017) found evidence for the condensation of FA with selected lignin models, whereas the topochemical investigations visualized the condensation of FA with cell wall lignin *in situ*.

No conclusive experimental evidence has so far been provided that gives a comprehensive explanation on the mode of action. It is still questioned as to what exactly influences the enhanced resistance of furfurylated wood to brown rot degradation. Hence, ongoing research focused, for instance, on information on accessible hydroxyl groups in furfurylated wood during brown rot decay (Beck et al. 2019) to identify changes in OH content at different degradation stages. These researchers found a significant increase of accessible OH groups after initiation of decay, which can be attributed to the opening of crystalline cellulose regions and the formation of new OH groups in lignin and the furfural polymer due to oxidative alteration. Furthermore, recent investigations on differential gene expression profiles of *R. placenta* degrading furfurylated wood by Skrede et al. (2019) showed, for instance, that the major difference is a delayed and elongated response for furfurylated wood compared to untreated wood. They further supposed that the furfurylation acts as both a physical barrier and a factor that lead to a less-hydrated environment for the fungus. In a critical discussion of moisture for brown rot degradation in modified wood, Ringman et al. (2019) showed that different theories regarding the influence of improved resistance play a role and do not appear mutually exclusive.

5 Knowledge gap

Knowledge of FA-lignin modification within the wood cell wall and its potential influence on brown rot degradation is still not fully understood. This research topic is of considerable interest, since wood cell wall lignin presents the most significant barrier to wood decay and influences degradation modes (Schwarze 2007). The UMSP method allows direct imaging of both hard- and softwood lignin distribution and lignin modification (biodegradation, delignification) (Fergus and Goring 1970a; Scott et al. 1969; Saka et al. 1982; Fukazawa 1992; Koch and Kleist 2001; Koch and Grünwald 2004; Rehbein and Koch 2011; Koch and Schmitt 2013). FA modified wood, as well as degraded FA modified wood has not yet been investigated with the UMSP method. However, it is still not definitively demonstrated how the furfurylation takes place in the wood cell wall with the cell wall compounds (Beck et al. 2019). In-depth knowledge of the topochemistry of furfurylated cell walls could reveal potential bindings of cell wall lignin and FA. Nordstierna et al. (2008) demonstrated this in a liquid-phase system with FA and a lignin model compound. Knowledge about the binding of FA and the cell wall lignin would improve our understanding of the mode of action of furfurylated cell walls against brown rot decay.

An entire picture of the degradation pattern during the early stages of brown rot decay and a comparison between untreated samples and FA modified samples would be of considerable interest. The early stages of brown rot decay are considered to be a critical step in identifying significant reduction in strength properties (Irbe et al. 2006). The ability to identify deterioration at an early stage is desirable due to the potential losses in wood strength at limited extents of decay (Kim et al. 2019). Decay tests with different wood species modified with varying FA treatments and conditions, as well as untreated wood species should be designed due to the different constitution of hard- and softwood lignin. Additionally, detailed knowledge of decomposition processes of wood decay fungi also can be used for biotechnology processes in the wood industry (Schwarze 2007). Sub-cellular studies of the fungi-related degradation process of untreated wood providing topochemical information are rare (e.g., Bauch et al. 1976; Kleist and Seehann 1997; Schmidt et al. 1997; Irbe et al. 2006; Rehbein and Koch 2011). Initial brown rot degraded cell walls analyzed by Irbe et al. (2006) and Rehbein and Koch (2011) revealed that UMSP and electron microscopy facilitated insights into the early stages of decay in untreated wood, and that the structural changes in wood tissues can be followed up with high spatial resolution. Furthermore, FT-IR imaging studies carried out by Fackler et al. (2010) and UMSP studies completed by Rehbein and Koch (2011) found that lignin modification occurs before any mass loss is detectable, and the lignin modification is proven at the outermost part of the S2 layer and the CML. However, visualization of non-enzymatic oxidative degradation at the initial decay stage still remains a major challenge; studies regarding untreated wood are rare (e.g., TEM coupled with immunocytochemistry Kim et al. 2002; Kim et al. 2015) and lacking in FA modified wood. The cellular characteristics of initial degradation of the cell wall structure by brown rot fungi need to be studied further. There are two major reasons for this. Firstly, brown rot fungi are generally considered the most important rot type for wood that is in-service and secondly, the

identification of early stages of decay is the key to successful maintenance of wood structures – increasing the service life of the products and saving costs (Kim et al. 2015). In practice, it would be helpful to have methods and structural features that can detect early signs of degradation.

To close this knowledge gap regarding the visualization of the initial stage of brown rot decay *in situ*, a combination of microscopy and spectroscopy studies should be performed. Studies with LM and UMSP have been performed successfully for hardwoods modified with an N-methylol melamine compound (Kielmann et al. 2013; Mahnert et al. 2013). Infrared and Raman, for instance, have been successfully applied to generate spectra of lignin substructures: coniferyl alcohol, abietin and coniferyl aldehyde (Bock and Gierlinger 2019) or SEM, nanoindentation, and imaging FTIR of surface modification of bamboo with FA by Liu et al. (2020). The suitability of Raman and cellular UV microspectrophotometry (UMSP) have not yet been proven for FA modified and degraded furfurylated wood.

FA modified wood is well established on the market as an environmentally friendly product (Gérardin, 2016 "Swan" ecological label (license number 2086 0001) for the furfurylation process adopted by Kebony ASA in Norway). Nevertheless, the studies by Goldstein and Dreher (1960), Stamm (1977) and Schneider (1995) do not reveal how the enhanced durability properties are exactly achieved. One aspect that could expand our understanding could be answering the question of what role the solvent plays during the furfurylation process regarding from the resulting characteristics (e.g., polymerized FA, filled lumen) of the modified wood. LM studies on the distribution of polymerized FA in wood tissue and assessments on possible differences of the polymerized FA in the cell wall and the lumen have not been carried out so far.

6 Objective and research questions

The main objective of this PhD-thesis was to spectroscopically examine FA modified wood on a (sub)cellular level, aiming for a better understanding of the mode of action of FA modified wood. *In situ* characterization on a cellular level was addressed and initial decay patterns by a brown rot fungus were investigated in a high timely and spatial resolution.

The detailed aims of this thesis were to study the following

1) Is the special cellular UV microspectrophotometry (UMSP) method suitable for investigating FA modified and degraded FA modified wood?

2) Undegraded and degraded FA modified wood by the brown rot fungus *Rhodonia placenta*:
   a. *in situ* characterization with light and electron microscopy to localize the polymerized FA and its distribution in wood tissue, as well as hyphal colonization.
   b. *in situ* characterization with UMSP to localize the polymerized FA, its distribution in the cell wall and to reveal initial decay patterns.
   c. with different wood species, different FA levels (measured as weight percent gain (WPG)) and different treatments.

3) The initial decay pattern of brown rot in FA modified wood:
   a. decay tests under laboratory conditions with different wood species, different FA levels, different treatments and with the brown rot fungus *Rhodonia placenta*.
   b. in combination with a cytochemical method.
   c. mapping out specific structural features characteristic for furfurylated wood during initial decay with spectroscopic methods.

4) Does the solvent, used during the furfurylation process, play a role in the characteristics of the modified wood?

5) The distribution of polymerized FA in the modified cell wall and the possibility of binding to cell wall lignin *in situ*.

7 Publications

7.1 Paper I

Improvement of a method for topochemical investigations of degraded furfurylated wood.

Gabriele Ehmcke, Annica Pilgård, Gerald Koch, Klaus Richter

2016 – International Wood Products Journal – Volume **7**(2) – Pages 96-101

Abstract

With regard to increasing environmental concerns and the finiteness of resources, the improved utilization of biobased resources is necessary and indispensable. As a result, there is an increasing demand for sustainable building materials and for wood protection systems that have no toxic mode of action. Furfurylation is one of the established wood modification techniques on the market with low environmental impact. Furfurylated softwoods and hardwoods are available with the equivalent quality to woods protected by copper, chromium and arsenic (CCA) solutions. However, not all the details of the furfurylation process are well understood. The aim of this study was to improve a method for investigating furfurylated *Pinus radiata*, both in terms of the furfuryl alcohol polymerization process in the wood cell wall and the detection of initial signs of brown rot degradation. It is an established theory today that brown rot degradation starts with lignin modification in the outermost part of the secondary cell wall and the combined middle lamella. Therefore, the established method (UV microspectrophotometry, UMSP) for *in situ* lignin investigation with respect to the lignin distribution and lignin modification was applied and adopted. The adaption to individual thresholds of UV intensities to a min of 1.00% and a max of 67.50% for the investigation of furfurylated wood. FA modified Radiata pine (*P. radiata*), incubated with *Rhodonia placenta* was subjected to the UMSP method. The UMSP area scans enable direct imaging of the lignin distribution and modification within individual cell wall layers. The modified and degraded samples were scanned with monochromatic UV-light at 280 nm. The results showed that USMP is a promising method to study furfurylated wood *in situ* as well as early fungal degradation damage in the cell wall of furfurylated wood. Further topochemical studies of furfurylated wood cell walls, and in particular, studies of FA modified cell wall lignin and initial brown rot decay are needed to expand our knowledge of the furfurylation- and fungal degradation-process on a subcellular level.

Contribution of the authors

For this publication, G. Ehmcke, together with A. Pilgård and G. Koch prepared the test design. G. Ehmcke conducted major parts of the laboratory work, in some cases supported by technical staff and students. In addition, Gabriele Ehmcke carried out all analyses and was responsible for drafting the paper. All co-authors contributed in terms of scientific advice, discussions, critical reading of the manuscript and language editing.

7.2 Paper II

Topochemical analyses of furfuryl alcohol modified radiata pine (*Pinus radiata*) by UMSP, light microscopy and SEM.

Gabriele Ehmcke, Annica Pilgård, Gerald Koch, Klaus Richter

2017 – Holzforschung – Volume 71(10) – Pages 821-831

Abstract

Furfurylation is one of the established wood modification techniques that has been widely investigated throughout the last decades and available on the market. However, it is still not clear how its enhanced durability is exactly achieved and how the FA molecule interacts with the wood cell wall. Furthermore, little is known about the topochemistry of furfurylated wood cell walls. With respect to incipient brown rot degradation, cell wall lignin acts as a natural barrier against fungal degradation processes. Therefore, it is of great interest to topochemically analyze the FA modified cell wall lignin in order to gain information as to what mechanism supports the advanced biodegradation resistance properties of the modified wood to improve wood modification. Furfurylated Radiata pine (*Pinus radiata*), with three different weight percent gains after FA uptake, were observed by cellular ultraviolet microspectrophotometry (UMSP) with the aim of analyzing possible topochemical alterations of the individual cell wall layers. Moreover, light microscopy (LM) and scanning electron microscopy (SEM) analyses supplemented UMSP investigations. Ultraviolet (UV) absorbance at 280 nm of the modified samples increased significantly compared to the untreated wood. That increment indicates a strong polymerization of the aromatic compounds. The highest UV absorbances were found in areas with the highest lignin concentration. The UV absorbance spectra with a spot size of 1 μm^2 in the wavelength range from 240 to 600 nm revealed approximately similar profiles of the polymerized FA in the lumina for all three modification types. The spectra of the strongly modified cell wall layers displayed a bathochromic shift and shoulders with lower intensities of around 320 nm compared to untreated wood. This can be interpreted as the formation of conjugated double bonds. The measurements clearly show that the entire wood cell wall is strongly modified. The UMSP images of the individual cell wall layers of furfurylated Radiata pine *in situ* support the hypothesis concerning condensation reactions between cell wall lignin and FA. The SEM images confirm the UMSP observations and provide detailed information on the cellular distribution of polymerized FA deposits. The polymerized FA is spatially displayed as a compact lumen-filling substance. LM studies revealed differently filled cell types and an uneven distribution of the polymerized FA in wood tissue. A homogenous modification is essential for the resistance of furfurylated wood against biodegradation processes.

Contribution of the authors

For this publication, G. Ehmcke and A. Pilgård developed the test design. G. Ehmcke analyzed the specimens, collected and evaluated the data, compiled the results and drafted the manuscript. The co-authors contributed to the content of the paper with scientific advice, discussions and language for the paper.

7.3 Paper III

Furfurylation result of Pinus Radiata depends on the solvent.

Lisbeth Gabrecht Thygesen, Gabriele Ehmcke, Søren Barsberg, Annica Pilgård
2020 – Wood Science and Technology – Volume 54 – Pages 929–942

Abstract

Furfurylation is a modification technique that improves wood properties in several ways, for instance, with the resistance against biodegradation. Furfuryl alcohol (FA) can be produced from agricultural waste. The wood is first impregnated with FA diluted in a solvent, and afterwards, the impregnated wood is cured, during which time a FA derived polymer is formed within the wood cell wall and, to some extent, within the cell lumina as well. The resulting modified wood does not pose an environmental hazard and can therefore be disposed of like natural wood at the end-of-service-life. In this study, the effect of the solvent used during the impregnation step of the process after the distribution of the FA polymer within the wood structure was investigated for Radiata pine (*Pinus radiata*). The hypothesis was tested to see if the solvent used during the impregnation step of the furfurylation process would play a role in the characteristics of the modified wood. Furthermore, it was assumed that these characteristics would correlate with the differences in marine durability, as previously reported. Radiata pine was subjected to spectroscopic methods: Light microscopy, Infrared spectroscopy and Infrared microspectroscopy and Flourescence spectroscopy. It was found that impregnation carried out using isopropanol, rather than water as solvent, resulted in more filled earlywood tracheid lumina, albeit this result may be confounded by a concomitant difference in weight percent gain. It was assumed that the degree of earlywood lumen filling would affect the durability of furfurylated wood in marine settings via an effect on the hardness on the microscale as perceived by gribble (*Limnoriidae*) and by shipworm (*Teredinidae*) larvae when they settle on wood.

Contribution of the authors

For this publication, L. Thygesen and S. Barsberg developed the test design. L. Thygesen managed the spectroscopy analyzation and G. Ehmcke conducted the light microscopy investigations. In addition, L. Thygesen and S. Barsberg analyzed the data and composed and wrote the paper. The co-authors contributed to the content of the paper with scientific advice, discussions and critical reading of the manuscript.

7.4 Paper IV

Topochemical and light microscopic investigations of non-enzymatic oxidative changes at the initial decay stage of furfuryl alcohol-modified radiata pine (*Pinus radiata*) degraded by the brown rot fungus *Rhodonia placenta.*

Gabriele Ehmcke, Annica Pilgård, Gerald Koch, Klaus Richter

2020 – International Biodeterioration & Biodegradation – Volume 154

Abstract

Brown rot fungi is one of the most common and dangerous house-rot fungus. Brown rot degradation of wood material leads to significant losses in strength and functionality at the initial stages of rot, even before any attack can be recognized. Therefore, a wood protection concept with low environmental impact that meets local requirements in place of application is essential. Wood modified with furfuryl alcohol (FA) can be used as a sustainable solution. Furfurylated wood provides, for instance, enhanced durability properties against biotic degradation, which leads to a prolonged service life. However, not all the details of the furfurylation of the wood cell walls are well understood. Wood has a natural barrier against fungal degradation processes – the cell wall lignin. It is an established theory today that brown rot degradation starts with lignin modification in the non-enzymatic oxidative degradation phase. The aim of this study was to visualize non-enzymatic oxidative degradation damages in furfurylated wood at the initial decay stage of the brown rot fungus *Rhodonia placenta*. A decay test with small wood blocks ($1.5 \times 1.5 \times 5$ mm^3) of untreated and furfurylated Radiata pine (*Pinus radiata*) selected from two different furfurylation processes was performed until the first mass loss occurred. The samples were exposed to the brown rot fungus *R. placenta*, monitored by light microscopy and analyzed topochemically by cellular UV microspectrophotometry (UMSP). The results showed that the FA modification process directly influenced: i) fungal colonization and hyphal growth, ii) spectral UV behavior, and iii) degradation patterns of the entire cell wall layers. For the first time, UMSP area scans and selective line scans of individual cell wall regions provided topochemical insights into oxidative degradation of furfuryl alcohol-modified *P. radiata* at the initial decay stage, visualizing oxidative degradation *in situ*. Knowledge of the initial decay stage of brown rot fungi in FA modified wood compared to untreated wood extends our understanding of the brown rot decay processes of FA modified and untreated wood cell wall compounds.

Contribution of the authors

For this paper, G. Ehmcke, together with A. Pilgård, developed the research idea and the test design. G. Ehmcke prepared the specimen and the decay test with support by technical staff and, in some cases, students. G. Ehmcke did the data analyses as well as the composition and writing of the paper. All co-authors contributed by means of scientific advice, critical reading of the manuscript and language for the paper.

The above listed papers are attached in the appendix.

8 Material and methods

The following methods were carried out at different institutes. If nothing else is stated, the method was carried out at the Chair of Wood Science at the Technical University of Munich, Germany.

8.1 Wood species, wood treatments and fungal strain

In this thesis, two softwood species Radiata pine (*Pinus radiata*), Southern yellow pine [*Pinus caribaea, P. echinata*, *P. elliottii*, *P. palustris* and *P. taeda]*) and one hardwood species (maple [*Acer* spec.]) were furfurylated under different process conditions. Radiata pine and maple were furfurylated at the pilot location by Kebony A/S (Skien, Norway) and distributed to project partners of the research project PolyWood (RCN project no. 219294/O30). The furfurylation processes were based on full cell impregnation with different FA solutions, followed by steam curing and kiln drying. The specific initiators and catalysts used are the property of Kebony AS and are not revealed in this context. This also goes for the details of the impregnation and curing procedures. Water based (process A) and alcohol solutions (process B) were used, both containing FA and standard catalysts. An experimental mix with a water based solution and alternative catalytic chemistry was used in process C. An untreated board matched each modified board used in this project. Southern yellow pine samples were furfurylated in the laboratory at the Norwegian Forest and Landscape Institute (NIBIO) (Ås, Norway), according to Lande et al. (2004) with the exception that the samples were soaked in the modification mixture overnight to ensure good penetration. The resulting weight percent gain (WPG) from the furfurylation processes are summarized in Table 4.

The European strain of *Rhodonia placenta* (former name *Postia placenta,* Paper I) (FPRL 280) was used in all decay tests described in this thesis. *R. placenta* is a well-studied brown rot species and it has previously been used in studies that are suitable for comparing the achieved results (Irbe et al. 2006; Kim et al. 2015; Martinez et al. 2009).

Table 4: Wood material, FA treatment, decay tests and applied analyzing method; Process A: water-based solvent; Process B: alcohol-based solvent (IPA); Process C: experimental mix, water-based solvent and alternative catalytic chemistry

	WPG (%)			*Rhodonia placenta*				
Wood species	**Process A**	**Process B**	**Process C**	**Mini-block test type I**	**Mini-block test type II**	**Cerium chloride test**	**Method**	**Published**
Pinus radiata	/	/	60	Pre-test (Algeier 2014)	/	/	UMSP, LM	Paper I
Pinus radiata	60	70	57	/	/	/	UMSP, SEM, LM, Raman	Paper II, IV, (Wadenspanner 2018)
Pinus radiata	52	67	57	/	/	/	LM, FT-IR, Fluorescence	Paper III
Pinus radiata	52	67	/	X	/	/	UMSP, LM	Paper IV
SYP	91.5	/	/	/	X	X	TEM, EDX	(Ehmcke et al. 2014)
Pinus sylvestris	/	/	/	/	X	X	TEM, EDX	(Ehmcke et al. 2014)

SYP: Southern Yellow Pine (*Pinus caribaea, P. echinata*, *P. elliottii*, *P. palustris* and *P. taeda*)

8.2 Laboratory decay tests

8.2.1 Mini-block test – type I

The decay tests were performed according to the approach of Rehbein and Koch (2011) with adaptions in frequency of harvesting and sample numbers per petri dish as a result of a pre-test (Algeier, 2014). For sample preparation, 10 discs with 5 mm thickness, in the direction of the tracheids, per furfurylated (type A and B) and the corresponding untreated board were processed. Afterwards, small blocks (1.5 x 1.5 x 5 mm³, R x T x L) from the center of the discs, excluding the surface of the boards, were prepared. The criterion for the subsamples was that a growth ring boundary, containing early wood and late wood tissues, had to be included. The benefit of the small sample size, as described by Rehbein and Koch (2011), is that the complete sample can be used for light microscopy and also embedded and prepared for cellular UMSP investigation in contrast to common degradation tests, for example, Bravery (1978) and DIN CEN/TS 15083-1(2005-10), where the samples had to be cut into pieces.
The samples were leached according to EN 84 (1997) and conditioned at 20°C and 65% RH for one week. All samples were sterilized with gamma radiation (>30 kGy). Petri dishes with standard malt agar according to EN 113:1996-11 (4% malt, Merck; and 2% agar, Roth) were prepared. Four samples (two untreated and two furfurylated) were placed in each petri dish, together with four mycelium flakes of *R. placenta* (strain FPRL 280). The transversal sections of each sample were in direct contact with the mycelium flake. The orientation of the samples was documented. In total, 560 FA-modified samples, including samples from process A and B, as well as 560 untreated samples were inoculated. Twelve samples of each treatment and 12 untreated samples were placed in petri dishes without fungi (correction values), respectively. The prepared petri dishes were incubated in a climate chamber (Memmert HPP 749, Germany) at 22 ± 1 °C and 70 ± 1 % RH. The decay test was terminated after 30 days. Two petri dishes (4 samples = mass loss and moisture; 4 samples = UMSP analyses) were harvested per day – and the non-inoculated samples at the end of the decay test. At harvest, the samples were either (1) weighed wet and dried (103°C, 18 h) for calculating mass loss and moisture content or (2) shock frozen in liquid nitrogen and then stored at -20°C, awaiting UMSP and light microscopy analyses.

8.2.2 Mini-block test – type II

The mini-block test (30 x 10 x 5 mm^3) was performed according to Bravery (1978). Southern Yellow Pine (SYP) sapwood samples were leached according to EN 84:1997 and dried to 103 °C. Half of the samples were furfurylated with a water based solution to an average WPG of 91.5% in the laboratory at NIBIO. The furfurylated samples were leached again according to EN 84 (1996) and sterilized with gamma radiation together with the untreated samples. The samples were placed two and two with the same treatment (Junga and Militz 2005) in petri dishes containing sterile soil and inoculated with *R. placenta* (strain FPRL 280) liquid culture. Samples were incubated at 22 ± 1 °C and 70 ± 1% relative humidity (RH) (Memmert HPP 749, Germany) and harvested after defined incubation times. The covering mycelia were

manually removed and the samples were either dried and weighed for mass loss or frozen at 80 °C.

This mini-block test was carried out at the Technical University of Munich by A. Pilgård and R. Ringman in the course of the project "Functional transcriptomics, proteomics and metabolomics of wood degradation: fungal strategies against modified wood" (2016-2019) funded by Formas – The Swedish Research Council for Environment, Agricultural Sciences and Spatial Planning.

8.3 Cytochemical test

The wood material comes from the mini-block test-type II. Untreated samples with a mass loss of 2.6%, 3.2% and furfurylated samples with 2% and 2.1% mass loss were chosen for hydrogen peroxide investigation. All samples were sliced with a razor blade into small sections of about 1 x 1 x 5 mm^3 size. The cerium chloride procedure presented by Kim et al. (2002) was applied to all sample variations with some changes in the procedure. Hand-sectioned wood samples were incubated for 1 hour or 4 hours in a solution of 5 mM $CeCl_3$ in 50 mM Mops at pH 7.2. The initial fixation of the samples were performed by a standard preparation with aldehydes (1.25% glutaraldehyde [GA]/1.25% paraformaldehyde [PA]) for 30 minutes at room temperature as described and followed by 3 washing steps with a sodium cacodylate buffer (pH 7.2). The second fixation and staining procedure was carried out using 1% Osmium tetroxide (OsO_4) in a cacodylate buffer. One series was incubated for 1 hour and another series was incubated for 12 hours. Three washing steps with sodium cacodylate buffer (pH 7.2) followed. The combination of material and cerium chloride procedure is summarized in Table 5.

Table 5: Wood material and treatment combinations (SYP = Southern Yellow Pine; PISY = *Pinus sylvestris*; GA= glutaraldehyde; PA= paraformaldehyde) (Ehmcke et al., 2014)

Material	Treatment									
	Rhodonia placenta		$CeCl_3$				washing	OsO_4		washing
		H_2O_2	0 h	1 h	4 h	GA/PA	steps	1 h	12 h	steps
SYP	X	–	X	X	X	X	X	X	X	X
SYP (FA)	X	–	X	X	X	X	X	X	X	X
PISY	–	X	X	X	X	X	X	X	X	X

Untreated and undegraded *Pinus sylvestris* (PISY) sapwood was also prepared to confirm the cerium chloride reaction as a positive control. The samples were incubated in 0.1% H_2O_2 or 1% H_2O_2 for 30 minutes, and afterwards, transferred into the cerium chloride procedure as described above. Further information can be retrieved from Ehmcke et al. (2014).

8.4 Light microscopy (LM)

To localize FA-impregnated cell elements, as well as filled lumen and hyphal growth, selected samples were analyzed by a conventional transmitted light microscope (Axiophot, Carl Zeiss AG, Oberkochen, Germany) equipped with a digital camera (AxioCam, Carl Zeiss AG, Oberkochen, Germany) combined with AxioVision software (Carl Zeiss AG, Oberkochen, Germany).

Small wood blocks (5 x 5 x 5 mm³, R x T x L), including a growth ring boundary containing early wood and late wood tissue if possible, were prepared. With a conventional sliding microtome (Leica SM 2000 R), microscopically thin transverse sections (18 – 24 µm) were processed for each treatment type and for untreated wood. The surface was moistened with distilled water. For light microscopic examination, an embedding system with Euparal (Carl Roth, Carl Roth GmbH + Co. KG, Karlsruhe, Germany) were chosen. The microscopic analyses and images were carried out with a light microscope (Axiophot, Carl Zeiss AG, Oberkochen, Germany), equipped with a digital camera (AxioCam, Carl Zeiss AG, Oberkochen, Germany) combined with AxioVision software (Carl Zeiss AG, Oberkochen, Germany). (Paper II, III)

Infected small wood blocks (1.5 x 1.5 x 5 mm³, R x T x L) of untreated and furfurylated Radiata pine coming from the mini-block test type I were processed. To analyze hyphal growth inside the harvested samples of untreated and FA-modified wood, A and B exposed to *R. placenta* was investigated by LM. Thin sections of about 15 – 20 µm of radial and tangential surfaces were processed: six sections per anatomical direction and day, respectively. To allow longitudinal sectioning of the small samples with a conventional sliding microtome (Leica SM 2000 R), all samples were glued on a suitable wood block for support. All sections were taken from a 500 µm zone below the surfaces. After sectioning, the thin tissues were stained for 5 minutes with aniline blue (0.1% aniline blue (Merck, VWR) dissolved in 50% lactic acid (Carl Roth GmbH)) to obtain a better contrast of fungal hyphae. Afterwards, the sections were washed in distilled water to clean them from unreacted stain, mounted on microscopic slides and dehydrated with a graded series of ethanol. The untreated samples were double stained with aniline blue and safranin (Merck, VWR). For light microscopic examination, an embedding system with Euparal (Carl Roth) was chosen. Overall, 1,375 sections were prepared. The microscopic analyses were carried out with a Zeiss Axiophot microscope, equipped with a digital camera adapted with an evaluation program (Axiophot). For visual evaluation of hyphae growth, the radial sections provide best insight into the different cell types (early and late wood tracheids, ray parenchyma and radial tracheids). A four-grade scale evaluation, where 0 means no growth and 3 means very abundant growth, was applied. If no hyphae were found in the radial section (grade 0), tangential sections were used instead. (Paper IV)

8.5 Fluorescence spectroscopy

Fluorescence spectroscopy measures transition between electronic states arising from the excitation of molecules by monochromatic light, followed by the detection of light emitted from the fluorophores (Rettig et al. 1999). It is a highly sensitive and non-invasive technique. A broad application field opens up for this technique such as biochemistry, analytical chemistry, food, and environmental science.

Fluorescence spectra are measured as a function of two variables, the excitation and the emission wavelength (Pedersen et al. 2002). The emission wavelength comes from molecules (fluorophores; few molecules exhibit fluorescence) that are going from an excited state to a ground state (Kotwa et al. 2013). Two-dimensional spectra (landscapes), a so-called excitation–emission matrix (EEM) representing intensities of the compounds for certain excitation and emission wavelengths are thereby generated (Kotwa et al. 2013).

With the parallel factor analysis (PARAFAC) (Bro, 1997), it is possible to mathematically explain the physical behavior of low-rank fluorescence data (‘mathematical chromatography’) (Pedersen et al. 2002). The complex fluorescence landscapes can be resolved by PARAFAC into excitation and emission profiles of the underlying fluorophores (Bro, 1997) and thus obtain their relative concentrations as presented for screening for dioxin contamination in fish oil (Pedersen et al. 2002).

In this thesis work a fluorescence landscape was obtained for a sample from a cross section of each treated board (A, B, C) and from six untreated boards using a Fluoromax 4 spectrofluorometer (Horiba Jobin Yvon; Kyoto, Japan). Each landscape spanned 36 excitation wavelengths in a range from 300 to 650 nm with a spacing of 10 nm, and 176 emission wavelengths in a range from 400 to 750 nm with a spacing of 2 nm. The integration time was 0.1 s, and the excitation and emission slits were both set to 1 nm. The landscapes obtained were analysed using parallel factor analysis (PARAFAC) as implemented in the N-way toolbox for Matlab by Rasmus Bro and Claus Andersson (http://www.models.life.ku.dk/nwaytoolbox).

PARAFAC modeling was run without constraints on the loadings. (Paper III)

The fluorescence spectroscopy investigations were carried out at the University of Copenhagen (Denmark), Department of Geosciences and Natural Resource Management by L.G. Thygesen. (Paper III)

8.6 Transmission electron microscopy (TEM)

The principle of the image generation by transmission electron microscope is based on transmission of electrons through an ultra-thin (˜0,1 µm) object in a vacuum environment. Depending on the electron density of the object itself, the structural composition, with a resolution capacity of 0.4 to 0.2 nm, can be revealed. The method is well suited, for example, to analyze individual wood cell wall layers (Liese 1960, 1970) and alterations during decay (Kim et al. 2002; Kim et al. 2015; Goodell et al. 2017).

The samples coming from the cytochemical test (section 8.3.) were subjected to TEM analyzes to detect and localize H_2O_2 during incipient *R. placenta* decay in untreated and furfurylated softwood. The fixation and staining was carried out using 1% Osmium tetroxide (OsO_4) in cacodylate buffer. As an embedding system, London Resin white (LR white) was chosen. The embedding process started with dehydration in a graded series of ethanol with an incubation time of 15 minutes for each level using a rotator. The last dehydrating step with 100 % ethanol was repeated twice, followed by an overnight incubation (12 hours) with a mixture of ethanol and LR white (1:1). The solution was exchanged with pure resin twice and vacuum infiltrated for 15 minutes. Afterwards the samples were embedded in pure resin and filled up in gelatin capsules (size 4, Plano GmbH). The polymerization process was catalyzed by thermal curing at 60 °C for 12 hours.

The samples were sectioned with an ultra-microtome (Ultra-tome nova LKB Bromma) equipped with a diamond knife using a cutting speed of 2 or 1 mm per second. Ultra-thin sections (90-100 nm) were transferred to Formvar (polyvinyl formal) film coated copper or nickel grids (100 mesh) and uncoated nickel grids (300 mesh). The samples were analyzed by TEM (Zeiss EM 10 C) at an acceleration voltage of 60 to 80 kV. Further information on the method is given by Ehmcke et al. (2014).

8.7 Scanning electron microscopy (SEM)

The principle of a scanning electron microscope is based on the interaction of electrons with a scanned surface to obtain information about its topography and chemical composition. A focused electron beam (cathode) emits electrons that are accelerated by electromagnetic conductors in a medium to high vacuum environment. The accelerated electrons penetrate the surface of the scanned object to a depth of a few microns, interact and produce signals – like secondary electrons and x-rays. The produced signals are collected by their corresponding detectors (x-ray-, backscatter electron-, secondary electron detectors) to create 3D images and/or elemental analysis.

Small cubes (1 cm^3) of untreated and furfurylated wood were prepared for SEM analyses. The specimens were boiled in water and then manually cut with a thin razorblade to obtain a plain surface perpendicular to the axial direction. The specimens were stored overnight under a vacuum setting and then sputter-coated by a coating unit (International Scientific Instruments Co, New Delhi, India) with a 10 – 15 nm thin layer of gold to provide conductivity. The SEM

that was used for the investigation of the untreated and furfurylated samples in this case was equipped with a tungsten cathode (EVO 40, 10–12 kV, Carl Zeiss AG, Oberkochen, Germany). (Paper II)

8.8 Cellular UV microspectrophotometry (UMSP)

In this study, untreated and furfurylated wood samples (infected and not infected) were illuminated by UV light. A certain spectral region was used to study lignin and lignin modification *in situ.* The principle of the Universal-Microscope-Spectrophotometer is based on the transmission and interaction of UV light with the sample according to Lambert-Beer's law (Eq. 1). Koch and Grünwald (2004) described the application of UV microscopic point measurements over the last seven decades. Progress in this highly sensitive method of development presents the UV spectrophotometric-scanning-device as described by Koch and Kleist (2001). In the present study, UV microscopic point measurements, as well as area scans, were performed.

The analyzed samples comprised 1 µm thick (*d*) transverse sections of untreated and furfurylated wood cells. According to Lambert-Beer's law,

Equation 1 $$\mathbf{A = \varepsilon \cdot C \cdot d}$$

wherein *A* is the emerging UV light intensity from the cell wall due to the absorbance of lignin. In equation (1), ε is the extinction coefficient, *C* is the volume concentration and *d* is the thickness of the absorbing layer. According to Koch and Grünwald (2004), the incident UV light intensity I_0 is measured by passing through the embedding medium in the cell lumen, resulting in the intensity emerging from the lumen (I_{lumen}). In case of the analyzed wood sections, I_{lumen} is reduced to the intensity of the cell wall ($I_{cell\ wall}$) and equation (1) can be expressed as

Equation 2 $$\mathbf{A = \log(I_{lumen}/I_{cell\ wall})}$$

For determining the lignin concentration in wood cell walls, the typical maximum UV absorbance of lignin (A_{max}) in the range of λ270 − 280 nm is used as stimulation wavelength (Musha and Goring 1975). The wood samples were scanned with a defined wavelength of λ280 nm for softwood and λ278 nm for hardwood, respectively. The scan program Automatic Photometric Analysis of Microscopic Objects by Scanning (APAMOS, Carl Zeiss AG, Oberkochen, Germany) digitizes square fields of a local geometrical resolution of 0.25 µm × 0.25µm and a photometrical resolution of 4,096 grayscale levels. To visualize the absorbance intensities, the grayscale levels were converted into 14 basic colors, as described by Koch and Kleist (2001). The scans can be depicted as two-dimensional (2D) or three-dimensional (3D) image profiles, and a statistical data evaluation results in a semi-quantitative lignin distribution.

The infected and uninfected samples coming from the pre-test (Algeier 2014) and the mini-block test type I (section 8.2.) were fixed in a glutaraldehyde solution (Karnovsky, 1965) and dehydrated in a graded series of ethanol or acetone. After dehydration, the samples were embedded in Spurr's (1969) epoxy resin under mild vacuum conditions. Thermal curing at 70°C for 12 hrs. catalyzed the polymerization process. For the infected samples, the cross sections, which were first colonized by the fungus, were used for sectioning. In the first step, the samples were trimmed with a razor blade to provide a trapezoid area of approximately 0.5 mm² and sectioned with an ultra-microtome (Reichert-Jung) equipped with a diamond knife. The semi-thin sections (1 µm) were transferred to quartz microscopic slides and then thermally fixed. At the same time, cross sections were also taken for light microscopy analyses. These sections were transferred to common microscopic slides, stained with toluidine blue and then thermally fixed, as well.

The sections for UMSP analyses were immersed in a drop of non-UV absorbing glycerine (glycerine/water mixture nD = 1.46) and covered with a quartz cover slip. As reference, non-degraded untreated samples were also prepared, following the same embedding process.

The sections were placed in a Zeiss UMSP 80 (Carl Zeiss AG, Oberkochen, Germany) equipped with a scanning stage. For control purposes, the lignin distribution within individual cell types and cell wall layers of untreated wood specimens were scanned.

For the topochemical analyses areas with microscopic intact cell walls, respective parts of the cell wall were selected. Wood cell walls of untreated and furfurylated wood were scanned, as well as cell lumens, and were filled with polymerized FA. For the infected samples by *R. placenta*, 10 measurements of individual cell wall layers per incubation day were scanned for semi-quantitative studies. If procurable (quality of the ultra-thin slices), two image profiles per area of interest were carried out: i) filled lumen cells, ii) intact tracheid cells, iii) cell walls with radial oriented compound middle lamella (CML).

Initial degradation stages and cell wall modifications were topochemically monitored by UMSP. To follow topochemical changes on the individual cell wall level of untreated and furfurylated wood exposed to *R. placenta*, the raw data (Intensity values) of the obtained 2D image profiles were analyzed in a standardized procedure following a defined line profile from the middle lamella cell corner (MLcc) via the corner cell wall to the cell lumen (Figure 1, Paper IV). With the scan program APAMOS, line profiles can only be generated in the direction of the x- and y-axes. However, for this study, a diagonal line profile was necessary. For this purpose, the raw data of one representative area scan per incubation day was transferred into MS Excel data and converted to absorbance values (A) based on equation 2.

MS excel was used to generate greyscale images of the scanned areas to obtain 2D images again. Origination from the highest absorption value in the MLcc, square fields of 36 x 36, were selected and a diagonal line (36 measuring points with a geometrical resolution of 0.25 x 0.25 µm^2 per pixel, 9 µm length) was displayed as a line profile. This special approach intuitively visualizes the local lignin concentration (measured at the absorbance maximum of λ280 nm) and the chemical cell wall modification from MLcc via corner cell wall to the cell lumen in the incipient decay stages. (Paper IV)

In addition, uninfected furfurylated wood samples were subjected to photometric point measurements with defined polychromatic light. A TIDAS MSP 800 microscope spectrometer (J&M Analytik AG, Esslingen, Germany) equipped with TIDAS-DAQ software was used. The principle of this technique is based on the transmission of semi-thin transverse sections by light with varying wavelengths. The spectrometer (CCD-MCS UVNIR) divides the light into separate wavelengths between λ190 - 1010 nm. Depending on the equipped microscope (Zeiss Axio Imager.D1m), a range of between λ240 - 900 nm can be used. In this case, the UV spectra of individual cell wall layers and FA-polymerized deposits in the lumen were recorded with a 40x object lens in a range between λ240 nm and λ600 nm and statistically evaluated. A spot size of 1 μm^2 was used and the transmitted wavelengths were detected by a Diode-Array detector. (Paper II)

All UMSP investigations were conducted by the author at the Thünen Institute of Wood Research, Germany.

8.9 Raman spectroscopy

The Raman spectroscopy technique is a non-destructive technique that is based on light scattering effects to determine molecular vibrations and thereby provides information about the chemical structure of the analyzed material. Monochromatic light from a high intensity laser source interacts with the chemical bonds within the sample (Göpel and Ziegler 1994). A shift in energy from that of the exciting radiation is defined as Raman scattering and should be referred to as Δcm^{-1}, but it is often expressed simply as cm^{-1} (Smith and Dent 2005). Most of the light merely transmits the specimen without any interactions or is scattered elastically without change of frequency (Rayleight scattering) and does not provide any useful information. Only a small amount (10^{-8}) is scattered inelastically (stokes scattering) or hyper-elastically (anti-stokes scattering) at different wavelengths (change of frequency), compared to the laser light source. This is called Raman scattering (Long 2002; Müller et al. 2003; Hesse et al. 2016). This is in accordance with the involved symmetric molecular vibration. For vibration stimulation, the alteration of the deformability of the electron cloud (polarizability α) in a chemical bond is required. Together with the correlating induced dipole moment μ and the field strength E of the light wave, a linear equation can be derived (Equation 3, Hesse et al. 2016) as

Equation 3 $$\mu(t) = \alpha\, E(t)$$

The obtained Raman spectrum shows the intensity and wavelength position of the scattered light. Furthermore, it is subject to a strong re-adsorption and intense fluorescence background radiation. Nevertheless, a number of valuable peaks can be detected (Müller et al. 2003).

Each peak corresponds to a specific molecular bond vibration that can result from systems which involve individual bonds, double bonds or groups of bonds, such as aromatic

compounds (Smith and Dent 2005) like lignin (Bock and Gierlinger 2019). This technique allows the linking of anatomical and chemical information.

Wadenspanner (2018) performed Raman investigations in the context of the elaboration of a master thesis. The measurements were carried out at Fraunhofer IVV (Freising, Germany) using the Raman Microscope Alpha 500 (WITec, Ulm, Germany). Uninfected wood blocks (10 x 10 x 10 mm³, R x T x L) of furfurylated Radiata pine from process A, B and C and untreated Radiata pine were investigated. For more detailed information about the sample preparation and the performed method, see Wadenspanner (2018).

8.10 Infrared spectroscopy and microspectroscopy

Compared to the Raman measurements, the infrared (IR) method uses the direct absorbance of the IR spectrum coming from the induced molecular vibrations described by the wave number $\tilde{\nu}$ (cm^{-1}) and the reciprocal wavelength λ (Hecht 2019). The IR radiation transmits the sample or is reflected using a special reflectance setup (attenuated total reflection [ATR] crystal) and the time depending intensities (interferogram) are recorded (Fox 2016). The interferogram is then converted by the Fourier transformation to a frequency depending spectra (Fox 2016). The detected absorbance bands are in a range of 4,000 – 400 cm^{-1} and display the functional group of a molecule that can be identified by comparing the bands with more than 100,000 published IR spectra (Fox 2016).

The Fourier transformed infrared (FT-IR) measurements were performed using a Nicolet 6700 FT-IR spectrometer (Thermo Scientific, Waltham, MA, USA) equipped with a deuterated triglycine sulfate (DTGS) detector and, additionally, a Perkin-Elmer Spectrum Spotlight 400 FT-IR microscope equipped with a mercury cadmium telluride (MCT) detector.

A Pike Technologies GladiATR diamond with a working temperature of 25 °C was used in combination with the Nicolet 6700 FT-IR spectrometer and a spectral resolution of 4.0 cm^{-1}. Small specimens of untreated and furfurylated wood with a thickness of about 0.5-1 mm and an area of approximately 5 x 5 mm² from the center parts of the boards (i.e., not the surfaces) were examined. The obtained spectra (using 64 scans per spectrum and 128 for the background) was recorded in a range between 4,000–600 cm^{-1}. The spectra were corrected via standard normal variate (SNV) (Barnes et al. 1989).

Additionally, IR microspectroscopy was used with a spectral range of 4,000-720 cm^{-1} and a spectral resolution of 8 cm^{-1}. The spectra were obtained using a Germanium (Ge) tip ATR add-on and each spectrum corresponded to an area of 1.56 µm x 1.56 µm. The Ge crystal was pressed against the sample surface and took 16 scans per spectrum. The background spectra were obtained in ambient air.

L.G. Thygesen carried out the infrared spectroscopy investigations at the University of Copenhagen (Denmark), Department of Geosciences and Natural Resource Management. (Paper III)

9 Results and discussion

The aim of this thesis was to topochemically reveal the mode of action of wood modified with FA and its biological initial degradation.

9.1 Studies on the suitability of a cellular UV microspectrophotometry (UMSP) method for analyzing FA modified and degraded FA modified wood

The cellular UV microspectrophotometry (UMSP) method was selected as a method to search for possible reactions of FA and cell wall lignin. This method enables direct imaging of the lignin distribution and lignin modification within individual cell wall layers. To investigate if this method was appropriate to use to investigate FA modified wood, decayed samples, analyzed in a decay test performed within a Master thesis (Algeier 2014), were processed and investigated preliminarily. It was shown that the standard settings for untreated softwood (thresholds at a min. of 10.00% and a max. of 80.00%) where not useful for image generation of furfurylated softwood. The thresholds of the UV intensities had to be adapted to a min. of 1.00% and a max. of 67.50%, for suitable image generation (Paper I). Furthermore, the results revealed changes in the UV absorbance values for non-degraded and degraded furfurylated wood. The furfurylated and colonized samples showed significantly lower UV absorbance values compared to the non-decayed control (Figure 3, Paper I). The initial absorbance values at 280 nm are 1.35 for S3; for the values of around 1.6 for CC and for the S2 layers, the initial absorbance values are in a range of 1.09-1.48. The absorbance values at 280 nm shifted to 0.56-0.82 for the S2 layer with a locally inhomogeneous pattern of lower intensities. The signals of the CML are partly undistinguishable from the S2 layer, and some small regions still absorb UV in the range of 0.82-0.95. The UV absorbance values of the CC distinctively changed from abs280 nm 1.48 to abs280 nm 1.09. This decrease in absorbance most likely originates from early fungal degradation processes (Rehbein and Koch 2011), wherein highly reactive hydroxyl radicals, produced in the non-enzymatic part of the chelator mediated Fenton degradation (Goodell et al. 1997; Hammel et al. 2002; Arantes et al. 2012), attack lignin. The absorbance values of the polymerized FA in the cell lumen changed after decay (Figure 2b, Paper I), as well. That lead to the assumption that *R. placenta*, besides lignin, also attacks polymerized FA deposits in the cell lumens.

The results showed that USMP, after adaptation of the UV intensity thresholds, is a promising method to study furfurylated wood and early fungal degradation damage in the cell walls of furfurylated wood.

9.2 *In situ* characterization of furfurylated wood that is undegraded and degraded by *R. placenta*

9.2.1 Undegraded samples

The polymerized FA in the impregnated wood tissue, the ratio of filled and empty lumens and the spatial distribution within the wood tissue were investigated. Therefore, furfurylated Radiata pine (*Pinus radiata*) and furfurylated maple (*Acer* sp.) with three different weight percent gains, after FA uptake under different process conditions (Table 3), were investigated by LM and SEM.

Table 6: Experimental formulations and procedures used for the preparation of furfurylated samples with their corresponding abbreviations.

FA solutions	WPG% Maple	WPG% Radiata pine	Vacuum step during curing	Abbreviations
water-based solvent	32	60	NO	A
alcohol-based solvent (IPA)	37	70	YES	B
experimental mix, water-based solvent and alternative catalytic chemistry	2 7	57	YES	C

9.2.1.1 Light microscopy and SEM analyses

After the modification process with FA, the furfurylated wood appears dark brown, independent of the species, and comparable with tropical hardwood. The texture and the anatomical features of the modified softwood or hardwood are still visible according to the cutting direction and surface finishing. The LM micrographs give insight into the cellular deposition of polymerized FA in the wood tissues. The spatial distribution can be followed in the three-dimensional SEM images. Figure 6 (Paper II) and Figure 5 present the light microscopic observations of untreated and furfurylated Radiata pine and maple, respectively. Microscopic sections of treatments A, B and C were processed for histologic analyses of the three anatomical directions (transverse, radial and tangential). The cross and radial sections include earlywood (EW) and latewood (LW).

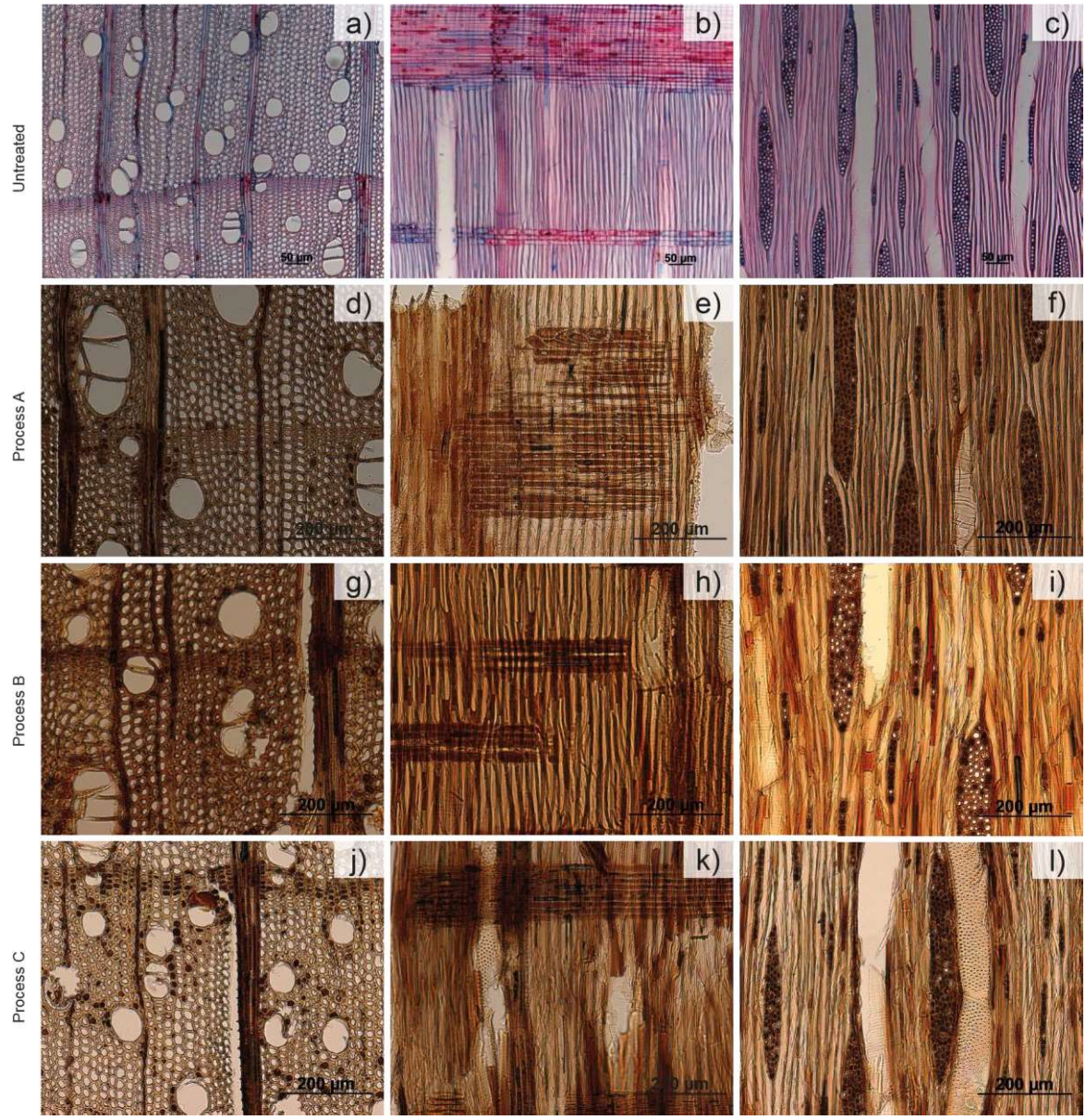

Figure 5: Light microscopic images of maple (processes A, B and C) in three anatomical directions (transverse, radial, tangential). 5a – c show untreated maple sections, stained with safranin and anelin blue.

LM of furfurylated Radiata pine (excluding samples from the experimental mix) allowed quantifying the number of tracheids with lumina filled with FA polymer vs. the number of tracheids without any visible filling (Table 7). In this section, the abbreviations for the treatments (A for water-based and C for alcohol-based solvent) changed due to the published Paper III.

Table 7: Number of filled and empty tracheids in earlywood and latewood counted in LM images of furfurylated wood using either water or IPA as a solvent (Paper III, Table 2)

Image no.	Treatment	Latewood tracheids				Earlywood tracheids			
		Empty	Filled	Sum	% Filled	Empty	Filled	Sum	% Filled
1	C	542	0	542	0.0	1457	554	2011	27.5
2	C					646	228	874	26.1
3	C					279	71	350	20.3
4	C	2362	8	2370	0.3	311	68	379	17.9
5	C	1187	9	1196	0.8	645	197	842	23.4
6	C					765	310	1075	28.8
7	C	1623	23	1646	1.4	746	260	1006	25.8
Total	C	**5714**	**40**	**5754**	**0.7**	**4849**	**1688**	**6537**	**25.8**
STD	C	*662*	*8*	*666*	*0.5*	*361*	*153*	*514*	*3.7*
1	A	1547	222	1769	14.4	672	126	798	15.8
2	A	2009	271	2280	13.5	262	39	301	13.0
3	A	599	107	706	17.9	397	48	445	10.8
4	A	2428	327	2755	13.5				
5	A					1023	81	1104	7.3
6	A					868	153	1021	15.0
7	A	2193	272	2465	12.4				
8	A	1487	200	1687	13.4	160	86	246	35.0
9	A					909	77	986	7.8
10	A					440	23	463	5.0
11	A	2132	288	2420	13.5				
Total	A	**12395**	**1687**	**14082**	**13.6**	**4731**	**633**	**5364**	**11.8**
STD	A	*574*	*67*	*640*	*1.6*	*301*	*41*	*323*	*8.8*

All images from each of the two types are from a single sample. The mean filled lumina percentage was significantly different (t test) on the 5% level between the earlywood of the specimens from treatments A and C, and on the 1%o level for the latewood.

The results show that there was a significant difference between the analyzed treatments. The samples treated with a water based FA solution from type A had, on average, 12% filled tracheids in both EW and LW. Compared to the samples from the process with isopropyl alcohol (IPA) as a solvent, with higher loading (70% WPG) compared to process A, next to no filled tracheids were counted in the LW, while, on average, 26% of the earlywood tracheids were filled. We assume that a certain amount of FA penetrated the cell wall of LW before polymerization sets during curing. Falco et al. (2018a) found that the use of IPA delays the onset of polymer formation during curing. That could explain the differences in filled lumen found between impregnation in water compared to IPA as a solvent, if the findings of Falco et al. (2018a) are transferred to FA modification of wood. A morphological aspect to be

considered is that, due to a larger amount of non-aspirated bordered pits in the LW, unpolymerized FA was transported out of the LW lumina together with IPA during the vacuum drying step. This phenomenon was not observed for the EW lumina. It is well-known that bordered pits aspirate more often in coniferous EW than in LW during drying (Liese and Bauch, 1967; Siau 1984). One explanation by Lehringer et al. (2009) is that, due to the morphology of the bordered pits in the LW, the deflection and adhesion is hindered because this process needed greater forces than in EW, and therefore, fewer pits in the LW are aspirated during drying. The analyzed transverse sections of furfurylated maple only show a few filled cell lumen – mainly in the parenchyma cells of the ground tissue. That can be observed for all three treatments, with an accumulation at the annual ring boundary for the samples that were furfurylated with an experimental water based solvent (Figure 5). The tangential sections revealed the filled lumens of the parenchyma cells of the wood rays. That can be explained by the accessibility of the parenchyma cells, as the treating solutions have the same pathways as the sap in the living tree (Siau 1984). In their permeability experiment with a tropical hardwood species (*Tectona grandis*), Ahmed and Chun (2011) found that the arrangement of pitted ray cells facilitates the efficient liquid flow in radial direction. In particular, the radial flow will be easier when the end and lateral wall pit number is numerous with a large diameter at the end wall. Whereas almost all parenchyma cells of the wood rays of the samples furfurylated with the water based solvent were filled, approximately half of the cells of the samples from the process with IPA as the solvent were filled (Figure 5c,f,i). As for furfurylated Radiata pine with IPA, the unpolymerized FA was also transported out of the lumina – in this case, the ray parenchyma cell – before polymerization sets in. However, there is a striking difference regarding the wood ray cell of the analyzed furfurylated maple samples compared to furfurylated Radiata pine. The latter revealed that the polymerized FA was accessorily deposited in the ray tracheids (Figure 6e, h, k, Paper II). One reason for this could be that the FA solution enters the ray tracheids predominantly via the large connecting pits of the EW tracheids, which, however, does not correspond to the studies made by Wardrop and Davies (1961) that showed an apparently selective penetration of ray parenchyma and less intensively penetrated ray tracheids of Radiata pine.

The variability in filled cell lumens in the axial and radial directions supports the findings of Lande et al. (2010) and Zimmer et al. (2014), manifesting the varying permeability found in Scots pine sapwood. This also seems to apply for Radiata pine sapwood. Aspirated tracheid bordered pits are assumed to function as physical barriers in case of impregnation (Stamm 1967; Zimmer et al. 2014). No matter which mechanisms were responsible for the final distribution of FA polymer resulting from the use of the two different solvents, the light microscopy based quantification indicated a marked difference in the location of the FA polymer between the water based and IPA treatments for both Radiata pine and maple.

The SEM images of furfurylated Radiata pine (Figure 7, Paper II) provide more spatial information on the cellular distribution of polymerized FA deposits. The polymerized FA is displayed as a compact lumen-filling substance. There are no obvious signs of separation between the bulk polymer and the cell wall that are visible, despite the forces acted upon the compound during surface preparation by hand with a razorblade. We suggest that the deposits are tightly attached to the S3 layers of the tracheids. As already observed under LM, the cell lumen of the ray parenchyma cells appear to be empty.

9.2.1.2 Topochemical characterization

The catalytic polymerization of the monomeric FA in the impregnated cell wall, the reactions between FA and lignin and chemical alterations of the individual cell wall layers were investigated. Therefore, furfurylated Radiata pine (*Pinus radiata*) and furfurylated maple (*Acer* sp.) with three different weight percentage gains after FA uptake under different process conditions (section 8.1, Table 4) were investigated by UMSP.

Furfurylated Radiata pine at 280 nm

Representative UV microscopic scanning profiles of untreated and furfurylated Radiata pine (type A 60% WPG) are presented in Figure 1 (Paper II). The colored pixels mark the absorbance intensities at λ280 nm. The data of each UV profile are statistically evaluated from their corresponding histogram. The high resolution (0.25 µm² per pixel) enables a detailed differentiation of the UV absorbance within the individual cell wall layers (Koch et al. 2003). In addition to the standard 2D UV micrograph, a selective line scan of an individual cell wall region intuitively visualizes the local lignin concentration and the chemical cell wall modification. For spatial illustration, the scanned area is also presented as a 3D image profile.

The lignin distribution via wood cell walls in general, except for the reaction of wood tissue, decreases from the CML and the CC with the highest concentration, in relation to the cell wall layer, to cell lumen (Fergus et al. 1969). In accordance with that, the highest absorbance values for untreated wood were recorded in the area of the CML and the CC (Figure 1a, Paper II) as previously described for softwood and hardwood species (Koch and Kleist 2001; Koch and Grünwald 2004), as well as for thermally (Fergus et al. 1969) and hydrothermally modified wood (Andersons et al. 2016). The broad S2 layer occurred with slightly varying values as previously described by Takabe (2002).

The scanned areas of type A showed the typical lignin distribution with a similar spectral behavior like that of untreated wood, with the difference that the entire cell wall of type A is displayed by significantly higher absorbance values. This shift was also detected in a pre-test for degraded furfurylated wood (Paper I). With reference to fluorescence studies by Thygesen et al. (2010), UMSP indicates a concentration decrement of polymerized FA from the CML to the S2 layer. This can be explained by the early observations of Wardrop and Davies (1961) that aspirated bordered pits lead directly to the CML and serve as entrance openings during impregnation of the cell wall.

The line scans in Figure 1 (Paper II) visualize the CML as a peak that is flanked by the S2 layers presented as broad plateaus of high UV intensities for furfurylated wood. Compared to untreated samples (Figure 1a, Paper II) and all other furfurylated materials (Figures 1b, 2 and 3, Paper II), the wood tissue of type A (Figure 1b, Paper II) shows the highest absorbance values with a clear shift to green, yellow and gray pixels (A280 nm 1.22–1.74).

The mean UV absorbance values did not increase proportionally to the loadings (i.e., to the WPGs) of the analyzed samples. The highest loading was generated by process B with 70% WPG, representing the lowest $A_{280\,nm}$ with 1.07, compared to process A with $A_{280\,nm}$ 1.16 and C with $A_{280\,nm}$ 1.09, but these differences are not significant (Table 1, Paper II).

Furfurylated Maple at 278 nm

The following representative UV microscopic scanning profiles of untreated and furfurylated maple were taken at λ278 nm, the A_{max} of hardwood lignin (Figure 6). The standard 2D UV micrographs are additionally displayed as a 3D image profile with selective line scans of an individual cell wall region that facilitates the high spatial resolution.

The untreated maple sections showing typical lignin distribution in fiber cell walls with the highest absorbance values in the cell corner (CC [↑]) and in the area of the compound middle lamella (CML, Figure 6a). Furfurylated maple fibre tissue from process A (Figure 7b) show a higher absorption compared to the untreated maple (6a) with a shift to red color and a clear reduction of blue pixel. Furfurylated maple fiber tissue form process B (Figure 6c) close to a vessel reveal a further increase in absorbance for all cell wall layers, dominated by purple colored pixels marking the S2 layer. The cell corners and compound middle lamella are pronounced and are depicted with a bluish green to yellow color.

Figure 6d shows the UV scanning profile of furfurylated maple from process C. The wood tissue surrounding a vessel showing the highest absorption level compared to the untreated samples and the two other FA modified samples. The absorbance intensity increases from the cell lumen (dark blue to purple) to the S2 layer (bluish green) and reaches the highest intensity in the CML and the CC (green, yellow to grey). A deposit of FA polymer was detected by an overflow signal [↑] in fibre cell lumen.

The UV profiles of all treatments reveal significantly higher UV-absorption within the entire cell wall, which correlates with the lignin distribution. The results show that the absorbance intensity does not depend on the loading (WPG) of the treated sample, but rather on the modification process/lignin modification/polymerization process.

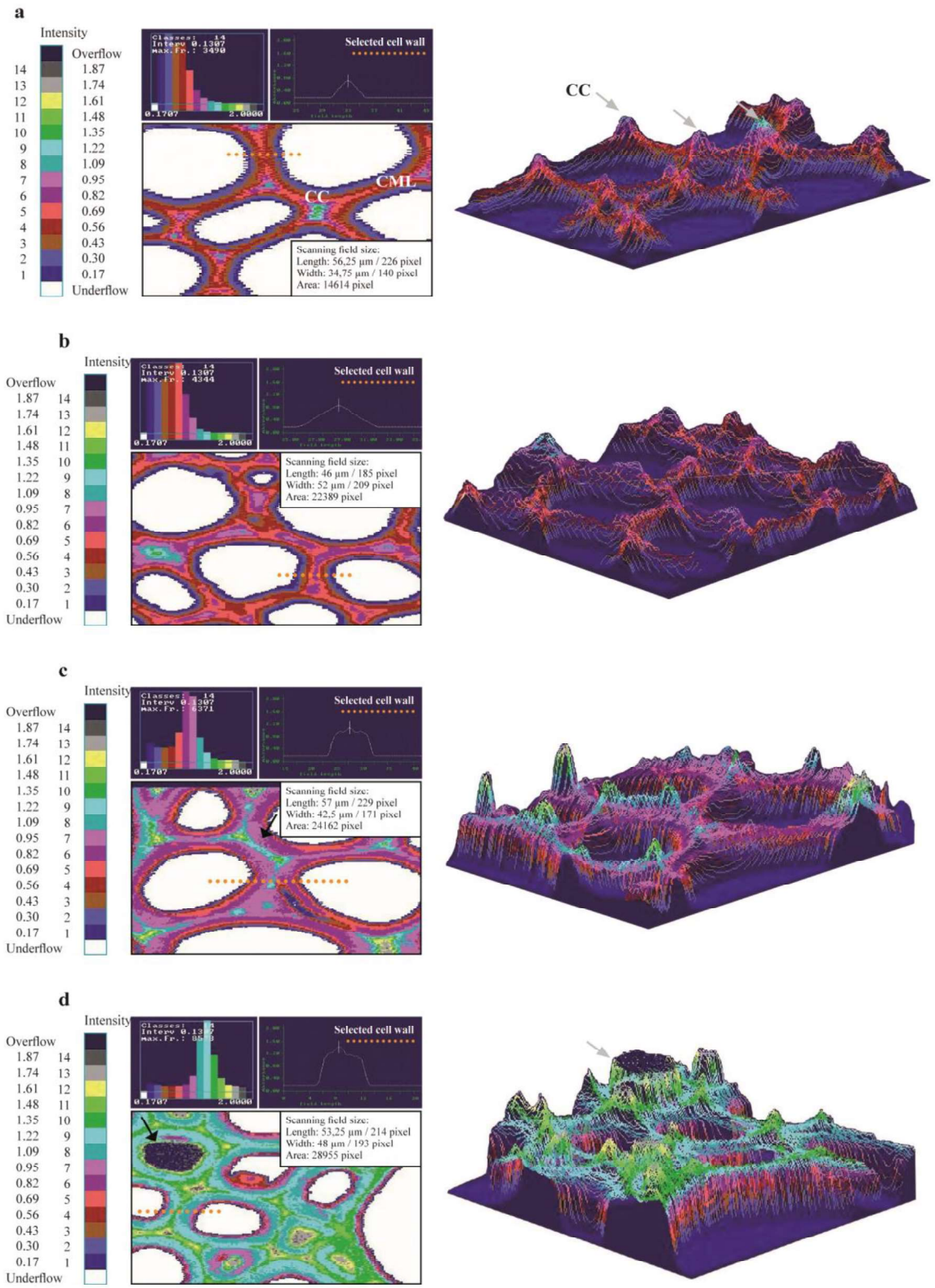

Figure 6: Representative UV microscopic scanning profiles (area, 3D and line scan) of maple and modified maple with statistical evaluation (histogram). The thresholds have been adapted (min. 1.00%; max. 67.50%) for all samples. The colored pixels mark the absorbance intensity at λ278 nm.

The wooden tissue of untreated maple is characterized by lower UV absorbance values compared to untreated Radiata pine (Figure 1a, Paper II). The detected differences in absorbance values of softwood and hardwood reflect those described by Koch and Grünwald (2004) for spruce (*Picea abies*) and beech (*Fagus sylvatica*). The furfurylated sample from process A revealed only slightly increasing absorbance values compared to the untreated sample (Figure 7b). The absorbance intensities increase in type A < type B < type C, but not proportionally to the loadings (i.e., to the WPGs) of the analyzed samples, as in the case of the analyzed furfurylated Radiata pine. The highest mean $A_{278\ nm}$ with 1.03 was recorded for process C, compared to process A with $A_{278\ nm}$ 0.69 and B with $A_{278\ nm}$ 0.72 (Table 7).

Table 8: Mean UV absorbance of untreated and furfurylated maple and maximum UV absorbance values (A_{max}) of polymerized deposits in the cell lumen.

Process	WPG (%)	UMSP-scanning profiles maple			UV-Abs. spectra[a]		
		$A_{278\ nm}$	STD	(pixel)[b]	λ (nm)	A_{max}	STD
Untr.	0	0.52	0.07	16581	-	-	-
Process A	32	0.69	0.11	29825	280	1.11	0.04
Process B	37	0.72	0.05	27853	280	1.14	0.07
Process C	27	1.03	0.07	27894	280	1.19	0.06

[a]Lumen filled with FA, [b]Field size.

UV absorption spectra (240 – 600 nm) of furfurylated wood

To study the spectral behavior of furfurylated wood, UV spectra of polymerized FA in the cell lumen, the S2 layers of fibers and vessels, or tracheids, as well as the CML and CC were recorded. The wavelength was adjusted in a range from 250 to 600 nm for both species – Radiata pine and maple.

The spectral characteristics of the polymerized FA deposits in the cell lumen of furfurylated tissues are shown in Figure 7. The UV spectra of the FA deposits from all three modification processes show approximately similar profiles. Common to all three modifications are (i) the high absorbance intensities, (ii) a distinct shoulder in the wavelength range between λ340 nm and λ380 nm and (iii) certain absorbance levels in the visible light range resulting from large chromophoric structures that were formed during the furfurylation processes.

The absorption maxima of the FA deposits in the cell lumen occurred at around λ278 nm for Radiata pine, except for treatment B, and at λ280 nm for maple (Table 7). These results are in accordance with the findings of Ünver and Öktem (2013) and Gandini and Belgacem (1997), who studied the photopolymerization and photocross-linking of simple furans and F with comparable peaks at around λ270 nm. The A_{max} of the polymerized FA in the tracheid lumen of the IPA treated samples was less pronounced and shifted hypsochromically (Nic et al. 2014) to λ256 nm (Figure 7). This phenomenon was not observed for the analyzed FA deposits in maple wood tissue.

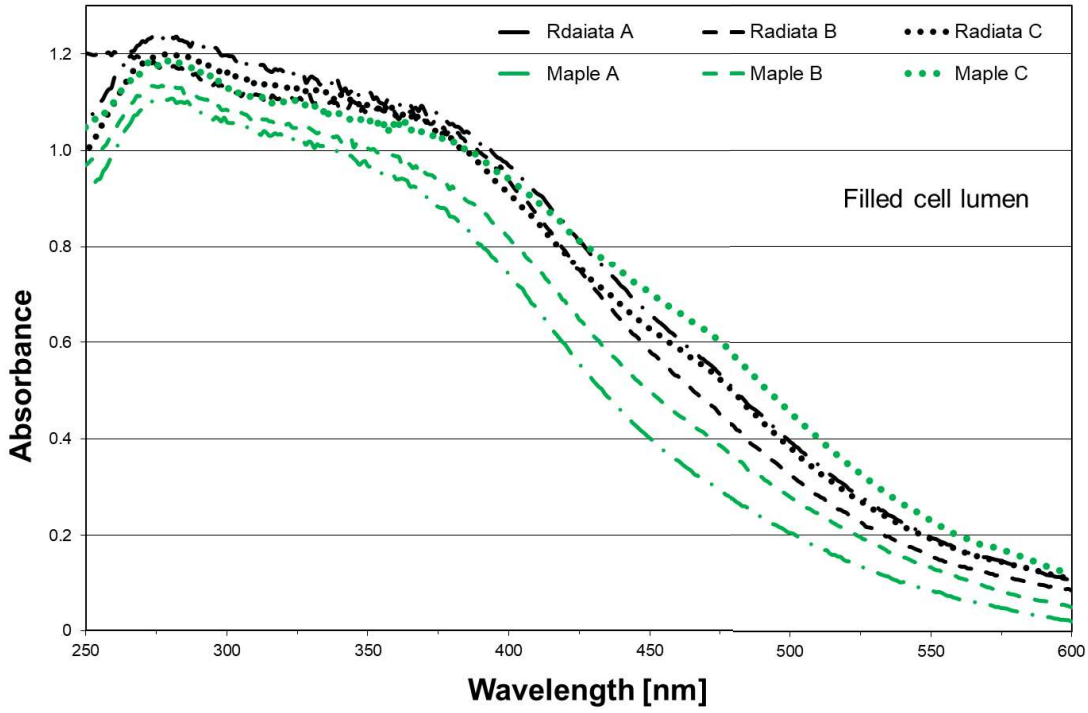

Figure 7: UV absorbance values of polymerized FA deposits in the cell lumen of Radiata pine and maple in a range between 450 and 600 nm.

Comparing the spectra within each process type, the absorbance values of polymerized FA Radiata pine are higher than the recorded values for maple of process A and B. The absorbance spectra of process C behaved differently. In a range between 262 nm and 382 nm, the values for maple were lower than for Radiata and changed at 383 nm – into slightly higher values. Overall, both spectra of process C tend to proceed together more than the spectra of processes A and B (Figure 7). The differences within the spectra of each process type could be due to extrapolation or evaporation of more volatile wood components. This could mean that the wood species was influenced in a certain process in A and B, whereas process C probably showed no reaction with the modified wood species itself.

The spectral characteristics of the individual cell wall layers of untreated (black line) and furfurylated wood are presented in Figures 8, 9 and 10. The cell wall layers (S2, CML and CC) of untreated wood show the typical UV spectra of lignified softwood tracheids (Figure 8) and hardwood cells (Figure 9). The characteristic Amax at λ280 nm for softwood is attributed to the strongly absorbing guaiacyl-type units, whereas the Amax between λ270-280 nm is attributed to hardwood lignin. The hardwood lignin consists of a varying amount of guaiacyl- and syringyl-type moieties with a less distinct absorbance maximum (Fergus and Goring 1970b, 1970a; Musha and Goring 1975; Takabe et al. 1992). The ratios of these monomers vary between individual cell types and cell wall layers and show lower UV absorbance at an increasing OCH_3/C_9 ratio (Musha and Goring 1975).

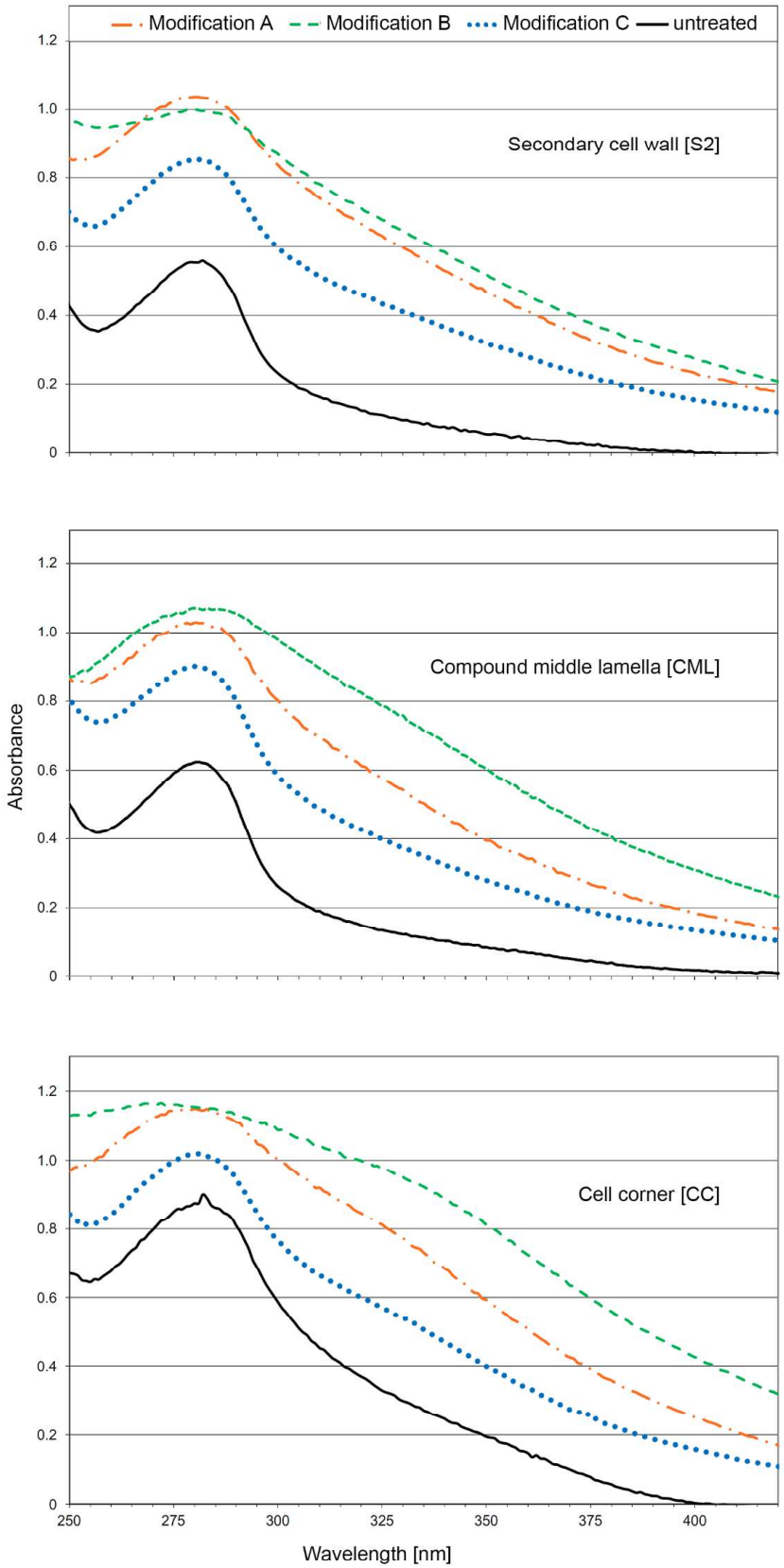

Figure 8: UV absorbance spectra in a range between λ240 and λ600 nm of untreated and furfurylated Radiata pine cell wall layers.

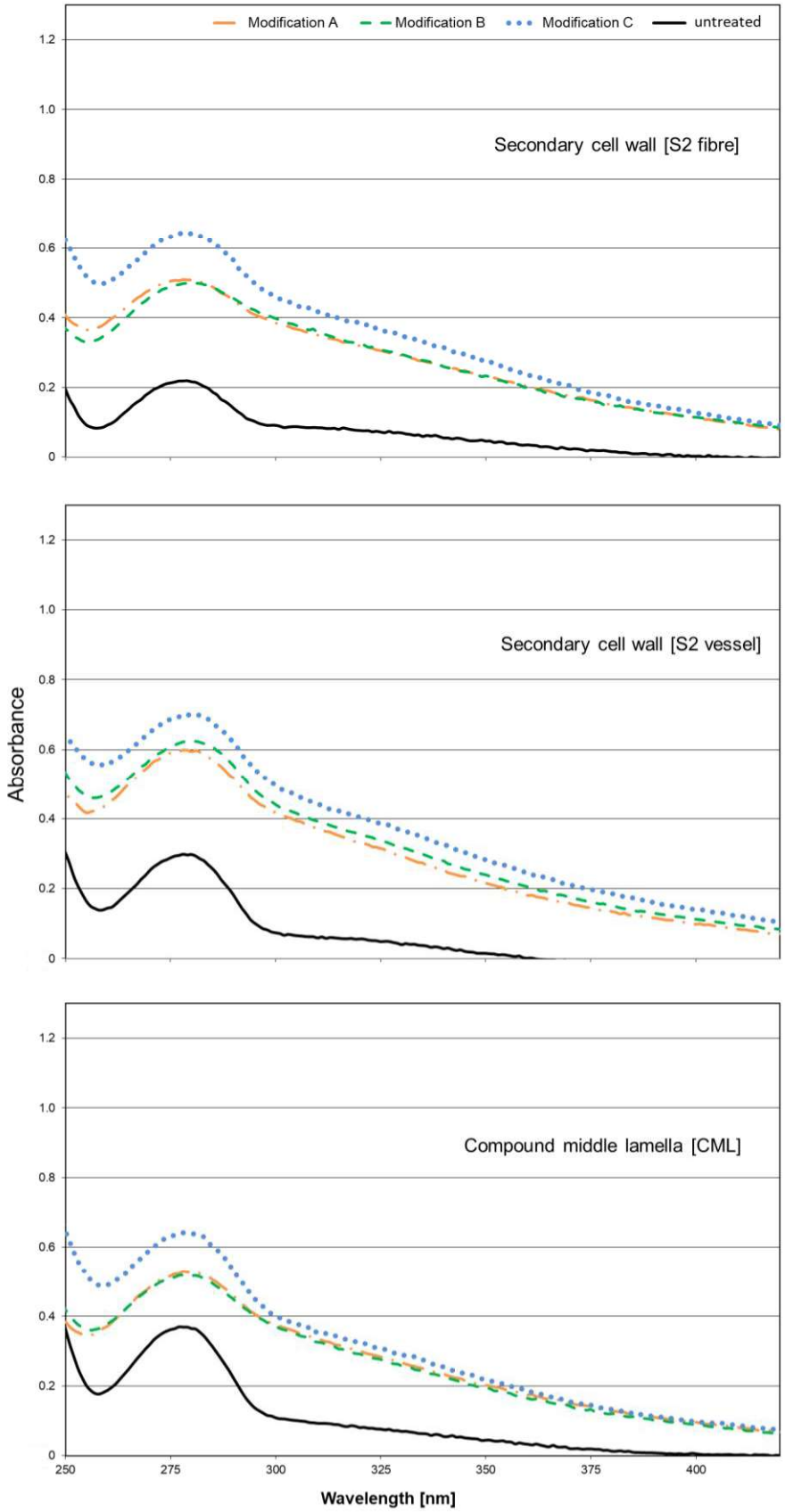

Figure 9: UV absorbance spectra in a range between λ240 and λ600 nm of untreated and furfurylated maple cell wall layers.

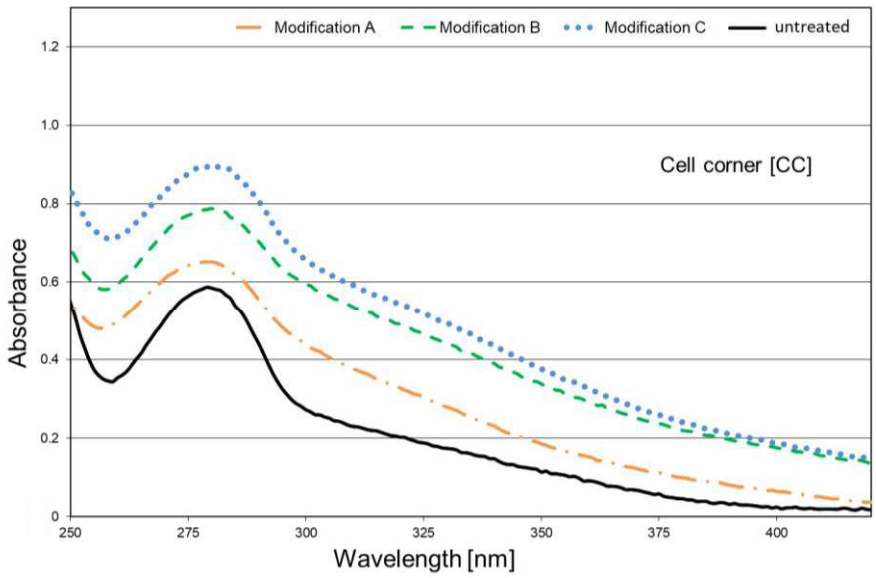

Figure 10: UV absorbance spectra of the cell corner (CC) in a range between λ240 and λ600 nm of untreated and furfurylated maple samples.

The different absorbance intensities at λ280 nm and λ278 nm, respectively, are strongly correlated to the lignin concentration, with the highest amount in the CC (Koch and Kleist 2001; Koch and Grünwald 2004). In the case of Radiata pine, the A_{max} of the CC in untreated wood is 1.6 times higher than in the A_{max} of the S2 layer and, for maple, even 2.7 times higher (Table 7). This large difference seen in untreated samples changed for the furfurylated samples into a less pronounced CC area compared to the S2 layers visualized by the line scans (Figure 1, Paper II and Figure 4).

The spectra of the furfurylated cell wall layers of Radiata pine and maple show similar characteristics, with significantly higher absorbance values for the individual cell wall layers compared to the untreated cell wall layers. For process C, the process which results in the lowest WPG, both for Radiata and maple, a clear distinction between the spectra of all cell wall layers of Radiata pine and maple can be seen. Whereas the spectra of Radiata pine type C (57% WPG) appear close to the course of the untreated wood, and the spectra of maple type C (27% WPG) are presented by the highest absorbance spectra. That supported the results of the recorded scanning profiles and the spectra of the filled lumens (Table 8). The different spectral behavior of modified maple from process C has to be strongly related to the wood species. The anatomical structure, cell types, cell wall compounds and chemical composition of the extractives and their localization result in the treatability behavior that directly influences the loading of the sample (Lande et al. 2010; Zimmer et al. 2014; Tarmian et al. 2020). The same process condition for maple and Radiata pine lead to different spectral characteristics, as can be seen for treatment C.

The spectra of these strongly modified cell wall layers of Radiata pine and maple have a commonality in that a bathochromic shift and shoulders with lower intensities of around 320 nm compared to untreated wood were detected. This is probably due to the formation of conjugated double bonds. The higher degree of conjugation stabilizes π - π * transitions

resulting in bathochromic shifts (Goldschmid 1971). The strong increase of absorbance intensities from untreated to furfurylated wood and the shift of the bands of the furfurylated wood cell walls indicate a higher condensation of carbonyl groups as a possible reaction of FA with the guaiacyl units of softwood lignin (Lande et al. 2004). A combined theoretical and FTIR spectroscopy study of a hybrid poly(FA) lignin material (Barsberg & Thygesen, 2017) support these hypotheses.

The UV absorbance of the modified samples increased significantly compared to the untreated samples, indicating a strong polymerization of the aromatic compounds. The highest UV absorbance values were found in areas with the highest lignin concentration. The results show that the absorbance intensities depend more on the wood species and the modification process parameters than on the FA loading (WPG) of the treated sample. The mean UV absorbance values are summarized in Table 9.

Table 9: Mean UV absorbance values of the secondary cell wall (S2), the compound middle lamella (CML) and the cell corner of untreated and A-, B- and C-type modified Radiata pine and maple.

Radiata pine	WPG (%)	S2			CML			CC		
		Λ(nm)	Abs.	Δ	λ (nm)	Abs.	Δ	λ (nm)	Abs.	Δ
Untr.	0	282	0.56		281	0.62		282	0.90	
A	60	278	1.04	0.48	280	1.03	0.41	278	1.15	0.25
B	70	280	1.00	0.44	280	1.07	0.45	272	1.17	0.27
C	57	280	0.86	0.30	280	0.90	0.28	281	1.02	0.12

Maple	WPG (%)	S2			CML			CC			S2 vessel		
		Λ (nm)	Abs.	Δ	Λ (nm)	Abs.	Δ	Λ (nm)	Abs.	Δ	Λ(nm)	Abs.	Δ
Untr.	0	279	0.22		277	0.37		279	0.59		278	0.30	
A	32	278	0.51	0.29	278	0.53	0.16	280	0.65	0.06	278	0.60	0.30
B	37	280	0.50	0.28	279	0.52	0.15	280	0.79	0.20	281	0.62	0.32
C	27	278	0.65	0.43	278	0.64	0.27	280	0.90	0.31	280	0.70	0.40

The data are averages of 15 to 20 individual spectra. Δ is the absorbance difference between the untreated control and the FA-modified samples.

9.2.2 Samples degraded by *Rhodonia placenta*

In the view of incipient fungal decay of furfurylated wood, laboratory degradation tests were performed. The tests were monitored daily over 18 days to provide different degradation levels of furfurylated (type A and B, Table 10) and untreated Radiata pine. The harvested samples were analyzed by LM, TEM and UMSP. Furthermore, the mass loss and the moisture content were measured for both modified and unmodified samples. These experiments are expected to visually depict initial brown rot degradation and support our understanding in how modified wood is protected against decay and what the role cell wall lignin and FA play in this process. The experimental formulations with their corresponding abbreviations and procedures used by Kebony can be taken from Table 6, section 9.2.1.

9.2.2.1 Light microscopy and TEM analyses

The initial colonization of *Rhodonia placenta* in untreated and furfurylated wood during decay test I was evaluated by using LM. Samples from the water based solvent process (A) and samples from the alcohol based solvent process (B) were examined.

The analyzed transverse sections revealed no structural changes (Figure 3d,h,l, Paper IV), confirming previous light microscopic studies of initial stages of brown rot decay (Irbe et al. 2006; Rehbein and Koch 2011). A mass loss of at least 10% is necessary for microscopic detection of cell wall damage (Carll and Highley 1999).

After 24 hours, a fungal colonization can be observed in untreated wood, but not in furfurylated wood (Figure 3, Paper IV). The vast presence of the fungal hyphae observed in untreated wood was not seen for either of the treatment types A or B during the entire decay test. That can be due to the physically blocked tracheids by polymerized FA in the cell lumen and/or lower wood moisture conditions in furfurylated samples. The observed fungal colonization progress corresponded to the moisture development of the untreated and furfurylated samples (Figure 2, Paper IV). It has to be considered that the presence of fungal hyphae is not a diagnostic characteristic useful in distinguishing stages of decay (Wilcox 1993).

When comparing the two treatments, the fungal colonization developed differently. This can be seen in the micrographs of the radial sections (Figure 3, Paper IV). On the day of the first observed ML, the hyphae growth rate in FA-modified wood was medium high, grade 2 (type A day 16), low in type B (grade 1, day 13) and high (3) in the untreated sample (day 9). The samples from type B performed slightly better (10 times grade 1) than from type A (8 times grade 1) (Figure 4, Paper IV). These findings support earlier studies in marine environments where Scots pine samples furfurylated using a methanol/ethanol solvent performed better than samples using water as a solvent (Westin et al. 2016). The differences in fungal colonization found in samples from treatment A and B can be attributed to i) the different solvents used in the furfurylation process, ii) the disparate WPG level, iii) the filled lumen ratio and iv) the lower MC of type B.

The possible reason/reasons for the delayed onset of brown rot degradation in FA modified wood is/are unclear. It would be of great interest to find the major mechanism behind this

occurrence in order to advance research regarding this topic. More research is needed to separately evaluate each of the possible reasons. Test designs with one fixed parameter should be developed to search for possible variable correlations.

The LM results of this study indicate that the presence of fungal hyphae in furfurylated wood is directly linked to protection from decay. Furfurylated wood is protected from decay for a prolonged period compared to untreated wood, which corresponds to earlier results (Eikenes et al. 2004; Lande et al. 2004b, 2004a; Venås 2008; Esteves et al. 2011; Li et al. 2015; Sejati et al. 2017). Furthermore, the observed fungal colonization emphasizes the non-biocidal character of FA modified wood, as it was found for white rot (Pilgård, Alfredsen et al. 2010) and marine organisms (Westin et al. 2016).

It is known that hydrogen peroxide (H_2O_2) is part of the Fenton reaction used by the brown rot fungus for producing hydroxyl radicals through the reaction with Fe2+ during the non-enzymatic oxidative degradation phase (Arantes and Goodell 2014). It has been suggested for the brown rot fungus *Gleophyllum trabeum* that H_2O_2 is produced through a reaction of hydroquinones and oxygen (Jensen et al. 2001). To detect and localize H_2O_2 during incipient *R. placenta* decay in untreated and furfurylated softwood, ultra-thin sections of the samples from the cytochemical test with cerium chloride ($CeCl_3$) were subjected to transmission electron microscopy. The cytochemical method, where cerium acts as a trapping agent for enzyme-generated H_2O_2, was introduced by Briggs et al. (1975) and applied by Kim et al. (2002) for two brown rot fungi species. Cerous ions and H_2O_2 precipitate as cerium perhydroxide [$Ce(OH)_2OOH$] as an electron-dense reaction product, which can be easily detected with TEM. Perhydroxide precipitates, detected as dark granules, were found in cell lumens that were mainly close to the wood cell wall and in the direct vicinity of bordered pits (Figure 1a and 1b, Ehmcke et al. 2014). These results are comparable with the findings of Kim et al. (2002) for the brown rot species *Tyromyces palustris* and *Coniophora puteana*. To confirm the specificity of $CeCl_3$ staining for H_2O_2 EDX, mapping and line scan analyzes were used. Selected sections verified that the detected precipitates include cerium (Figure 11).

Precipitates, similar to those in untreated wood, were also detected in furfurylated wood colonized by *R. placenta*. That shows that FA modified wood is comparable with untreated wood regarding the decay pattern of *R. placenta*. To provide visual information about specific fungal activities in furfurylated wood, further cytochemical and immunolabelling studies are desirable.

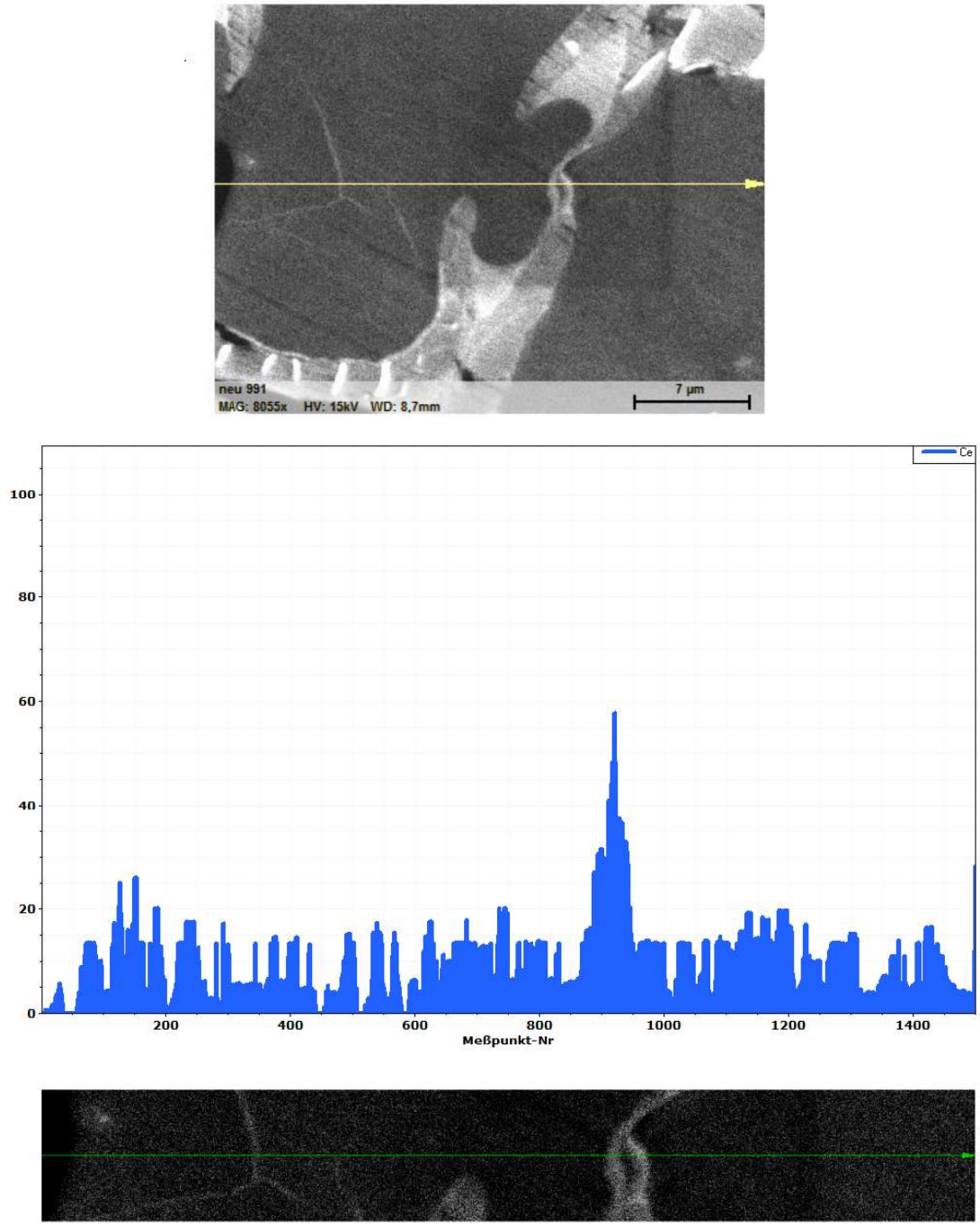

Figure 11: EDX analysis: line scan of detected precipitates adjacent the aspired bordered pit of a tracheid from the cytochemical test with cerium chloride. (blue line – Ce)

9.2.2.2 Topochemical characterization

Furfurylated and untreated samples from the mini-block test-type I were topochemically analyzed to visualize non-enzymatic oxidative degradation changes of lignin within individual cell wall layers at the initial decay phase of the brown rot fungus *R. placenta*. To ensure that the period of initial decay was included, the mass loss (ML) and, additionally, the moisture

content (MC) were calculated daily. The results of the ML and MC are presented in Table 1 (Paper IV). The topochemical monitoring included the harvest points until the first detectable ML + 2 days. Selected sample sections of untreated and furfurylated wood tissues of *P. radiata* incubated with *R. placenta* were scanned with monochromatic UV-light at a λ280nm wavelength. The mean absorbance values, two- and three-dimensional UMSP profiles and the UV absorbance values as a function of distance from the middle lamella cell corner (MLcc, 0 µm) to the cell lumen were evaluated.

Mean UV absorbance values

The analyzed areas in this study were particularly characterized by increased absorbance values compared to the uninoculated samples during the first 4 days of the decay test. This finding corresponds with results reported for untreated *Pinus sylvestris* degraded by the brown rot species *Andtrodia vailantii* (Rehbein and Koch 2011) and *Coniophora puteana* (Irbe et al. 2006). The absorbance values of the untreated and furfurylated samples fluctuated around the values before decay during the first 11 days. After 11 days, the mean absorbance values of furfurylated samples fluctuated between $A_{280\ nm}$ 0.57 and $A_{280\ nm}$ 0.73 with a decreasing amplitude until day 18. The sample from treatment A showed slightly lower values compared to treatment B. Common to all three variations (untreated, A, and B) was that the minimum mean absorbance value was lower than the reference value before decay. The development of the evaluated mean absorbance values (based on 11,100 to 12,900 scanned measuring points) over the entire decay period of cell wall regions with radially oriented combined middle lamella (CML) of untreated and furfurylated (type A and B) samples is displayed in Figure 5 (Paper IV).

Two- and three-dimensional UMSP profiles

Representative two-dimensional UMSP profiles of undegraded samples are presented in Figure 6.1a-c (Paper IV). The UV absorbance intensities within the individual cell wall layers are displayed by the differently colored pixels. The highest absorbance intensities occurred in the area of the CML and the corner cell wall (CC), as previously described for untreated wood (Koch and Kleist 2001; Koch and Grünwald 2004), thermally modified wood (Mahnert et al. 2013) and furfurylated wood (Paper II). The furfurylated profiles (Figure 6.1 b,c, Paper IV) show significantly higher UV absorbance levels of the entire cell wall compared to untreated wood, confirming the observations presented in Paper II. The reason for the detected high absorbance values are the condensing reaction of FA and lignin during the furfurylation process, as previously proposed by Barsberg and Thygesen (2017) for hybrid poly(furfuryl) alcohol to lignin models. To illustrate the decrease in absorbance values caused by initial decay activities, seen in this study, the most characteristic UV scans are presented in Figure 6.2 (Paper IV).

The detected inhomogeneous changes in the spectral behavior of the scanned cell wall layers originate from early fungal degradation processes. Both Irbe et al. (2006) and Rehbein and Koch (2011) have reported similar findings for untreated softwood. This topochemically visualizes the suggested re-aggregation of modified lignin during brown rot degradation followed by an immediate filling of opened pores with repolymerized lignin, which support

the findings of Goodell et al. (2017). The removal of poly-saccharide components and the partial depolymerization of the native lignin in combination with modifications in its side chains could explain the increase in absorbance values seen in this study and previously shown by Irbe et al. (2006).

The results of the scanned cells filled with polymerized FA showed distinct variations in absorbance signals after decay (Figure 7, Paper IV), confirming earlier observations of degradation-causing changes of absorbance values of polymerized FA deposits in the cell lumen (Paper I). The changes of absorbance values are most likely explained by the attack of highly reactive hydroxyl radicals, produced in the non-enzymatic oxidative degradation (B. Goodell et al. 1997; Hammel et al. 2002; Arantes et al. 2012) process.

UV absorbance – from the middle lamella via the cell corner (MLcc) to the cell lumen

The UV absorbance values of areas ranging from the MLcc, via the corner cell wall to the cell lumen, were analysed to generate specific information on alterations during brown rot decay. The absorbance changes found at the MLcc could be related to the suggested preferential degradation of middle lamella regions at incipient decay stages by *R. placenta,* as described by Kim et al. (2015). The adjacent area revealed further absorbance changes, supporting findings for untreated wood relating to i) the perception that the brown rot degradation starts at the outermost part of the S2 layer and ii) the degradation pattern Type 1 as described by Kim et al. (2015). The results indicate that initial lignin modification through brown rot degradation affected the entire cell wall (Figure 8-1,2, Paper IV). Furthermore, our results support findings by Kim et al. (2015) regarding disrupted lamellae of lignin aggregates and cellulose microfibril bundles in the outermost S2 layer of early stage decayed spruce tracheids.

The differences found in the absorbance behavior of treatments A and B could be explained by the impact of the solvents used in the different furfurylation processes and the resulting WPGs. Whereas the absorbance values of type A remained beneath or rather close to the undegraded sample curve, the values of type B fluctuated, which can be seen in all topochemical analyzing methods. The results indicate that areas damaged by hydroxyl radicals, produced through the initial degradation activities of *R. placenta,* can be detected and analyzed *in situ* by two- and three-dimensional UMSP images.

9.3 Initial decay pattern in furfurylated wood

Non-enzymatic oxidative degradation patterns in wood are neither macroscopically visible nor are they visible by LM. It has been shown that the initial brown rot decay phase and rapid depolymerization results in essential losses of engineering properties (e.g., bending strength) – even before any mass loss can be detected (Schultze-Dewitz 1966; Bariska et al. 1983; Winandy and Morrell 1993; Curling et al. 2002; Witomski et al. 2016). Therefore, it is of great importance to identify the onset of brown rot degradation in the earliest stages of decay (Kim et al. 2019). Methods of investigating fungal activity in timber and trees are listed by Schmidt (2006b). Detection by microscopic methods were presented by Schwarze (2007), DNA and gene expression studies were presented in a review by Alfredsen et al. (2014) and further methods were recently reviewed by Kim et al. (2019) with regard to implementing modern fungal decay research into a wood building standard of practices. Nevertheless, methods to detect initial decay *in situ* for practical purpose have not yet been presented.

Therefore, it is of great interest to learn more about non-enzymatic oxidative degradation by brown rot fungi. Close monitoring of initial fungal activity in untreated and FA modified Radiata pine attempting to follow *in situ* the non-enzymatic oxidative degradation processes was carried out. To identify topochemically visible features of cell wall alterations that are characteristic for the initial degradation phase, a special UMSP technique were applied. According to TEM studies by Kim et al. (2015), the area of interest was defined from the middle lamella cell corner (MLcc) via the corner cell wall to the lumen (Figure 12).

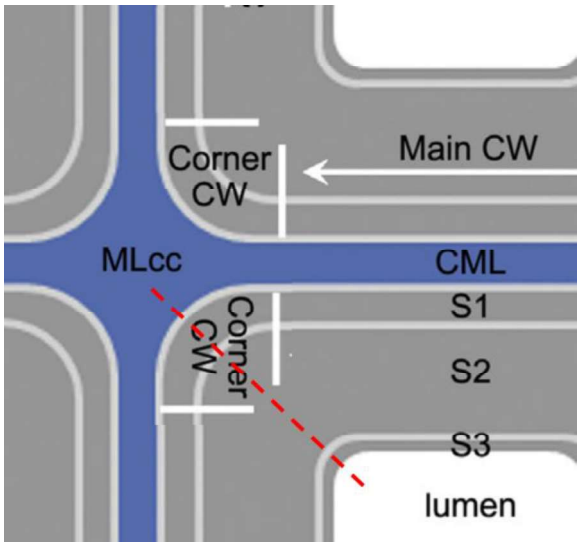

Figure 12: Schematic diagram according to Kim et al. (2015) of untreated cell wall ultrastructure of tracheids. The red dotted line shows the area of interest (the line profile). The line profile is defined from the middle lamella cell corner (MLcc) via the corner cell wall to the cell lumen. CML, compound middle lamella; CW, cell wall; S1, secondary cell wall outer layer; S2, secondary cell wall middle layer; S3, secondary cell wall inner layer. (Paper IV, detail Figure 1)

Topochemical scanning profiles recorded during the first 4 days of the decay test partly increased absorbance values compared to the uninoculated samples for both untreated and furfurylated samples. A relative increase in lignin in the degraded lignocellulosic cell wall matrix by brown rot, as previously reported by Rehbein et al. (2011) and Irbe et al. (2006b), can basically explain this effect. The topochemically scanned cell wall layers revealed inhomogeneous changes in the spectral behavior of the cell wall layers with spots of higher and lower UV absorbance values (Figure 13). These detected UV alterations originated from a) early fungal degradation processes, as reported by Irbe et al. (2006b) and Rehbein et al. (2011), and b) the suggested re-aggregation of modified lignin during brown rot degradation followed by an immediate filling of opened pores with repolymerized lignin, as suggested by Goodell et al. (2017).

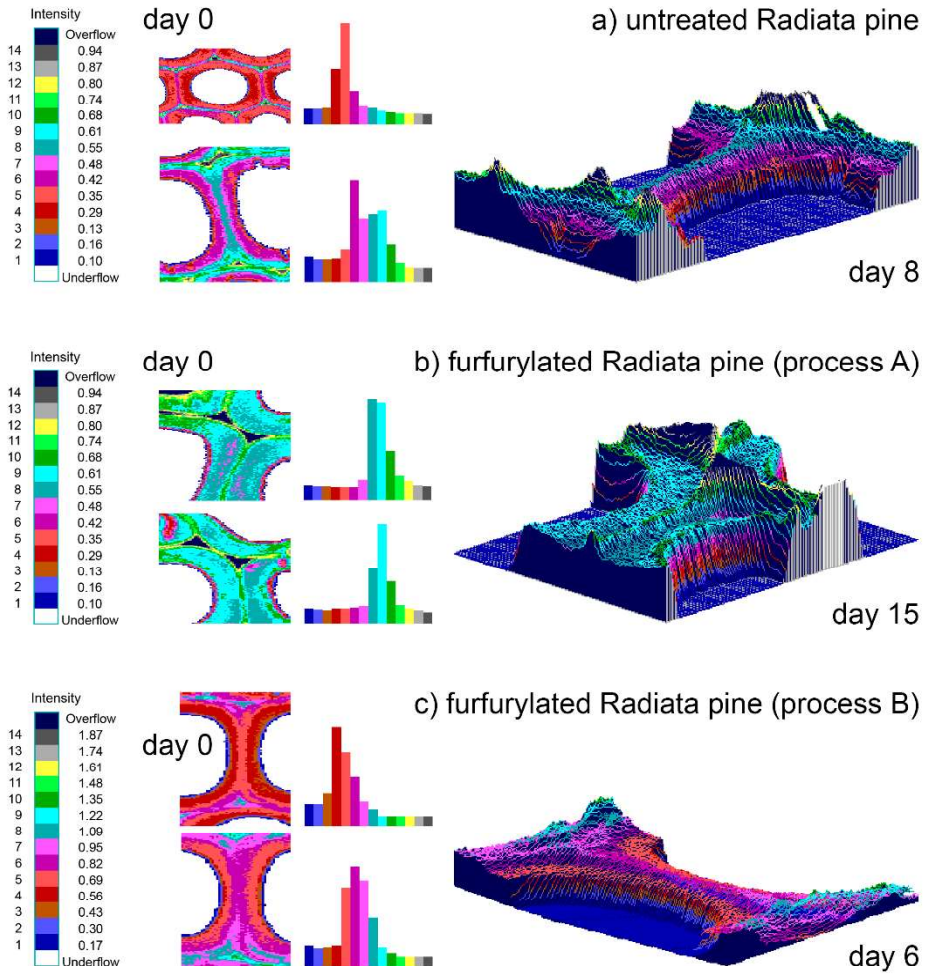

Figure 13: Representative UV microscopic scanning profiles (area and 3-D) at λ280nm of early stages of decay in untreated (a) and furfurylated (b,c) Radiata pine cell walls by *R. placenta*. The data are valuated from their corresponding histograms. The 3D image profiles intuitively visualize topochemical changes and cell wall modification at the initial stage of decay. (Paper IV, Figure 8b)

To obtain non-enzymatic oxidative degradation activities in the defined area of interest (Figure 12) the individual UV absorbance values at λ280nm were analyzed and plotted as function of distance (Figure 14).

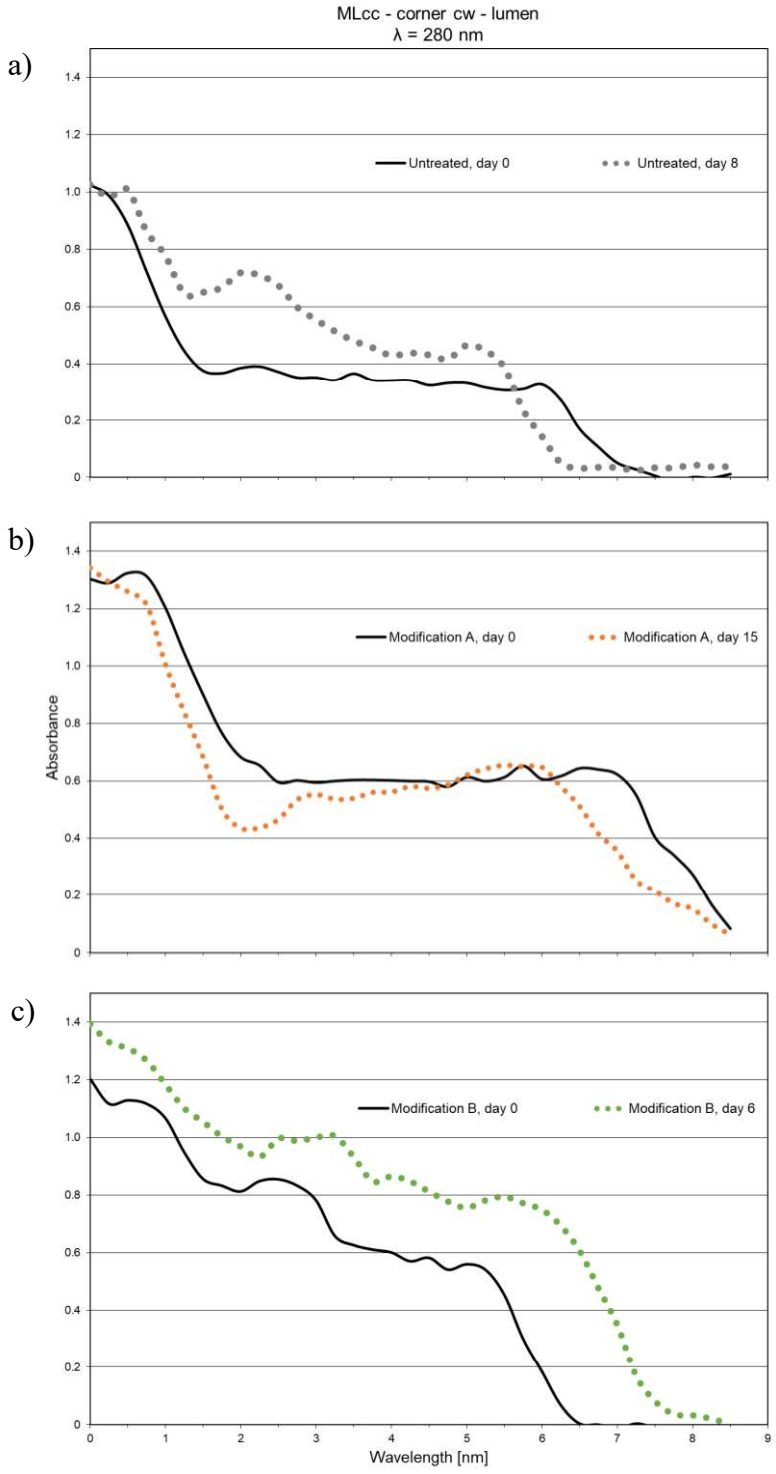

Figure 14: UV absorbance values at λ280nm as a function of distance at the initial stages of decay by *R. placenta* in pine tracheid corner cell walls. (according to Paper IV, Figure 8a)

Figure 14a-c present representative line profiles of undegraded (day 0, solid line) and infected *Pinus radiata* (a – untreated; b – modification A; c – modification B). The UV absorption changes already mentioned before can now be precisely localized at a cell wall layer level. After 8 days of exposure, the absorbance values increased in the region of the primary and secondary wall for untreated wood (Figure 14a). The line profile of furfurylated *P. radiata*, type A, revealed decreased absorbance values – especially in the region of MLcc after 15 days of exposure (Figure 14b). For process B, the evaluated UV absorbance values of the entire cell wall shifted to higher values after 6 days. Cell wall characteristics of non-enzymatic oxidative degradation can be derived from the evaluation of the line profiles of the entire decay test. The features found in this study are combined with those of Irbe et al. (2006), Rehbein and Koch (2011) and Kim et al. (2015) in Table 10. In the Table, the most characteristic cell wall features, which could help to identify brown rot activity in FA modified softwood at initial stages, are summarized. Figure 15 displays the location of described initial decay patterns.

Table 10: Structural features of initial brown rot decay according to Kim et al. (2015) in comparison to findings of Rehbein and Koch (2011) and own studies (Paper IV).

TEM investigations	**UMSP investigations**			
Features according to Kim et al. (2015) of untreated *Picea abies* degraded by *R. placenta*	Rehbein and Koch (2011), untreated *Pinus sylvestris* degraded by *A. vailantii*		Own studies (paper IV), FA modified *Pinus radiata* degraded by *R. placenta*	
	present	absent*	present	absent*
degradation of middle lamella regions (Figure 15)		X	X	
outermost part of the S2 layer (Figure 15)	X		X	
degradation pattern Type 1 (Figure 15): primary cell wall (PW), outermost S2 layer including S1/S2 boundary inner S2/S3 layers middle S2 layer		X	X	
degradation pattern Type 2 (Figure 15): notable structural changes in inner S2/S3 layers without notable degradation in the outermost S2 layer		X		X
differences in organism attacks between cell corners (corner cell wall) and the main cell wall (i.e., cell walls between cell corners) apparent even in the same tracheid cell wall	X		X	

*absent refers to the analyzed cell wall area; this does not preclude the possibility of further degradation patterns located in the wood tissue.

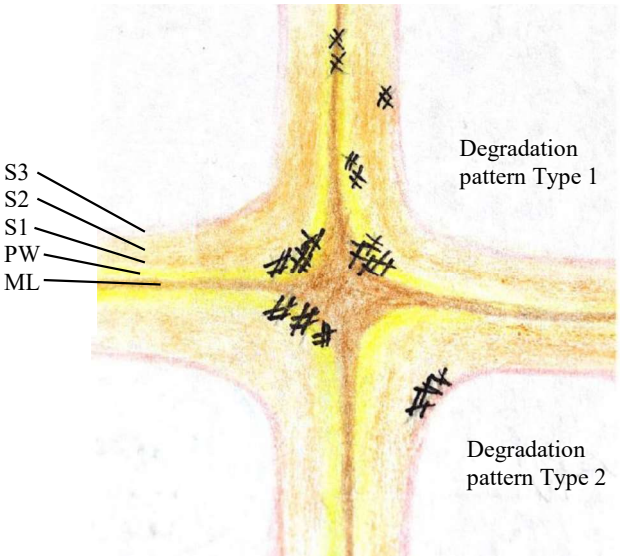

Figure 15: Schematic drawing of the cell wall corner of four adjacent tracheids. (#) marks the structural features of initial brown rot decay found in the analyzed samples.

The topochemical observations in this study confirm earlier TEM studies by Kim et al. (2015). The results revealed that the entire zones, essential for the stability of the cell wall and responsible for the absorbance of the interfacial shearing forces, are attacked. The brown rot induced hydroxyl radicals involved in the Fenton degradation system are responsible for the attack of the cell wall integrity (Yelle et al., 2008, 2011). These zones are displayed in Figure 15: i) middle lamella – responsible for cohesion of two wood cells (tracheids); ii) primary cell wall (PW), outermost S2 layer including S1/S2 boundary – connecting the main cell wall layer with the middle lamella; iii) middle S2 layer – the main part of the wood cell wall featuring the wood's core.

The sophisticated system of linkages between cellulose fibrils, hemicelluloses and lignin is seriously affected by the initial decay carried out by brown rot. This confirms the hypothesis of oxidatively cleaved linkages between lignin and polysaccharides, as supposed by Irbe et al. (2006).

The key to understanding wood properties and their effects is to understand the wood cell wall ultrastructure (Donaldson, 2019). This also applies to modified wood cell walls. Investigations on possible strength reaction within the wood cell wall revealed reactions of the individual layers under applied forces. The assessment results of mechanical characterizations of the S2 layers and the ccML (Wimmer and Lucas, 1997) suggested that the combination of lignin and cellulose is more closely related to hardness than solely on layer. Studies on cell wall fractures by Donaldson (1995) revealed that fractures occur mainly between the ML and S1 layers or between the S1 and S2 layers. Wimmer and Lucas (1997) concluded that the shearing forces first lead to a failure of the S1 layer. Bergander and Salmén (2002) investigated the wood cell wall properties and their effects on the mechanical properties of fibers with a model analysis. It was found that the S1 layer has a minor effect on the properties in longitudinal direction, whereas the influence in the transverse direction is larger.

Bergander and Salmén (2002) further concluded that morphology and structure of the wood fiber material of the S1 layer are important for the cell wall's mechanical properties in the transverse direction. Studies on the deformation and failure mechanism of the S2 layer by *in situ* SEM compression of Focused Ion Beam machined micropillars revealed, for instance, that the shear band formation occurs as a result of failure of the hemicellulose-lignin matrix, which is supported by the buckling and misalignment of the microfibrils (Adusumalli et al. 2010). Through FA modification, a reinforcement of the initially affected zones under stress can be assumed, since studies on FA distribution (Venås and Rinnan 2008; Thygesen et al. 2010) revealed the highest concentration in the area of the ccML, CML and S1. Further nanoindentation studies by Li et al. (2016) showed improvements in indentation modulus and hardness of FA modified wood cells. This reinforcement can be clearly visualized by UMSP by higher absorbance values, indicating strong modification of the cell wall. The 3D images and the detailed line scans of the furfurylated cell walls (Figure 1b, 2 and 3, Paper II) show a modification with broader plateaus adjacent to the ML compared to the untreated wood. To apply, for instance, the test design described by Adusumalli et al. (2010) on the CML area of untreated and furfurylated wood at the initial stages of brown rot decay could extend our understanding of cell wall alteration during decay.

9.4 The role of the solvent

The differences found in the absorbance behavior of the two treatments A and B could be explained by the impact of solvents used in the different furfurylation processes and the resulting WPGs. In order to clarify if the solvent plays a role during the furfurylation process for the characteristics of the modified wood LM, infrared (IR) and fluorescence spectroscopy procedures were applied.

In this section, the abbreviations for the treatments were changed due to Paper III being published. The abbreviation for the process with alcohol-based solvent (IPA) changed from 'B' into 'C'; the abbreviation for the process with the experimental mix of water-based solvent changed from 'C' into 'B'; and the abbreviation for water-based solvent process A remains the same.

Infrared spectra of the untreated and the furfurylated Radiata pine, with three different furfurylation formulations, are given in Figure 1 (Paper III). The spectra show that samples from the alcohol based treatment C stand out from the water based treatments A and B, which can be attributed to the effect of the solvent. The absorbance peak seen at approximately 1,510 cm^{-1} for untreated softwood (Faix, 1991; Schwanninger et al. 2004) occurred for furfurylated wood with downshifts at approximately 5 cm^{-1}, as would be expected if FA binds to a ring position within the lignin of the wood cell wall (Barsberg & Thygesen, 2017). However, it needs to be considered that the polymerized FA itself also has a peak at the downshifted position. Therefore, it is not possible to assign the increased absorbance at the new peak position to the binding of FA and lignin.

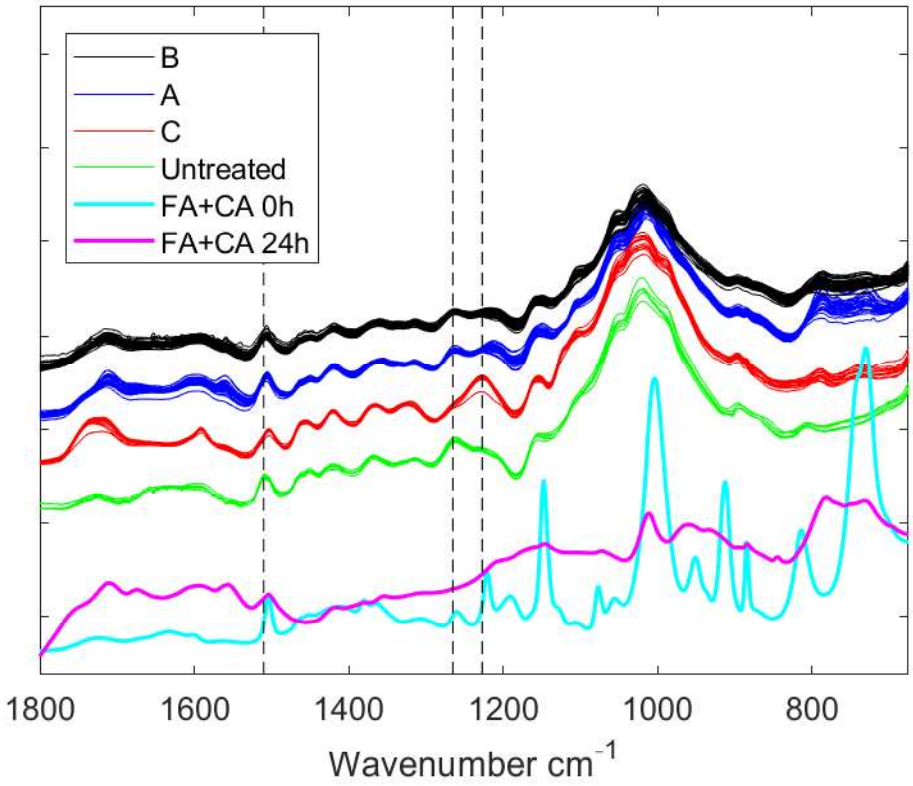

Figure 16: Standard normal variate (SNV) corrected ATR-IR spectra of untreated samples and the three types of furfurylated Radiata pine samples. SNV corrected ATR-IR spectra of furfuryl alcohol containing citric acid (CA) as catalysts are also shown for comparison, both before and after curing. The vertical lines mark band positions 1,510, 1,265 and 1,227 cm^{-1}. A: water-based solvent; B: water-based solvent with alternative catalytic chemistry C: alcohol-based solvent (IPA); (Paper III, Figure 2)

Falco et al. (2018) described a furan ring opening effect that also can be observed in the IR spectra by the carbonyl peak at approximately 1,750 cm^{-1} (Figure 14). All three of these furfurylation processes had a relative increase in this functionality in common. In contrast to the two water-based treatments A and B, treatment C showed a broadening of this peak position due to the suggested formation of isopropyl levulinate and the ester bond therein (Falco et al. 2018).

The results from the fluorescence spectroscopy confirmed three aspects of earlier results found by Thygesen et al. (2010).

1) Mean excitation-emission landscapes were prepared for the untreated and furfurylated samples (Paper III, Figure 2) by applying fluorescence spectroscopy. The observed emission shifting towards higher wavelengths for furfurylated wood compared to the untreated wood was also seen in the previous study by Thygesen et al. (2010). When comparing the three treatments, the signals of treatment A appeared close to those of untreated wood. This confirms results from the UV spectroscopy of furfurylated Radiata pine and maple in treatment A (section 9.2.1).

2) The fluorescence emission properties of the analyzed material regarding populations of fluorophores confirm earlier results found for a different sample set of furfurylated wood

using a different wood species. It might be speculated that these populations are generic representatives of different conjugation lengths of the FA oligomers present in the material.

3) The analyzed PARAFAC models (Figure 3, Paper III) of the fluorescence landscapes confirm earlier results, however, that no differences between the herein analyzed treatments were observed.

With fluorescence spectroscopy, it was not possible to verify the differences seen between alcohol-based and water-based furfurylated samples observed with IR spectroscopy. Another option that can be used to search for fluorescence differences/similarities localized to the position in the wood is to use pixel-wise CLSM landscapes and analyze these by use of chemometrics such as PARAFAC or multivariate curve resolution-alternating least squares (MCR-ALS), or alternatively, by capturing emission curves for a few different excitation wavelengths – for each pixel, as well.

In this context, we decided to use IR micro-spectroscopy to identify differences in the distribution of the polymerized FA in the wood tissue.

Further IR micro-spectroscopy of furfurylated cell walls and filled lumen of treatment A and C revealed that there was a difference between the spectra of cell walls and filled lumens that was independent of the treatment (Figure 5. Paper III). This means that the polymer that formed in the cell wall is the same for treatment A and C and the polymer that formed in the lumen for these two treatments. Whereas the formed polymer in the cell wall and the one in the lumen is not the same. This could be explained 1) by the length of conjugated chains formed in the lumen (longer chains that give a red shift in fluorescence) and 2) due to the possibility that the chain length in the cell wall is reduced because of sterical hindrance; it could also be due to bonds to cell wall polymers – probably lignin. The LM quantification of the number of tracheids with lumina filled with FA polymer vs. the number of tracheids without any visible filling showed that there was a significant difference between the analyzed treatments of Radiata pine. Differences were also observed for furfurylated maple. The analyzed transverse section of furfurylated maple only revealed a few filled cell lumen, mainly in the parenchyma cells of the ground tissue, independent from LW and EW. A more prominent difference was found in the wood rays, in that almost all parenchyma cells of the water-based solvent were filled, whereas approximately half of the cells of the samples from the process with IPA as a solvent were filled. These differences could be related to i) the wood species-dependent morphological pathways in general and through different amounts of non-aspired bordered pits in LW and EW; and ii) the IPA-dependent delay of the onset of polymer formation during curing, based on findings by Falco et al. (2018a)

No matter which mechanisms were responsible for the final distribution of FA polymer resulting from the use of the two different solvents, the LM based quantification indicated a marked difference in the location of the FA polymer between the water-based and IPA treatments for both Radiata pine and maple. It has to be considered that the missing information of the specific initiators and catalysts used in the furfurylation process could probably act as a limiting factor for further interpretation.

9.5 FA and cell wall lignin

The previously mentioned structural features (Table 10, section 9.3) that were detected at the initial stages of brown rot occur mainly in lignin rich areas – the CML and the S1 layer. The results from the decay tests indicate that lignin plays an important role in untreated and furfurylated wood when it comes to resistance against brown rot degradation. These results confirm the findings from Schwarze (2007): that lignin presents the most significant barrier to wood decay and influences degradation modes. Furthermore, Lee et al. (2019) suggested that, in living plant cells, e.g., the lignin-deposited structure, functions as a physical barrier comparable to the Casparian strip, catching hold of pathogens and thereby limiting their growth.

During wood modification with FA, there might have been a grafting reaction between lignin and FA, as suggested by Lande et al. (2004). NMR studies by Nordstierna et al. (2008) revealed that there is a formation of covalent bonds between FA and a lignin model compound in a liquid-phase system. Recently, a combined theoretical and FTIR spectroscopy study of a hybrid poly(FA)-lignin material (Barsberg and Thygesen 2017) support these findings. They found evidence for condensation of FA with selected lignin models. The results from the IR studies (section 9.4) revealed that the absorbance peak, seen at approximately 1,510 cm^{-1} (Figure 13) for untreated softwood (Faix 1991; Schwanninger et al. 2004), occurred in furfurylated wood with downshifts of approximately 5 cm^{-1}. This downshift is expected when part of the polymerized FA forms during curing and is covalently bonded to lignin within wood cell walls, but only a fraction of the cross-condensation reactions take place at lignin ring positions (Barsberg and Thygesen 2017). However, it needs to be considered that the polymerized FA itself also has a peak at the downshifted position. Therefore, it is not possible to assign the increased absorbance at the new peak position to chemical covalent bond formations between polymerized FA and wood cell wall lignin. Our UMSP studies (section 9.2.1.) of furfurylated Radiata pine and maple showed an absorbance increment at 280nm/278nm that can be interpreted as a manifestation of the preferred deposition of condensed UV-active compounds at places of high lignin concentration in the cell wall *in situ*. Chemical bonds between FA and wood cell wall lignin were most likely also produced, but this has to be further verified.

To study and characterize possible chemical bonds between FA and cell wall lignin, FA modified wood was also subjected to Raman spectroscopy in the context of a master thesis (Wadenspanner 2018). The comprehensive review of Fackler and Thygesen (2013) presented microspectroscopic techniques like Raman that can map lignin by having marker bands that do not overlap with contributions from cellulose and hemicelluloses, which is explained by its smaller means of orientation than cellulose within the wood cell wall (Stevanic and Salmén, 2009; Gierlinger et al. 2010). Bock and Gierlinger (2019) were aiming to provide more information on the structure of lignin by vibrational spectroscopy to improve the assignment of vibrational spectra of lignin. In the Raman spectra of lignin, they found that the majority of the aromatic rings (unconjugated ones) can only be seen as weak bands, and they concluded that stronger Raman scatterers masked the weak scattering structures. Furthermore, Raman

analyses of untreated wood is partly limited due to laser-induced fluorescence (LIF) (Agarwal 1999; Lähdetie et al. 2013), which caused a strong background signal to form. Furfurylated wood also has a strong LIF that limits the possibility of generating acceptable Raman spectra with the same setting parameters as untreated wood. Aiming to reduce these limitations, we studied several hardwood and software modules and settings to reduce the interfering fluorescence – attempting to generate evaluable spectra.

A Raman spectroscope equipped with a Nikon CFI Achro 100x/1.25 objective was used at the Fraunhofer-Institute (IVV), Freising.

The size of the scanning field was 20 x 20µm² with 250 points per line (PPl, LPI) to generate an image scan that enabled us to differentiate the single cell wall layers (Figure 17, left). The obtained spectra from the cell wall corner showed a clearer peak at the rel. wavenumber of 1,600cm^{-1}, representing one band from the aromatic part of softwood lignin and confirming the results of Bock and Gierlinger (2019). In addition, a small peak in a range of 2,900cm^{-1} to 3,000 cm^{-1} occurred. In the fingerprint area, below 1,500cm^{-1} (Hesse 2016), no peaks appeared. That is due to the high intensity of fluorescence that covered the Raman scattering in the fingerprint area. The fingerprint area is of great importance for evaluating the Raman spectra, as the peaks in this area characterize the chemical compound as a whole (Smith & Dent, 2005). Furthermore, Bock and Gierlinger (2019) concluded that the cell corner spectrum mainly shows conjugated aromatic substructures, whereas unconjugated rings, although in the majority, can hardly be seen in the Raman spectrum.

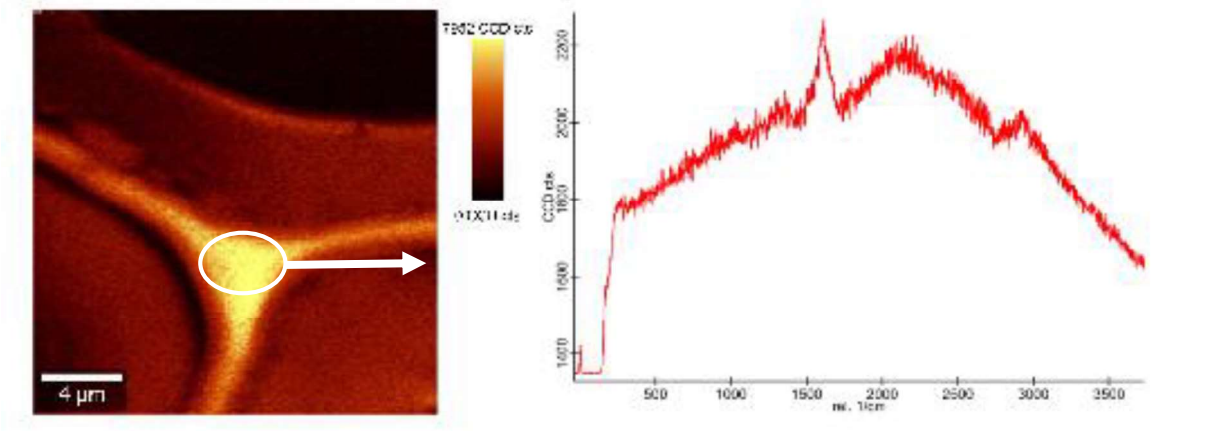

Figure 17: Image scan of the cell wall corner of furfurylated Radiata pine with a sum filter at 1,600cm^{-1} and the corresponding spectrum, retrieved from Wadenspanner (2018).

To quench fluorescence Zięba-Palus and Michalska (2014) recommended, e.g., photo bleaching as an opportunity, which did not work for furfurylated wood. Unfortunately, the further applied adaptions like spatial resolution, integration times, scanning depth or variations in sample thickness did not enhance the fingerprint area. Only the peak, at approx. 1,600 cm^{-1}, continuously had a clear appearance.

Since water can help to suppress fluorescence as an extinguishing substance by returning the excited molecule to its ground state via the extinguishing substance instead of fluorescence

emission (Wadenspanner 2018), Raman investigations were performed underwater. These investigations were carried out with the Zeiss Objective 63x W plan apochromat with no improvement of the spectra of furfurylated wood, whereas the spectra of untreated wood was improved.

Overall, the results of the Raman analyses performed can be summarized as follows: for untreated wood, analyzable Raman spectra were able to be recorded in contrast to furfurylated wood. It was not possible to analyze FA modified wood using the available equipment at the Fraunhofer Institute and the given combination of devices (Raman spectroscope, laser, objectives and analyzing software). Comparable drawbacks like lasers with other wavelengths and oil-immersible objectives were also raised in previous studies by Gierlinger et al. (2010). Nevertheless, the referenced master thesis (Wadenspanner 2018) provides a suitable methodology for sample preparation and, additionally, a comprehensive assembly of different setting parameters with their corresponding effect on the data. Thus, the present study serves as basic research regarding Raman spectroscopy of furfurylated wood.

10 Conclusions and future prospects

10.1 Conclusions

The main objective of this thesis was to study FA modified wood regarding its topochemistry for a better understanding of the mode of action of FA modified wood. *In situ* characterization on a cellular level was addressed and initial decay patterns by a brown rot fungus were investigated in a high timely and spatial resolution.

The FA modified wood is characterized by very high UV absorbance values (overflow) of the condensed phenolic/aromatic compounds in the modified tissue, which require individual threshold adaption of the UV intensities to a min. of 1.00% and a max. of 67.50%. The results of the absorbance increment at 280nm/278nm of undegraded furfurylated Radiata pine and maple lead to the conclusion that a manifestation of the preferred deposition of condensed UV-active compounds at places of high lignin concentration in the cell wall *in situ* has taken place. The strong increase of absorbance intensities from untreated to furfurylated wood and the shift of the bands of the furfurylated wood cell walls lead to the conclusion that a strong polymerization of the aromatic compounds as a possible reaction of FA with the cell wall lignin occurred. This conclusion is supported by current literature on predicted and measured FT-IR spectra of FA – lignin models' reactions as well as experimental data from previous studies on the basic chemistry of furfurylated wood. Deeper knowledge of the nature of these bonds might be helpful to understand and to improve the biological resistance of furfurylated wood. Furthermore, our topochemical results lead to the conclusion that the absorbance intensities depend rather on the wood species and the modification process parameters than on the FA loading (WPG) of the treated samples.

In summary, the results of this thesis lead to the conclusion that the USMP method, with its high spatial resolution, is well-suited to analyze the cell wall layer topochemistry of furfurylated wood *in situ*.

The LM investigation of the distribution of the polymerized FA in the wood tissue of Radiata pine showed a solvent-dependent distribution in the cross sections. The radial sections reveal that the ray parenchyma cells of furfurylated Radiata pine appeared empty. The results of the SEM analyses of furfurylated Radiata pine show that the polymerized FA is a cell wall-attaching, compact lumen-filling substance. The furfurylated maple had fewer filled cells in the cross sections, and the radial sections reveal almost all parenchyma cells of the water-based solvent were filled and approximately half of the cells of the samples from the process with IPA as solvent were filled. These results lead to the conclusion that the observed differences within Radiata pine and maple might be related to i) the wood species dependent morphological pathways in general and the different number of pits – non-aspired bordered pits in LW an EW; and ii) the IPA dependent delay of the onset of polymer formation during curing.

The results of the decay test show that *R. placenta* was already able to colonize untreated Radiata pine samples within the first days of incubation compared to the furfurylated samples, where the fungal colonization occurred with significantly less success. This led to the conclusion that physically blocked tracheid cell lumens filled with polymerized FA affect the fungal hyphae spread in the furfurylated samples. That can be seen as one possible reason for the impaired fungal colonization. The data from monitoring the LM are not sufficient for a conclusive answer to what is more important for the biological resistance of furfurylated wood – FA filled lumens or cell wall penetration of FA molecules and reaction with lignin. These results imply that a combination of both parameters impede brown rot degradation by giving a physical barrier for the hyphal expanse and an improved cell wall lignin by FA modification that is more difficult to degrade.

For the first time, brown rot infected FA modified Radiata pine was topochemically analyzed. UMSP area scans and selective line scans of an individual cell wall region provided detailed insights into non-enzymatic oxidative lignin modification at the initial decay stage, visualizing non-enzymatic oxidative degradation *in situ*. The UMSP results of the analyzed degraded furfurylated and untreated Radiata pine samples revealed comparable decay patterns in untreated and furfurylated samples. This led to the conclusion that FA modified wood has non-toxic properties regarding fungal degradation. This conclusion was supported by current literature on the chemical analysis of leachates from furfurylated wood, as well as experimental data from previous studies on fungal degradation of FA modified wood. Degradation patterns in the form of modified lignin did not only occur in the area of the outermost S2 layer, but also on local spots over the entire wood cell wall of the analyzed untreated and FA-modified samples. The highly reactive hydroxyl radicals, produced in the non-enzymatic oxidative degradation of *R. placenta*, are responsible for the damaged areas in the cell wall as well as for the attacked FA deposits in the cell lumen. These results lead to the conclusion, that *R. placenta* is able to degrade polymerized FA. The results in this thesis revealed further that initial lignin modification through brown rot degradation affected the entire cell wall. The results of the topochemical analysis reveal features for the identification of initial brown rot decay. The affected zones of the cell wall are: i) middle lamella; ii) the primary cell wall (PW), the outermost S2 layer including the S1/S2 boundary and iii) the middle S2 layer. These attacked areas are essential for the stability of the cell wall and are responsible for the absorbance of the interfacial shearing forces. These results imply that the ingenious system of the interfaces between the cell wall layers and the linkages between cellulose fibrils, hemicelluloses and lignin is seriously affected, which might explain the enormous strength loss in this decay phase. This conclusion was supported by literature on the mechanical properties of brown rot degraded wood.

In summary, the results of this thesis reveal that the decay pattern of *R. placenta* in FA modified wood were similar to those in untreated wood, which underlines the non-toxic mode of action of furfurylated wood. These results lead to the conclusion that FA modified cell wall lignin influences the fungal degradation process and, therefore, presents another possible reason for the enhanced brown rot resistance properties of furfurylated wood.

The exact role that FA modified cell wall lignin plays is yet not sufficiently understood. Studies on FA modified cell wall lignin and on the visualization of non-enzymatic oxidative degradation patterns should be focused on in the future. Therefore, further topochemical, cytochemical, and immunolabeling studies are desirable.

10.2 Future prospects

To enhance our current knowledge of the wood degradation of FA-modified wood at the initial stage, studies of a wider range in laboratory and fieldwork need to be conducted. The effects of sample design, different wood species and different FA modification processes need to be investigated further to produce reliable data for the choice of the best raw materials and process conditions for furfurylation. Decay tests with adopted test and sample designs, for instance, according to Schilling et al. (2013) and Kölle et al. (2019), should be performed to develop models for the initial decay activity, especially for non-enzymatic oxidative degradation. The wood-moisture relation at the initial decay stage should also be monitored in order to find answers regarding the role of moisture at the early fungal colonization stage. Furthermore, applying Scanning Near-Field Optical Microscopy (SNOM in reflection mode) according to Keplinger et al. (2014) is a rather universal principle of spatial cellulose and lignin assembly in secondary cell walls, and is therefore highly relevant for the understanding of cell wall structure and its enzymatic degradation.

The development of (short-time) field tests based on the obtained data from the laboratory decay test could help transfer the knowledge gained to practical means. This can be realized through the development of application standards for furfurylated wood, like use classes according DIN 68800, predictions of maintenance intervals and service life. Furthermore, this information of FA-modified wood would lead to the admission of further construction details and other building applications with special restrictions.

Not only are studies on brown rot as the most important house-rot fungi of great importance; studies on white and soft rot degradation are important, too. With regard to Europe's climate goals for 2050, more hardwood species will be used in building environments, which should initiate the expansion of our views of house-rot fungi.

The preferred scenario would be a topochemical evaluation of FA-modified wood degraded by *R. placenta* combined with fungal gene expression analyses. The obtained image data from the scanned wood tissue *in situ* could be accomplished by the fungal gene expression to provide information for a better understanding of the degradation pattern, therefore increase our knowledge of the mode of action of furfurylated wood. Topochemical point measurements with varying wavelengths can provide a high spatial resolution of the topochemistry of the colonized cell wall.

To reveal information on the chemical bonds of FA and cell wall lignin, Raman investigations with appropriate setting parameters and spectroscopy design are required. More information is needed on the properties of these chemical bonds to enhance our understanding of FA modified cell wall lignin and its role during brown rot degradation. Finally, this could help to improve the modification process, especially polymerization.

To further study the mechanical characteristics of the furfurylated cell walls (undegraded and at the initial decay stages) regarding deformation and failure mechanisms of the CML, the shearing forces under load in *in situ* SEM micro-compression investigations of micropillars according to Adusumalli et al. (2010) is needed. This data is needed to be able to conclude if

the identified features of initial brown rot decay in the interfaces of the cell wall layers are attacked in their structural integrity.

With respect to the long-term strategic vision for a climate neutral European Union economy by 2050, the improved utilization of biobased resources will be necessary, and this will push the utilization of modified wood forward. Therefore, it is highly relevant to emphasize and promote the carbon storage benefits of FA-modified timers in a constructed environment to be included in future synthesis reports of the Intergovernmental Panel on Climate Change (IPPC). LCA analysis of FA-modified wood, the furfurylation process and the furfurylated wood species studied could be a useful tool for gathering data.

11 References

Adusumalli, R. B., Raghavan, R., Ghisleni, R., Zimmermann, T., & Michler, J. (2010). Deformation and failure mechanism of secondary cell wall in Spruce late wood. *Applied Physics A: Materials Science and Processing*, *100*(2), 447–452. https://doi.org/10.1007/s00339-010-5847-1

Agarwal, U. P. (1999). An Overview of Raman Spectroscopy as Applied to Lignocellulosic Materials. In D. Argyropoulos (Ed.), *Advances in Lignocellilosics Characterization* (pp. 201–225). Tappi Press.

Ahmed, S. A., & Chun, S. K. (2011). Permeability of Tectona grandis L. as affected by wood structure. *Wood Science and Technology*, *45*(3), 487–500. https://doi.org/10.1007/s00226-010-0335-5

Alfredsen, G., Ringman, R., Pilgård, A., & Fossdal, C. G. (2015). New insight regarding mode of action of brown rot decay of modified wood based on DNA and gene expression studies: a review. *International Wood Products Journal*, *6*(1), 5–7. https://doi.org/10.1179/2042645314Y.0000000085

Algeier, S. M. (2014). *Biologischer Abbau von furfuryliertem Holz durch ausgewählte Basidiomyceten* (Issue Master thesis). Technische Universität München.

Arantes, V., & Goodell, B. (2014). Current understanding of brown-rot fungal biodegradation mechanisms: a review. In *Deterioration ...* (pp. 3–21). American Chemical Society. https://doi.org/10.1021/bk-2014-1158

Arantes, V., Jellison, J., & Goodell, B. (2012). Peculiarities of brown-rot fungi and biochemical Fenton reaction with regard to their potential as a model for bioprocessing biomass. *Applied Microbiology and Biotechnology*, *94*(2), 323–338. https://doi.org/10.1007/s00253-012-3954-y

Arantes, V., Milagres, A. M. F., Filley, T. R., & Goodell, B. (2011). Lignocellulosic polysaccharides and lignin degradation by wood decay fungi: the relevance of nonenzymatic Fenton-based reactions. *Journal of Industrial Microbiology & Biotechnology*, *38*(4), 541–555. https://doi.org/10.1007/s10295-010-0798-2

Bariska, M., Osuský, A., & Bosshard, H. H. (1983). Änderung der Mechanischen Eigenschaften von Holz nach Abbau durch Basidiomyceten. *Holz Als Roh- Und Werkstoff*, *41*(6), 241–245. https://doi.org/10.1007/BF02608570

Barsberg, S. T., & Thygesen, L. G. (2017). A Combined Theoretical and FT-IR Spectroscopy Study of a Hybrid Poly(furfuryl alcohol) - Lignin Material: Basic Chemistry of a Sustainable Wood Protection Method. *ChemistrySelect*, *2*(33), 10818–10827. https://doi.org/10.1002/slct.201702104

Bauch, J., Seehann, G., & Fitzner, H. (1976). Microspectrophotometrical investigations on lignin of decayed wood. *Mat Org*, *3*, 141–152.

Beck, G., Hill, C. A. S., Cocher, P. M., & Alfredsen, G. (2019). Accessibility of hydroxyl groups in furfurylated wood at different weight percent gains and during Rhodonia placenta decay. *European Journal of Wood and Wood Products*, *77*(5), 953–955. https://doi.org/10.1007/s00107-019-01445-4

Bergander, A., & Salmén, L. (2002). Cell wall properties and their effects on the mechanical properties of fibers. *Journal of Materials Science*, *37*(1), 151–156. https://doi.org/10.1023/A:1013115925679

Bock, P., & Gierlinger, N. (2019). Infrared and Raman spectra of lignin substructures: Coniferyl alcohol, abietin, and coniferyl aldehyde. *Journal of Raman Spectroscopy*, *February*, 778–792. https://doi.org/10.1002/jrs.5588

Bollmus, S., Beeretz, C., & Militz, H. (2020). Tensile and impact bending properties of chemically modified scots pine. *Forests*, *11*(1). https://doi.org/10.3390/f11010084

Booker, R. E. (1990). Changes in transverse wood permeability during the drying of Dacrydium cupressinum and Pinus radiata. *New Zealand Journal of Forestry Science*, *20*(2), 231–244.

Bravery, Anthony F. (1979). A miniaturised wood-block test for rapid evaluation of wood preservative fungicides. In A. F. Bravery & D. J. Dickinson (Eds.), *In: Screening techniques for potential wood preservative chemicals. Proceedings of a special seminar held in association with the 10th annual meeting of the IRG, Peebles 1978.* Swedish Wood Preservation Institute Report No. 136. Stockholm.

Briggs, R. T., Drath, D. B., Karnovsky, M. L., & Karnovsky, M. J. (1975). Localization of NADH oxidase on the surface of human polymorphonuclear leukocytes by a new cytochemical method. *Journal of Cell Biology*, *67*(3), 566–586. https://doi.org/10.1083/jcb.67.3.566

Brischke, C., & Alfredsen, G. (2020). Wood-water relationships and their role for wood susceptibility to fungal decay. *Applied Microbiology and Biotechnology*, *104*(9), 3781–3795. https://doi.org/10.1007/s00253-020-10479-1

Brischke, C., & Meyer-Veltrup, L. (2016). Modelling timber decay caused by brown rot fungi. *Materials and Structures/Materiaux et Constructions*, *49*(8), 3281–3291. https://doi.org/10.1617/s11527-015-0719-y

Bro, R. (1997). PARAFAC. Tutorial and applications. *Chemometrics and Intelligent Laboratory Systems*, *38*(2), 149–171. https://doi.org/10.1016/S0169-7439(97)00032-4

Candelier, K. (2018). Heat Treatments (ISPM 15) and Thermal Modifications of Wood. *RACEWOOD Technical Conferences*, *June*.

Candelier, K., & Dibdiakova, J. (2020). A review on life cycle assessments of thermally modified wood. *Holzforschung*, *August*. https://doi.org/10.1515/hf-2020-0102

Candelier, K., Thevenon, M.-F., Petrissans, A., Dumarcay, S., Gerardin, P., & Petrissans, M. (2016). Control of wood thermal treatment and its effects on decay resistance: a review. *Annals of Forest Science*, *73*(3), 571–583. https://doi.org/10.1007/s13595-016-0541-x

Carll, C. G., & Highley, T. L. (1999). Decay of Wood and Wood-Based Products Above Ground in Buildings. *Journal of Testing and Evaluation*, *27*(2), 150–158. https://doi.org/10.1520/JTE12054J

Civardi, C., Schubert, M., Fey, A., Wick, P., & Schwarze, F. W. M. R. (2015). Micronized copper wood preservatives: Efficacy of ion, nano, and bulk copper against the brown rot fungus rhodonia placenta. *PLoS ONE*, *10*(11). https://doi.org/10.1371/journal.pone.0142578

Comstock, G. L., & Côté, W. A. (1968). Factors affecting permeability and pit aspiration in coniferous sapwood. *Wood Science and Technology*, *2*(4), 279–291. https://doi.org/10.1007/BF00350274

Curling, S., Clausen, C., & Winandy, J. (2002). Relationships between mechanical properties, weight loss and chemical composition of wood during incipient brown rot decay. *Forest Products Journal*, *52*, 34–40.

Daniel, G., & Nilsson, T. (1998). Developments in the Study of Soft Rot and Bacterial Decay. In A. Bruce & J. W. Palfreyman (Eds.), *Forest Products Biotechnology* (pp. 37–62). Taylor & Francis. https://doi.org/10.1201/9781482272734-5

Durability of wood and wood-based products. Natural durability of solid wood. Part 1: General, (2016).

Donaldson, L. A. (2001). Lignification and lignin topochemistry - An ultrastructural view. *Phytochemistry*, *57*(6), 859–873. https://doi.org/10.1016/S0031-9422(01)00049-8

Donaldson, L. A. (2019). Wood cell wall ultrastructure the key to understanding wood properties and behaviour. *IAWA Journal*, *40*(4), 645–672. https://doi.org/10.1163/22941932-40190258

Eastwood, D. C., Floudas, D., Binder, M., Majcherczyk, A., Schneider, P., Aerts, A., Asiegbu, F. O., Baker, S. E., Barry, K., Bendiksby, M., Blumentritt, M., Coutinho, P. M., Cullen, D., de Vries, R. P., Gathman, A., Goodell, B., Henrissat, B., Ihrmark, K., Kauserud, H., … Watkinson, S. C. (2011). The Plant Cell Wall–Decomposing Machinery Underlies the Functional Diversity of Forest Fungi. *Science*, *333*(6043), 762–765. https://doi.org/10.1126/science.1205411

Eaton, R. A., & Hale, M. D. C. (1993). *Wood: Deacy, Pests and Protection* (1st ed.). Chapman & Hall.

Ehmcke, G., Ringman, R., Pilgård, A., & Richter, K. (2014). Improvement of a cytochemical method for localization of hydrogen peroxide and adaptation to furfurylated wood. *Proceedings of the 10th Meeting of the Nordic Baltic Network in Wood Material Science & Engineering (WSE)*.

Eikenes, M., Flæte, P. O., Haartveit, E. Y., & Lande, S. (2004). Prediction of Weight Percent Gain (WPG) of furfurylated wood by FT-NIR spectroscopy. *The 35th Annual Meeting on the International Research Group on Wood Preservation*, *June*, 9.

Epmeier, H., Westin, M., & Rapp, A. (2004). Differently modified wood: comparison of some selected properties. *Scandinavian Journal of Forest Research*, *19*(sup5), 31–37. https://doi.org/10.1080/02827580410017825

Eriksson, K.-E. L., Blanchette, R. A., & Ander, P. (1990). *Biodegradation of Cellulose* (pp. 89–180). https://doi.org/10.1007/978-3-642-46687-8_2

Esteves, B. M., Nunes, L., & Pereira, H. (2011). Properties of furfurylated wood (Pinus pinaster). *European Journal of Wood and Wood Products*, *69*(4), 521–525. https://doi.org/10.1007/s00107-010-0480-4

European Commission. (2018). A Clean Planet for all. A European strategic long-term vision for a prosperous, modern, competitive and climate neutral economy. In *COMMUNICATION FROM THE COMMISSION TO THE EUROPEAN PARLIAMENT, THE EUROPEAN COUNCIL, THE COUNCIL, THE EUROPEAN ECONOMIC AND SOCIAL COMMITTEE, THE COMMITTEE OF THE REGIONS AND THE EUROPEAN INVESTMENT BANK: Vol. COM* (Issue 773 final).

Fackler, K., Stevanic, J. S., Ters, T., Hinterstoisser, B., Schwanninger, M., & Salmén, L. (2010). Localisation and characterisation of incipient brown-rot decay within spruce wood cell walls using FT-IR imaging microscopy. *Enzyme and Microbial Technology*, *47*(6), 257–267. https://doi.org/10.1016/j.enzmictec.2010.07.009

Fackler, K., & Thygesen, L. G. (2013). Microspectroscopy as applied to the study of wood molecular structure. *Wood Science and Technology*, *47*(1), 203–222. https://doi.org/10.1007/s00226-012-0516-5

Faix, O. (1991). Classification of Lignins from Different Botanical Origins by FT-IR Spectroscopy. *Holzforschung*, *45*(s1), 21–28. https://doi.org/10.1515/hfsg.1991.45.s1.21

Falco, G., Guigo, N., Vincent, L., & Sbirrazzuoli, N. (2018a). FA polymerization disruption by protic polar solvents. *Polymers*, *10*(5), 1–14. https://doi.org/10.3390/polym10050529

Falco, G., Guigo, N., Vincent, L., & Sbirrazzuoli, N. (2018b). Opening Furan for Tailoring Properties of Bio-based Poly(Furfuryl Alcohol) Thermoset. *ChemSusChem*, *11*(11), 1805–1812. https://doi.org/10.1002/cssc.201800620

Fengel, D., & Wegener, G. (1983). *Wood* (D. Fengel & G. Wegener (eds.)). DE GRUYTER. https://doi.org/10.1515/9783110839654

Fergus, B. J., & Goring, D. A. I. (1970a). The Distribution of Lignin in Birch Wood as Determined by Ultraviolet Microscopy. *Holzforschung*, *24*(4), 118–124. https://doi.org/10.1515/hfsg.1970.24.4.118

Fergus, B. J., & Goring, D. A. I. (1970b). The Location of Guaiacyl and Syringyl Lignins in Birch Xylem Tissue. *Holzforschung*, *24*(4), 113–117. https://doi.org/10.1515/hfsg.1970.24.4.113

Fergus, B. J., Procter, A. R., Scott, J. A. N., & Goring, D. A. I. (1969). The distribution of lignin in sprucewood as determined by ultraviolet microscopy. *Wood Science and Technology*, *3*(2), 117–138. https://doi.org/10.1007/BF00639636

Fernandes, A. N., Thomas, L. H., Altaner, C. M., Callow, P., Forsyth, V. T., Apperley, D. C., Kennedy, C. J., & Jarvis, M. C. (2011). Nanostructure of cellulose microfibrils in spruce wood. *Proceedings of the National Academy of Sciences of the United States of America*, *108*(47). https://doi.org/10.1073/pnas.1108942108

Ferreira, J., Esteves, B. M., Nunes, L., & Domingos, I. (2016). Life Cycle Assessment as a tool to promote sustainable Thermowood boards: a Portuguese case study. *International Wood Products Journal*, *7*(3), 124–129. https://doi.org/10.1080/20426445.2016.1160592

Fox, T. (2016). Infrarot- und Raman-Spektren. In M. Hesse, H. Meier, & B. Zeh (Eds.), *Spektroskopische Methoden in der organischen Chemie* (9th ed., pp. 38–40). Thieme.

Fredriksson, M. (2019). On Wood–Water Interactions in the Over-Hygroscopic Moisture Range—Mechanisms, Methods, and Influence of Wood Modification. *Forests*, *10*(9), 779. https://doi.org/10.3390/f10090779

Fukazawa, K. (1992). Ultraviolet Microscopy. In L. D. C. SY (Ed.), *Lignin chemestry* (pp. 110–121). Springer Verlag. https://doi.org/10.1007/978-3-642-74065-7_8

Gandini, A., & Belgacem, M. N. (1997). Furans in polymer chemistry. *Progress in Polymer Science*, *22*(6), 1203–1379. https://doi.org/10.1016/S0079-6700(97)00004-X

Garzuglia, M. (FAO). (2018). The Global Forest Resources Assessment 2015. In S. Russell & D. Henderson-Howat (Eds.), *Seventy years of FAO's Global Forest Resources Assessment(1948-2018). Historical overview and future prospects* (pp. 52–53). FAO.

Gérardin, P. (2016). New alternatives for wood preservation based on thermal and chemical modification of wood— a review. *Annals of Forest Science*, *73*(3), 559–570. https://doi.org/10.1007/s13595-015-0531-4

Gierlinger, N., Luss, S., König, C., Konnerth, J., Eder, M., & Fratzl, P. (2010). Cellulose microfibril orientation of Picea abies and its variability at the micron-level determined by Raman imaging. *Journal of Experimental Botany*, *61*(2), 587–595. https://doi.org/10.1093/jxb/erp325

Goldschmid, O. (1971). Ultraviolet Spectra. In K. V. Sarkanen & C. H. Ludwig (Eds.), *Lignins. Occurence, Formation, Structure and Reactions.* (pp. 241–266).

Goldstein, I. S., & Dreher, W. A. (1960). *Stable Furfuryl Alcohol Impregnating Solutions*. *52*(1), 57–58.

Goodell, B., Jellison, J., Liu, J., Daniel, G., Paszczynski, a., Fekete, F., Krishnamurthy, S., Jun, L., & Xu, G. (1997). Low molecular weight chelators and phenolic compounds isolated from wood decay fungi and their role in the fungal biodegradation of wood1This is paper 2084 of the Maine Agricultural and Forest Experiment Station.1. *Journal of Biotechnology*, *53*(2–3), 133–162. https://doi.org/10.1016/S0168-1656(97)01681-7

Goodell, Barry, Zhu, Y., Kim, S., Kafle, K., Eastwood, D., Daniel, G., Jellison, J., Yoshida, M., Groom, L., Pingali, S. V., & O'Neill, H. (2017). Modification of the nanostructure of lignocellulose cell walls via a non-enzymatic lignocellulose deconstruction system in brown rot wood-decay fungi. *Biotechnology for Biofuels*, *10*(1), 179. https://doi.org/10.1186/s13068-017-0865-2

Göpel, W., & Ziegler, C. (1994). *Struktur der Materie: Grundlagen, Mikroskopie und Spektroskopie*. Vieweg+Teubner Verlag. https://doi.org/10.1007/978-3-322-99522-3

Gradeci, K., Labonnote, N., Köhler, J., & Time, B. (2017). Mould Models Applicable to Wood-Based Materials-A Generic Framework. *Energy Procedia*, *132*, 177–182. https://doi.org/10.1016/j.egypro.2017.09.751

Hammel, K. E., Kapich, A. N., Jensen, K. A., & Ryan, Z. C. (2002). Reactive oxygen species as agents of wood decay by fungi. *Enzyme and Microbial Technology*, *30*(4), 445–453. https://doi.org/10.1016/S0141-0229(02)00011-X

Hecht, T. (2019). Physikalische Grundlagen der IR-Spektroskopie. In *Klima, Kälte, Heizung* (Vol. 18, Issue 3). Springer Fachmedien Wiesbaden. https://doi.org/10.1007/978-3-658-27535-8

Henriksson, G., Brännvall, E., & Lennholm, H. (2009). 2. The Trees. In *Wood Chemistry and Wood Biotechnology* (pp. 13–44). De Gruyter. https://doi.org/https://doi.org/10.1515/9783110213409.13

Hesse, M. (2016). Raman-Spektroskopie. In Hesse, Meier, & Zeeh (Eds.), *Spektroskopische Methoden in der organischen Chemie* (9th ed., pp. 68–74). Georg Thieme Verlag KG. http://doi.wiley.com/10.1002/prac.19813230126

Hill, C. A. S. (2006). Wood Modification. In *Wood Modification: Chemical, Thermal and Other Processes*. John Wiley & Sons, Ltd. https://doi.org/10.1002/0470021748

Hill, C. A. S. (2011). Wood modification: An update. *BioResources*, *6*(2), 918–919. https://doi.org/10.15376/biores.6.2.918-919

Hill, C. A. S. (2019). The Environmental Consequences Concerning the Use of Timber in the Built Environment. *Frontiers in Built Environment*, *5*(October), 1–10. https://doi.org/10.3389/fbuil.2019.00129

Hingston, J. A., Collins, C. D., Murphy, R. J., & Lester, J. N. (2001). Leaching of chromated copper arsenate wood preservatives: A review. *Environmental Pollution*, *111*(1), 53–66. https://doi.org/10.1016/S0269-7491(00)00030-0

Höglmeier, K., Weber-Blaschke, G., & Richter, K. (2017). Erratum: Potentials for cascading of recovered wood from building deconstruction—A case study for south-east Germany (Resources, Conservation and Recycling (2013) 78 (81–91) (S0921344913001444)(10.1016/j.resconrec.2013.07.004)). *Resources, Conservation and Recycling*, *117*, 304–314. https://doi.org/10.1016/j.resconrec.2015.10.030

Homan, W. J., & Jorissen, A. J. M. (2004). Wood modification developments. *Heron*, *49*(4), 361–386.

Homan, W. J., & Tjeerdsma, B. (2000). Structural and other properties of modified wood. *Congress WCTE*, *January*.

Hosseinpourpia, R., & Mai, C. (2016). Mode of action of brown rot decay resistance of acetylated wood: resistance to Fenton's reagent. *Wood Science and Technology*, *50*(2), 413–426. https://doi.org/10.1007/s00226-015-0790-0

Huckfeldt, T., & Schmidt, O. (2015). *Hausfäule- und Bauholzpilze: Diagnose und Sanierung* (R. Müller (ed.); 2nd ed.).

Hunt, C. G., Zelinka, S. L., Frihart, C. R., Lorenz, L., Yelle, D. J., Gleber, S.-C., Vogt, S., & Jakes, J. E. (2018). Acetylation increases relative humidity threshold for ion transport in wood cell walls – A means to understanding decay resistance. *International Biodeterioration & Biodegradation*, *133*(September), 230–237. https://doi.org/10.1016/j.ibiod.2018.06.014

Ibach, R. E. (2013). Biological Properties. In R. M. Rowell (Ed.), *Wood Chemistry and Wood Composites* (2nd ed., pp. 99–126). CRC Press.

Irbe, I., Noldt, G., Koch, G., Andersone, I., & Andersons, B. (2006). Application of scanning UV microspectrophotometry for the topochemical detection of lignin within individual cell walls of brown-rotted Scots pine (Pinus sylvestris L.) sapwood. *Holzforschung*, *60*(6), 601–607. https://doi.org/10.1515/HF.2006.102

Jakes, J. E., Hunt, C. G., Zelinka, S. L., Ciesielski, P. N., & Plaza, N. Z. (2019). Effects of Moisture on Diffusion in Unmodified Wood Cell Walls: A Phenomenological Polymer Science Approach. *Forests*, *10*(12), 1–48. https://doi.org/10.3390/f10121084

Jebrane, M., & Sèbe, G. (2007). A novel simple route to wood acetylation by transesterification with vinyl acetate. *Holzforschung*, *61*(2), 143–147. https://doi.org/10.1515/HF.2007.026

Jensen, K. A., Houtman, C. J., Ryan, Z. C., & Hammel, K. E. (2001). Pathways for Extracellular Fenton Chemistry in the Brown Rot Basidiomycete Gloeophyllum trabeum. *Applied and Environmental Microbiology*, *67*(6), 2705–2711. https://doi.org/10.1128/AEM.67.6.2705-2711.2001

Jones, D., Sandberg, D., Goli, G., & Todaro, L. (2019). Wood Modification in Europe. In D. Jones, D. Sandberg, G. Goli, & L. Todaro (Eds.), *Wood Modification in Europe a state-of-the-art about processes, products and applications* (Proceedings e Report, Vol. 124). Firenze University Press. https://doi.org/10.36253/978-88-6453-970-6

Junga, U., & Militz, H. (2005). Particularities in agar block tests of some modifed woods caused by different protection and decay principles. In H. Militz & C. A. S. Hill (Eds.), *Proceedings of the 2nd European Conference on Wood Modification* (pp. 354–362). University of Göttingen.

Karnovsky, M. J. (1965). A formaldehyde-glutaraldehyde fixative of high osmolaty for use in electron microscopy. *The American Society for Cell Biology*, *27*, 137–138. http://www.jstor.org/stable/1604673

Keplinger, T., Konnerth, J., Aguié-Béghin, V., Rüggeberg, M., Gierlinger, N., & Burgert, I. (2014). A zoom into the nanoscale texture of secondary cell walls. *Plant Methods*, *10*(1), 1–7. https://doi.org/10.1186/1746-4811-10-1

Kielmann, B. C., Adamopoulos, S., Militz, H., Koch, G., & Mai, C. (2013). Modification of three hardwoods with an N-methylol melamine compound and a metal-complex dye. *Wood Science and Technology*, *48*(1), 123–136. https://doi.org/10.1007/s00226-013-0595-y

Kim, J. H., Sutley, E. J., & Martin, F. (2019). Review of Modern Wood Fungal Decay Research for Implementation into a Building Standard of Practice. *Journal of Materials in Civil Engineering*, *31*(12). https://doi.org/10.1061/(ASCE)MT.1943-5533.0002998

Kim, J. S., Gao, J., & Daniel, G. (2015). Ultrastructure and immunocytochemistry of degradation in spruce and ash sapwood by the brown rot fungus Postia placenta: Characterization of incipient stages of decay and variation in decay process. *International Biodeterioration & Biodegradation*, *103*, 161–178. https://doi.org/10.1016/j.ibiod.2015.05.005

Kim, Y. S., & Singh, A. P. (2000). Micromorphological chracteristics of wood biodegradation in wet environments: a review. *IAWA Journal*, *21*(2), 135–155. https://doi.org/10.1163/22941932-90000241

Kim, Y. S., Wi, S. G., Lee, K. H., & Singh, A. P. (2002). Cytochemical Localization of Hydrogen Peroxide Production during Wood Decay by Brown-Rot Fungi Tyromyces palustris and Coniophora puteana. *Holzforschung*, *56*(1), 7–12. https://doi.org/10.1515/HF.2002.002

Klaassen, R. K. W. M., & van Overeem, B. S. (2012). Factors that influence the speed of bacterial wood degradation. *Journal of Cultural Heritage*, *13*(3 SUPPL.), S129–S134. https://doi.org/10.1016/j.culher.2012.02.016

Kleist, G., & Seehann, G. (1997). Colonization patterns and topochemical aspects of sap streak in Norway spruce caused by Stereum sanguinolentum. *European Journal for Path*, *27*, 351–361.

Koch, G., & Grünwald, C. (2004). Application of UV microspectrophotometry for the topochemical detection of lignin and phenolic extractives in wood fibre cell walls. In U. Schmitt, P. Ander, J. R. Barnett, A. M. C. Emons, G. Jeronimidis, P. Saranpää, & S. Tschegg (Eds.), *Wood Fibre Cell Walls: Methods to Study their Formation, Structure and Properties* (pp. 119–130). Swedish University of Agricultural Sciences.

Koch, G., & Kleist, G. (2001). Application of Scanning UV Microspectrophotometry to Localise Lignins and Phenolic Extractives in Plant Cell Walls. *Holzforschung*, *55*(6), 563–567. https://doi.org/10.1515/HF.2001.091

Koch, G., Rose, B., Patt, R., & Kordsachia., O. (2003). Topochemical Investigations on Delignification of Picea abies [L.] Karst. during Alkaline Sulfite (ASA) and Bisulfite Pulping by Scanning UV Microspectrophotometry. *Holzforschung*, *57*(6), 611–618. https://doi.org/10.1515/HF.2003.092

Koch, G., & Schmitt, U. (2013). Topochemical and Electron Microscopic Analyses on the Lignification of Individual Cell Wall Layers During Wood Formation and Secondary Changes. In J. Fromm (Ed.), *Cellular Aspects of Wood Formation* (Vol. 20, pp. 41–69). Springer Berlin Heidelberg. https://doi.org/10.1007/978-3-642-36491-4_2

Kölle, M., Ringman, R., & Pilgård, A. (2019). Initial Rhodonia placenta Gene Expression in Acetylated Wood: Group-Wise Upregulation of Non-Enzymatic Oxidative Wood Degradation Genes Depending on the Treatment Level. *Forests*, *10*(12), 1117. https://doi.org/10.3390/f10121117

Kollmann, F., & Fengel, D. (1965). Änderungen der chemischen Zusammensetzung von Holz durch thermische Behandlung. *Holz Als Roh- Und Werkstoff*, *23*(12), 461. https://doi.org/10.1007/BF02627217

Kotwa, E., Jørgensen, B., Brockhoff, P. B., & Frosch, S. (2013). Automatic scatter detection in fluorescence landscapes by means of spherical principal component analysis. *Journal of Chemometrics*, *27*(1–2), 3–11. https://doi.org/10.1002/cem.2485

Künniger, T., Gerecke, A. C., Ulrich, A., Huch, A., Vonbank, R., Heeb, M., Wichser, A., Haag, R., Kunz, P., & Faller, M. (2014). Release and environmental impact of silver nanoparticles and conventional organic biocides from coated wooden façades. *Environmental Pollution*, *184*, 464–471. https://doi.org/10.1016/j.envpol.2013.09.030

Lähdetie, A., Nousiainen, P., Sipilä, J., Tamminen, T., & Jääskeläinen, A.-S. (2013). Laser-induced fluorescence (LIF) of lignin and lignin model compounds in Raman spectroscopy. *Holzforschung*, *67*(5), 531–538. https://doi.org/10.1515/hf-2012-0177

Lande, S., Eikenes, M., & Westin, M. (2004). Chemistry and ecotoxicology of furfurylated wood. *Scandinavian Journal of Forest Research*, *19*(sup5), 14–21. https://doi.org/10.1080/02827580410017816

Lande, S., Eikenes, M., Westin, M., & Schneider, M. H. (2008). *Furfurylation of Wood: Chemistry, Properties, and Commercialization* (pp. 337–355). https://doi.org/10.1021/bk-2008-0982.ch020

Lande, S., Høibø, O., & Larnøy, E. (2010). Variation in treatability of Scots pine (Pinus sylvestris) by the chemical modification agent furfuryl alcohol dissolved in water. *Wood Science and Technology*, *44*(1), 105–118. https://doi.org/10.1007/s00226-009-0272-3

Lande, S., Westin, M., & Schneider, M. H. (2004a). Eco-efficient wood protection. *Management of Environmental Quality: An International Journal*, *15*(5), 529–540. https://doi.org/10.1108/14777830410553979

Lande, S., Westin, M., & Schneider, M. H. (2004b). Properties of furfurylated wood. *Scandinavian Journal of Forest Research*, *19*(sup5), 22–30. https://doi.org/10.1080/0282758041001915

Larsson Brelid, P. (2013). Benchmarking and state of- the-art report for modified wood. *SP Report No. 54, SP Technical Research Institute of Sweden, Stockholm, Sweden*, 1–31. http://www.diva-portal.org/smash/get/diva2:96 2771/FULLTEXT01.pdf

Larsson Brelid, P., Simonson, R., Bergman, Ö., & Nilsson, T. (2000). Resistance of acetylated wood to biological degradation. *Holz Als Roh- Und Werkstoff*, *58*(5), 331–337. https://doi.org/10.1007/s001070050439

Lebow, S. T. (2004). Alternatives to chromated copper arsenate for residential construction. In *U.S. Department of Agriculture, Forest Service, Forest Products Laboratory*. https://doi.org/10.2737/FPL-RP-618

Lee, M., Jeon, H. S., Kim, S. H., Chung, J. H., Roppolo, D., Lee, H., Cho, H. J., Tobimatsu, Y., Ralph,

J., & Park, O. K. (2019). Lignin-based barrier restricts pathogens to the infection site and confers resistance in plants. *The EMBO Journal*, *38*(23), 1–17. https://doi.org/10.15252/embj.2019101948

Lehringer, C., Richter, K., Schwarze, F. W. M. R., & Militz, H. (2009). A review on promising approaches for liquid permeability improvement in softwoods. *Wood and Fiber Science*, *41*(4), 373–385.

Li, W., Ren, D., Zhang, X., Wang, H., & Yu, Y. (2016). The Furfurylation of Wood: A Nanomechanical Study of Modified Wood Cells. *BioResources*, *11*(2), 3614–3625. https://doi.org/10.15376/biores.11.2.3614-3625

Li, W., Wang, H., Ren, D., Yu, Y., & Yu, Y. (2015). Wood modification with furfuryl alcohol catalysed by a new composite acidic catalyst. *Wood Science and Technology*, *49*(4), 845–856. https://doi.org/10.1007/s00226-015-0721-0

Liese, W. (1960). Die Struktur der Tertiärwand in Tracheiden und Holzfasern. *Holz Als Roh- Und Werkstoff*, *18*(8), 296–303. https://doi.org/10.1007/BF02626118

Liese, W. (1970). Ultrastructural Aspects of Woody Tissue Disintegration. *Annual Review of Phytopathology*, *8*(1), 231–258. https://doi.org/10.1146/annurev.py.08.090170.001311

Liese, W., & Bauch, J. (1967). On the closure of Bordered Pits in Conifers. *Wood Science and Technology*, *1*, 1–13.

Liu, M., Li, W., Wang, H., Zhang, X., & Yu, Y. (2020). The distribution of furfuryl alcohol (FA) resin in bamboo materials after surface furfurylation. *Materials*, *13*(5). https://doi.org/10.3390/ma13051157

Long, D. A. (2002). The Raman effect: a unified treatment of the theory of Raman scattering by molecules. 2002. In *West Sussex, England: John Wiley & Sons Ltd* (Vol. 8).

Mahnert, K.-C., Adamopoulos, S., Koch, G., & Militz, H. (2013). Topochemistry of heat-treated and N-methylol melamine-modified wood of koto (Pterygota macrocarpa K. Schum.) and limba (Terminalia superba Engl. et. Diels). *Holzforschung*, *67*(2), 137–146. https://doi.org/10.1515/hf-2012-0017

Mantanis, G. I. (2017). Chemical Modification of Wood by Acetylation or Furfurylation: A Review of the Present Scaled-up Technologies. *BioResources*, *12*(2), 4478–4489. https://doi.org/10.15376/biores.12.2.Mantanis

Martínez, Á. T., Rencoret, J., Nieto, L., Jiménez-Barbero, J., Gutiérrez, A., & del Río, J. C. (2011). Selective lignin and polysaccharide removal in natural fungal decay of wood as evidenced by in situ structural analyses. *Environmental Microbiology*, *13*(1), 96–107. https://doi.org/10.1111/j.1462-2920.2010.02312.x

Martínez, Á. T., Speranza, M., Ruiz-Dueñas, F. J., Ferreira, P., Camarero, S., Guillén, F., Martínez, M. J., Gutiérrez, A., & Del Río, J. C. (2005). Biodegradation of lignocellulosics: Microbial, chemical, and enzymatic aspects of the fungal attack of lignin. *International Microbiology*, *8*(3), 195–204. https://doi.org/10.2436/im.v8i3.9526

Martinez, D., Challacombe, J., Morgenstern, I., Hibbett, D., Schmoll, M., Kubicek, C. P., Ferreira, P., Ruiz-Duenas, F. J., Martínez, Á. T., Kersten, P., Hammel, K. E., Vanden Wymelenberg, A., Gaskell, J., Lindquist, E., Sabat, G., Splinter BonDurant, S., Larrondo, L. F., Canessa, P., Vicuna, R., … Cullen, D. (2009). Genome, transcriptome, and secretome analysis of wood decay fungus Postia placenta supports unique mechanisms of lignocellulose conversion. *Proceedings of the National Academy of Sciences*, *106*(6), 1954–1959. https://doi.org/10.1073/pnas.0809575106

Maschek, D., Goodell, B., Jellison, J., Lessard, M., & Mllitz, H. (2013). A new approach for the study of the chemical composition of bordered pit membranes: 4Pi and confocal laser scanning microscopy. *American Journal of Botany*, *100*(9), 1751–1756. https://doi.org/10.3732/ajb.1300004

Mead, D. J. (2013). Sustainable management of Pinus radiata plantations. In *FAO Forestry Paper* (No. 170). FAO.

Meyer, L., & Brischke, C. (2015). Fungal decay at different moisture levels of selected European-grown wood species. *International Biodeterioration and Biodegradation*, *103*. https://doi.org/10.1016/j.ibiod.2015.04.009

Militz, H. (1991). Die Verbesserung des Schwind- und Quellverhaltens und der Dauerhaftigkeit von Holz mittels Behandlung mit unkatalysiertem Essigsäureanhydrid. *Holz Als Roh- Und Werkstoff*, *49*(4), 147–152. https://doi.org/10.1007/BF02607895

Militz, H. (2002). Thermal treatment of wood: European Processes and their background. *The 33rd Annual Meeting on the International Research Group on Wood Preservation*, *IRG/WP 02*-(May), IRG/WP 02-40241.

Müller, J., Ibach, W., Weishaupt, K., & Hollricher, O. (2003). Confocal Raman Microscopy. *Microscopy and Microanalysis*, *9*(S02), 1084–1085. https://doi.org/10.1017/S143192760344542X

Musha, Y., & Goring, D. A. I. (1975). Distribution of syringyl and guaiacyl moieties in hardwoods as indicated by ultraviolet microscopy. *Wood Science and Technology*, *9*(1), 45–58. https://doi.org/10.1007/BF00351914

Nordstierna, L., Lande, S., Westin, M., Karlsson, O., & Furó, I. (2008). Towards novel wood-based materials: Chemical bonds between lignin-like model molecules and poly(furfuryl alcohol) studied by NMR. *Holzforschung*, *62*(6), 709–713. https://doi.org/10.1515/HF.2008.110

Pedersen, D. K., Munck, L., & Engelsen, S. B. (2002). Screening for dioxin contamination in fish oil by PARAFAC and N-PLSR analysis of fluorescence landscapes. *Journal of Chemometrics*, *16*(8–10), 451–460. https://doi.org/10.1002/cem.735

Pereira, L., Flores-Borges, D. N. A., Bittencourt, P. R. L., Mayer, J. L. S., Kiyota, E., Araújo, P., Jansen, S., Freitas, R. O., Oliveira, R. S., & Mazzafera, P. (2018). Infrared nanospectroscopy reveals the chemical nature of pit membranes in water-conducting cells of the plant xylem. *Plant Physiology*, *177*(4), 1629–1638. https://doi.org/10.1104/pp.18.00138

Pilgård, A., Alfredsen, G., & Hietala, A. (2010). Quantification of fungal colonization in modified wood: Quantitative real-time PCR as a tool for studies on Trametes versicolor. *Holzforschung*, *64*(5), 645–651. https://doi.org/10.1515/hf.2010.074

Pilgård, A., Treu, A., van Zeeland, A. N. T., Gosselink, R. J. a, & Westin, M. (2010). Toxic hazard and chemical analysis of leachates from furfurylated wood. *Environmental Toxicology and Chemistry / SETAC*, *29*(9), 1918–1924. https://doi.org/10.1002/etc.244

Preston, A. F. (2000). Wood Preservation – Trends of Today that Will Influence the Industry Tomorrow. *Forest Products Journal*, *50*(9), 12–19.

Rademacher, P., Németh, R., Bak, M., Fodor, F., & Hofmann, T. (2017). European Co-Operation in Wood Research from Native Wood to Engineered Materials. Part 1: Chemical Modification with Native Impregnation Agents. *Pro Ligno*, *13*(4), 341–350.

Rehbein, M., & Koch, G. (2011). Topochemical investigation of early stages of lignin modification within individual cell wall layers of Scots pine (Pinus sylvestris L.) sapwood infected by the brown-rot fungus Antrodia vaillantii (DC.: Fr.) Ryv. *International Biodeterioration & Biodegradation*, *65*(7), 913–920. https://doi.org/10.1016/j.ibiod.2011.04.009

Rehbein, M., Koch, G., Schmitt, U., & Huckfeldt, T. (2013). Topochemical and transmission electron microscopic studies of bacterial decay in pine (Pinus sylvestris L.) harbour foundation piles. *Micron*, *44*(1), 150–158. https://doi.org/10.1016/j.micron.2012.05.012

Reinprecht, L., & Repák, M. (2019). The impact of paraffin-thermal modification of beech wood on its biological, physical and mechanical properties. *Forests*, *10*(12). https://doi.org/10.3390/f10121102

Riley, R., Salamov, A. A., Brown, D. W., Nagy, L. G., Floudas, D., Held, B. W., Levasseur, A., Lombard, V., Morin, E., Otillar, R., Lindquist, E. A., Sun, H., LaButti, K. M., Schmutz, J., Jabbour, D., Luo, H., Baker, S. E., Pisabarro, A. G., Walton, J. D., … Grigoriev, I. V. (2014). Extensive sampling of basidiomycete genomes demonstrates inadequacy of the white-rot/brown-rot paradigm for wood decay fungi. *Proceedings of the National Academy of Sciences*, *111*(27), 9923–9928. https://doi.org/10.1073/pnas.1400592111

Ringman, R., Beck, G., & Pilgård, A. (2019). The Importance of Moisture for Brown Rot Degradation of Modified Wood: A Critical Discussion. *Forests*, *10*(6), 522. https://doi.org/10.3390/f10060522

Ringman, R., Pilgård, A., Brischke, C., & Richter, K. (2014). Mode of action of brown rot decay resistance in modified wood: a review. *Holzforschung*, *68*(2), 239–246. https://doi.org/10.1515/hf-2013-0057

Ringman, R., Pilgård, A., Brischke, C., Windeisen, E., & Richter, K. (2017). Incipient brown rot decay in modified wood: patterns of mass loss, structural integrity, moisture and acetyl content in high resolution. *International Wood Products Journal*, *8*(3), 172–182. https://doi.org/10.1080/20426445.2017.1344382

Rowell, R. M. (1983). Wood modification: a review. *Commonwealth Forestry Bureau*, *6*(12), 363–382.

Rowell, R. M. (2005a). Chemical modification of wood. In R. M. Rowell (Ed.), *Handbook of Wood Chemistry and Wood Composites* (pp. 381–420). Taylor & Francis.

Rowell, R. M. (2005b). *Handbook of wood chemistry and wood coposites* (R. M. Rowell (ed.)). Taylor & Francis.

Rowell, R. M. (2012). Chemical modification of wood to procedure stabele and durable composites. *Cellulose Chemistry and Technology*, *46*(7–8), 537–598.

Rowell, R. M. (2016). Dimensional stability and fungal durability of acetylated wood. *Drewno*, *59*(197), 139–150. https://doi.org/10.12841/wood.1644-3985.C14.04

Rowell, R. M., Hess, S., Plackett, D. V, Cronshaw, D., & Dunningham, E. (1994). Acetyl Distribution in Acetylated Whole Cell-Wall Components To Acetic Anhydride. *Wood and Fiber Science*, *26*(1), 11–18.

Rowell, R. M., Ibach, R. E., James, M., & Thomas, N. (2009). Understanding decay resistance, dimensional stability and strength changes in heat-treated and acetylated wood. *Wood Material Science and Engineering*, *4*(1–2), 14–22. https://doi.org/10.1080/17480270903261339

Rowell, R. M., Pettersen, R., & Tshabalala, M. (2012). Cell Wall Chemistry. In R. M. Rowell (Ed.), *Handbook of Wood Chemistry and Wood Composites, Second Edition* (2nd ed., Issue May, pp. 33–72). CRC Press. https://doi.org/10.1201/b12487-5

Saka, S., Whiting, P., Fukazawa, K., & Goring, D. A. I. (1982). Comparative studies on lignin distribution by UV microscopy and bromination combined with EDXA. *Wood Science and Technology*, *16*(4), 269–277. https://doi.org/10.1007/BF00353151

Salmén, L. (2004). Micromechanical understanding of the cell-wall structure. *Comptes Rendus Biologies*, *327*, 873–880. https://doi.org/10.1016/j.crvi.2004.03.010

Salmén, L., & Burgert, I. (2009). Cell wall features with regard to mechanical performance. A review COST Action E35 2004–2008: Wood machining – micromechanics and fracture. *Holzforschung*, *63*(2). https://doi.org/10.1515/HF.2009.011

Sandberg, D., Kutnar, A., & Mantanis, G. (2017). Wood modification technologies - a review. *IForest - Biogeosciences and Forestry*, *10*(6), 895–908. https://doi.org/10.3832/ifor2380-010

Schilling, J. S., Duncan, S. M., Presley, G. N., Filley, T. R., Jurgens, J. A., & Blanchette, R. A. (2013). Colocalizing incipient reactions in wood degraded by the brown rot fungus Postia placenta.

International Biodeterioration & Biodegradation, *83*, 56–62. https://doi.org/10.1016/j.ibiod.2013.04.006

Schmidt, O. (2006a). Damages by Viruses and Bacteria. In D. Czeschlik & A. Schlitzberger (Eds.), *Wood and Tree Fungi* (pp. 109–118). Springer Berlin Heidelberg. https://doi.org/10.1007/3-540-32139-X_5

Schmidt, O. (2006b). Habitat of Wood Fungi. In D. Czeschlik & A. Schlitzberger (Eds.), *Wood and Tree Fungi* (pp. 161–236). Springer Berlin Heidelberg. https://doi.org/10.1007/3-540-32139-X_8

Schmidt, O. (2006c). Physiology. In D. Czeschlik & A. Schlitzberger (Eds.), *Wood and Tree Fungi* (pp. 53–85). Springer Berlin Heidelberg. https://doi.org/10.1007/3-540-32139-X_3

Schmidt, O. (2006d). Wood Cell Wall Degradation. In D. Czeschlik & A. Schlitzberger (Eds.), *Wood and Tree Fungi* (pp. 87–107). Springer Berlin Heidelberg. https://doi.org/10.1007/3-540-32139-X_4

Schmidt, O. (2006e). Wood Rot. In D. Czeschlik & A. Schlitzberger (Eds.), *Wood and Tree Fungi* (pp. 135–159). Springer Berlin Heidelberg. https://doi.org/10.1007/3-540-32139-X_7

Schmidt, O., Schmitt, U., Moreth, U., & Potsch, T. (1997). Wood Decay by the White-Rotting Basidiomycete Physisporinus vitreus from a Cooling Tower. *Holzforschung*, *51*(3), 193–200. https://doi.org/10.1515/hfsg.1997.51.3.193

Schneider, M. H. (1995). New cell wall and cell lumen wood polymer composites. *Wood Science and Technology*, *29*(2), 121–127. https://doi.org/10.1007/BF00229341

Schneider, M. H., Phillips, J. G., & Lande, S. (2000). Physical andmechanical properties of wood polymer composites. *J. Forest Eng.*, *11*, 83–89.

Schultze-Dewitz, G. (1966). Beziehungen zwischen der Elastizität und der statischen sowie dynamischen Biegefestigkeit von Kiefernholz nach dem Angriff durch echte holzzerstörende Pilze. *Holz Als Roh- Und Werkstoff*, *24*(10), 506–512. https://doi.org/10.1007/BF02612884

Schwanninger, M., Rodrigues, J. C., Pereira, H., & Hinterstoisser, B. (2004). Effects of short-time vibratory ball milling on the shape of FT-IR spectra of wood and cellulose. *Vibrational Spectroscopy*, *36*(1), 23–40. https://doi.org/10.1016/j.vibspec.2004.02.003

Schwarze, F. W. M. R. (2007). Wood decay under the microscope. *Fungal Biology Reviews*, *21*(4), 133–170. https://doi.org/10.1016/j.fbr.2007.09.001

Scott, J. A. N., Procter, A. R., Fergus, B. J., & Goring, D. A. I. (1969). The application of ultraviolet microscopy to the distribution of lignin in wood description and validity of the technique. *Wood Science and Technology*, *3*(1), 73–92. https://doi.org/10.1007/BF00349985

Sejati, P. S., Imbert, A., Gérardin-Charbonnier, C., Dumarçay, S., Fredon, E., Masson, E., Nandika, D., Priadi, T., & Gérardin, P. (2017). Tartaric acid catalyzed furfurylation of beech wood. *Wood Science and Technology*, *51*(2), 379–394. https://doi.org/10.1007/s00226-016-0871-8

Siau, J. F. (1984). *Transport processes in wood*. Springer Verlag.

Singh, A. P., & Butcher, J. A. (1991). Bacterial degradation of wood cell walls: a review of degradation patterns. *Journal of the Institute of Wood Science*, *12*(3), 143–157.

Singh, A. P., Kim, Y. S., & Singh, T. (2016). Bacterial Degradation of Wood. In *Secondary Xylem Biology: Origins, Functions, and Applications* (Issue July, pp. 169–190). Elsevier Inc. https://doi.org/10.1016/B978-0-12-802185-9.00009-7

Singh, A. P., & Singh, T. (2014). Biotechnological applications of wood-rotting fungi: A review. *Biomass and Bioenergy*, *62*, 198–206. https://doi.org/10.1016/j.biombioe.2013.12.013

Singh, T., & Singh, A. P. (2012). A review on natural products as wood protectant. *Wood Science and Technology*, *46*(5), 851–870. https://doi.org/10.1007/s00226-011-0448-5

Skrede, I., Solbakken, M. H., Hess, J., Fossdal, C. G., Kenar, O., & Alfredson, G. (2019). Wood

Modification by Furfuryl Alcohol Resulted in a Delayed. *Applied and Environmental Microbiology*, *85*(14), 1–21.

Smith, E., & Dent, G. (2005). Modern Raman Spectroscopy - A Practical Approach. In *Modern Raman Spectroscopy - A Practical Approach*. https://doi.org/10.1002/0470011831

Spatafora, J. W., Aime, M. C., Grigoriev, I. V, Martin, F., Stajich, J. E., & Blackwell, M. (2017). The Fungal Tree of Life: From Molecular Systematics to Genome-Scale Phylogenies. In *The Fungal Kingdom* (Issue September, pp. 3–34). American Society of Microbiology. https://doi.org/10.1128/microbiolspec.FUNK-0053-2016

Spurr, A. R. (1969). A low-viscosity epoxy resin embedding medium for electron microscopy. *Journal of Ultrastructure Research*, *26*(1–2), 31–43. https://doi.org/10.1016/S0022-5320(69)90033-1

Stamm, A. J. (1977). Dimensional stabilization of wood with furfuryl alcohol. In I. Goldstein (Ed.), *Wood Chemical Aspects* (pp. 141–149). American Chemical Society.

Stamm, A. J., Burr, H. K., & Kline, A. A. (1946). Staybwood—Heat-Stabilized Wood. *Industrial & Engineering Chemistry*, *38*(6), 630–634. https://doi.org/10.1021/ie50438a027

Stevanic, J. S., & Salmén, L. (2009). Orientation of the wood polymers in the cell wall of spruce wood fibres. *Holzforschung*, *63*(5), 497–503. https://doi.org/10.1515/HF.2009.094

Takabe, K. (2002). Wood Formation in Trees. In N. Chaffey (Ed.), *Wood Formation in Trees: Cell and Molecular Biology Techniques1* (1st ed.). CRC Press. https://doi.org/10.1201/9780203166444

Takabe, K., Miyauchi, S., Tsunoda, R., & Fukazawa, K. (1992). Distribution of Guaiacyl and Syringyl Lignins in Japanese Beech (Fagus Crenata): Variation Within an Annual Ring. *IAWA Journal*, *13*(1), 105–112. https://doi.org/10.1163/22941932-90000561

Tarmian, A., Zahedi Tajrishi, I., Oladi, R., & Efhamisisi, D. (2020). Treatability of wood for pressure treatment processes: a literature review. *European Journal of Wood and Wood Products*, *78*(4), 635–660. https://doi.org/10.1007/s00107-020-01541-w

Terashima, N., & Fukushima, K. (1988). Heterogeneity in formation of lignin?XI: An autoradiographic study of the heterogeneous formation and structure of pine lignin. *Wood Science and Technology*, *22*(3), 259–270. https://doi.org/10.1007/BF00386021

Terashima, N., Kitano, K., Kojima, M., Yoshida, M., Yamamoto, H., & Westermark, U. (2009). Nanostructural assembly of cellulose, hemicellulose, and lignin in the middle layer of secondary wall of ginkgo tracheid. *Journal of Wood Science*, *55*(6), 409–416. https://doi.org/10.1007/s10086-009-1049-x

Thermowood. (2003). ThermoWood® handbook. In *International ThermoWood Association*. www.thermowood.fi

Thybring, E. E. (2013). The decay resistance of modified wood influenced by moisture exclusion and swelling reduction. In *International Biodeterioration and Biodegradation* (Vol. 82, pp. 87–95). Elsevier Ltd. https://doi.org/10.1016/j.ibiod.2013.02.004

Thybring, E. E. (2017). Water relations in untreated and modified wood under brown-rot and white-rot decay. *International Biodeterioration and Biodegradation*, *118*, 134–142. https://doi.org/10.1016/j.ibiod.2017.01.034

Thybring, E. E., Kymäläinen, M., & Rautkari, L. (2018). Moisture in modified wood and its relevance for fungal decay. *IForest*, *11*(3), 418–422. https://doi.org/10.3832/ifor2406-011

Thygesen, L. G., Barsberg, S., & Venås, T. M. (2010). The fluorescence characteristics of furfurylated wood studied by fluorescence spectroscopy and confocal laser scanning microscopy. *Wood Science and Technology*, *44*(1), 51–65. https://doi.org/10.1007/s00226-009-0255-4

Thygesen, L. G., Ehmcke, G., Barsberg, S. T., & Pilgård, A. (2020). Furfurylation result of Radiata pine depends on the solvent. *Wood Science and Technology*, *0123456789*.

https://doi.org/10.1007/s00226-020-01194-1

Tjeerdsma, B. F., Boonstra, M., Pizzi, A., Tekely, P., & Militz, H. (1998). Characterisation of thermally modified wood: molecular reasons for wood performance improvement. *Holz Als Roh-Und Werkstoff*, *56*(3), 149–153. https://doi.org/10.1007/s001070050287

Townsend, T., Dubey, B., Tolaymat, T., & Solo-Gabriele, H. (2005). Preservative leaching from weathered CCA-treated wood. *Journal of Environmental Management*, *75*(2), 105–113. https://doi.org/10.1016/j.jenvman.2004.11.009

Treu, A., Zimmer, K., Brischke, C., Larnøy, E., Gobakken, L. R., Aloui, F., Cragg, S. M., Flæte, P. O., Humar, M., Westin, M., Borges, L., & Williams, J. (2019). Durability and protection of timber structures in marine environments in Europe: An overview. *BioResources*, *14*(4), 10161–10184. https://doi.org/10.15376/biores

Ünver, H., & Öktem, Z. (2013). Controlled cationic polymerization of furfuryl alcohol. *European Polymer Journal*, *49*(5), 1023–1030. https://doi.org/10.1016/j.eurpolymj.2013.01.025

van Eetvelde, G., de Geyter, S., Marchal, P., & Stevens, M. (1998). Aquatic toxicity research of structural materials. *THE INTERNATIONAL RESEARCH GROUP ON WOOD PRESERVATION*.

Venås, T. M. (2008). A study of mechanisms related to the fungal decay protection rendered by wood furfurylation. In *Faculty of Life Sciences*. University of Copnehagen.

Venås, T. M., & Rinnan, Å. (2008). Determination of weight percent gain in solid wood modified with in situ cured furfuryl alcohol by near-infrared reflectance spectroscopy. *Chemometrics and Intelligent Laboratory Systems*, *92*(2), 125–130. https://doi.org/10.1016/j.chemolab.2008.02.002

Vlosky, R. (2009). *Statistical overview of the U . S . wood preserving industry : 2007* (Issue October).

Wadenspanner, A. (2018). *Raman Analysis of Furfuryl Alcohol Modified Radiata Pine (pinus radiata)* (Issue April). Technische Universität München.

Wagenführ, R. (2007). *Holzatlas* (6th ed.). Hanser Verlag.

Wardrop, A. B., & Davies, G. W. (1961). Morphological Factors Relating to the Penetration of Liquids into Wood. *Holzforschung*, *15*(5), 129–141. https://doi.org/10.1515/hfsg.1961.15.5.129

Westin, M. (2003). *Furan polymer impregnated wood: Vol. PCT/NO2003* (Patent No. CA2493512 C). Westin, Mats.

Westin, M., Larsson Brelid, P., Nilsson, T., Rapp, A. O., Dickerson, J. P., Lande, S., & Cragg, S. M. (2016). Marine Borer Resistance of Acetylated and Furfurylated Wood – Results from up to 16 years of Field Exposure. *Proceedings IRG Annual Meeting*, *IRG/WP 16-40756*, 1–9.

Wilcox, W. (1993). Comparative Morphology of Early Stages of Brown-Rot Wood Decay. *IAWA Journal*, *14*(2), 127–138. https://doi.org/10.1163/22941932-90001306

Wimmer, R., & Lucas, B. N. (1997). Comparing Mechanical Properties of Secondary Wall and Cell Corner Middle Lamella in Spruce Wood. *IAWA Journal*, *18*(1), 77–88. https://doi.org/10.1163/22941932-90001463

Winandy, J. E., & Morrell, J. J. (1993). *Relationship between incipient decay, strength, and chemical composition of Douglas-fir heartwood*. http://ir.library.oregonstate.edu/jspui/handle/1957/14208

Winandy, J. E., & Morrell, J. J. (2017). Improving the utility, performance, and durability of wood- and bio-based composites. *Annals of Forest Science*, *74*(1), 1–11. https://doi.org/10.1007/s13595-017-0625-2

Witomski, P., Olek, W., & Bonarski, J. T. (2016). Changes in strength of Scots pine wood (Pinus silvestris L.) decayed by brown rot (Coniophora puteana) and white rot (Trametes versicolor). *Construction and Building Materials*, *102*, 162–166. https://doi.org/10.1016/j.conbuildmat.2015.10.109

Worrall, J. J., Anagnost, S. E., & Zabel, R. A. (1997). Comparison of wood decay among diverse lignicolous fungi. *Mycologia*, *89*(2), 199–219. https://doi.org/10.2307/3761073

Yelle, D. J., Ralph, J., Lu, F., & Hammel, K. E. (2008). Evidence for cleavage of lignin by a brown rot basidiomycete. *Environmental Microbiology*, *10*(7), 1844–1849. https://doi.org/10.1111/j.1462-2920.2008.01605.x

Yelle, D. J., Wei, D., Ralph, J., & Hammel, K. E. (2011). Multidimensional NMR analysis reveals truncated lignin structures in wood decayed by the brown rot basidiomycete Postia placenta. *Environmental Microbiology*, *13*(4), 1091–1100. https://doi.org/10.1111/j.1462-2920.2010.02417.x

Zelinka, S. L., Kirker, G. T., Bishell, A. B., & Glass, S. V. (2020). Effects of Wood Moisture Content and the Level of Acetylation on Brown Rot Decay. *Forests*, *11*(3), 299. https://doi.org/10.3390/f11030299

Zelinka, S. L., Passarini, L., Matt, F., & Kirker, G. (2019). Corrosiveness of Thermally Modified Wood. *Forests*, *11*(1), 50. https://doi.org/10.3390/f11010050

Zelinka, S. L., Ringman, R., Pilgård, A., Thybring, E. E., Jakes, J. E., & Richter, K. (2016). The role of chemical transport in the brown-rot decay resistance of modified wood. *International Wood Products Journal*, *7*(2), 66–70. https://doi.org/10.1080/20426445.2016.1161867

Zhang, J., Presley, G. N., Hammel, K. E., Ryu, J. S., Menke, J. R., Figueroa, M., Hu, D., Orr, G., & Schilling, J. S. (2016). Localizing gene regulation reveals a staggered wood decay mechanism for the brown rot fungus Postia placenta. *Proceedings of the National Academy of Sciences of the United States of America*, *113*(39), 10968–10973. https://doi.org/10.1073/pnas.1608454113

Zhang, J., & Schilling, J. S. (2017). Role of carbon source in the shift from oxidative to hydrolytic wood decomposition by Postia placenta. *Fungal Genetics and Biology*, *106*, 1–8. https://doi.org/10.1016/j.fgb.2017.06.003

Zhu, Y., Plaza, N., Kojima, Y., Yoshida, M., Zhang, J., Jellison, J., Pingali, S. V., O'Neill, H., & Goodell, B. (2020). Nanostructural Analysis of Enzymatic and Non-enzymatic Brown Rot Fungal Deconstruction of the Lignocellulose Cell Wall†. *Frontiers in Microbiology*, *11*(June). https://doi.org/10.3389/fmicb.2020.01389

Zięba-Palus, J., & Michalska, A. (2014). Photobleaching as a useful technique in reducing of fluorescence in Raman spectra of blue automobile paint samples. *Vibrational Spectroscopy*, *74*, 6–12. https://doi.org/10.1016/j.vibspec.2014.06.007

Zimmer, K., Treu, A., & McCulloh, K. A. (2014). Anatomical differences in the structural elements of fluid passage of Scots pine sapwood with contrasting treatability. *Wood Science and Technology*, *48*(2), 435–447. https://doi.org/10.1007/s00226-014-0619-2

12 List of publications

Publications in the context of this dissertation:

Paper I

Reprinted with kind permission from Taylor & Francis: International Wood Products Journal

G. Ehmcke, A. Pilgård, G. Koch and K. Richter (2016) Improvement of a method for topochemical investigations of degraded furfurylated wood. *Int Wood Products Journal*, **7**(2): 96-101.

The original can be accessed at doi.org/10.1080/20426445.2016.1161866

Paper II

Reprinted with kind permission from DeGruyter: Holzforschung

G. Ehmcke, A. Pilgård, G. Koch and K. Richter (2017) Topochemical analyses of furfuryl alcohol modified radiata pine (*Pinus radiata*) by UMSP, light microscopy and SEM. *Holzforschung* **71**(10): 821–831.

The original can be accessed at doi.org DOI 10.1515/hf-2016-0219

Paper III

Reprinted with kind permission from Springer: Wood Science and Technology

L.G. Thygesen, G. Ehmcke, S. Barsberg and A. Pilgård (2020) Furfurylation result of Pinus Radiata depends on the solvent. *Wood Sci Technol* **54,** 929–942.

The original can be accessed at doi.org/10.1007/s00226-020-01194-1

Paper IV

Reprinted with kind permission from Elsevier B. V.: International Biodeterioration & Biodegradation

G. Ehmcke, G. Koch, K. Richter and A. Pilgård (2020) Topochemical and light microscopic investigations of non-enzymatic oxidative changes at the initial decay stage of furfuryl alcohol-modified Radiata pine (*Pinus radiata*) degraded by the brown rot fungus *Rhodonia placenta*. *Int Biodeterioration & Biodegradation* **154,** 105020.

The original can be accessed at doi.org/10.1016/j.ibiod.2020.105020

Conference proceedings

Ehmcke, G., Ringman, R., Pilgård, A., Richter, K. (2014) Improvement of a cytochemical method for localization of hydrogen peroxide and adaptation to furfurylated wood. Proceedings of the 10th Meeting of the Nordic Baltic Network in Wood Material Science & Engineering (WSE). October 13-14, 2014, Edinburgh Scotland. (Oral presentation by G. Ehmcke)

Ehmcke, G., Pilgård, A., Koch, G., Richter, K. (2014) A method for topochemical investigation of furfurylated maple. Proceedings of the International Academy of Wood Science (IAWS) Plenary Meeting 2014 – Sopron (Hungary) – Vienna (Austria) – Eco Efficient Resource Wood with Special Focus on Hardwoods. September 15-18, 2014, Sopron and Vienna. (Oral presentation by G. Ehmcke)

Ehmcke, G., Pilgård, A., Koch, G., Richter, K. (2015) Improvement of a method for topochemical investigations of degraded furfurylated wood. Proceedings of the 8ght European Conference on Wood Modification (ECWM), October 26-27, 2015, Helsinki, Finland. (Oral presentation by G. Ehmcke)

Ehmcke, G., Pilgård, A., Koch, G., Richter, K. (2017): Topochemical analyzes of furfuryl alcohol modified Radiata pine (*Pinus radiata*). Proceedings of the 13th Meeting of the Nordic Baltic Network in Wood Material Science and Engineering (WSE). September 28-29, 2017, Copenhagen, Denmark. (Oral presentation by G. Ehmcke)

13 Annex

Paper I

Improvement of a method for topochemical investigations of degraded furfurylated wood.

Paper II

Topochemical analyses of furfuryl alcohol modified radiata pine (*Pinus radiata*) by UMSP, light microscopy and SEM.

Paper III

Furfurylation results of Pinus Radiata depends on the solvent.

Paper IV

Topochemical and light microscopic investigations of non-enzymatic oxidative changes at the initial decay stage of furfuryl alcohol-modified radiata pine (*Pinus radiata*) degraded by the brown rot fungus *Rhodonia placenta*.

I

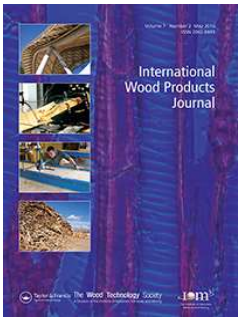

International Wood Products Journal

ISSN: 2042-6445 (Print) 2042-6453 (Online) Journal homepage: http://www.tandfonline.com/loi/ywpj20

Improvement of a method for topochemical investigations of degraded furfurylated wood

G. Ehmcke, A. Pilgård, G. Koch & K. Richter

To cite this article: G. Ehmcke, A. Pilgård, G. Koch & K. Richter (2016) Improvement of a method for topochemical investigations of degraded furfurylated wood, International Wood Products Journal, 7:2, 96-101, DOI: 10.1080/20426445.2016.1161866

To link to this article: http://dx.doi.org/10.1080/20426445.2016.1161866

Published online: 16 Jun 2016.

Improvement of a method for topochemical investigations of degraded furfurylated wood

G. Ehmcke*[1], A. Pilgård[1,2], G. Koch[3] and K. Richter[1]

Today there is an increasing demand for wood protection systems which are based on low environmental impact technologies. The aim of this study was to improve a method for investigating furfurylated *Pinus radiata*, both in terms of the furfuryl alcohol polymerisation process in the wood cell wall and the detection of initial signs of brown rot degradation. It is an established theory today that brown rot degradation starts with lignin modification in the outermost part of the secondary cell wall and the combined middle lamella. We adapted a method (cellular UV microspectrophotometry, UMSP) which enables direct imaging of the lignin distribution and modification within individual cell wall layers. Furfurylated *P. radiata*, incubated with *Postia placenta*, were scanned with monochromatic UV-light at 280 nm. The results showed that USMP is a promising method to study furfurylated wood and early fungal degradation damages in the cell wall of furfurylated wood.

Keywords: Brown rot degradation, Furfuryl alcohol, Lignin modification, Modified wood, *Postia placenta*, UV microspectrophotometry

Introduction

Wood applications in building and construction are faced with and influenced by varying environmental conditions and a permanent presence of microbial organisms. Brown rot basidiomycetes are reckoned to cause the most destructive type of wood decay, even before any mass loss is detectable (Schultze-Dewitz 1966; Bariska, Osusk and Bosshard 1983; Winandy and Morrell 1993). Brown rot fungi attack the structural basis of the wood cell wall, cellulose and hemicelluloses, leaving a modified lignin behind (Danninger, Messner and Rohr 1980; Eriksson, Blanchette and Ander 1990; Goodell 2003). Lignin maintains their macromolecular nature throughout brown rot decay (Kirk 1975; Niemenmaa, Uusi-Rauva and Hatakka 2008; Yelle, Ralph, Lu and Hammel 2008), but their structure is modified substantially by hydroxyl radicals produced by the fungi (Yelle *et al.* 2008; Arantes *et al.* 2009; Arantes, Milagres, Filley and Goodell 2011; Martinez *et al.* 2011; Yelle, Wei, Ralph and Hammel 2011).

To delay or even prevent biodegradation processes, different wood protection and modification systems are available. Today there is an increasing demand for wood preservative methods which are based on technologies with low environmental impact. Wood modification involves the action of a chemical, biological or physical agent upon the material, resulting in increased durability and dimensional stability (Hill 2006). In contrast to treatments with traditional wood preservatives, where the decay resistance is caused mainly by the toxicity of the chemicals added, little is known about the mode of action of modified wood. Furfurylation of wood is a chemical modification where furfuryl alcohol (FA) penetrates into the wood cell wall, polymerises *in situ*, resulting in a permanent swelling of the wood cell wall (Goldstein 1955, 1960; Stamm 1977). It has been shown that furfurylation of wood leads to higher durability against biodegradation (Lande, Westin and Schneider 2004) and a low environmental impact (van Eetvelde, De Geyter, Marchal and Stevens 1998; Lande, Eikenes and Westin 2004a; Lande, Westin and Schneider 2004b; Pilgård, De Vetter, Van Acker and Westin 2010a; Pilgård *et al.* 2010b). UV microspectrophotometry (UMSP) is an established analytical technique which enables direct imaging of lignin distribution and lignin modification (biodegradation, delignification) within individual cell wall layers (Fergus, Procter, Scott and Goring 1969; Scott, Procter, Fergus and Goring 1969; Saka, Whiting, Fukazawa and Goring 1982; Fukazawa 1992; Koch and Kleist 2001; Koch and Grünwald 2004; Rehbein and Koch 2011; Koch and Schmitt 2013). Rehbein and Koch (2011) detected topochemical indications of incipient lignin modification by the brown rot fungus *Antrodia vailantii* in the S2 layer in *Pinus sylvestris* already after 3 days of incubation. The aim of this study was to improve a method for investigating furfurylated *Pinus radiata* in order to gain a better understanding of the furfuryl alcohol polymerisation process in the wood cell wall and to be able to detect and localise early appearance of brown rot degradation.

[1]Technische Universität München, Chair of Wood Science, Winzererstraße 45, D-80797 München, Germany
[2]SP Technical Research Institute of Sweden, Box 857, SE-501 15 Borås, Sweden
[3]Thünen Institute of Wood Research, Leuschnerstr. 91, D-21031 Hamburg, Germany

*Corresponding author, email ehmcke@hfm.tum.de

Received 29 November 2015; accepted 27 February 2016
DOI 10.1080/20426445.2016.1161866

Experimental

Sample preparation

Small blocks (1.5 × 1.5 × 5 mm³, R × T × L) of furfurylated *P. radiata* sapwood, a research product, were trimmed, leached according to EN 84 (1996) and sterilised by gamma radiation. The benefit of the small sample size is that the complete sample can be embedded and prepared for cellular UMSP investigation in contrast to common degradation tests, for example Bravery (1979) and DIN CEN/TS 15083-1(2005). The underlying decay test of this paper (Algeier 2014) was performed according to Rehbein and Koch (2011). Four samples were placed into each petri dish, prepared with a standard malt agar, in front of a mycelium flake of *Postia placenta* (FRIES), M.J. LARSEN & LOMB. (FPRL 280) and stored in a climate chamber at 22 ± 1°C and 70 ± 1% r.H. for a period of 23 days. The inoculation of the petri dish and sample mounting were performed at the same time to avoid contamination. Samples were harvested at 12 different times according to Rehbein and Koch (2011). For this paper, we chose a sample after 21 days of incubation.

Light microscopy and scanning UMSP

The samples were carefully cleaned (with a soft paintbrush) from surrounding mycelia and dehydrated in a graded series of ethanol. Afterwards the samples were embedded in epoxy resin according to Spurr (1969), trimmed with a razor blade and sectioned with a rotary microtome (Leica, RM2265) equipped with a diamond knife. The sections were taken from the surface at a depth between 20 and 30 µm. The cutting process is a delicate issue in the sample preparation for USMP investigations to obtain a homogenous thickness of the slices to avoid the effect of thickness differences, previously described by Irbe *et al.* (2006). The semithin sections (1 µm), with a size of approximately 0.5 mm², were transferred to quartz microscopic slides and thermally fixed. Prior to placing the microscopic slide into the microspectrophotometer, the sections were immersed in a drop of non-UV absorbing glycerine (glycerine/water mixture $n_D = 1.46$) and covered with a quartz cover slip. The sections for the light microscopy were transferred to microscopic slides without staining. Previous studies by Algeier (2014) showed that staining of furfurylated *P. radiata* with anilinblue and astrablue did not increase the contrast. Light microscopic analyses were carried out with a microscope (Axiophot, Zeiss) equipped with a digital camera (AxioCam, Zeiss) using AxioVision software.

For the topochemical analyses, the sections were placed into a microspectrophotometer (Zeiss UMSP 80) equipped with a scanning stage. The principle of UMSP investigation is based on the fact that lignin is able to absorb UV light with absorbance maximum in the range of $\lambda_{270–280\ nm}$ (Musha and Goring 1975) displaying a characteristic spectrum in contrast to the other cell wall compounds, cellulose and hemicelluloses. The scan program APAMOS (automatic photometric analysis of microscopic objects by scanning, Zeiss) digitises square fields of a local geometrical resolution of 0.25 µm × 0.25 µm and a photometrical resolution of 4096 greyscale levels. The high resolution enables a high differentiation of the UV absorbance within the individual cell wall layers. To visualise the absorbance intensities, the greyscale levels were converted into 14 basic colours (Koch and Kleist 2001). The scan can be depicted as two- or three-dimensional image profiles with a statistical evaluation of the semi-quantitative lignin distribution. For the scanning analyses of the prepared sections of *P. radiata* (21 days of incubation) a defined wavelength of 280 nm (absorbance maximum of softwood lignin) was selected and applied to study the lignification of the earlywood and latewood tissues.

Results and discussion

Light microscopy

Light microscopy observation of uninfected and embedded furfurylated *P. radiata* showed intact tracheid tissue with an uneven distribution of polymerised FA located in the cell lumen (brown deposits) (Fig. 1*a*). After 21 days of incubation, no degradation of the cell wall structures could be seen in the inner parts of the samples (Fig. 1*b*). However, the cell structures of the outer parts were degraded. The preparation process of semithin sections of undegraded and degraded furfurylated *P. radiata* caused material-dependent artefacts which are marked with arrows in Fig. 1. The slices were

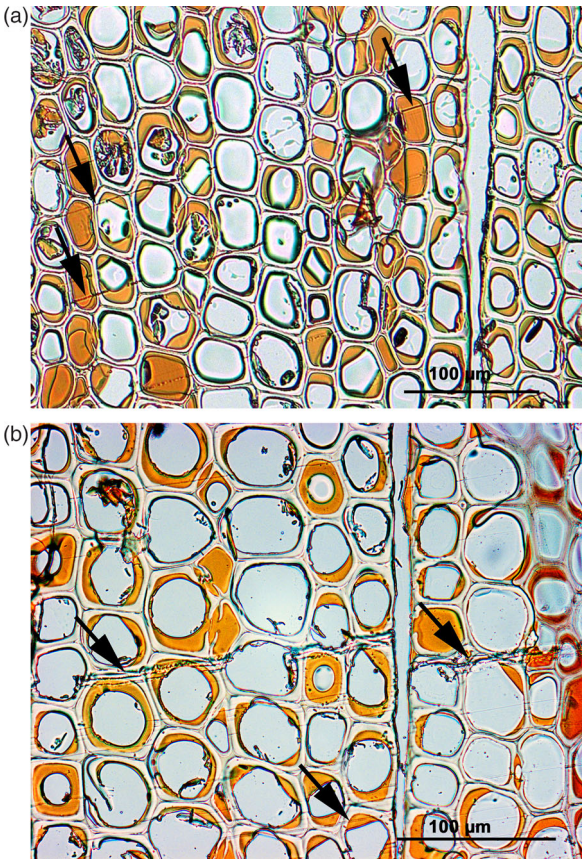

1 Light microscope cross sections of (a) modified *Pinus radiata* and (b) *Pinus radiata* exposed to *Postia placenta* (incubation time: 21 days). Both samples showed an uneven distribution of polymerised FA in the cell lumen (brown deposits). The arrows mark preparation artefacts

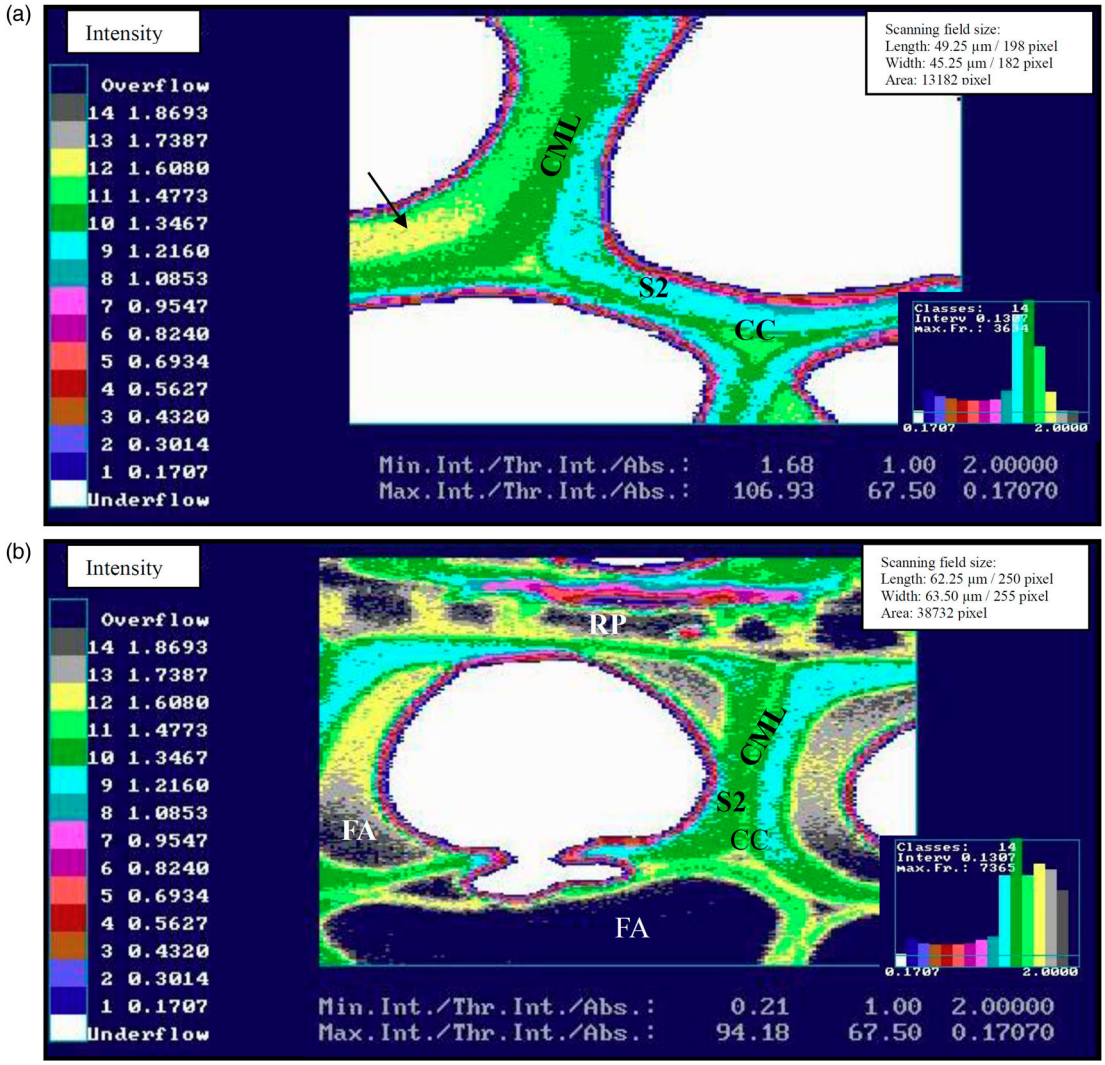

2 UV microscopic scanning profiles of modified *Pinus radiata* with statistical evaluation (histogram). The coloured pixels mark the absorbance intensity at $\lambda_{280\,nm}$. The highest absorbance values in the cell wall tissue are in the area of the compound middle lamella (CML) and cell corners (CC). (a) The secondary wall (S2) revealed lower intensities and a spot of high absorbance (↑) which could be an indication of an accumulation of polymerised furfuryl alcohol in the cell wall. (b) Polymerised furfuryl alcohol (FA) deposits in the lumen and ray parenchyma (RP) display absorbance intensities above 1.87 (overflow)

partly brittle and fragile. A possible reason could be that FA hinders the epoxy resin impregnation.

UV microscopic scanning profiles

For the first time, degraded furfurylated wood tissue was investigated by cellular UMSP. Selected sample sections of *P. radiata* incubated with *Postia placenta* and undegraded furfurylated references were scanned with monochromatic UV-light at 280 nm. The thresholds of the UV intensities have been individually adapted to min 1.00% and max 67.50% for all investigated samples, to obtain a comparable evaluation and image generation. Normally, the thresholds are set to a standard of min 10.00% and max 80.00%, but with those parameters it was not possible to generate the very high UV absorbance (overflow) of the condensed phenolic/aromatic compounds in the modified tissue. The intensities of UV absorbance within the individual cell wall layers are displayed by the different colour pixels. Figure 2*a* and *b* show representative UV microscopic scanning profiles of undegraded furfurylated *P. radiata*. The treated controls show distinct UV absorbance signals of the individual cell wall layers and cell types. The highest absorbance intensities in the cell wall tissue occur in the area of the compound middle lamella (CML) and the cell corners (CC) as previously described for untreated (Koch and Kleist 2001; Koch and Grünwald 2004) and also for thermally modified wood (Mahnert, Adamopoulos, Koch and Militz 2013). The absorbance values increase from the S3 layer to the area of the CML with approximately $abs_{280\,nm}$ 1.35 and the CC with values around $abs_{280\,nm}$ 1.6. UV absorbance intensities of the S2 layers are in the range of $abs_{280\,nm}$ 1.09–1.48. A spot of high absorbance values in the S2 layer ($abs_{280\,nm}$ 1.61) could be an indication of a local accumulation of polymerised furfuryl alcohol in the cell wall (Fig. 2*a*). Polymerised furfuryl alcohol in the cell lumen was distinctively detected as overflow with UV absorbance values >1.9 (Fig. 2*b*).

After 21 days of incubation the entire wood tissue of the furfurylated and colonised sample appears with significant lower UV absorbance values compared to the undecayed control (Fig. 3). This decrease in absorbance most likely originates from early fungal degradation processes

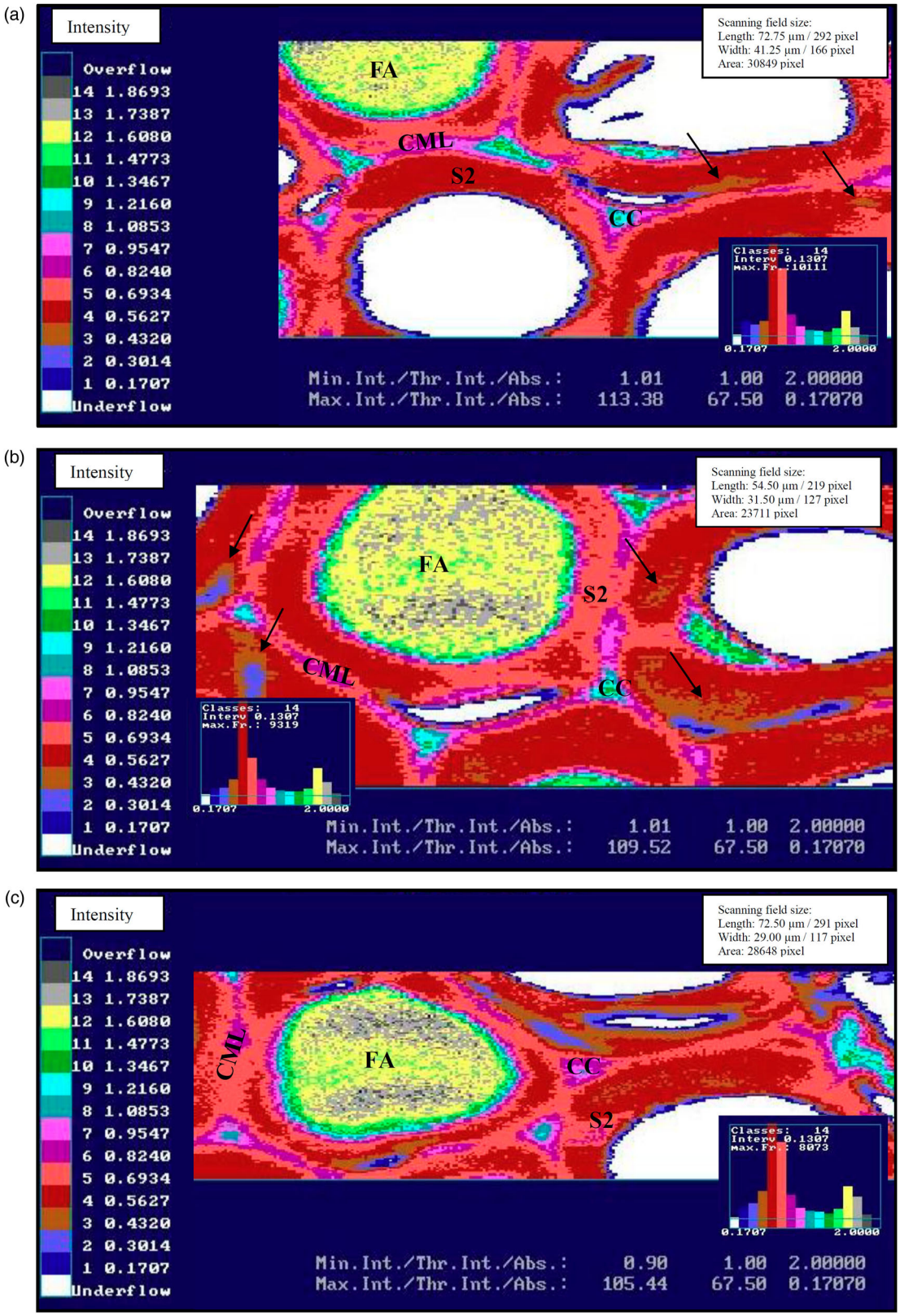

3 UV microscopic scanning profiles at $\lambda_{280\ nm}$ of modified *Pinus radiata* degraded by *Postia placenta*. The degraded sample revealed a significant decrease of the absorbance intensity from greenish to reddish pixels compared to the controls (Fig. 2*a*, *b*) as the statistical evaluation displays (histogram). *a* The secondary wall (S2) revealed lower and locally inhomogeneous pattern of lower intensities (↑) and the onset of lignin modification. The compound middle lamella (CML) is partly degraded, the absorbance values of the cell corners (CC) and the furfuryl alcohol (FA) in the cell lumen decreased. *b* and *c* show the same trends with locally inhomogeneous pattern of lower intensities (↑) and partially dissolved CMLs

(Rehbein and Koch 2011), where highly reactive hydroxyl radicals, produced in the non-enzymatic part of the chelator mediated Fenton degradation (Goodell *et al*. 1997; Hammel, Kapisch, Jensen and Ryan 2002; Arantes, Jellison and Goodell 2012) attack lignin as well as furfuryl alcohol, since no structural cell wall damages could be seen in the light microscope. The absorbance values of the polymerised furfuryl alcohol in the cell lumen changed from overflow (Fig. 2*b*) to values around $abs_{280\,nm}$ 1.61. The absorbance of the S2 layers shifted from $abs_{280\,nm}$ 1.09–1.48 to $abs_{280\,nm}$ 0.56–0.82 with locally inhomogeneous pattern of lower intensities (Fig. 3 ↑). The signals of the CML are partly not distinguishable from S2 and some small regions are still absorbing in the range of $abs_{280\,nm}$ 0.82–0.95. The UV absorbance values of the CC distinctively changed from $abs_{280\,nm}$ 1.48 to $abs_{280\,nm}$ 1.09.

The present results of the topochemical analyses confirm the findings of Fackler *et al*. (2010) and Rehbein and Koch (2011) that brown rot degradation starts with a lignin modification in the outermost part of the secondary cell wall and the combined middle lamella, through the chelator mediated Fenton degradation (Goodell 2003), also in furfurylated wood. This degradation process is evidenced by the strong decrease of the UV absorbance values documented in Figs. 2 and 3. The highest amount of condensed lignin is topochemically detectable in the middle lamella and the cell corners where we also found the highest amounts of furfuryl alcohol in the furfurylated samples. Thygesen, Barsberg and Venås (2010) also described that the highest amount of furfuryl alcohol was located in the lignin rich parts of the wood cell wall (CML and CC). This together with our results indicate the importance of a homogenous (good) penetration and polymerisation of furfuryl alcohol in the CML to improve the decay resistance of the furfurylated wood since brown rot degradation starts at this location. In a study performed by Irbe *et al*. (2006), a gradual decrease in lignin absorbance in CML and CC during the progress of brown rot decay was detected. However, Rehbein and Koch (2011) noticed an increase in UV absorbance intensities in the inner parts of the S2 layer after 3 days of exposure. Other factors which are contributing according to Irbe *et al.* (2006) are the thickness of decayed cell walls compared to undecayed cell walls, partial depolymerisation of the native lignin and the changed ratio of lignin to carbohydrates. However, we could not see any physical damages and natural variations which might influence the provided basic results on lignin modification (topochemistry) in the cell wall layers of furfurylated wood at early degradation stages. We therefore assume that thickness differences, due to degradation, are minor problems for our application of the UMSP method to studies of early degradation stages in furfurylated wood.

Conclusions

Cellular UMSP investigations of furfurylated *P. radiata*, characterised by very high UV absorbance (overflow) of the condensed phenolic/aromatic compounds in the modified tissue, require individual threshold adaption of the UV intensities to min 1.00% and max 67.50%. After 21 days of incubation with *Postia placenta*, no structural cell wall damages were seen in the light microscope, but changes in chemical distribution of modified lignin could be detected with the UMSP in the entire cell wall which most likely indicate early brown rot decay. These results show that cellular UMSP is a promising method to study furfurylated wood and early fungal degradation damages in the cell wall of furfurylated wood. Further degradation studies including more (individual) decay stages are planned to complement the results from this study.

Acknowledgements

The authors thank S. M. Algeier for sample preparation and performing the decay test in the context of his master thesis, A. Vieler for sectioning, D. Paul and K. Brandt, Hamburg, for assistance in UMSP analysis.

References

Algeier, S. M. 2014. Biologischer Abbau von furfuryliertem Holz durch ausgewählte Basidiomyceten, MS Thesis, Technische Universität München, München, Germany.

Arantes, V., Jellison, J. and Goodell, B. 2012. Peculiarities of brown-rot fungi and biochemical Fenton reaction with regard to their potential as a model for bioprocessing biomass. *Applied Microbiology and Biotechnology*. **94**(2): 323–338.

Arantes, V., Milagres, A. M., Filley, T. R. and Goodell, B. 2011. Lignocellulosic polysaccharides and lignin degradation by wood decay fungi: the relevance of nonenzymatic Fenton-based reactions. *Journal of Industrial Microbiology Biotechnology*. **38**(4): 541–555.

Arantes, V., Qian, Y., Kelley, S. S., Milagres, A. M. F., Filley, T. R., Jellison, J. and Goodell, B. 2009. Biomimetic oxidative treatment of spruce wood studied by pyrolysis-molecular beam mass spectrometry coupled with multivariate analysis and ^{13}C-labeled tetramethylammonium hydroxide thermochemolysis: implications for fungal degradation of wood. *Journal of Biological Inorganic Chemistry*. **14**(8): 1253–1263.

Bariska, M., Osusk, A. and Bosshard, H. H. 1983. Änderung der mechanischen Eigenschaften von Holz nach Abbau durch Basidiomyceten. *Holz als Roh- und Werkstoff*. **41**(6): 241–245.

Bravery, A. F. 1979. Screening techniques for potential wood preservative chemicals. A miniaturised wood-block test for the rapid evaluation of preservative fungicides, in: Principles of a Special Seminar Held in Association with the 10th Annual Meeting of the IRG, Peebles. Reports No. 136. Stockholm, Sweden.

CEN/TS 15083-1 2005. Durability of wood and wood-based products – determination of the natural durability of solid wood against wood- destroying fungi, test methods – Part 1: Basidiomycetes, 18.

Danninger, E., Messner, K. and Rohr, M. 1980. Abbauschema der Braun- und Weißfäulepilze auf heimischen Hölzern (Buche, Fichte). *Holzforschung und Holzverwertung*. **32**(5): 126–130.

EN 84. 1996. Wood preservatives. Accelerated ageing of treated wood prior to biological testing, Leaching procedure, European Committee for Standardization (CEN), Brussels, Belgium, 7.

Eriksson, K. E. L., Blanchette, R. A. and Ander, P. 1990. *Microbial and enzymatic degradation of wood and wood components*. 407, Berlin: Springer.

Fackler, K., Stevanic, J. S., Ters, T., Hinterstoisser, B., Schwanninger, M. and Salmén, L. 2010. Localisation and characterisation of incipient brown-rot decay within spruce wood cell walls using FT-IR imaging microscopy. *Enzyme and Microbial Technology*. **47**(6): 257–267.

Fergus, B. J., Procter, A. R., Scott, J. A. N. and Goring, D. A. I. 1969. The distribution of lignin in sprucewood as determined by ultraviolet microscopy. *Wood Science and Technology*. **3**(2): 117–138.

Fukazawa, K. 1992. Ultraviolet microscopy. In: Lin S. Y. and Dence C. W. (eds). *Methods in Lignin Chemistry*. Berlin: Springer-Verlag, 110–121.

Goldstein, I. S. 1955. The impregnation of wood to impart resistance to alkali and acid. *Forest Products Journal*. **5**(4): 265–267.

Goldstein, I. S. 1960. Impregnating solutions and methods. GB Patent 846,680.

Goodell, B. 2003. Brown rot fungal degradation of wood: our evolving view, in Wood deterioration and preservation: Advances in our changing world, (eds. B. Goodell, D. Nicholas, and T. Schultz), 845, (6), 97–118, Washington D.C., American Chemical Society.

Goodell, B., Jellison, J., Liu, J., Daniel, G., Paszczynski, A., Fekete, F., Krishnamurthy, A., Jun, L., Xu, G. 1997. Low molecular weight

chelators and phenolic compounds isolated from wood decay fungi and their role in the fungal biodegradation of wood. *Journal of Biotechnology*. **53**(2–3): 133–162.

Hammel, K. E., Kapisch, A. N., Jensen jr, K. A. and Ryan, Z. C. 2002. Reactive oxygen species as agents of wood decay by fungi. *Enzyme and Microbial Technology*. **30**(4): 445–453.

Hill, C. 2006. *Wood Modification: Chemical, Thermal and Other Processes*. 239, Oxford, UK: John Wiley & Sons.

Irbe, I., Noldt, G., Koch, G., Andersone, I. and Andersons, B. 2006. Application of scanning UV microspectrophotometry for the topochemical detection of lignin within individual cell walls of brown-rotted Scots pine (*Pinus sylvestris* L.) sapwood. *Holzforschung*. **60** (6): 601–607.

Kirk, T. 1975. Effects of the brown-rot fungus *Lentzites trabea*, on lignin in spruce wood. *Holzforschung*. **29**(3): 99–107.

Koch, G. and Grünwald, C. 2004. Application of UV microspectrophotometry for the topochemical detection of lignin and phenolic extractives in wood fibre cell walls. In: Schmitt U., Ander P., Barnett J. R., Emons A. M. C., Jeronimidis G., Saranpää P., Tschegg S. (eds). *Wood Fibre Cell Walls: Methods to Study Their Formation, Structure and Properties*. Uppsala: Swedish University of Agricultural Sciences, 119–130.

Koch, G. and Kleist, G. 2001. Application of scanning UV microspectrophotometry to localise lignins and phenolic extractives in plant cell walls. *Holzforschung*. **55**(6): 563–567.

Koch, G. and Schmitt, U. 2013. Topochemical and electron microscopic analyses on the lignification of individual cell wall layers during wood formation and secondary changes. In: Fromm J., Robinson D. G. (eds). *Cellular Aspects of Wood Formation, Plant Cell Monographs 20*. Berlin, Heidelberg: Springer-Verlag, 41–69.

Lande, S., Eikenes, M. and Westin, M. 2004. Chemistry and ecotoxicology of furfurylated wood. *Scandinavian Journal of Forest Research*. **19**(5): 14–21.

Lande, S., Westin, M. and Schneider, M. 2004a. Properties of furfurylated wood. *Scandinavian Journal of Forest Research*. **19**(5): 22–30.

Lande, S., Westin, M. and Schneider, M. H. 2004b. Eco-efficient wood protection: Furfurylated wood as alternative to traditional wood preservation. *Management of Environmental Quality: An International Journal*. **15**(5): 529–540.

Mahnert, K.-C., Adamopoulos, S., Koch, G. and Militz, H. 2013. Topochemistry of heat-treated and N-methylol melamine modified wood of Koto (*Pterygota macrocarpa* K. Schum.) and Limba (*Terminalia superba* Engl. et Diels). *Holzforschung*. **67**(2): 137–146.

Martínez, A. T., Rencoret, J., Nieto, L., Jiménez-Barbero, J., Gutiérrez, A. and Del Río, J. C. 2011. Selective lignin and polysaccharide removal in natural fungal decay of wood as evidenced by in situ structural analyses. *Environmental Microbiology*. **13**(1): 96–107.

Musha, Y. and Goring, D. A. I. 1975. Distribution of syringyl and guaicyl moieties in hardwoods as indicated by ultraviolet microscopy. *Wood Science and Technology*. **9**(1): 45–58.

Niemenmaa, O., Uusi-Rauva, A. and Hatakka, A. 2008. Demethoxylation of [$O_{14}CH_3$]-labelled lignin model compounds by the brown-rot fungi *Gloeophyllum trabeum* and *Poria* (*Postia*) *placenta*. *Biodegradation*. **19**(4): 555–565.

Pilgård, A., De Vetter, L., Van Acker, J. and Westin, M. 2010a. Toxic hazard of leachates from furfurylated wood: Comparison between two different aquatic organisms. *Environmental Toxicology and Chemistry*. **29**(5): 1067–1071.

Pilgård, A., Treu, A., Van Zeeland, A. N. T., Gosselink, R. J. A. and Westin, M. 2010b. Toxic hazard and chemical analysis of leachates from furfurylated wood. *Environmental Toxicology and Chemistry*. **29**(9): 1918–1924.

Rehbein, M. and Koch, G. 2011. Topochemical investigation of early stages of lignin modification within individual cell wall layers of Scots pine (*Pinus sylvestris* L.) sapwood infected by the brown-rot fungus *Antrodia vaillantii* (DC.: Fr.) Ryv. *International Biodeterioration & Biodegradation*. **65**(7): 913–920.

Saka, S., Whiting, K. Fukazawa, K. and Goring, D. A. I. 1982. Comparative studies on lignin distribution by UV microscopy and bromination combined with EDXA. *Wood Science and Technology*. **16**(4): 269–277.

Schultze-Dewitz, G. 1966. Beziehungen zwischen der Elastizität und der statischen sowie dynamischen Biegefestigkeit von Kiefernholz nach dem Angriff durch echte holzzerstörende Pilze. *Holz als Roh- und Werkstoff*. **24**(10): 506–512.

Scott, J. A. N., Procter, A. R., Fergus, B. J. and Goring, D. A. I. 1969. The application of ultraviolet microscopy to the distribution of lignin in wood: description and validity of the technique. *Wood Science and Technology*. **3**(1): 73–92.

Spurr, A. R. 1969. A low-viscosity epoxy resin embedding medium for electron microscopy. *Journal of Ultrastructure Research*. **26**(1–2): 31–43.

Stamm, A. J. 1977. Dimensional stabilization of wood with furfuryl alcohol resin, in Wood Technology: Chemical Aspects, (ed. I. Goldstein), 43, (9), 141–149, Washington D.C., American Chemical Society.

Thygesen, L. G., Barsberg, S. and Venås, T. M. 2010. The fluorescence characteristics of furfurylated wood studied by fluorescence spectroscopy and confocal laser scanning microscopy. *Wood Science and Technology*. **44**(1): 51–65.

Van Eetvelde, G., De Geyter, S., Marchal, P. and Stevens, M. 1998. Aquatic toxicity research of structural materials, in Proceedings of the International Research Group on Wood Preservation (IRG), IRG/WP 98-50114, 1–10, Maastricht, The Netherlands.

Winandy, J. E. and Morrell, J. J. 1993. Relationship between incipient decay, strength, and chemical composition of Douglas-fir heartwood. *Wood and Fibre Science*. 25(3): 278–288.

Yelle, D. J., Ralph, J., Lu, F. and Hammel, K. E. 2008. Evidence for cleavage of lignin by a brown rot basidiomycete. *Environmental Microbiology*. 10(7): 1844–1849.

Yelle, D. J., Wei, D., Ralph, J. and Hammel, K. E. 2011. Multidimensional NMR analysis reveals truncated lignin structures in wood decayed by the brown rot basidiomycete Postia placenta. *Environmental Microbiology*. 13(4): 1091–1100.

II

Gabriele Ehmcke*, Annica Pilgård, Gerald Koch and Klaus Richter

Topochemical analyses of furfuryl alcohol-modified radiata pine (*Pinus radiata*) by UMSP, light microscopy and SEM

DOI 10.1515/hf-2016-0219
Received November 25, 2016; accepted May 11, 2017; previously published online June 16, 2017

Abstract: Furfurylation is one of the wood modification techniques via catalytic polymerization of the monomeric furfuryl alcohol (FA) in the impregnated cell wall. Little is known about the topochemistry of this process. Brown rot degradation begins with lignin modification and therefore, the reactions between FA and lignin was one focus of this research. Furfurylated radiata pine (*Pinus radiata*) with three different weight percent gains (WPGs of 57%, 60% and 70%) after FA uptake was observed by cellular ultraviolet microspectrophotometry (UMSP) to analyze chemical alterations of the individual cell wall layers. Moreover, light microscopy (LM) and scanning electron microscopy (SEM) analyses were performed. The ultraviolet (UV) absorbance of the modified samples increased significantly compared to the untreated controls, indicating a strong polymerization of the aromatic compounds. Highest UV absorbances were found in areas with the highest lignin concentration. The UMSP images of individual cell wall layers support the hypothesis concerning condensation reactions between lignin and FA.

Keywords: brown rot, furfurylation, light microscopy (LM), lignin modification, scanning electron microscopy (SEM), ultraviolet microspectrophotometry (UMSP), wood modification

***Corresponding author: Gabriele Ehmcke,** Chair of Wood Science, Technical University of Munich, Winzererstraße 45, D-80797 München, Germany, Phone: +49 89 2180 6431, e-mail: ehmcke@hfm.tum.de
Annica Pilgård: Chair of Wood Science, Technical University of Munich, Winzererstraße 45, D-80797 München, Germany; and RISE Research Institutes of Sweden AB, Box 857, SE-501 15 Borås, Sweden
Gerald Koch: Thünen Institute of Wood Research, Leuschnerstr. 91, D-21031 Hamburg, Germany
Klaus Richter: Chair of Wood Science, Technical University of Munich, Winzererstraße 45, D-80797 München, Germany

Introduction

Brown rot basidiomycetes cause the most destructive type of wood decay, even before any mass loss (ML) of the wood is detectable (Schultze-Dewitz 1966; Bariska et al. 1983; Winandy and Morrell 1993). Cellulose and hemicelluloses are mainly metabolized, leaving a modified lignin behind (Danninger et al. 1980; Eriksson 1990; Goodell 2003). Lignin maintains its macromolecular nature throughout the brown rot decay (Kirk 1975; Niemenmaa et al. 2008; Yelle et al. 2008), but its structure is modified substantially by hydroxyl radicals produced by the fungi (Yelle et al. 2008, 2011; Arantes et al. 2009, 2011; Martínez et al. 2011). The lignin modification begins in the outermost part of the secondary cell wall (S2) and the compound middle lamella (CML) (Fackler et al. 2010; Rehbein and Koch 2011).

Wood preservation based on technologies with low environmental impact are mandatory today. Different approaches are known in this regard, for instance, modifications with melamine formaldehyde (Stamm 1964), with acetic anhydride (Rowell et al. 1994), or thermal modification (Militz 2002), the effects of which are based on chemical, biological and physical interactions, resulting in increased durability and dimensional stability (Hill 2006; Ringman et al. 2014). Another promising approach is the furfurylation process. Furfuryl alcohol (FA) is obtained from renewable resources of agricultural crop waste (corn or sugar cane production) consisting of pentosans, which are easily hydrolyzed, and the pentoses obtained are dehydrated to furfural (F) (Hill 2006; Uppal et al. 2008; Moghaddam et al. 2016), which is then converted to FA. F and FA are by far the most important furan derivates (Gandini and Lacerda 2015), which can be polymerized by several organic and mineral acids, such as by Lewis acids (Lande et al. 2004a). Ünver and Öktem (2013) investigated controlled cationic polymerization of FA, visualized by the UV bands at $\lambda_{228\,nm}$ and $\lambda_{286\,nm}$.

Furfurylation begins with FA impregnation of wood followed by *in situ* polymerization, which leads to a permanent swelling of the cell wall (Goldstein 1955, 1960; Stamm 1977; Schneider 1995; Bryne et al. 2010). In the last decade, FA impregnation was, for example, applied to

improve plasticization and fixation during the densification of wood (Pfriem et al. 2012), and new catalysts were developed (Li et al. 2015; Sejati et al. 2017). Not all the details of the furfurylation process are well understood. The FA solution enters the cell wall to some extent but also fills the cell lumens completely or partially (Schneider et al. 2000). Depending on wood species and FA concentration, the curing temperature ranges from 45°C to 140°C (Westin 2003). Furfurylated wood (W_{FA}) has better durability against biodegradation (Lande et al. 2004c; Esteves et al. 2011; Gascon-Garrido et al. 2013; Li et al. 2015; Sejati et al. 2017) and has a low environmental impact (van Eetvelde 1998; Lande et al. 2004a,b,c; Pilgård et al. 2010a, 2010b). Furfurylated softwoods and hardwoods are available on the market with the equivalent quality to woods protected by copper, chromium and arsenic (CCA) solutions. W_{FA} is darker than native wood and has an aesthetic appeal similar to that of natural durable (and dark) tropical timbers like teak, ipé or azobé. W_{FA} fulfills the requirements for hazard classes 3 and 4 applications according to EN 335. Furfurylated southern yellow pine and radiata pine are admitted as "proven" for window frames on the German market (VFF-Merkblatt HO.06-4 2016). Previous studies by infrared (Venås and Rinnan 2008) and fluorescence microscopy (Thygesen et al. 2010) on W_{FA} have shown that FA polymerization takes place within the wood tissue. Higher fluorescence occurs in lignin-rich parts, mainly in the cell wall corner regions (CC) and the CML (Thygesen et al. 2010). Nuclear magnetic resonance (NMR) spectra of early stages of FA polymerization demonstrated that lignin model compounds form covalent bonds in a liquid-phase system with the FA polymer (Nordstierna et al. 2008). Chemical bonds between the FA polymer and wood tissue, however, have not yet been proven.

To learn more about furfurylation, ultraviolet microspectrophotometry (UMSP) was applied in the present study. UMSP is an established analytical technique which enables the direct imaging of lignin distribution and lignin modification in the course of biodegradation and technological delignification within individual cell wall layers *in situ* (Fergus et al. 1969; Scott et al. 1969; Saka et al. 1982; Fukazawa 1992; Koch and Kleist 2001; Koch et al. 2003a; Koch et al. 2003b; Koch and Grünwald 2004; Rehbein and Koch 2011; Koch and Schmitt 2013; Aguayo et al. 2014; Kojima et al. 2014; Bianchi et al. 2016; Ehmcke et al. 2016). The π electron-rich lignin shows UV maxima at around $\lambda_{212\,nm}$ and $\lambda_{280\,nm}$ (Scott et al. 1969; Goldschmid 1971; Fukazawa 1992). Softwood lignin is mainly composed of guaiacylpropane moieties with an absorbance maximum (A_{max}) at around $\lambda_{280\,nm}$ (Musha and Goring 1975; Takabe 1992). The UV-A_{max} data are lower in lignins with higher syringpropan unit participation, seen on the increasing OCH_3/C_9 ratios (Musha and Goring 1975; Fujii et al. 1987). Modified timbers, such as heat-treated and N-methylol melamine-modified hardwoods (Kielmann et al. 2013; Mahnert et al. 2013; Sint et al. 2013), hydrothermal-modified wood (Andersons et al. 2016) and degraded furfurylated softwood (Ehmcke et al. 2016), were also studied by UMSP.

The aim of the present study was to investigate FA-modified radiata pine (*Pinus radiata*) by the UMSP method to search for indications of lignin modification via chemical bonds with FA.

Materials and methods

Radiata pine (*P. radiata*) sapwood boards were industrially furfurylated under different process conditions and distributed to project partners of an ongoing research project (Research council of Norway project 219294/O30). The furfurylation processes are based on a full-cell impregnation with different FA solutions, buffer agents and catalysts followed by steam curing and kiln drying. Water-based [process A, a weight percent gain (WPG) of 60%] and alcohol solutions (process B, 70% WPG) were applied, both containing FA and standard catalysts. Process C was performed with an experimental mix of a water-based solution and an alternative catalyst leading to a WPG of 57%. The wood from process A is a commercial product and available on the market. Each modified board in this project was matched by an untreated board (W_{untr}).

Sample preparation for UMSP: Small blocks of W_{FA} 1 mm × 1 mm × 5 mm (R × T × L) were prepared for each treatment type ($W_{FA,A}$, $W_{FA,B}$ and $W_{FA,C}$) and for W_{untr}. Selected wood blocks were dehydrated in a graded series of ethanol and then embedded in Spurr's (1969) epoxy resin (Electron Microscopy Sciences, Hatfield, PA, USA) under mild vacuum conditions. The polymerization process was catalyzed by thermal curing at 70°C for 12 h. The embedded specimens were trimmed with a razor blade (Plano GmbH, Wetzlar, Germany) to provide an area of approximately 0.5 mm^2 and sectioned with a rotary microtome (Leica, RM2265, Leica Mikrosysteme Vertrieb GmbH Wetzlar, Germany) equipped with a diamond knife (DiATOME histo, 4.0 mm, 45°, Diatome AG, Biel, Switzerland). The semi-thin sections (1 μm) were transferred to quartz microscopic slides (Plano GmbH, Wetzlar, Germany) and thermally fixed. The sections were immersed in a drop of non-UV-absorbing glycerine (glycerine/water mixture $n_D = 1.46$) and covered with a quartz cover slip. As reference, unmodified radiata pine sapwood specimens were also prepared, following the same embedding process.

In addition, small cubes (1 cm^3) of W_{untr} and W_{FA} were prepared for light microscopy (LM) and scanning electron microscopy (SEM) analyses. For conventional LM, the cubes were sectioned with a sliding microtome (Leica SM 2000 R, Leica Mikrosysteme Vertrieb GmbH Wetzlar, Germany) and sections of the three anatomical directions (transverse, radial and tangential) were mounted on microscopic slides and embedded in Euparal (Carl Roth, Carl Roth GmbH + Co. KG, Karlsruhe, Germany). For SEM analysis, specimens were boiled in water and then manually cut with a thin razorblade to obtain a plain surface perpendicular to the axial direction. The specimens were stored overnight

under vacuum and then sputter-coated by a coating unit (International Scientific Instruments Co, New Delhi, India) with a 10–15-nm gold film.

Cellular UMSP: The ultrathin sections were placed in a Zeiss UMSP 80 (Carl Zeiss AG, Oberkochen, Germany) equipped with a scanning stage. The principle of the UMSP investigation is based on the typical UV absorbance of lignin in the range of $\lambda_{270–280\ nm}$ (Musha and Goring 1975). For scanning, a defined wavelength of $\lambda_{280\ nm}$ (the A_{max} of softwood lignin) was selected. The scan program Automatic Photometric Analysis of Microscopic Objects by Scanning (APAMOS, Carl Zeiss AG, Oberkochen, Germany) digitizes square fields of a local geometrical resolution of 0.25 µm × 0.25 µm and a photometrical resolution of 4096 grayscale levels. To visualize the absorbance intensities, the grayscale levels were converted into 14 basic colors as described in detail by Koch and Kleist (2001). The scans can be depicted as two-dimensional (2D) or three-dimensional (3D) image profiles, and a statistical data evaluation results in a semi-quantitative lignin distribution. For control purposes, the lignin distribution within individual cell types and cell wall layers of three W_{untr} specimens were scanned.

In addition, the specimens were also subjected to photometric point measurements with a spot size of 1 µm². The UV spectra of individual cell wall layers were recorded in the range between $\lambda_{250\ nm}$ and $\lambda_{420\ nm}$ and statistically evaluated. A TIDAS MSP 800 microscope spectrometer (J&M Analytik AG, Esslingen, Germany) equipped with TIDAS-DAQ software was available. The spectral characteristics of 15–20 point measurements of individual cell wall layers and FA-polymerized deposits in the lumen were evaluated.

LM and SEM: To localize FA-impregnated cell elements, selected samples were analyzed by conventional LM (Axiophot, Carl Zeiss AG, Oberkochen, Germany) equipped with a digital camera (AxioCam, Carl Zeiss AG, Oberkochen, Germany) combined with AxioVision software (Carl Zeiss AG, Oberkochen, Germany). The SEM was equipped with a tungsten cathode (EVO 40, 10–12 kV, Carl Zeiss AG, Oberkochen, Germany).

Results and discussion

Transverse sections of W_{untr} and W_{FA} from the FA modification processes were observed by cellular UV microscopy at $\lambda_{280\ nm}$. Preliminary tests showed that the standard thresholds for the UMSP analyses of untreated wood tissue (min 10% and max 80%) were not suitable to evaluate W_{FA} due to the high absorbance intensities (Ehmcke et al. 2016). To obtain a comparable evaluation and image generation, the thresholds were therefore individually adapted to a minimum of 1.0% and a maximum of 67.5% for all investigated specimens.

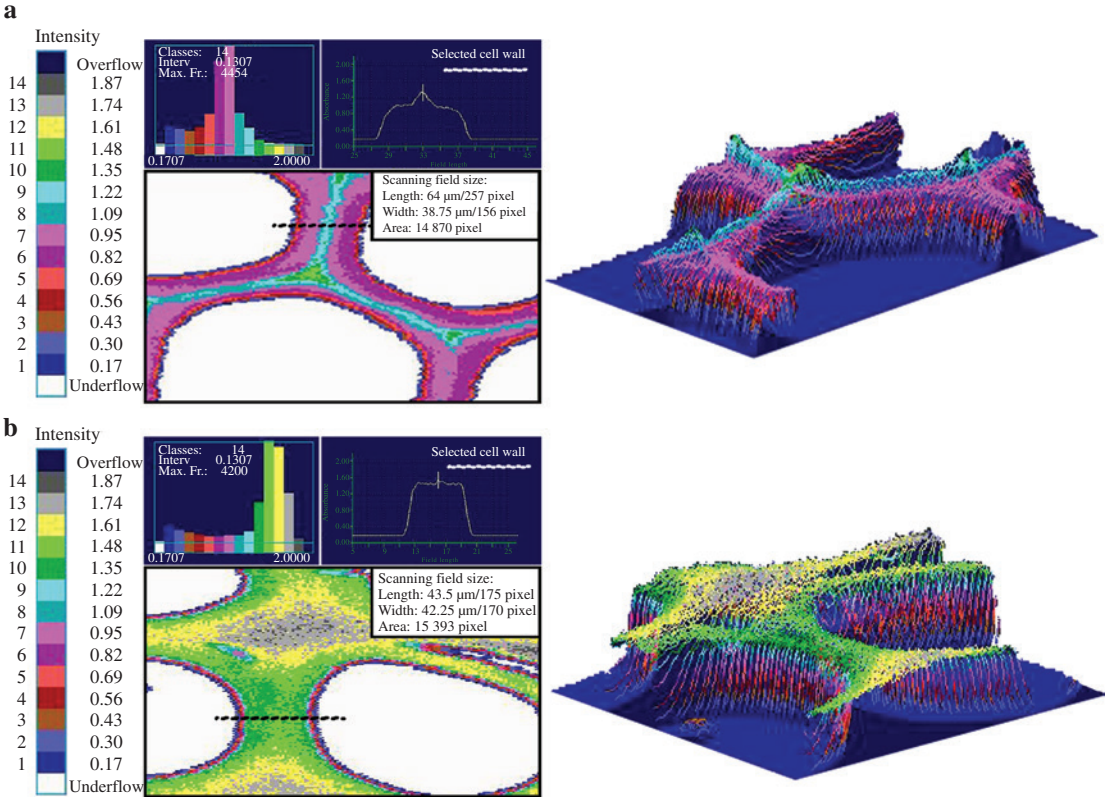

Figure 1: UV microscopic scanning profiles of untreated (a) and furfurylated (b) radiata pine (process A, 60% WPG).
The data are statistically evaluated from their corresponding histograms. The colored pixels mark the absorbance intensity at $\lambda_{280\ nm}$. A selective line scan of an individual cell wall region intuitively visualizes the local lignin concentration and chemical cell wall modification.

UV microscopic scanning profiles

In Figure 1, representative UV microscopic scanning profiles of W_{untr} and $W_{FA,A}$ (60% WPG, commercial product) are presented. The colored pixels mark the absorbance intensities at $\lambda_{280\ nm}$. The data of each UV profile are statistically evaluated from its corresponding histogram. The high resolution (0.25 µm² per pixel) enables a detailed differentiation of the UV absorbance within the individual cell wall layers (Koch et al. 2003a). In addition to the standard 2D UV micrograph, a selective line scan of an individual cell wall region intuitively visualizes the local lignin concentration and the chemical cell wall modification. For spatial illustration, the scanning area is also presented as a 3D image profile.

A representative profile of natural lignin distribution in cell walls of W_{untr} is presented in Figure 1a. The highest absorbances occur in the area of the CML and the CC as previously described for W_{untr} (Koch and Kleist 2001; Koch and Grünwald 2004) and also for thermally (Mahnert et al. 2013) and hydrothermally modified wood (Andersons et al. 2016). For the W_{untr} tissue, the following UV absorption data ($A_{280\ nm}$) are typical: 1.22 for the CML, 1.48 for the CC and lower, slightly varying values for the S2 layer (0.69–0.95). The fluctuating values for the S2 layer were already described by Takabe (2002). The line scan of a double cell wall in the radial direction and the corresponding 3D image illustrates the high absorbance intensities of the CML as a pronounced peak and a highly absorbing band.

For comparison, the UV scanning profiles of W_{untr} and $W_{FA,A}$ (60% WPG) are presented in Figure 1. The profiles (Figure 1b) show significantly higher absorbances of the entire cell wall compared to W_{untr}. With regard to the typical lignin distribution, both UV micrographs of W_{untr} and W_{FA} reveal a similar spectral behavior, where the absorbance intensities are increasing from the S3 layer towards the area of the CML and the CC. For W_{FA}, a clear shift is visible to green-, yellow-, and gray-colored pixels, representing higher UV intensities in the range of 1.22–1.74 ($A_{280\ nm}$), as it was already documented by Ehmcke et al. (2016). With reference to fluorescence studies (Thygesen et al. 2010), the highest amount of polymerized FA was detected in the lignin-rich areas. The line scan in Figure 1b visualizes a distinct increase of the absorbance values from the outer cell wall towards the CML. On the other hand, the CML evinces a less-pronounced peak compared to W_{untr} in Figure 1a. The CML in Figure 1b is associated with a broad plateau of high UV intensities representing the S2 layer ($A_{280\ nm}$ 1.22–1.35), which indicates an intensive modification of the cell wall.

$W_{FA,B}$ (70% WPG) and $W_{FA,C}$ (57% WPG) are presented in Figures 2 and 3. The cell wall layers of $W_{FA,B}$ (Figure 2) reveal relatively homogenous absorbance intensities in the green color range ($A_{280\ nm}$ 1.22–1.35). The CC and CML are somewhat more pronounced and characterized by rare yellow pixels ($A_{280\ nm}$ 1.48). Figure 3 shows lower intensities with bluish-green colors for $W_{FA,C}$. The cell wall layers of $W_{FA,C}$ show increasing intensities beginning with the cell lumen ($A_{280\ nm}$ 0.17–0.56) to S2 ($A_{280\ nm}$ 1.09–1.22), to the CML and the CC ($A_{280\ nm}$ 1.35–1.61), where the absorbance intensities culminate. Compared to W_{untr} (Figure 1a) and all other treated materials (Figures 1b, 2 and 3), the wood tissue of $W_{FA,A}$ (Figure 1b) shows the highest absorbances with a clear shift to green, yellow and gray pixels ($A_{280\ nm}$ 1.22–1.74).

The mean UV absorbances did not increase proportionally to the loadings (i.e. to the WPGs) of the analyzed samples (Table 1). The highest loading was generated by process B with 70% WPG, representing the lowest $A_{280\ nm}$ with 1.07, compared to process A with $A_{280\ nm}$ 1.16 and C with $A_{280\ nm}$ 1.09, but these differences are not significant. The slight deviations could be explained by differences in the anatomical structure and the high resolution of the individual measuring fields. In general, the individual parameters of the FA modification (in terms of catalyst concentration,

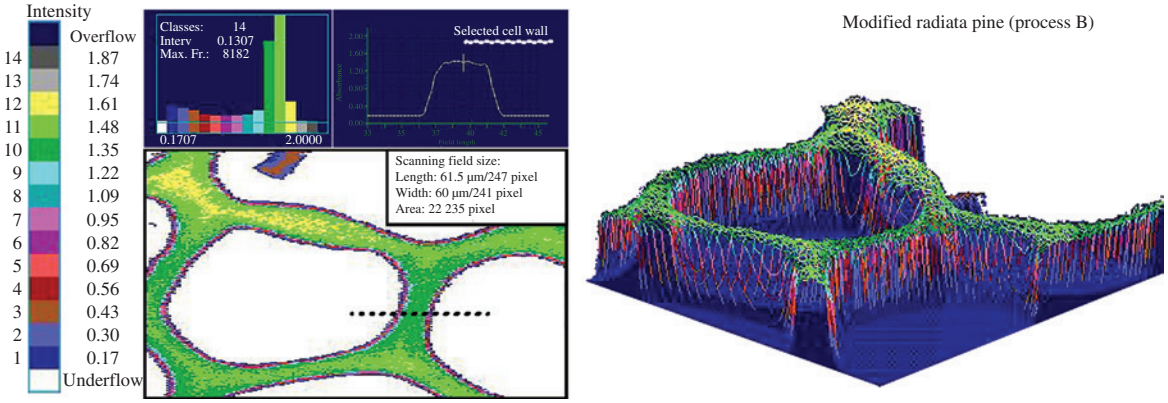

Figure 2: UV microscopic scanning profiles of furfurylated radiata pine (process B, 70% WPG).

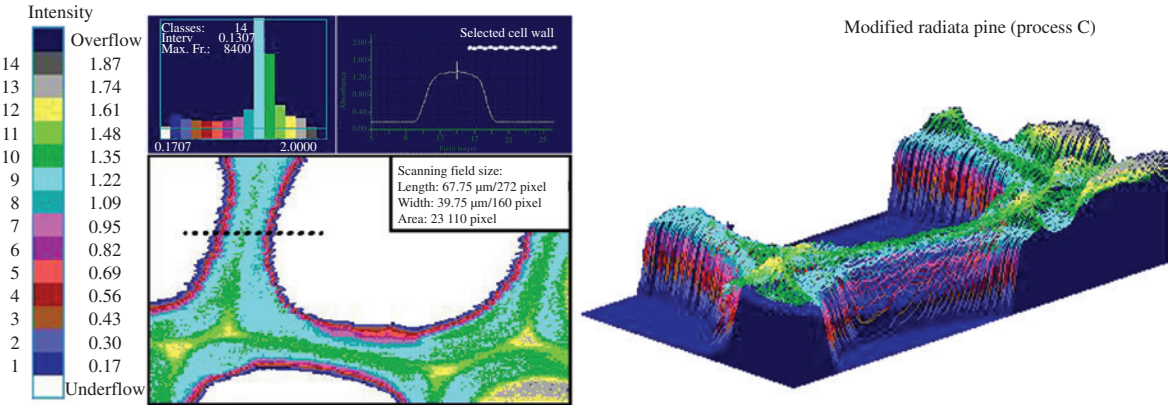

Figure 3: UV microscopic scanning profiles of furfurylated radiata pine (process C, 57% WPG).

Table 1: Mean UV absorbance (A_{280nm}) of untreated and modified radiata pine and maximum UV absorbance values (A_{max}) of polymerized FA deposits (processes A, B and C, threshold minimum 1.0% and maximum 67.5%).

		UMSP-scanning profiles			UV-Abs. spectra[a]		
Process	WPG (%)	$A_{280\,nm}$	StD	(pixel)[b]	λ (nm)	A_{max}	StD
Untr.	0	0.74	0.05	12 733	–	–	–
A	60	1.16	0.07	19 752	278	1.24	0.07
B	70	1.07	0.06	14 426	256	1.21	0.07
C	57	1.09	0.09	23 103	278	1.20	0.06

[a]Lumens filled with FA, [b]Field size. WPG is for weight percentage gain. StD is for standard deviation.

processing temperature and time and pH value of the solution) strongly affect the final product by the degree and type of chemical bonds (Lande et al. 2004a).

Compared to W_{untr}, higher UV absorbances were also observed by UMSP on thermally modified wood (160°C–180°C) (Mahnert et al. 2013). Andersons et al. (2016) reported similar results at lower temperatures, but at 140°C for 1 h only a slight impact on the UV absorbance was seen. The furfurylation occurs below 140°C (Westin 2003). The chemical reactivity of the lignin is induced above a temperature of 80°C (Koch et al. 2003a) and real thermal changes of lignin are expected to begin at 150°C (Fengel and Przyklenk 1970). Ünver and Öktem (2013) showed that polymerized FA is characterized by a UV-A_{max} at around $\lambda_{280\,nm}$, i.e. which is also the case for untreated softwood lignins. Accordingly, the presented results concerning the absorbance increment at 280 nm can be unambiguously interpreted as a manifestation of the preferred deposition of (condensed) UV-active compounds at places of high lignin concentration in the cell wall. Most likely chemical bonds between FA and lignin were also produced, but of course, this assumption is not yet proved definitively.

UV absorption spectra

UV spectra with a spot size of 1 µm² in the wavelength range from 240 to 600 nm were recorded to study the spectral behavior of W_{FA} on a cellular level. The spectral characteristics of the polymerized FA deposits in the cell lumen of W_{FA} tissues are given in Figure 4. The UV spectra of the FA deposits from all three modification processes show approximately similar profiles. Common to all three modifications are (i) the high absorbance intensities, (ii) a distinct shoulder in the wavelength range between $\lambda_{340\,nm}$ and $\lambda_{380\,nm}$ and (iii) certain absorbance levels in the visible light range resulting from large chromophoric structures that were formed during the furfurylation processes. The absorption maxima of the FA deposits detected in $W_{FA,A}$ and $W_{FA,C}$ around $\lambda_{278\,nm}$ are similar to the findings of Ünver and Öktem (2013). Comparable peaks around $\lambda_{270\,nm}$ are also described by Gandini and Belgacem (1997), who studied the photopolymerization and photocrosslinking

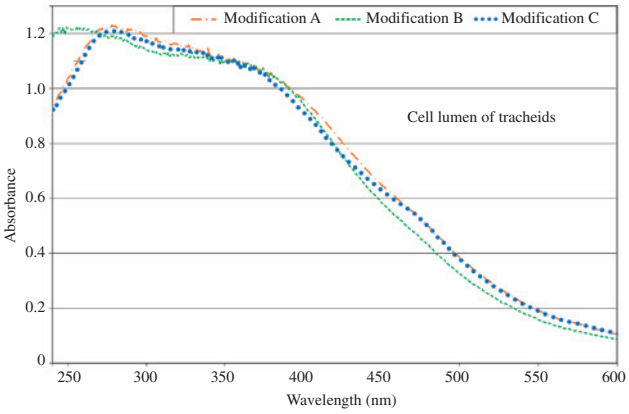

Figure 4: Representative UV absorbance spectra of polymerized FA deposited from all three modification processes in the cell lumens of radiata pine.

of simple furans and F. The A_{max} of the deposits detected in $W_{FA,B}$ are less pronounced and shifted hypsochromically (Nic et al. 2014) to $\lambda_{256\ nm}$. This slight variation of the spectral behavior may have been caused by the individual process parameters of the furfurylation and are independent of sample loading (Table 1).

In Figure 5, representative lignin spectra of the individual cell wall layers of W_{untr} (black line) and the three furfurylated wood types are presented. The cell wall layers (S2, CML and CC) of W_{untr} show typical UV spectra of lignified softwood tracheids, with the characteristic A_{max} at

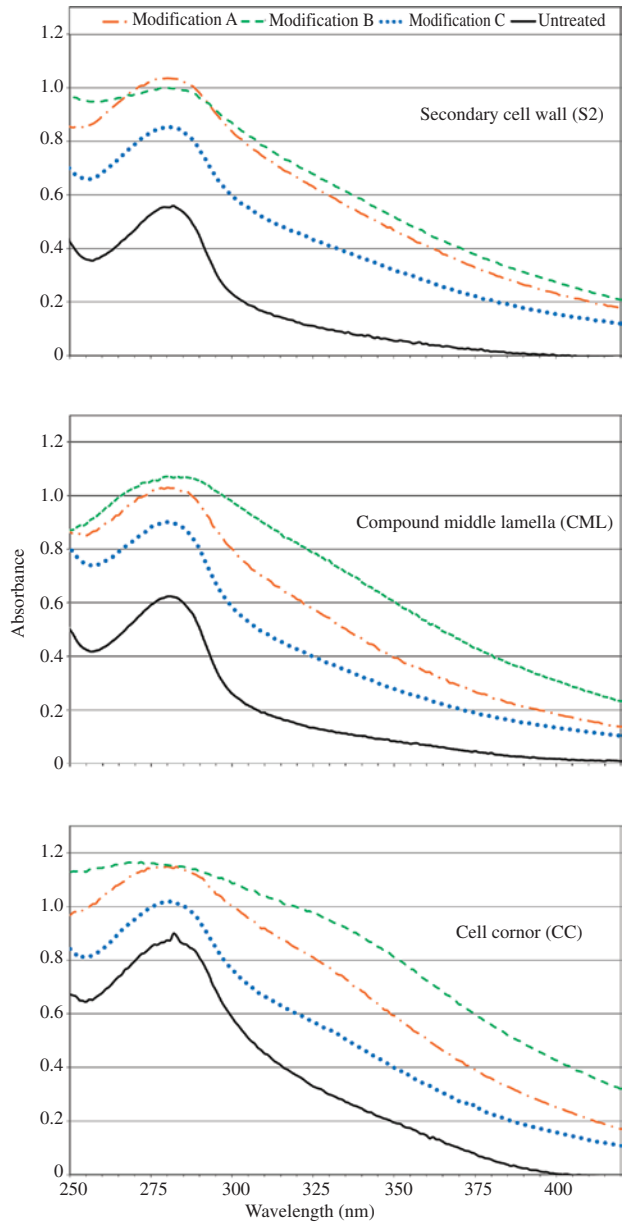

Figure 5: Representative UV absorbance spectra of the individual cell wall layers (S2, CML and CC) of untreated and furfurylated radiata pine (processes A, B and C).

$\lambda_{280\ nm}$ attributed to the strongly absorbing guaiacyl-type units (Musha and Goring 1975; Fujii et al. 1987). The different absorbance intensities at $\lambda_{280\ nm}$ are strongly correlated to the lignin concentration, with the highest amount in the CC (Koch and Kleist 2001; Koch and Grünwald 2004). In this case, the absorbance in the CC of W_{untr} is 1.6 times higher than in the S2 (Table 2). The spectra of the modified cell wall layers show similar characteristics, with significantly higher absorbance values for the individual cell wall layers (Figure 5) as was already demonstrated by the UV scanning analyses.

The spectra of $W_{FA,C}$ (57% WPG) appear close to the course of the W_{untr}, with generally higher absorbance intensities. The highest absorbances can be detected for the CC with 1.17 ($A_{272\ nm}$) and for the CML with 1.07 ($A_{280\ nm}$) for $W_{FA,B}$, i.e. for specimens with the highest WPG (70%) (Table 2). The spectra of these strongly modified cell wall layers display a bathochromic shift and shoulders with lower intensities around 320 nm (compared to W_{untr}). This is probably due to the formation of conjugated double bonds. The higher degree of conjugation stabilizes π-π^* transitions resulting in bathochromic shifts (Goldschmid 1971). In comparison, the spectra of the CML and CC show a course more similar to the spectra of polymerized FA in the lumina ($\lambda_{300\ nm}$ and $\lambda_{370\ nm}$, Figure 4), whereas the spectra of the S2 show only a shoulder with lower intensity. The strong increase from 0.56 (S2 in W_{untr}, $A_{282\ nm}$) to 1.04 (S2 in $W_{FA,A}$, $A_{278\ nm}$) and the shift of the bands of the W_{FA} cell walls indicate a higher condensation of carbonyl groups as a possible reaction of FA with the guaiacyl units of softwood lignin (Lande et al. 2004c).

Light microscopy and SEM

The LM and SEM images give insight into the cellular deposition of polymerized FA in the tissues. Figure 6 presents the LM observations in the three anatomical directions (transverse, radial and tangential) of W_{untr} and W_{FA} samples from the three process variants. The cross and radial sections include earlywood (EW) and latewood (LW). LW is easier to treat due to a larger amount of non-aspirated bordered pits compared to the EW (Phillips 1933; Liese and Bauch 1967; Zimmer et al. 2009). The sections in $W_{FA,A}$ (60% WPG, Figure 6d) and $W_{FA,C}$ (57% WPG, Figure 6j) show filled lumens in the LW. The transverse section of $W_{FA,B}$ (70% WPG, Figure 6g) unexpectedly displays less filled lumens in the LW tracheids. As the treating solutions have the same pathways as in the living tree (Nicholas and Siau 1973), it was assumed that

Table 2: Mean UV absorbances of the secondary cell wall (S2), compound middle lamella (CML) and cell corners (CC) of untreated and A-, B- and C-type modified radiata pine.

		S2			CML			CC		
Process	**WPG (%)**	**λ (nm)**	**Abs.**	**Δ**	**λ (nm)**	**Abs.**	**Δ**	**λ (nm)**	**Abs.**	**Δ**
Untr.	0	282	0.56		281	0.62		282	0.90	
A	60	278	1.04	0.48	280	1.03	0.41	278	1.15	0.25
B	70	280	1.00	0.44	280	1.07	0.45	272	1.17	0.27
C	57	280	0.86	0.30	280	0.90	0.28	281	1.02	0.12

The data are averages of 15–20 individual spectra. Δ is the absorbance difference between the untreated control and the FA-modified samples.

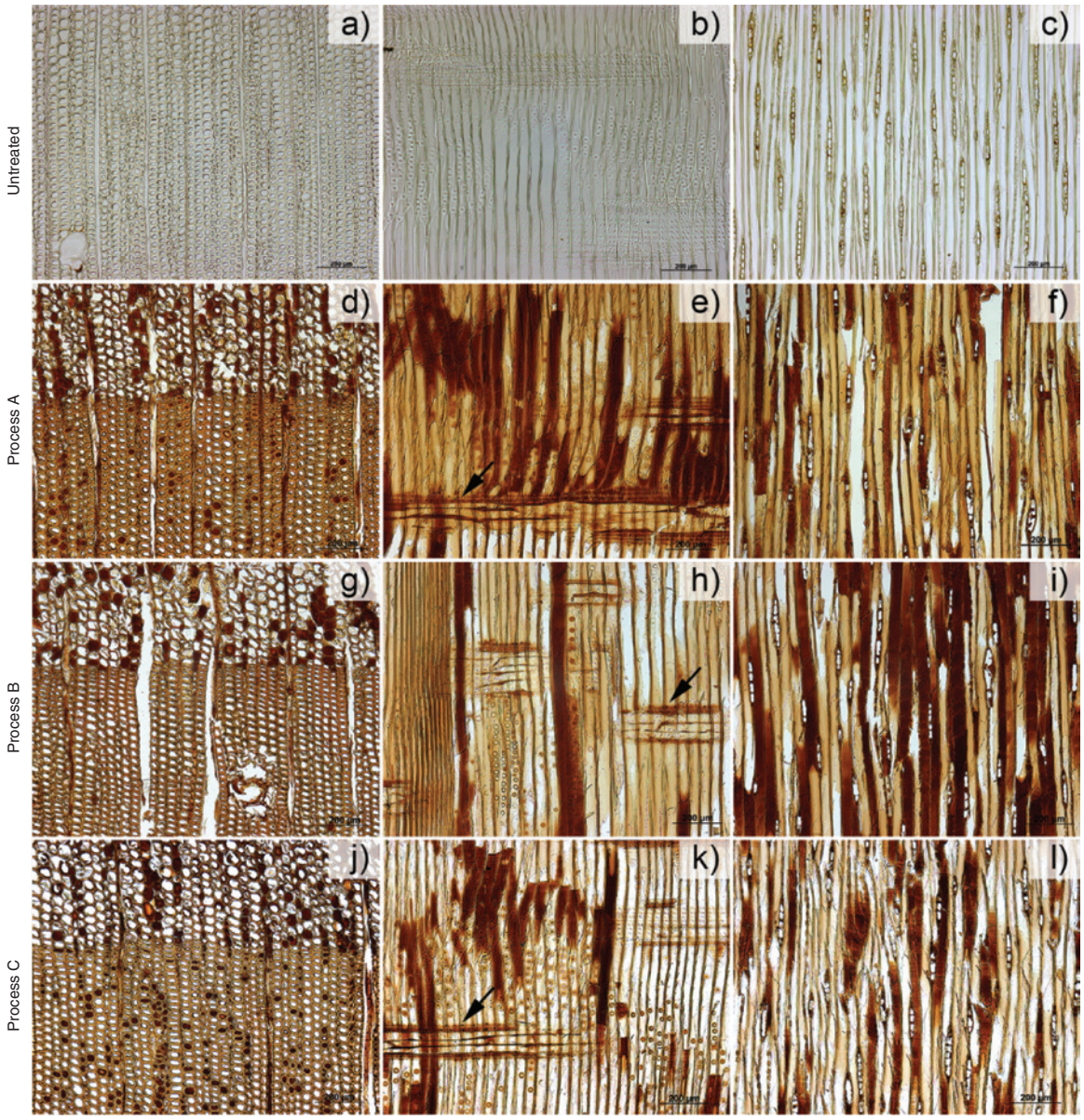

Figure 6: Light microscopic images of untreated (6a–c) and furfurylated radiata pine (processes A, B and C) in the three anatomical directions (transverse 6a, d, g, j; radial 6b, e, h, k; tangential 6c, f, g, l).
Compared to the untreated material, the furfurylated tissue appears darker with polymerized FA deposits in cell lumens. Filled ray tracheids are marked by arrows.

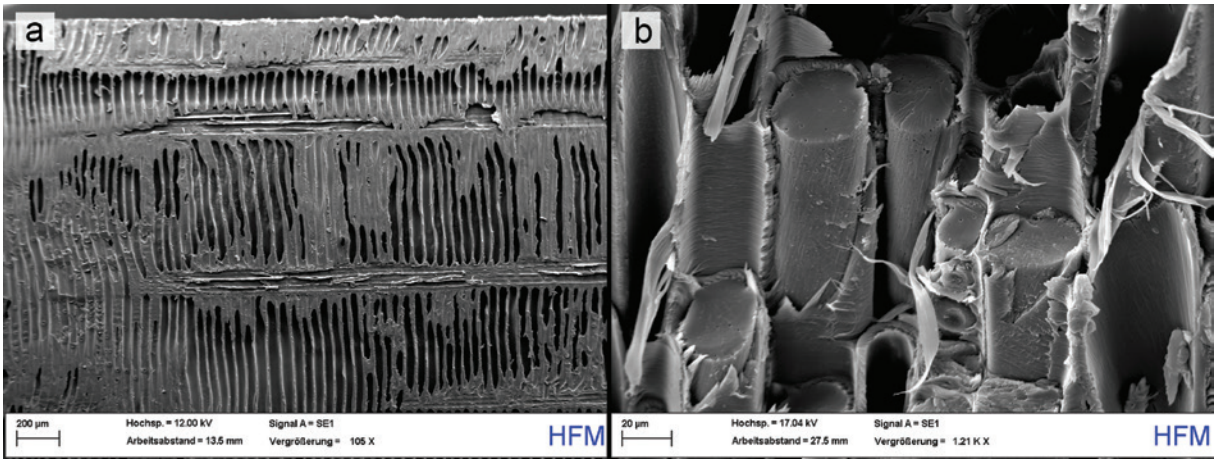

Figure 7: SEM images of furfurylated radiata pine.
The overview image shows the cellular distribution of polymerized FA deposits in the radial section (a). The polymerized FA is spatially displayed as a compact, lumen filling substance (b).

polymerized FA would be located in the easily accessible parenchyma cells of the wood rays. Radiata pine investigated by Wardrop and Davies (1961) showed an apparently selective penetration of ray parenchyma and less intensively penetrated ray tracheids. However, the radial and tangential sections of the W_{FA} samples revealed that the FA was accessorily deposited in the ray tracheids (Figure 6e, h, k). One reason could be that the FA solution enters the ray tracheids predominantly via the connecting pits of the EW tracheids. The variability in filled cell lumens in the axial and radial directions supports the findings of Lande et al. (2010) or Zimmer et al. (2014) and are manifestations of varying permeability in Scots pine sapwood. This seems to also apply for radiata pine sapwood.

Aspirated tracheid bordered pits are assumed to function as physical barriers in case of impregnation (Stamm 1946; Zimmer et al. 2014). UMSP indicates a concentration decrement of polymerized FA from CML to S2. This can be explained by the early observation of Wardrop and Davies (1961) that aspirated bordered pits lead directly to the CML and serve as entrance openings during impregnation of the cell wall.

An uneven distribution and differently filled cell types can be seen. The permeability of W_{untr} may vary due to various physiological parameters in the living tree and also by the drying parameters (Booker 1990; Booker and Evans 1994; Zimmer et al. 2009, 2014; Lande et al. 2010). For successful wood protection system performance, a homogenous distribution of the treating solution in the wooden tissue is essential (Zimmer et al. 2012). Degradation studies reveal the importance of a consistent penetration and polymerization of FA during the production of W_{FA} (Venås 2008). Certainly, more systematic studies are needed in this context.

The SEM images (Figure 7) confirm the UMSP observations and provide more detailed information on the cellular distribution of polymerized FA deposits. The cell lumens of the ray parenchyma cells appear empty (Figure 7a), as already observed under LM. In Figure 7b, the polymerized FA is spatially displayed as a compact lumen-filling substance. These deposits are obviously attached to the tracheid walls.

Conclusions

UMSP is an appropriate method for topochemical studies of W_{FA} subjected to various processes of modification. The measurements clearly show that the entire wood cell wall is modified, especially in the regions with the highest lignin concentration. The analyzed samples are characterized by strongly increased UV absorbances as a result of the formation of (condensed) aromatic compounds. This leads to the assumption that chemical bonds between FA and lignin may have been present. More specific knowledge of the nature of these bonds would probably be helpful in improving the biological resistance of furfurylated wood.

Acknowledgments: The authors extend their sincere thanks to the Research Council of Norway (RCN project 219294/O30, Wood-polymer composites for use in marine environments) for providing the test material. We also thank A. Vieler for sectioning, SEM preparations and analysis, and D. Paul and K. Brandt, Hamburg, for assistance in the UMSP analysis.

References

Aguayo, M.G., Ferraz, A., Elissetche, J.P., Masarin, F., Mendonça, R.T. (2014) Lignin chemistry and topochemistry during kraft delignification of *Eucalyptus globulus* genotypes with contrasting pulpwood characteristics. Holzforschung 68:623–629.

Andersons, B., Noldt, G., Koch, G., Andersone, I., Meija-Feldmane, A., Biziks, V., Grinins, J. (2016) Scanning UV microspectrophotometry as a tool to study the changes of lignin in hydrothermally modified wood. Holzforschung 70:215–221.

Arantes, V., Qian, Y., Kelley, S.S., Milagres, A.M.F., Filley, T.R., Jellison, J., Goodell, B. (2009) Biomimetic oxidative treatment of spruce wood studied by pyrolysis-molecular beam mass spectrometry coupled with multivariate analysis and ^{13}C-labeled tetramethylammonium hydroxide thermochemolysis: implications for fungal degradation of wood. J. Biol. Inorg. Chem. 14:1253–1263.

Arantes, V., Milagres, A.M., Filley, T.R., Goodell, B. (2011) Lignocellulosic polysaccharides and lignin degradation by wood decay fungi: the relevance of nonenzymatic Fenton-based reactions. J. Ind. Microbiol. Biotechnol. 38:541–555.

Bariska, M., Osusk, A., Bosshard, H.H. (1983) Änderung der mechanischen Eigenschaften von Holz nach Abbau durch Basidiomyceten. Holz Roh- Werkst. 41:241–245.

Bianchi, S., Koch, G., Janzon, R., Mayer, I., Saake, B., Pichelin, F. (2016) Hot water extraction of Norway spruce (Picea abies [Karst.]) bark: analyses of the influence of bark aging and process parameters on the extract composition. Holzforschung 70:619–631.

Booker, R.E. (1990) Changes in transverse wood permeability during the drying of *Dacrydium cupressinum* and *Pinus radiata*. New Zeal. J. For. Sci. 20:231–44.

Booker, R.E., Evans, J.M. (1994) The effect of drying schedule on the radial permeability of *Pinus radiata* D. Don. Holz Roh- Werkst. 52:150–156.

Bryne, L.E., Walinder, M.E.P. (2010) Ageing of modified wood. Part 1: wetting properties of acetylated, furfurylated, and thermally modified wood. Holzforschung 64:295–304.

Danninger, E., Messner, K., Rohr, M. (1980) Abbauschema der Braun- und Weißfäulepilze auf heimischen Hölzern (Buche, Fichte). Holzforsch. Holzverw. 32:126–130.

Ehmcke, G., Pilgård, A., Koch, G., Richter, K. (2016) Improvement of a method for topochemical investigations of degraded furfurylated wood. Int. Wood Prod. J. 7:96–100.

Eriksson, K.E.L., Blanchette, R.A., Ander, P. Microbial and Enzymatic Degradation of Wood and Wood Components. Springer, Berlin, 1990.

Esteves, B., Nunes, L., Pereira, H. (2011) Properties of furfurylated wood (*Pinus pinaster*). Eur. J. Wood. Prod. 69:521–525.

Fackler, K., Stevanic, J.S., Ters, T., Hinterstoisser, B., Schwanninger, M., Salmén, L. (2010) Localisation and characterisation of incipient brown-rot decay within spruce wood cell walls using FT-IR imaging microscopy, Enzyme Microbial. Technol. 47:257–267.

Fengel, D., Przyklenk, M. (1970) Einfluß einer Wärmebehandlung auf das Lignin in Fichtenholz. Holz Roh- Werkst. 28:254–263.

Fergus, B.J., Procter, A.R., Scott, J.A.N., Goring, D.A.I. (1969) The distribution of lignin in spruce wood as determined by ultraviolet microscopy. Wood Sci. Technol. 3:117–138.

Fujii, T., Shimizu, K., Yamaguchi, A. (1987) Enzymatic saccharification on ultrathin sections and ultraviolet spectra of Japanese hardwoods and softwoods. Mokuzai Gakkaishi 33:400–407.

Fukazawa, K. (1992) Ultraviolet microscopy. In: Methods in Lignin Chemistry. Eds. Lin, S.Y., Dence, C.W., Springer-Verlag, Berlin. pp. 110–121.

Gandini, A., Belgacem, M.N. (1997) Furans in polymer chemistry. Prog. Polym. Sci. 22:1203–1379.

Gandini, A., Lacerda, T.M. (2015) From monomers to polymers from renewable resources: Recent advances. Prog. Polym. Sci. 48:1–39.

Gascon-Garrido, P., Oliver-Villanueva, J.V., Ibiza-Palacios, M.S., Militz, H., Mai, C., Adamopoulos, S. (2013) Resistance of wood modified with different technologies against Mediterranean termites (*Reticulitermes* spp.). Int. Biodeter. Biodegr. 82:13–16.

Goodell, B. (2003) Brown rot fungal degradation of wood: our evolving view. In: Wood deterioration and preservation: Advances in our changing world. Eds. Goodell, B., Nicholas, D., Schultz, T. American Chemical Society, Washington DC. pp. 97–118.

Goldschmid, O. (1971) Ultraviolet spectra. In: Lignins. Occurrence, Formation, Structure and Reactions. Eds. Sarkanen, K.V., Ludwig, C.H. Wiley-Interscience, New York. pp. 241–266.

Goldstein, I.S. (1955) The impregnation of wood to impart resistance to alkali and acid. Forest Prod. J. 5:265–267.

Goldstein, I.S. (1960) Impregnating solutions and methods. GB Patent 846,680.

Hill, C. Wood Modification: Chemical, Thermal and Other Processes. John Wiley & Sons, Oxford, 2006.

Kielmann, B.C., Adamopoulos, S., Militz, H., Koch, G., Mai, C. (2013) Modification of three hardwoods with an N-methylol melamine compound and a metal-complex dye. Wood Sci. Technol. 48:123–136.

Kirk, T. (1975) Effects of the brown-rot fungus *Lentzites trabea*, on lignin in spruce wood, Holzforschung 29:99–107.

Koch, G., Grünwald, C. (2004) Application of UV microspectrophotometry for the topochemical detection of lignin and phenolic extractives in wood fibre cell walls. In: Wood Fibre Cell Walls: Methods to Study their Formation, Structure and Properties. Eds. Schmitt, U., Ander, P., Barnett, J.R., Emons, A.M.C., Jeronimidis, G., Saranpää, P., Tschegg, S. Swedish University of Agricultural Sciences, Uppsala. pp. 119–130.

Koch, G., Kleist, G. (2001) Application of scanning UV microspectrophotometry to localise lignins and phenolic extractives in plant cell walls. Holzforschung 55:563–567.

Koch, G., Schmitt, U. (2013) Topochemical and electron microscopic analyses on the lignification of individual cell wall layers during wood formation and secondary changes. In: Cellular Aspects of Wood Formation, Plant Cell Monographs 20. Ed. Fromm, J. Springer-Verlag, Berlin, Heidelberg. pp. 41–69.

Koch, G., Puls, J., Bauch, J. (2003a) Topochemical characterisation of phenolic cxtractives in discoloured beechwood (*Fagus sylvatica* L.). Holzforschung 57:339–545.

Koch, G., Rose, B., Patt, R., Kordsachia, O. (2003b) Topochemical Investigations on Delignification of *Picea abies* [L.] Karst. during alkaline sulfite (ASA) and bisulfite pulping by scanning UV microspectrophotometry. Holzforschung 57:611–618.

Kojima, Y., Kato, Y., Ishikura, Y., Yoon, S.-L., Ona, T. (2014) Photoyellowing of chemically modified chemithermomechanical pulps (CTMP) from *Eucalyptus globulus* under various atmospheres. Holzforschung 68:143–149.

Lande, S., Eikenes, M., Westin, M. (2004a) Chemistry and ecotoxicology of furfurylated wood. Scand. J. Forest Res. 19:14–21.
Lande, S., Westin, M., Schneider, M. (2004b) Properties of furfurylated wood. Scand. J. Forest Res. 19:22–30.
Lande, S., Westin, M., Schneider, M.H. (2004c) Eco-efficient wood protection: Furfurylated wood as alternative to traditional wood preservation. Manage. Environ. Qual.: Int. J. 15:529–540.
Lande, S., Høibø, O., Larnøy, E. (2010) Variation in treatability of Scots pine (*Pinus sylvestris*) by the chemical modification agent furfuryl alcohol dissolved in water. Wood Sci. Technol. 44:105–118.
Li, W., Wang, H., Ren, D., Yu, Y.S., Yu, Y. (2015) Wood modification with furfuryl alcohol catalysed by a new composite acidic catalyst. Wood Sci. Technol. 49:845–856.
Liese, W., Bauch, J. (1967) On the closure of bordered pits in conifers. Wood Sci. Technol. 1:1–13.
Mahnert, K.-C., Adamopoulos, S., Koch, G., Militz, H. (2013) Topochemistry of heat-treated and N-methylol melamine modified wood of Koto (*Pterygota macrocarpa* K. Schum.) and Limba (*Terminalia superba* Engl. et Diels). Holzforschung 67:137–146.
Martínez, A.T., Rencoret, J., Nieto, L., Jiménez-Barbero, J., Gutiérrez, A., Del Río, J.C. (2011) Selective lignin and polysaccharide removal in natural fungal decay of wood as evidenced by in situ structural analyses. Environ. Microbiol. 13:96–107.
Militz, H. (2002) Thermal treatment of wood: European prosesses and their background. IRG/WP 02-40241. In: Proceedings, International Research Group on Wood Protection, 12–17 May, Cardiff.
Moghaddam, M., Wålinder, M.E.P., Claesson, P.M., Swerin, A. (2016) Wettability and swelling of acetylated and furfurylated wood analyzed by multicycle Wilhelmy plate method. Holzforschung 70:69–77.
Musha, Y., Goring, D.A.I. (1975) Distribution of syringyl and guaicyl moieties in hardwoods as indicated by ultraviolet microscopy. Wood Sci. Technol. 9:45–58.
Nic, M., Jirat, J., Kosata, B. Compendium of Chemical Terminology (Gold Book). IUPAC, Durham, North Carolina. 2014.
Nicholas, D.D., Siau, J.F. (1973) Factors influencing the treatability of wood. In: Wood Deterioration and its Prevention by Preservative Treatment. Vol. 2. Ed. Nicholas, D.D. University Press, Syracuse. pp. 299–343.
Niemenmaa, O., Uusi-Rauva, A., Hatakka, A. (2008) Demethoxylation of [O14CH3]-labelled lignin model compounds by the brown-rot fungi *Gloeophyllum trabeum* and *Poria* (*Postia*) *placenta*. Biodegradation 19:555–565.
Nordstierna, L., Lande, S., Westin, M., Karlsson, O., Furó, I. (2008) Towards novel wood-based materials: Chemical bonds between lignin-like model molecules and poly(furfuryl alcohol) studied by NMR. Holzforschung 62:709–713.
Pfriem, A., Dietrich, T., Buchelt, B. (2012) Furfuryl alcohol impregnation for improved plasticization and fixation during the densification of wood. Holzforschung 66:215–218.
Phillips, W.W.J. (1933) Movement of the pit membrane in coniferous woods, with special reference to preservative treatment. Forestry 7:109–120.
Pilgård, A., De Vetter, L., Van Acker, J., Westin, M. (2010a) Toxic hazard of leachates from furfurylated wood: Comparison between two different aquatic organisms. Environ. Toxicol. Chem. 29:1067–1071.
Pilgård, A., Treu, A., Van Zeeland, A.N.T., Gosselink, R.J.A., Westin, M. (2010b) Toxic hazard and chemical analysis of leachates from furfurylated wood. Environ. Toxicol. Chem. 29:1918–1924.
Rehbein, M., Koch, G. (2011) Topochemical investigation of early stages of lignin modification within individual cell wall layers of Scots pine (*Pinus sylvestris* L.) sapwood infected by the brown-rot fungus *Antrodia vaillantii* (DC.: Fr.) Ryv. Int. Biodeter. Biodegr. 65:913–920.
Ringman, R., Pilgård, A., Brischke, C., Richter, K. (2014) Mode of action of brown rot decay resistance in modified wood: a review. Holzforschung 68:239–246.
Rowell, R.M., Simonson, R., Hess, S., Placket, D.V., Cronshaw, D., Dunningham, E. (1994) Acetyl distribution in acetylated whole wood and reactivity of isolated wood cell wall components to acetic anhydride. Wood Fibre Sci. 26:11–18.
Saka, S., Whiting, K., Fukazawa, K., Goring, D.A.I. (1982) Comparative studies on lignin distribution by UV microscopy and bromination combined with EDXA. Wood Sci. Technol. 16:269–277.
Schneider, M.H. (1995) New cell wall and cell lumen wood polymer composites. Wood Sci. Technol. 29:121–127.
Schneider, M.H., Philips, J.G., Lande, S. (2000) Physical and mechanical properties of wood polymer composites. J. Forest Eng. 11:83–89.
Schultze-Dewitz, G. (1966) Relations between elasticity and static and impact bending strength of pinewood after exposure to basidiomycetes. Holz Roh- Werkst. 24:506–512.
Scott, J.A.N., Procter, A.R., Fergus B.J., Goring, D.A.I. (1969) The application of ultraviolet microscopy to the distribution of lignin in wood: description and validity of the technique. Wood Sci. Technol. 3:73–92.
Sejati, P.S., Imbert, A., Gérardin-Charbonnier, C., Dumarçay, S., Fredon, E., Masson, E., Nandika, D., Priadi, T., Gérardin, P. (2017) Tartaric acid catalyzed furfurylation of beech wood. Wood Sci. Technol. 51:379–394.
Sint, K.M., Adamopoulos, S., Koch, G., Hapla, F., Militz, H. (2012) Impregnation of *Bombax ceiba* and *Bombax insigne* wood with a N-methylol melamine compound. Wood Sci. Technol. 47:43–58.
Stamm, A.J. (1946) Passage of liquids, vapours and dissolved materials through softwoods. U.S. Forest Products Laboratory. Techical Bullentin 929.
Spurr, A.R. (1969) A low viscosity epoxy resin embedding medium for electron microscopy. J. Ultra. Mol. R. 26:31–43.
Stamm, A.J. (1977) Dimensional stabilization of wood with furfuryl alcohol resin. In: Wood Technology: Chemical Aspects. Ed. Goldstein, I. American Chemical Society, Washington DC. 43:141–149.
Stamm, A.J. Wood and Cellulose Science. The Ronald Press Company, New York, 1964.
Takabe, K. (2002) Cell walls of woody plants: Autoradiography and ultraviolet microscopy. In: Wood Formation in Trees. Ed. Chaffey, N. Taylor & Francis, Singapore. pp. 159–177.
Thygesen, L.G., Barsberg, S., Venås, T.M. (2010) The fluorescence characteristics of furfurylated wood studied by fluorescence spectroscopy and confocal laser scanning microscopy. Wood Sci. Technol. 44:51–65.
Uppal, S.K., Gupta, R., Dhillon, R.S. (2008) Potential of sugarcane bagasse for production of furfural and its derivatives. Sugar Tech. 10:298–301.

Ünver, H., Öktem, Z. (2013) Controlled cationic polymerization of furfuryl alcohol. Eur. Polym. J. 49:1023–1030.
van Eetvelde, G., De Geyter, S., Marchal, P., Stevens, M. (1998) Aquatic toxicity research of structural materials. IRG/WP 98-50114. In: Proceedings, International Research Group on Wood Protection, 19–19 June, Maastricht.
Venås, T.M. (2008) A study of mechanisms related to the fungal decay protection rendered by wood furfurylation. University of Copenhagen, Copenhagen.
Venås, T.M., Rinnan, Å. (2008) Determination of weight percent gain in solid wood modified with *in situ* cured furfuryl alcohol by near-infrared reflectance spectroscopy. Chemometr. Intell. Lab. 92:125–130.
VFF-Merkblatt HO.06-4 (2016). Holzarten für den Fensterbau – Teil 4: Modifizierte Hölzer.
Wardrop, A.B., Davies, G.W. (1961) Morphological factors relating to the penetration of liquids in wood. Holzforschung 15:129–141.
Westin, M. (2003) Furan polymer impregnated wood. Patent CA 2493512 C.
Winandy, J.E., Morrell, J.J. (1993) Relationship between incipient decay, strength, and chemical composition of Douglas-fir heartwood. Wood Fibre Sci. 25:278–288.
Yelle, D.J., Ralph, J., Lu, F., Hammel, K.E. (2008) Evidence for cleavage of lignin by a brown rot basidiomycete. Environ. Microbiol. 10:1844–1849.
Yelle, D.J., Wei, D., Ralph, J., Hammel, K.E. (2011) Multidimensional NMR analysis reveals truncated lignin structures in wood decayed by the brown rot basidiomycete *Postia placenta*. Environ. Microbiol. 13:1091–1100.
Zimmer, K.P., Larnøy, E., Koch, G. (2009) Wood properties affecting permeability of furfuryl alcohol in Scots pine sapwood. IRG/WP 09-40470. In: Proceedings, International Research Group on Wood Protection, 24–28 May, Beijing.
Zimmer, K.P., Larnøy, E., Høibø, O. (2012) Assessment of fluid flow paths and distribution in conifers. Wood Res. 57:1–14.
Zimmer, K.P., Høibø, O., Vestøl, G.I., Larnøy, E. (2014) Variation of treatability of Scots pine sapwood: A survey of 25 different northern European locations. Wood Sci. Technol. 48:435–447.

III

Wood Science and Technology
https://doi.org/10.1007/s00226-020-01194-1

ORIGINAL

Furfurylation result of Radiata pine depends on the solvent

L. G. Thygesen[1] · G. Ehmcke[2] · S. Barsberg[1] · A. Pilgård[2]

Received: 26 October 2019

Abstract

Furfurylation is a modification technique that improves many wood properties. The wood is first impregnated with furfuryl alcohol (FA) diluted in a solvent, and afterward the impregnated wood is cured, during which time a FA derived polymer is formed within the wood cell wall and to some extent also within the cell lumina. In this study, the effect of the solvent used during the impregnation step of the process on the distribution of the FA polymer within the wood structure was investigated for Radiata pine (*Pinus radiata*). It was found that impregnation carried out using isopropanol rather than water as solvent resulted in more filled earlywood tracheid lumina, albeit this result may be confounded by a concomitant difference in weight percent gain. It was hypothesized that the degree of earlywood lumen filling affects the durability of furufrylated wood in marine settings via an effect on the hardness on the microscale as perceived by gribble (*Limnoriidae*) and by shipworm (*Teredinidae*) larvae when they settle on wood.

Introduction

Furfurylation is a wood modification process in which wood is impregnated with furfuryl alcohol supplemented with a catalyst and afterward cured, during which time a furfuryl alcohol (FA) polymer is formed inside the wood. Wood modification by furfurylation has an environmentally friendly profile; the modified wood does not pose an environmental hazard (Lande et al. 2004a; Pilgard et al. 2010a, b; van Eetvelde et al. 1998), and FA can be produced from agricultural waste (Chuang et al. 1984; Gonzalez et al. 1992; Maciel et al. 1982). Furfurylation makes the material more versatile as it improves wood properties in several ways. The reduced water uptake increases dimensional stability (Epmeier et al. 2007a, b; Epmeier and Kliger

✉ L. G. Thygesen
lgt@ign.ku.dk

[1] Department of Geosciences and Natural Resource Management, University of Copenhagen, Rolighedsvej 23, 1958 Frederiksberg C, Denmark

[2] Chair of Wood Science, Technical University of Munich, Winzererstrasse 45, 80797 Munich, Germany

Published online: 06 June 2020

2005; Herold and Pfriem 2014; Lande et al. 2004b; Stamm 1964; Westin 2004) and makes the treated wood less susceptible to fungal degradation (Lande et al. 2005). While these positive effects of furfurylation for the use of wood on land are well-known, only a few studies have explored the possible effects of this modification method on wood durability in marine applications (Lande et al. 2004c; Slevin et al. 2015; Westin et al. 2016). New alternatives for wood protection in marine environments are, however, relevant to explore as traditional treatments for this type of applications, like for example CCA, are no longer legal in Europe due to the associated environmental problems (Hingston et al. 2001; Ibach 2005; Townsend et al. 2005). In a field test, it was found that furfurylated Scots pine sapwood with a weight percent gain of 29, 50 or 120% was sound after 4 years of exposure in the sea, while specimens with a weight percent gain (WPG) of 11% failed within this time frame (Lande et al. 2004b). In another experiment, it was found that furfurylation reduced attacks of both crustacean and bivalve borers, both in field tests and in laboratory trials (Slevin et al. 2015). In a recent study, Westin et al. (2016) tested the long-term suitability of furfurylation in marine environments. They found that there seem to be some critical effects of the solvent used during the furfurylation process on the durability of the modified wood when exposed in the sea for several years, and that these effects are not seen for applications on land. Specifically, they found that Scots pine specimens furfurylated using methanol/ethanol solvent and with a WPG ranging from 29 to 120% were sound or only slightly attacked after 16 years, while Scots pine specimens furfurylated using water as solvent and with a WPG of 64% failed within 8 years.

The main wood degraders in marine environments in European coastal waters are shipworms (*Teredinidae*) and gribble (*Limnoriidae*) (Borges et al. 2014a, b). These animals disintegrate the wood mechanically and use it as a food source. In some species in a symbiosis with bacteria, while other species have been found to be able to digest the material on their own (Besser et al. 2018; Cragg et al. 2015; Kern et al. 2013; King et al. 2010; Sabbadin et al. 2018). Because the first step of the degradation is similar to grinding, it is suggested that the physical–mechanical properties of the material as perceived on the microscale relevant for gribble and for shipworm larvae when they settle on wood could influence the durability of furfurylated wood in marine applications. If hardness plays a role, it implies that the physical properties of the FA-derived polymer as well as its distribution within the wood structure could influence how efficient this type of modification functions in such settings. In any case, the mechanisms involved are likely to differ from those at land where the main degraders are fungi. However, although the mechanisms might be different they depend on the end point of the wood furfurylation process and the properties of the ensuing poly(FA)-wood composite, i.e., of the furfurylated wood.

Polymerization of FA is a complicated process. It requires a catalyst and is at present believed to take place in three steps (Choura et al. 1996). The first step is the formation of linear FA chains, which in a second step form conjugated FA oligomers. These steps take place while the system is still liquid. In the final step, the linear oligomers cross-link via Diels–Alder cycloadditions forming a branched structure, which causes the emergence of a rubbery state, a process that, if allowed to proceed sufficiently far, results in a hard, stiff and glassy polymer. Furan ring opening may

also occur as a side reaction during the polymerization process and can affect the mechanical properties of the final polymer (Falco et al. 2018b).

Consistent with this overall three-step mechanism, it has been found that wood furfurylation causes a strong fluorescence originating from the FA-derived conjugated polymer segments situated both within cell walls as well as within lumens, i.e., neat FA polymer material within lumina. The fluorescence characteristics are closely coupled with the location of the polymer. Thus, the emission from cell lumen material is significantly red-shifted as compared to emission originating from within cell walls (Thygesen et al. 2010), indicating that the propensity of the FA polymer to form longer conjugated segments is higher in the less constrained (empty) cell lumina.

Whether or not FA links to lignin inside wood cell walls in furfurylated wood has been discussed for some years. Experiments in vitro have shown that FA links to ring positions of simple lignin monomers (Nordstierna et al. 2008), while molecular modeling using larger, more realistic lignin models indicates that FA just as readily binds to other molecular positions not present in the simpler lignin models (Barsberg and Thygesen 2017). Topochemical investigations of furfurylated wood cell walls in situ (Ehmcke et al. 2017) supported these findings. The study by Barsberg and Thygesen (2017) indicates relatively low selectivity that may also include binding to the aliphatic C-alpha or C-gamma positions within the lignin polymer. An important implication of this work is that cross-linking between lignin and FA that consumes lignin hydroxyl groups can be ruled out for thermodynamic reasons.

A few studies have investigated the possible differences between polymerization of neat FA and FA in the presence of an added solvent that is miscible with FA. In an earlier study (Barsberg and Thygesen 2009), polymerization of neat FA was compared with polymerization in cymene, and it was found that the latter induced a "boost" phase with rapid chain length growth not seen in the neat system. Another study found that for a fixed catalyst and catalyst concentration, the rate of polymerization significantly decreased when polymerization took place in ethanol, n-butanol or iso-butanol compared to pure FA (Kim et al. 2013). Falco et al. (2018a) recently published a FA polymerization study, where water or isopropyl alcohol (IPA) was used as solvent and maleic anhydride (MA) as catalyst. They found that IPA reduces the rate of the initial steps of the process, causing the initiation of the polymerization to take place at a higher temperature than in water, which again leads to a less complete polymerization in the end. The effect of using neat FA vs. FA diluted in ethanol for the furfurylation of veneers has also been studied (Herold et al. 2013). They found that ethanol dilution resulted in lower WPG. Apart from the direct effect of the amount of FA present in the wood when curing starts, i.e., a simple dilution effect of the solvent compared to neat FA, the furfurylation result also depends on the nature of the impregnation liquid as well as on the inherent properties of the wood (Lande et al. 2010; Treu and Zimmer 2014).

In the present study, the hypothesis was tested that the solvent used during the impregnation step of the furfurylation process plays a role in the characteristics of the modified wood, and that these characteristics correlate with the differences in marine durability reported by Westin et al. (2016). The same two solvents as in the study by Falco et al. (2018b) were included, i.e., water and isopropyl alcohol (IPA).

It was also investigated whether a vacuum step during the curing of samples impregnated using a water-based formulation affected the characteristics of the furfurylated wood.

Materials and methods

Furfurylated wood

Radiata pine (*Pinus radiata* (D.Don)) boards (25 × 140 × 1500 mm) were furfurylated using experimental formulations delivered by the company Kebony A/S. Twenty boards were furfurylated per treatment at the pilot plant at Kebony A/S. The specific initiators and catalysts used are the property of Kebony AS and are not revealed in this paper. This also goes for the details of the impregnation and curing procedures apart from the overview given in Table 1.

Light microscopy

Small wood blocks (size of about 5 mm × 5 mm × 5 mm) were prepared such that they included a growth ring boundary containing early wood and late wood tissue, if possible. With a conventional sliding microtome (Leica SM 2000 R), microscopic thin transverse sections (18–24 µm) were processed for each treatment type. The surface was moistened with distilled water. For light microscopic examination, an embedding system with Euparal (Carl Roth, Carl Roth GmbH + Co. KG, Karlsruhe, Germany) was chosen. The cutting process was very delicate and caused material-dependent artifacts, as the slices were to some extent brittle and fragile. The microscopic analyses and imaging were carried out with a light microscope (Axiophot, Carl Zeiss AG, Oberkochen, Germany), equipped with a digital camera (AxioCam, Carl Zeiss AG, Oberkochen, Germany) combined with AxioVision software (Carl Zeiss AG, Oberkochen, Germany).

Infrared spectroscopy

ATR-FTIR measurements were taken with five replicates using a Nicolet 6700 FT-IR spectrometer (Thermo Scientific, Waltham, MA, USA) equipped with a DTGS detector and a Pike Technologies GladiATR diamond ATR with a working temperature of 25 °C. Spectra were obtained from small specimens of wood (about

Table 1 Experimental formulations and procedures used for the preparation of furfurylated samples

Treatment	Furfuryl alcohol (V/V %)	Water (V/V %)	Isopropyl alcohol (V/V %)	Additive (V/V %)	Vacuum step during curing
A	37.6	60.8	0	1.6	No
B	37.6	60.8	0	1.6	Yes
C	39.9	3.7	55.1	1.3	Yes

0.5–1 mm thickness, area approximately 5×5 mm) from the center parts of the wooden boards (i.e., not the surfaces). The specimens were obtained by use of first sawing, and then by use of a razor blade. The spectral range was 4000–600 cm^{-1}, and spectra were obtained using 64 scans (128 for the background) and a spectral resolution of 4.0 cm^{-1}. Two spectra per board were obtained, but a few had to be discarded due to poor data quality (problems with atmospheric signal). Reference spectra of two times distilled furfuryl alcohol with 1% citric acid added as polymerization catalyst were also obtained in the uncured state and after curing at 130 °C for 24 h. The spectra were SNV corrected (Barnes et al. 1989).

Infrared microspectroscopy

Infrared spectra were obtained from cross sections of untreated wood specimens and wood specimens from treatment A and C using a PerkinElmer Spectrum Spotlight 400 FT-IR microscope equipped with a MCT detector. The spectral range was 4000–720 cm^{-1}, the spectral resolution was 8 cm^{-1}, and the number of scans was 16 per spectrum. Cross sections were prepared by hand using razor blades of specimens wetted in water. Wetting was carried out using vacuum and water with the addition of 1% EDTA. Spectra were obtained using a Ge tip ATR add-on, which was pressed against the sample surface. Each spectrum corresponds to an area of 1.56 µm×1.56 µm. Background spectra were obtained in air. Spectra were obtained for lumina and for cell walls for 3–5 specimens from each treatment analyzed.

Fluorescence spectroscopy

Using a Fluoromax 4 spectrofluorometer (Horiba Jobin–Yvon; Kyoto, Japan), a fluorescence landscape was obtained for a sample from a cross section of each treated board (A,B, C) and from six untreated boards. Each landscape spanned 36 excitation wavelengths in the range from 300 to 650 nm with a spacing of 10 nm, and 176 emission wavelengths in the range from 400 to 750 nm with a spacing of 2 nm. The integration time was 0.1 s, and the excitation and emission slits were both set to 1 nm. The landscapes obtained were analyzed using parallel factor analysis (PARAFAC) as implemented in the N-way toolbox for Matlab by Rasmus Bro and Claus Andersson (http://www.models.life.ku.dk/nwaytoolbox). PARAFAC modeling was run without constraints on the loadings.

Results and discussion

Infrared spectra of the untreated and of the three different furfurylation formulations and procedures show that specimens from treatment C stand out from treatment A and B (Fig. 1). A principal component analysis confirmed this (results not shown). This implies that for furfurylation using water as solvent, no effects of the vacuum drying step prior to curing were discernable using infrared spectroscopy, while a clear effect of the solvent was seen. In the IR wood spectra, a new

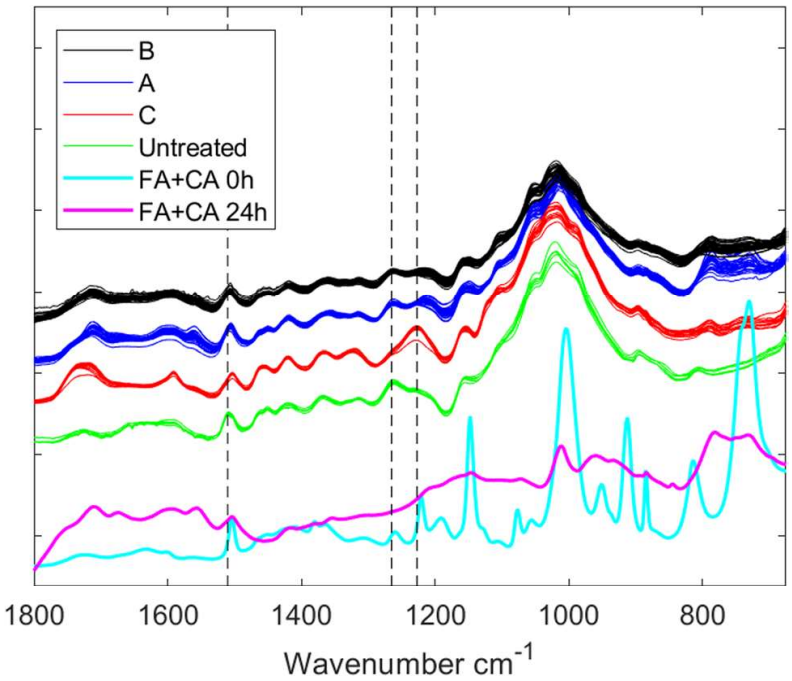

Fig. 1 SNV corrected ATR-IR spectra of untreated and the three types of furfurylated Radiata wood samples included in the study. SNV corrected ATR-IR spectra of furfuryl alcohol containing citric acid as catalyst are also shown for comparison, both before and after curing. The vertical lines mark band positions 1510, 1265 and 1227 cm^{-1}

absorbance peak at approximately 1260 cm^{-1} is seen for treatment C. When comparing the wood spectra to the spectra of neat cured and uncured furfuryl alcohol in Fig. 1, both show higher infrared absorbance in the 1300–1250 cm^{-1} range than in the 1250–1200 cm^{-1} range. However, since the spectra for the furfurylated wood samples are not dominated by the other strong absorbance bands seen in the uncured neat FA, it was found most likely that this band is due to polymerized FA.

Figure 1 also shows that the lignin absorbance peak seen at approximately 1510 cm^{-1} for untreated softwood (Faix 1991; Schwanninger et al. 2004) downshifts approximately 5 cm^{-1} as would be expected if FA binds to a ring position within the lignin of the wood cell wall (Barsberg and Thygesen 2017). However, as also seen in the figure, polymerized FA itself also has a peak at the downshifted position, so it is not possible to assign the increased absorbance at the new peak position to one or the other of these two possibilities. Another interesting region in the IR spectra is the carbonyl peak at approximately 1750 cm^{-1}. All three furfurylation procedures give a relative increase in this functionality, thus confirming the furan ring opening effect of both water and alcohol found by Falco et al. (2018b). A broadening of the peak position is also seen for the alcohol-based treatment C in contrast to the two water-based treatments A and B, again confirming the observations by Falco et al. (2018b), which they suggested to be due to the formation of isopropyl levulinate and the ester bond therein.

Regarding fluorescence spectroscopy results, mean excitation-emission landscapes were prepared for the untreated controls and for each of the three different furfurylation treatments (Fig. 2). The mean landscapes confirm earlier results (Thygesen et al. 2010), with emission shifting toward higher wavelengths with

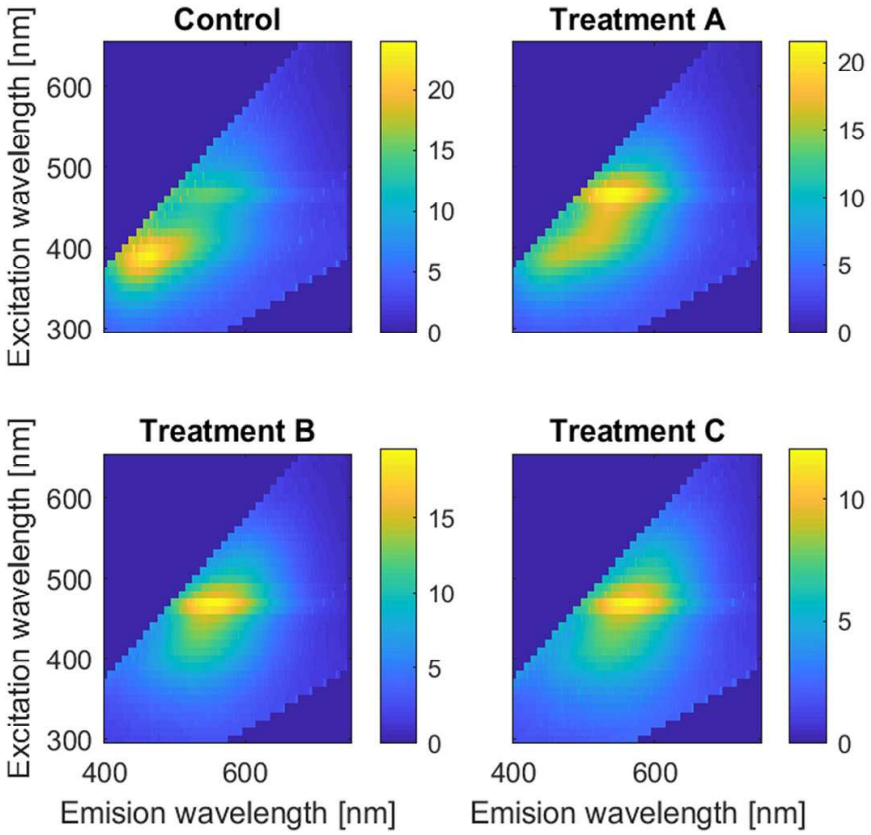

Fig. 2 Mean fluorescence excitation-emission landscapes of untreated Radiata wood and of the three types of furfurylated Radiata wood specimens included in the study

furfurylation compared to the untreated wood. When comparing treatments A, B and C, treatment A shows a trace of the signal from untreated wood. The PARAFAC model of the fluorescence landscapes (Fig. 3) also confirms earlier results (Thygesen et al. 2010). Three populations of fluorophores were found in the furfurylated wood, of which the one with the excitation-emission pair corresponding to the lowest wavelengths dominates in the untreated wood. The excitation and emission wavelengths are not completely identical to, but close to the three fluorophore populations found for a different sample set of furfurylated wood and using a different wood species (Thygesen et al. 2010), i.e., one with an excitation/emission maximum at ~ 390/450 nm, a second at ~ 460/520 nm and a third at ~ 480/600 nm. This similarity allows us to speculate that these populations are generic representatives of different conjugation lengths of the FA oligomers present in the material. When comparing the scores and loadings of the PARAFAC model, there is no indication of any qualitative differences between the three treatments regarding the emission characteristics of the FA polymer formed. Further, the relation between the scores for the three factors appears to be similar for all three types of furfurylation, again indicating no striking differences between the treatments. It should, however, be noted that only the fluorescent conjugated FA oligomers are expected to be observable in the visible range represented by the three components deduced from the emission data. The initially formed non-conjugated oligomers should not absorb or emit in the visible range (essentially represented by isolated 1,4-disubstituted furan rings), and late

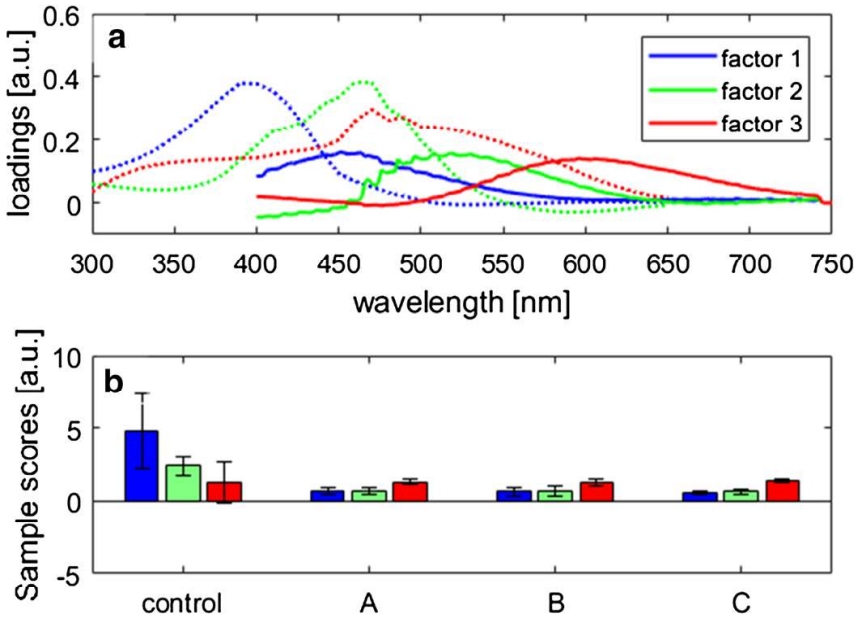

Fig. 3 PARAFAC decomposition of the fluorescence landscapes summarized in Fig. 2 using three factors. **a** shows the loadings in the excitation and emission directions, and **b** shows the mean sample scores for the four different sample types included (error bars: ± standard deviation)

stage cross-linking should effectively reduce conjugation length and thereby reduce visible range fluorophores. Thus, the fluorescence emission properties of the material are dynamically changing with the progress of the furfurylation reaction and are likely further affected by emission quenching due to the spatial closeness of the fluorophores. This implies that the size of the scores seen in Fig. 3 cannot be simply interpreted as expressions of fluorophore concentrations.

The lack of differences in polymer characteristics found between the treatments using fluorescence spectroscopy did not agree with the IR spectroscopy results, which as mentioned earlier indicated that specimens furfurylated in IPA were different from specimens furfurylated in water. This disparity prompted us to turn to microscopic methods to possibly identify differences in the distribution of the FA polymer within the wood structure. Light microscopy of specimens from treatments A and C was carried out with the aim of quantifying the number of tracheids with lumina filled with FA polymer versus the number of tracheids without any visible filling (Fig. 4 and Table 2). The results show that there was a significant difference between these two treatments. The specimens prepared using water as solvent had on average about 12% filled tracheids in both earlywood and latewood, while the specimens prepared using IPA as solvent had next to no filled tracheids in the latewood, while on average 26% of the earlywood tracheids were filled. If the results of Falco et al. (2018a) can be transferred to the situation during wood furfurylation, then the use of IPA as solvent should delay the onset of polymer formation during curing compared to wood specimens impregnated with FA in water. This would imply that FA in IPA has better possibilities for further penetration from lumen into the cell wall before polymerization sets in during curing. On the other hand, the lower boiling point of IPA compared to water means that FA has less time to be transported within the wood structure during the curing step before the solvent

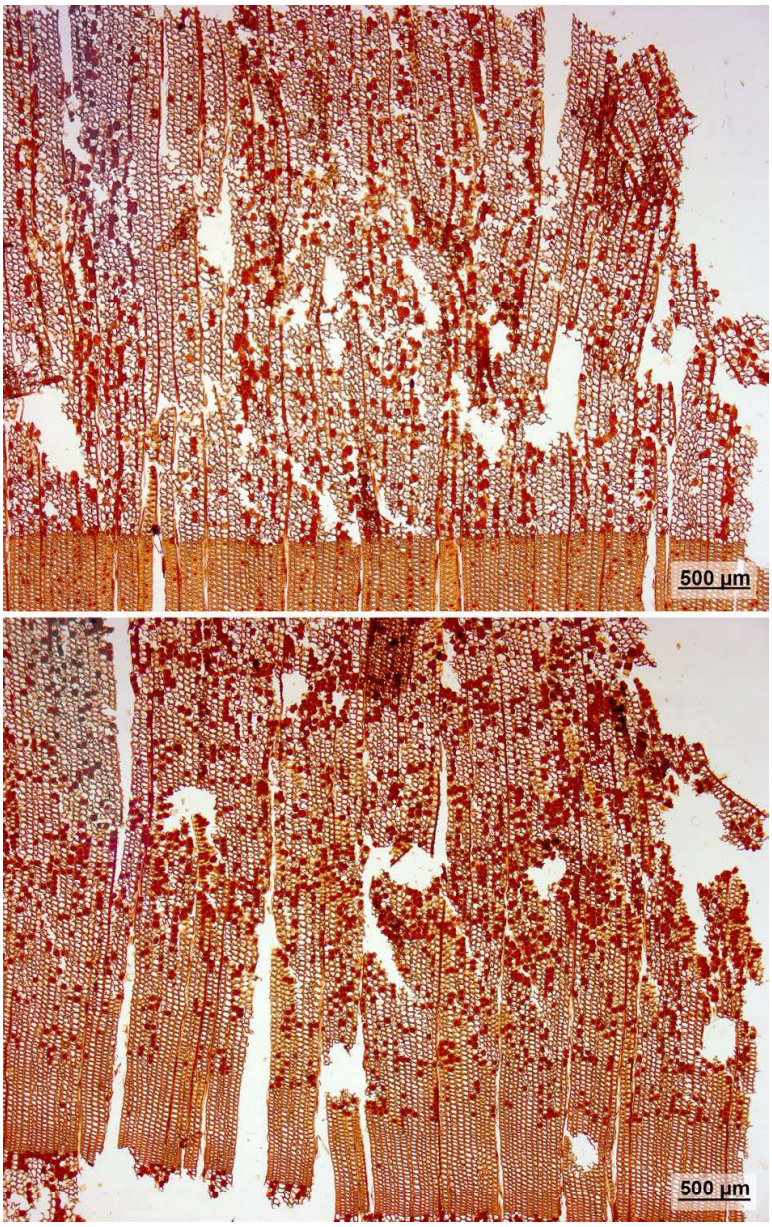

Fig. 4 Examples of light microscopy images of the treatment A (upper) and C (lower) specimens used for the counting of filled tracheid lumina (results shown in Table 2). The WPG of the treatment A specimen used was 52%, while it was 67% for the treatment C specimen

evaporates. It is suggested that the fact that lumen filling is higher in earlywood but lower in latewood for impregnation in IPA compared to water could reflect that the effect of the lower solvent boiling point dominates in earlywood, while the delay of the onset of polymerization dominates in latewood. An alternative explanation to the observed difference could be that unpolymerized FA was transported out of the latewood lumina together with IPA but not the earlywood lumina during the vacuum drying step of the C treatment. This would agree with the well-known fact that bordered pits between tracheids close more often in earlywood than in latewood during drying of softwood (Siau 1984). The A treatment did not include a vacuum drying step prior to curing (Table 1).

Table 2 Number of filled and empty tracheids in earlywood and latewood counted in light microscopy images of samples furfurylated using either water or IPA as solvent

Image no.	Treatment	Latewood tracheids				Earlywood tracheids			
		Empty	Filled	Sum	% Filled	Empty	Filled	Sum	% Filled
1	C	542	0	542	0.0	1457	554	2011	27.5
2	C					646	228	874	26.1
3	C					279	71	350	20.3
4	C	2362	8	2370	0.3	311	68	379	17.9
5	C	1187	9	1196	0.8	645	197	842	23.4
6	C					765	310	1075	28.8
7	C	1623	23	1646	1.4	746	260	1006	25.8
Total	C	5714	40	5754	0.7	4849	1688	6537	25.8
Std	C	662	8	666	0.5	361	153	514	3.7
1	A	1547	222	1769	12.5	672	126	798	15.8
2	A	2009	271	2280	11.9	262	39	301	13.0
3	A	599	107	706	15.2	397	48	445	10.8
4	A	2428	327	2755	11.9				
5	A					1023	81	1104	7.3
6	A					868	153	1021	15.0
7	A	2193	272	2465	11.0				
8	A	1487	200	1687	11.9	160	86	246	35.0
9	A					909	77	986	7.8
10	A					440	23	463	5.0
11	A	2132	288	2420	11.9				
Total	A	12,395	1687	14,082	12.0	4731	633	5364	11.8
Std	A	573	67	640	1.3	301	41	323	8.8

All images from each of the two types are from a single sample. The mean filled lumina percentage was significantly different (*t* test) on the 5% level between the earlywood of specimens from treatments A and C, and on the 1 ‰ level for the latewood

No matter which mechanisms were responsible for the final distribution of FA polymer resulting from the use of the two different solvents, the light microscopy-based quantification indicated a marked difference in the location of the FA polymer between treatments A and C. In a last experiment, it was tested whether the polymer itself showed any difference between these two treatments when individual cell lumina and cell walls were investigated using infrared microspectroscopy. Figure 5 shows the infrared spectra in the 1300–1200 cm^{-1} range for these two treatments as well as for the untreated control. Both treatments show the same pattern, with a difference between cell wall and filled lumen. This indicates that the polymers are the same for the same locations independent of the treatment, i.e., the polymer formed in the cell wall is the same for treatment A and C, and so is the polymer formed in the lumen for these two treatments. However, the polymer in the lumen and the polymer within the cell wall are not the same. Based on earlier results (Thygesen et al. 2010), the lumen polymer presumably has a longer conjugation length than

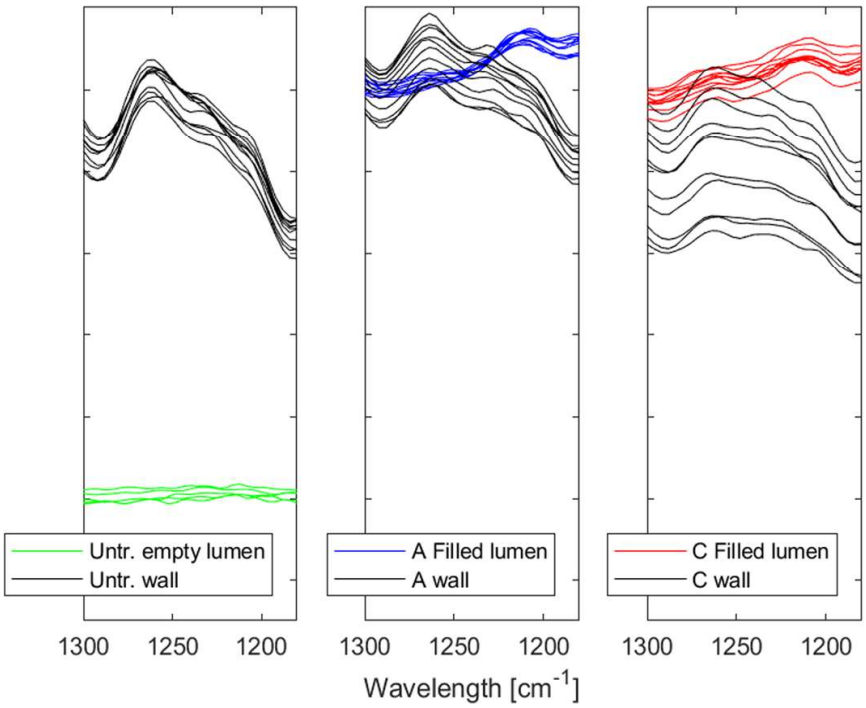

Fig. 5 Infrared micro-spectroscopy spectra of lumina and cell wall regions from untreated Radiata and from specimens of type A and C

the polymer in the cell wall. Further, when comparing to Fig. 1, IR spectra obtained from a filled lumen are seen to be similar to the spectral pattern for treatment C in Fig. 1 in the 1300–1200 cm^{-1} range, while spectra from the cell walls are similar to spectra for treatments A and B. The authors' interpretation of these observations is that the difference seen in this spectral range between specimens furfurylated in IPA and water with regards to their bulk IR spectra (Fig. 1) is due to a difference in the degree of the filling of the dominant cell type—the earlywood tracheids. That is, in this experiment, treatment C is characterized by having more filled earlywood tracheids than treatment A, but the polymer appears to be the same. Further, it is suggested that the more abundant sample filling of the earlywood tracheids of the specimens furfurylated in IPA could contribute to the efficiency of treatments using an alcohol as solvent versus treatments using water when it comes to durability in marine environments as reported by Westin et al. (2016). This would agree with the role of hardness in the resistance toward marine borers found by Cragg et al. (2007), as filled lumina will increase the macro-scale hardness. That is, it will likely be more difficult for shipworm larvae to settle, and for gribble to disintegrate the wood when a larger percentage of the earlywood lumina are filled with a hard FA polymer instead of being empty. However, these deductions are preliminary, and whether the solvent used for furfurylation affected the hardness of the cell wall cannot be inferred from these results. Further, the fact that the WPG happened to be rather different between the particular treatment A and C specimens studied using light microscopy may have confounded the results regarding lumen filling. The treatment C specimen studied had more filled earlywood tracheids and a higher WPG than the treatment A specimen studied (Fig. 4—WPG of 52 vs. 67%). In an earlier study on

the marine durability of furfurylated wood (Lande et al. 2004b), water was used as solvent during impregnation, and a clear effect of WPG was found after 4 years of exposure, illustrating the importance of WPG per se for marine durability. However, the present results from IR and fluorescence spectroscopy as well as from IR microspectroscopy are independent of the unfortunate sample selection for light microscopy. This strengthens the hypothesis that while the polymer formed appears to be similar between the furfurylation procedures tested for the same anatomical location within the wood, the distribution within the structure seems to be affected by the solvent used.

Conclusion

No data obtained in this study indicated that the FA polymer formed within Radiata wood was affected by the solvent used during the impregnation step of the furfurylation. However, there were preliminary indications that the distribution of the polymer between the cell walls and the cell lumina was affected, with more earlywood tracheid lumina filled and less late wood tracheid lumina filled when IPA was used instead of water. This would agree with the role of hardness within resistance toward marine borers found earlier (Cragg et al. 2007), as preliminary results have indicated better marine durability for furfurylated wood specimens prepared in alcohol than for those prepared in water.

Acknowledgements The study was carried out with financial support from the Norwegian Research Council (Grant No. 219294/O30) to the Project *Wood-polymer composites for use in marine environments* and from the Regional Norwegian Research Council for the Oslo Fjord region (Grant No. 268707) to the Project *Alcohol-based process for wood furfurylation*. LGT thanks Professor Thomas Günther-Pomorski at the University of Copenhagen, Department of Plant and Environmental Sciences for access to fluorescence spectroscopy. AP gratefully acknowledge financial support from The Swedish Research Council Formas 213-2011-1481 and 942-2015-530.

References

Barnes RJ, Dhanoa MS, Lister SJ (1989) Standard normal variate transformation and de-trending of near-infrared diffuse reflectance spectra. Appl Spectrosc 43:772–777

Barsberg S, Thygesen LG (2009) Poly(furfuryl alcohol) formation in neat furfuryl alcohol and in cymene studied by ATR-IR spectroscopy and density functional theory (B3LYP) prediction of vibrational bands. Vib Spectrosc 49:52–63

Barsberg ST, Thygesen LG (2017) A combined theoretical and FT-IR spectroscopy study of a hybrid poly(furfuryl alcohol)—lignin material: basic chemistry of a sustainable wood protection method. ChemistrySelect 2:10818–10827

Besser K, Malyon GP, Eborall WS et al (2018) Hemocyanin facilitates lignocellulose digestion by wood-boring marine crustaceans. Nat Commun 9:5125

Borges LMS, Merckelbach LM, Cragg SM (2014a) Biogeography of wood-boring crustaceans (Isopoda: Limnoriidae) established in european coastal waters. PLoS ONE 9(10):e109593

Borges LMS, Merckelbach LM, Sampaio I, Cragg SM (2014b) Diversity, environmental requirements, and biogeography of bivalve wood-borers (Teredinidae) in European coastal waters. Front Zool 11:13

Choura M, Belgacem NM, Gandini A (1996) Acid-catalyzed polycondensation of furfuryl alcohol: mechanisms of chromophore formation and cross-linking. Macromolecules 29:3839–3850
Chuang IS, Maciel GE, Myers GE (1984) C-13 NMR-study of curing in furfuryl alcohol resins. Macromolecules 17:1087–1090
Cragg SM, Danjon C, Mansfield-Williams H (2007) Contribution of hardness to the natural resistance of a range of wood species to attack by the marine borer. Limnoria Holzforschung 61:201–206
Cragg SM, Beckham GT, Bruce NC et al (2015) Lignocellulose degradation mechanisms across the Tree of Life. Curr Opin Chem Biol 29:108–119
Ehmcke G, Pilgård A, Koch G, Richter K (2017) Topochemical analyses of furfuryl alcohol-modified radiata pine (Pinus sradiata) by UMSP, light microscopy and SEM. Holzforschung 71:821–831
Epmeier H, Kliger R (2005) Experimental study of material properties of modified Scots pine. Holz Roh-Werkst 63:430–436
Epmeier H, Johansson M, Kliger R, Westin M (2007a) Bending creep performance of modified timber. Holz Roh-Werkst 65:343–351
Epmeier H, Johansson M, Kliger R, Westin M (2007b) Material properties and their interrelation in chemically modified clear wood of Scots pine. Holzforschung 61:34–42
Faix O (1991) Classification of lignins from different botanical origins by ft-ir spectroscopy. Holzforschung 45:21–27. https://doi.org/10.1515/hfsg.1991.45.s1.21
Falco G, Guigo N, Vincent L, Sbirrazzuoli N (2018a) FA polymerization disruption by protic polar solvents. Polymers 10(529):1–14
Falco G, Guigo N, Vincent L, Sbirrazzuoli N (2018b) Opening furan for tailoring properties of bio-based poly(furfuryl alcohol) thermoset. Chemsuschem 11:1805–1812. https://doi.org/10.1002/cssc.201800620
Gonzalez R, Martinez R, Ortiz P (1992) Polymerization of furfuryl alcohol with trifluoroacetic-acid - the influence of experimental conditions. Makromolekulare Chemie-Macromol Chem Phys 193:1–9
Herold N, Pfriem A (2014) Shape retention of furfurylated and moulded wood veneer. BioResources 9:545–553
Herold N, Dietrich T, Grigsby WJ, Franich RA, Winkler A, Buchelt B, Pfriem A (2013) Effect of maleic anhydride content and ethanol dilution on the polymerization of furfuryl alcohol in wood veneer studied by differential scanning calorimetry. BioResources 8:1064–1075
Hingston JA, Collins CD, Murphy RJ, Lester JN (2001) Leaching of chromated copper arsenate wood preservatives: a review. Environ Pollut 111:53–66
Ibach R (2005) Biological properties. In: Rowell RM (ed) Wood chemistry and wood composites. Taylor & Francis, Milton Park
Kern M, McGeehan JE, Streeter SD et al (2013) Structural characterization of a unique marine animal family 7 cellobiohydrolase suggests a mechanism of cellulase salt tolerance. Proc Natl Acad Sci U S A 110:10189–10194
Kim T, Assary RS, Kim H, Marshall CL, Gosztola DJ, Curtiss LA, Stair PC (2013) Effects of solvent on the furfuryl alcohol polymerization reaction: UV Raman spectroscopy study. Catal Today 205:60–66
King AJ, Cragg SM, Li Y et al (2010) Molecular insight into lignocellulose digestion by a marine isopod in the absence of gut microbes. Proc Natl Acad Sci USA 107:5345–5350
Lande S, Eikenes M, Westin M (2004a) Chemistry and ecotoxicology of furfurylated wood. Scand J For Res 19:14–21
Lande S, Westin M, Schneider M (2004b) Properties of furfurylated wood. Scand J For Res 19:22–30
Lande S, Westin M, Schneider MH (2004c) Eco-efficient wood protection—furfurylated wood as alternative to traditional wood preservation. Manag Environ Qual Int J 15:529–540
Lande S, Westin M, Schneider MH (2005) Eco-efficient wood protection: furfurylated wood as alternative to traditional wood preservation. Abstr Pap Am Chem Soc 229:U304–U304
Lande S, Hoibo O, Larnoy E (2010) Variation in treatability of Scots pine (*Pinus sylvestris*) by the chemical modification agent furfuryl alcohol dissolved in water. Wood Sci Technol 44:105–118
Maciel GE, Chuang IS, Myers GE (1982) C-13 NMR-study of cured furfuryl alcohol resins using cross polarization and magic-angle spinning. Macromolecules 15:1218–1220
Nordstierna L, Lande S, Westin M, Karlsson O, Furó I (2008) Towards novel wood-based materials: chemical bonds between lignin-like model molecules and poly(furfuryl alcohol) studied by NMR. Holzforschung 62:709–713
Pilgard A, De Vetter L, Van Acker J, Westin M (2010a) Toxic hazard of leachates from furfurylated wood: comparison between two different aquatic organisms. Environ Toxicol Chem 29:1067–1071

Pilgard A, Treu A, van Zeeland ANT, Gosselink RJA, Westin M (2010b) Toxic hazard and chemical analysis of leachates from furfurylated wood. Environ Toxicol Chem 29:1918–1924

Sabbadin F et al (2018) Uncovering the molecular mechanisms of lignocellulose digestion in shipworms. Biotechnol Biofuels 11:59

Schwanninger M, Rodrigues JC, Pereira H, Hinterstoisser B (2004) Effects of short-time vibratory ball milling on the shape of FT-IR spectra of wood and cellulose. Vib Spectrosc 36:23–40

Siau JF (1984) Transport processes in wood. Springer-Verlag, Berlin

Slevin C, Westin M, Lande S, Cragg SM (2015) Laboratory and marine trials of resistance of furfurylated wood to marine borers. In: 8th European conference on wood modification, Helsinki, Finland, pp 464–471

Stamm A (1964) Dimensional stabilization. In: Stamm AJ (ed) Wood and cellulose science. The Ronald Press Company, New York, pp 312–342

Thygesen LG, Barsberg S, Venas TM (2010) The fluorescence characteristics of furfurylated wood studied by fluorescence spectroscopy and confocal laser scanning microscopy. Wood Sci Technol 44:51–65

Townsend T, Dubey B, Tolaymat T, Solo-Gabriele H (2005) Preservative leaching from weathered CCA-treated wood. J Environ Manag 75:105–113

Treu A, Zimmer K (2014) Furfurylated wood for the use in marine environment—the influence of wood species on the polycondensation of furfuryl alcohol. In: Paper presented at the Northern European Network for Wood Science & Engineering (WSE) 10th Annual Meeting, Edinburgh, Scotland

Van Eetvelde G, De Geyter S, Marchal P, Stevens M (1998) Aquatic toxicity research of structural materials. IRG/WP 98-50114. Proceedings of the International Research Group on Wood Preservation, Maastricht, The Netherlands, June 14–19. pp 1–10

Westin M (2004) Furan polymer impregnated wood PCT/NO2003/000248 [WO 2004/011216 A2], 1–11. Patent

Westin M, Larson Brelid P, Nilsson T, Rapp AO, Dickerson JP, Lande S, Cragg S (2016) Marine borer resistance of acetylated and furfurylated EWood—results from up to 16 years of field exposure. In: 47th IRG annual meeting Lisbon, Portugal, 2016. The international research group on wood protection, pp WP 16-40756

IV

International Biodeterioration & Biodegradation 154 (2020) 105020

Contents lists available at ScienceDirect

International Biodeterioration & Biodegradation

journal homepage: www.elsevier.com/locate/ibiod

Topochemical and light microscopic investigations of non-enzymatic oxidative changes at the initial decay stage of furfuryl alcohol-modified radiata pine (*Pinus radiata*) degraded by the brown rot fungus *Rhodonia placenta*

G. Ehmcke[a,*], G. Koch[c], K. Richter[a], A. Pilgård[a,b]

[a] Technische Universität München, Chair of Wood Science, Winzererstraße 45, D-80797, München, Germany
[b] RISE Research Institute of Sweden, Box 857, SE-501 15, Borås, Sweden
[c] Thünen Institute of Wood Research, Leuschnerstr. 91, D-21031, Hamburg, Germany

ARTICLE INFO

Keywords:
Furfurylation
Lignin modification
UV microspectrophotometry (UMSP)
Wood modification
Rhodania placenta

ABSTRACT

The aim of this study was to visualize non-enzymatic oxidative degradation damages in the initial decay stage of the brown rot fungus *Rhodonia placenta* degradation in furfuryl alcohol (FA) modified wood cell walls and untreated wood cell walls of radiata pine (*Pinus radiata*) sapwood. A decay test with small wood blocks (1.5 × 1.5 × 5 mm^3) of untreated and furfurylated radiata pine selected from two different furfurylation processes was performed until the first mass loss occurred. The samples were exposed to the brown rot fungus *R. placenta*, monitored by light microscopy and analyzed topochemically by cellular UV microspectrophotometry (UMSP). The results showed that the FA modification process directly influenced: i) the fungal colonization and hyphal growth, ii) the spectral UV behavior, and iii) degradation patterns of the entire cell wall layers. For the first time, UMSP area scans and selective line scans of individual cell wall regions provide topochemical insights into oxidative degradation at the initial decay stage of furfuryl alcohol-modified *P. radiata* visualizing oxidative degradation *in situ*. Knowledge of the initial decay stage of brown rot degradation in FA-modified wood compared to untreated wood extends our understanding of the brown rot decay processes of cell wall compounds.

1. Introduction

Wood protection technologies, such as wood modification, are aiming for enhanced wood properties such as improved decay resistance facilitating a prolonged service life and easy disposal at the end of life (Hill, 2006). Among those wood protection technologies, wood modification with furfuryl alcohol (FA) is a commercial technology. Laboratory, in ground and marine field tests revealed that furfurylation of wood provides improved durability against biodegradation (Lande et al., 2004a; De Vetter et al., 2008; Westin et al., 2016). Studies on ecotoxicity and toxic hazard of leachates from furfurylated wood revealed that furfurylated wood has low environmental impact (Van Eetvelde et al., 1998; Lande et al., 2004b,c; Pilgård et al., 2010a,b; De Vetter et al., 2008). In general, wood modification involves the action of a chemical, biological or physical agent upon the material, resulting in increased durability and dimensional stability (Hill, 2006). FA is the key agent for the furfurylation of wood, which is obtained from renewable resources of agricultural crop waste (corn or sugar cane production). Chemically, it consists of easily hydrolysed pentosanes, and the pentoses obtained are dehydrated to furfural (Hill, 2006; Uppal et al., 2008), which is then converted to FA. The wood FA-modification process is characterized by a full cell impregnation with FA solution followed by *in situ* polymerization, which leads to a permanent swelling of the wood cell wall (Goldstein, 1955, 1960; Stamm, 1977; Schneider, 1995; Bryne and Walinder, 2010). Schneider et al. (2000) showed that the FA solution filled the cell lumen completely or partially and penetrated the cell walls to some extent. That FA polymerization takes place within the wood cell wall has been shown on furfurylated wood by infrared microscopy (Venås and Rinnan, 2008), fluorescence microscopy (Thygesen et al., 2010) and cellular UV microspectrophotometry (UMSP) (Ehmcke et al., 2017) studies. The investigations revealed concordantly higher (poly)FA concentrations in lignin-rich parts, mainly in the cell wall corner regions (CC) and the compound middle lamella (CML). Nordstierna et al. (2008) examined the possibility of a covalent bond formation to lignin during the FA polymerization process. Nuclear magnetic resonance (NMR) spectra of a liquid-phase

* Corresponding author.
E-mail addresses: ehmcke@hfm.tum.de (G. Ehmcke), gerald.koch@thuenen.de (G. Koch), richter@hfm.tum.de (K. Richter), annica.pilgard@ri.se (A. Pilgård).

https://doi.org/10.1016/j.ibiod.2020.105020
Received 17 February 2020; Received in revised form 1 June 2020; Accepted 1 June 2020

system of a lignin model compound and FA were studied. The results showed the formation of covalent bonds in the early stages of FA polymerization. Two different studies, a topochemical investigation of furfurylated wood cell walls (Ehmcke et al., 2017) and a combined theoretical and FTIR spectroscopy study of a hybrid poly(FA) – lignin material (Barsberg and Thygesen, 2017), support these findings. The latter found evidence for the condensation of FA with selected lignin models, whereas the topochemical investigations visualized the condensation of FA with cell wall lignin *in situ*. However, not all the details of the furfurylation process on the wood cell wall level are equally well understood. Hence, ongoing research deals with, for example, FA impregnation technology in the field of wood densification (Pfriem et al., 2012) or the development of new catalysts (Li et al., 2015; Sejati et al., 2017).

In order to assess the protection effect of the wood modification, standardized wood decay tests are applied. Wood degradation by brown rot fungi is one the most destructive types of component failure in wooden constructions (Zabel and Morell, 1992; Goodell, 2003). Parts of the structural basis of the wood cell wall, cellulose and hemicelluloses, are attacked (Danninger et al., 1980; Eriksson et al., 1990; Goodell, 2003; Kim et al., 2019) resulting in losses of essential engineering properties (e.g. bending strength) even before any mass loss can be detected (Schultze-Dewitz, 1966; Bariska et al., 1983; Winandy and Morrell, 1993; Curling et al., 2002; Witomski et al., 2016). The high-energy multiple impact (HEMI) test provides information about the loss of strength and structural integrity during initial decay (Brischke et al., 2006; Rapp et al., 2006; Ringman et al., 2017).

DNA and gene expression studies, as presented in a review by Alfredsen et al. (2014), provide insights into fungal activity during the decay of modified wood. The biodegradation process of brown rot organisms involves two parts, non-enzymatic oxidative degradation and enzymatic degradation (Goodell et al., 1997; Arantes et al., 2012). The non-enzymatic mechanism deconstructs the lignocellulose framework by catalytically modifying lignin (Yelle et al., 2008, 2011; Arantes et al., 2009, 2011; Martinez et al. 2009, 2011). Hydroxyl radicals initially do not only depolymerize the polysaccharide components, but also lignin (Yelle et al., 2008, 2011). Lignin is depolymerized and then rapidly repolymerized (Yelle et al., 2011). Atomic force microscopy (AFM) studies and small angle neutron scattering (SANS) data presented by Goodell et al. (2017) lead to the postulation that the majority of repolymerized and redistributed lignin deposits occurred in the first 18 days of decay by the brown rot fungus *Gloeophyllum trabeum*. Immunocytochemistry coupled with transmission electron microscopy (TEM) provides another analytical technique for ultrastructural degradation studies. Kim et al. (2015) investigated the initial degradation pattern of *Postia placenta (R. placenta*) and revealed two different degradation types distinct from previous concepts of brown rot decay. Type 1 showed ultrastructural changes in the primary cell wall (P), outermost second secondary cell wall layer (S2) and inner S2 and third secondary cell wall layer (S3). Type 2 showed structural changes in the latter areas but no changes in the outermost S2 layer. Based on the revealed degradation of the S3 layer and preferential degradation of middle lamella regions at incipient decay stages, previous ideas concerning decomposition process of tracheids and fibers need improving (Kim et al., 2015).

It is still challenging to monitor and visualize non-enzymatic oxidative degradation at the initial decay stage. Hence, basic studies on cellular characteristics of incipient brown rot degradation of the cell wall structure are rare (Irbe et al., 2006a,b; Rehbein et al., 2011; Kim et al. 2015; Goodell et al., 2017).

Brown rot degradation studies of untreated (Irbe et al., 2006b; Rehbein et al., 2011) and FA-modified softwood (Ehmcke et al., 2016) showed that cellular UV microspectrophotometry is a well-suited method to study early fungal degradation on a subcellular level. With the high spatial resolution (0.25 μm^2 per pixel) of the UV microspectrophotometry (UMSP) technique, structural changes in the cell wall layers can be detected precisely. Since lignin, as a complex and heterogeneous polymer (Fengel and Wegener, 1989; Donaldson, 2001), presents the most significant barrier to wood decay and influences the degradation modes (Schwarze, 2007), knowledge of FA-lignin modification and its potential influence on brown rot degradation is of great interest. The UMSP method allows for direct imaging of lignin distribution, lignin modification (biodegradation, delignification) (Fergus et al., 1969; Scott et al., 1969; Saka et al., 1982; Fukazawa, 1992; Koch and Kleist, 2001; Koch and Grünwald, 2004; Rehbein et al., 2011; Koch and Schmitt, 2013) and FA-lignin interaction within individual cell wall layers *in situ* (Ehmcke et al., 2017).

The aim of this study was to topochemically visualize non-enzymatic oxidative changes and lignin modification, within individual cell wall layers, in the initial decay stage of the brown rot fungus *Rhodonia placenta* degrading untreated and furfuryl alcohol (FA) modified radiata pine (*Pinus radiata*) sapwood. Thus, a detailed monitoring over 18 days of fungal colonization by the brown rot fungus *R. placenta* in wood furfurylated with two different impregnation methods and untreated wood was performed and investigated with UMSP. Light microscopic evaluation of hyphal growth, daily measured mass loss and moisture content complemented the experimental studies.

2. Materials and methods

2.1. Wood material and fungal exposure

Radiata pine (*Pinus radiata*) sapwood boards were furfurylated under different process conditions and distributed to project partners of the research project PolyWood (RCN project no 219294/O30). The furfurylation processes were based on a full cell impregnation with different FA solutions, buffer agents and catalysts. Process A was a water-based process leading to a weight percent gain (WPG) of 52%. Process B was an ethanol-based process resulting in a WPG of 67%.

The decay test was performed according to the approach of Rehbein et al. (2011) with adaptions in frequency of harvesting and sample numbers per Petri dish as a result of a pre-test (Algeier, 2014). Ten discs with 5 mm thickness, in the longitudinal direction, per furfurylated and the corresponding untreated board were processed. Afterwards, small blocks (1.5 × 1.5 × 5 mm^3, R x T x L) from the center of the discs, excluding the surface of the boards, were prepared. The criterion for the subsamples was that a growth ring boundary, containing early wood and late wood tissues, had to be included. The benefit of the small sample size, as described by Rehbein et al. (2011), is that the complete sample can be used for light microscopy and also embedded and prepared for cellular UMSP investigation in contrast to common degradation tests, for example Bravery (1979) and DIN CEN/TS 15083–1(2005) where the samples had to be cut into pieces.

The samples were dried at 103 °C for 18 h and weighed afterwards to document the dry weight for each sample before decay with a Sartorius Cubis® (Germany; 0.0001 g) analytical balance. According to EN 84 (1996), the samples were leached and conditioned at 20 °C and 65% relative humidity (RH) for one week. All samples were sterilized with gamma radiation (> 30 kGy). Petri dishes with standard malt agar according to EN 113:1996 (4% malt, Merck; and 2% agar, Roth) were prepared. Four samples (two untreated and two furfurylated) were placed without spacer on the agar in each Petri dish, together with four mycelium flakes of *R. placenta* (strain FPRL 280). The transversal sections of each sample were in direct contact with the mycelium flake. The orientation of the samples was documented. Per harvest point 4 replicates, including samples from process A and B, and 4 replicates of untreated samples were inoculated. The prepared Petri dishes were stored in a climate chamber (Memmert HPP 749, Germany) at 22 ± 1 °C and 70 ± 1% RH. The decay test was terminated after 30 days.

Two Petri dishes (4 replicates for mass loss and moisture; 4 replicates for UMSP analyses) were harvested per day and the non-

inoculated samples at the end of the decay test. At harvest, the samples were carefully rolled out from the covering mycelium. Four samples were weighed wet and dried (103 °C, 18 h) for calculating mass loss (ML) (analytical balance, Sartorius Cubis®, Germany; 0.0001 g) and moisture content (MC). For comparison of decayed, untreated and, to varying extent, modified wood samples, it is necessary to correct for mass loss according to Thybring (2017) and for mass gain due to modification (WPG) as described by Thybring (2013). The corrected MC in decayed wood was calculated by multiplying the normal MC with (1-ML) for the untreated samples or by multiplying with (1 + WPG) and (1-ML) for the modified samples. The other four samples were shock frozen in liquid nitrogen without wrapping and then stored at − 20 °C, until UMSP and light microscopy analyses.

The samples for UMSP analyses were fixed in a glutaraldehyde solution (Karnovsky, 1965) and dehydrated in a graded series of acetone. After dehydration, the samples were embedded in Spurr's (1969) epoxy resin under mild vacuum conditions. Thermal curing at 70 °C for 12 h catalyzed the polymerization process. The cross sections, which were colonized first by the fungus, were used for sectioning. In a first step the samples were trimmed with a razor blade to provide a trapezoid area of approximately 0.5 mm^2 and sectioned with an ultramicrotome (Reichert-Jung) equipped with a diamond knife. The semi-thin sections (1 µm) were transferred to quartz microscopic slides and then thermally fixed. Furthermore, cross sections for light microscopy analyses were transferred to microscopic slides, stained with toluidine blue and then thermally fixed as well.

The sections were immersed in a drop of non-UV absorbing glycerine (glycerine/water mixture $n_D = 1.46$) and covered with a quartz cover slip. As reference, non-degraded untreated and non-degraded FA-modified sapwood samples (process A, B) were also prepared, following the same embedding process.

2.2. Light microscopy

Hyphae growth inside the harvested samples of untreated and FA-modified wood exposed to *R. placenta* was investigated by light microscopy. Six sections of the radial and tangential surfaces with a thickness of 15–20 µm were processed. The microscopic sections were prepared for each harvest point and treatment. To allow longitudinal sectioning of the small samples with a conventional sliding microtome (Leica SM 2000 R, Leica Biosystems Nussloch GmbH, Germany), all samples were glued on a suitable wood block for support. All sections were taken from a 500 µm zone below the surfaces. After sectioning, the thin tissues were stained for 5 min with aniline blue (0.1% aniline blue (Merck, VWR) dissolved in 50% lactic acid (Carl Roth GmbH)) to obtain a better contrast of fungal hyphae. Afterwards, the sections were washed in distilled water to clean from unreacted stain, mounted on microscopic slides and dehydrated with a graded series of ethanol. The untreated samples were double stained with aniline blue and safranin (Art. 1382, Merck, VWR). For light microscopic examination, an embedding system with Euparal (Carl Roth GmbH) was chosen. The microscopic analyses were carried out with a Zeiss Axiophot microscope, equipped with a digital camera adapted with an evaluation program (Axiophot). For visual evaluation of hyphae growth, the radial sections provide best insight into the different cell types (early and late wood tracheids, ray parenchyma and radial tracheids). A four-grade scale evaluation where 0 means no growth and 3 means very abundant growth was applied. If no hyphae were found in the radial section (grade 0), tangential sections were used for grading.

2.3. Cellular UMSP

To study the initial degradation stages of furfurylated and untreated wood exposed to *R. placenta*, cell wall modifications were topochemically monitored by UMSP.

Quartz microscope slides prepared with ultrathin sections were placed into the microscope UMSP 80 (Carl Zeiss AG, Oberkochen, Germany). The slides were automatically scanned with a constant wavelength of λ_{280nm} (the A_{max} of softwood lignin) and analyzed with the scan program Automatic Photometric Analysis of Microscopic Objects (APAMOS, Carl Zeiss AG, Oberkochen, Germany). The principle is based on the characteristic of lignin to display an ultraviolet absorbance maximum in the range of $\lambda_{270–280\ nm}$ (Musha and Goring, 1975). Combined with the high local geometrical resolution of 0.25 $µm^2$ per pixel and a statistical evaluation of the data, the obtained data provides a semi-quantitative lignin distribution, visualized by absorbance intensities. The scans can be depicted as 2D or 3D image profiles by converting 4096 greyscale levels into 14 basic colors as described in detail by Koch and Kleist (2001).

For the topochemical analyses of the wood cell wall (furfurylated and untreated) and cell lumen filled with polymerized FA, areas with microscopically intact cell walls were selected. 10 measurements of individual cell wall layers per incubation day were scanned for semi-quantitative studies. If procurable (for good quality of the ultrathin slices), two image profiles per area of interest were carried out: i) filled lumen cells, ii) intact tracheid cells, iii) cell walls with radial oriented compound middle lamella (CML).

To follow topochemical changes on the individual cell wall level, the raw data of the obtained 2D image profiles were analyzed in a standardized procedure following a defined line profile from the middle lamella cell corner (MLcc) via the corner cell wall to the cell lumen (Fig. 1). With the scan program APAMOS line profiles can be generated merely in the direction of the x- and y-axes. However, for this study a diagonal line profile was necessary. For this purpose, the data of one representative area scan per incubation day was transferred into MS Excel data. Conditional formatting was used to highlight cells by rules to generate greyscale images. Starting from the highest absorption value in the MLcc, square fields of 36 × 36 were selected and a diagonal line (36 measuring points with a geometrical resolution of 0.25 × 0.25 $µm^2$ per pixel, 9 µm length) was displayed as a line profile. This special approach intuitively visualizes the local lignin concentration (measured at the absorbance maximum of λ_{280nm}) and the chemical cell wall modification from MLcc via corner cell wall to the cell lumen during early decay stages.

3. Results

3.1. Mass loss and moisture content

The mass loss (ML) and moisture content (MC) were calculated daily over a period of 18 days. The first detectable ML for the modified samples of type A occurred at day 16 (1.0% ML) and for the corresponding untreated samples at day 9 with 0.9% ML. The first detected mass loss for the furfurylated samples of type B occurred after 13 days (1.1% ML). In the corresponding untreated samples, the first weight reduction occurred after 8 days (0.5% ML). During the first days, all samples had a negative ML.

In Table 1, ML and equilibrium moisture content (EMC) of untreated and modified samples at the beginning of the experiment (20 °C, 65 % RH) and the MC at harvest time point when the first ML occurred are listed. By modification with FA, the EMC at equilibrium at standard climate conditions (20 °C, 65%RH) was decreased compared to the untreated samples (Table 1). Nevertheless, an increased MC was calculated after harvesting for both FA process variations with 69.4% MC for type A and 51.8% MC for type B. The progression of the MC values of the untreated and furfurylated samples during the experiment is presented in Fig. 2. After 24 h, the MC of the untreated wood samples for type A increased from 11.7% up to 47.1% and 55.5% for type B and exceeded 100% MC after 8 and 5 days, respectively. The MC of the furfurylated samples increased significantly slower compared to the untreated samples and both modified variations exceeded 30% MC after 4 days, with one outlier of type B at day 3. Until the first ML was

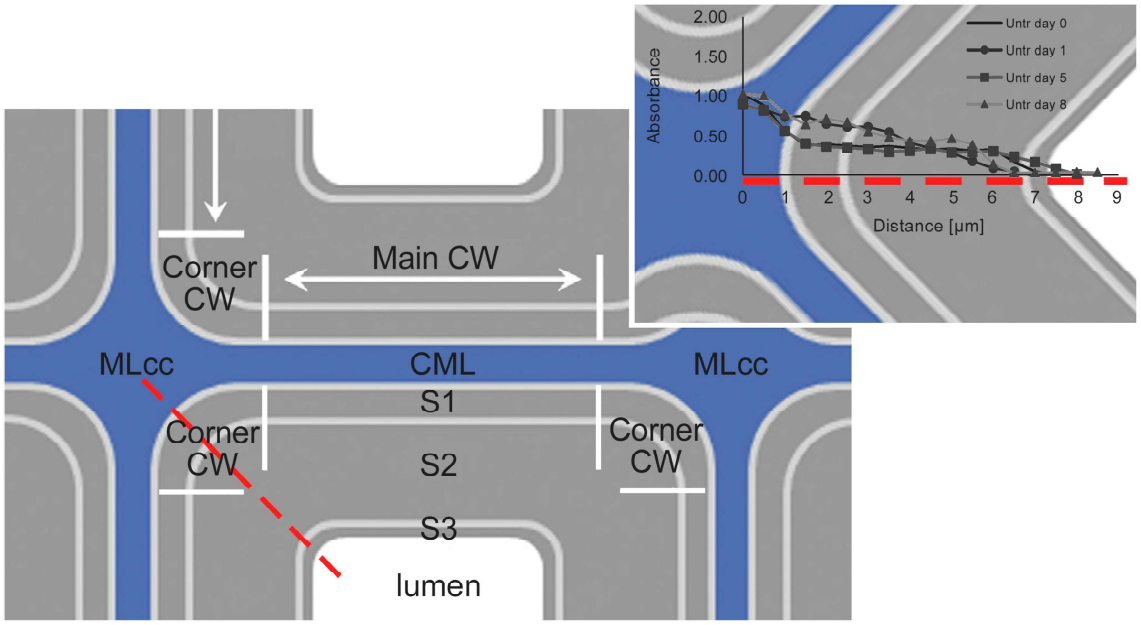

Fig. 1. Schematic diagram of untreated cell wall ultrastructure of tracheids. The red dashed line shows the area of the line profile. The line profile illustrates the absorbance values from the middle lamella cell corner (MLcc) via the corner cell wall to the cell lumen (inset). CML, compound middle lamella; CW, cell wall; S1, secondary cell wall outer layer; S2, secondary cell wall middle layer; S3, secondary cell wall inner layer.

Table 1
Equilibrium moisture content (EMC) of untreated wood and the EMC corrected for modification mass gain before decay; mass loss (ML) according to exposure to *R. placenta* at harvest point when the first ML occurred; Moisture content (MC) at harvest point corrected for ML and for mass gain due to modification. The decay test was terminated after 18 days. Samples n = 4.

Process	EMC 20/65	Exposure (day of ML)	ML [%]			MC at harvest point [%]
	[%]	[days]	Min	Average	Max	Average
A	7.0	16	0	1	1.9	69.4
untreated A	11.7	9	−3.1	0.9	6.9	113.2
B	7.5	13	−1.1	1.1	2.2	51.8
untreated B	11.7	8	−3.2	0.5	3.5	117.7

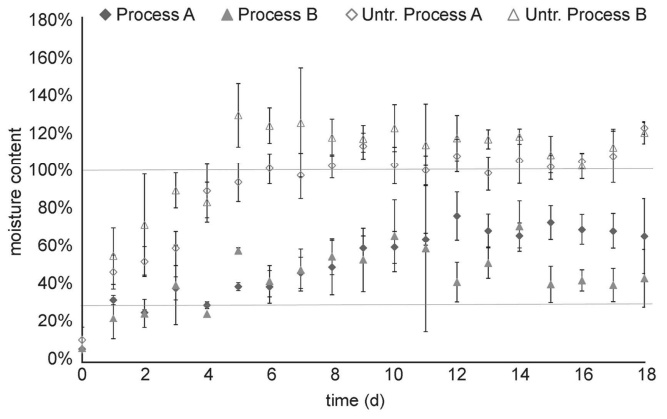

Fig. 2. Moisture content (MC) before and during the decay test, mean values (n = 4) with error bars representing standard deviation. The MC is corrected for mass loss and the MC of the furfurylated samples additionally for mass gain due to modification. Filled rhombus – furfurylated wood, process A; filled triangles - furfurylated wood, process B; rhombus – untreated wood, process A; triangles - untreated wood, process B.

measured, the MC of the furfurylated samples still increased. Throughout the course of the decay test (18 days), type B performed better with a lower mean MC of 46% than type A with a mean value of 54% MC.

3.2. Light microscopy

The incipient development of fungal hyphae colonization of untreated and modified wood samples was studied by light microscopy throughout 18 days.

Fungal colonization was seen already after one day in untreated wood (Fig. 3a ↑) and in the furfurylated sample of type B. After two days, hyphae were seen in the furfurylated sample of type A. Micrographs of radial sections of day 3 (type A) and day 2 (type B) are shown exemplarily in Fig. 3e,i. Fungal hyphae colonized initially from the direction of the cross sections into the tracheid lumina and ray parenchyma cells. The fungal colonization progress during the first days was characterized by a distinct hyphal growth in untreated wood and a moderate to low growth in type A and type B furfurylated samples. An intense spread of the fungal hyphae in untreated wood started already on the second day (growth rate 2) and then within the following two days it increased to grade 3 (very abundant), which can be seen exemplarily in Fig. 3b, and stayed there for the rest of the experiment with one exception, day 18 The vast presence of the fungal hyphae observed in untreated wood was never recorded for modified samples during the entire decay test. Compared to the untreated samples, type A reached only three times grade 3 (days 6, 8 and 9), whereas type B fluctuated between grade 1 and 2. The samples from type B performed slightly better (10 times grade 1) than from type A (8 times grade 1) (Fig. 4). This is demonstrated in an exemplary manner by day 6 in Fig. 3f,j. By the day of the first observed ML, the hyphae growth rate in FA-modified wood was medium high, grade 2 (type A day 16), low in type B (grade 1, day 13) and high (3) in the untreated sample day 9. The corresponding micrographs (radial and transverse section details) of the first ML are presented in Fig. 3. Light microscopic analysis of the transverse sections revealed no structural changes (Fig. 3d,h,l).

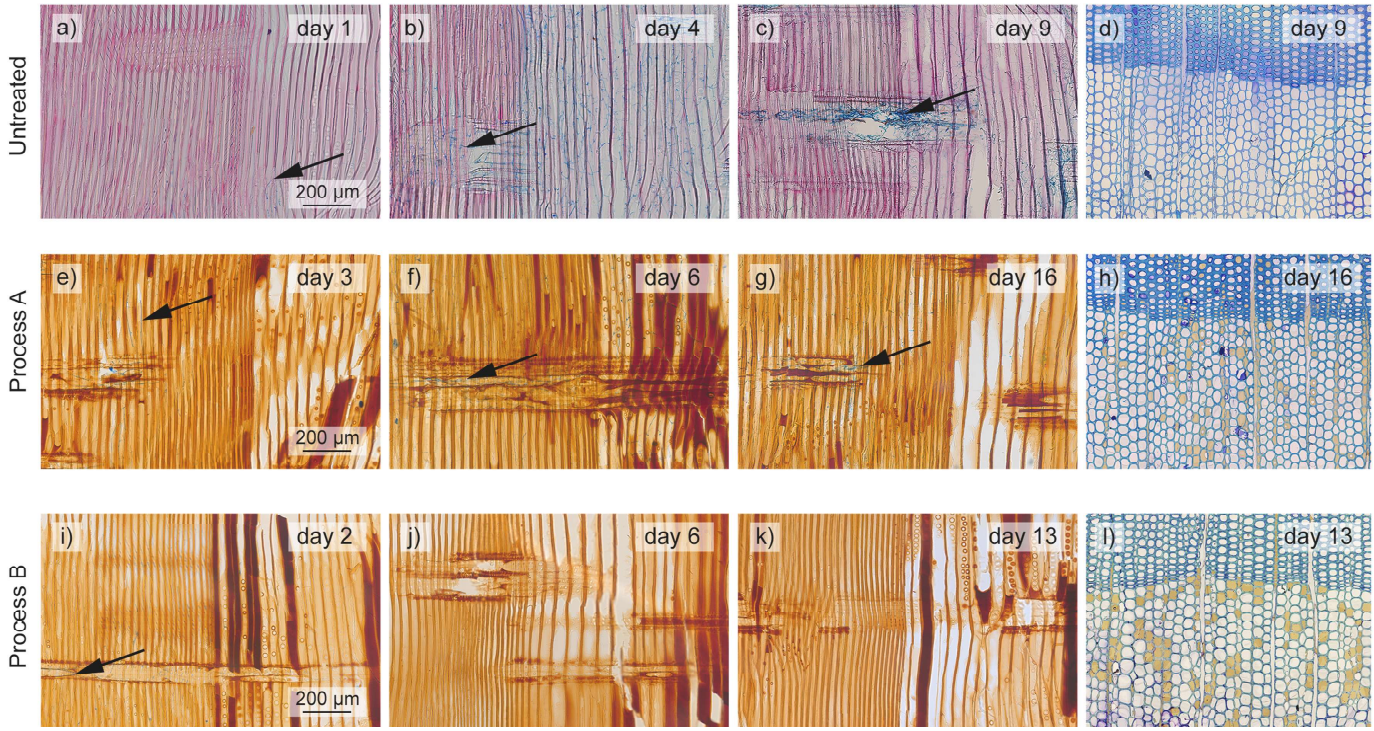

Fig. 3. Light microscope radial and transverse sections containing late and early wood of untreated and furfurylated *Pinus radiata* in ascending stages of exposure to *Rhodonia placenta*. The fungal hyphae are stained blue. 3a-d: Untreated *P. radiata* stained with safranin and aniline blue; 3a: After 1 day first hyphae occurred (↑) and spread over the entire sample after the following days (3b). 3c,d: After 9 days, the first ML occurred; no hyphae can be seen in the transverse sections, whereas the radial section is full of hyphae. 3e-h: Furfurylated *P. radiata*, type A, 52 WPG%, stained with aniline blue. 3e,f: A few hyphae can be seen in the wood ray on day 3 and 6 (↑). 3g,h: After 16 days, first ML occurred; the wood tissue remained intact. 3i-l: Furfurylated *P. radiata*, type B, 67 WPG%, stained with aniline blue; Hyphae were observed sporadically (↑); no structural changes were found. Bars: 200 µm.

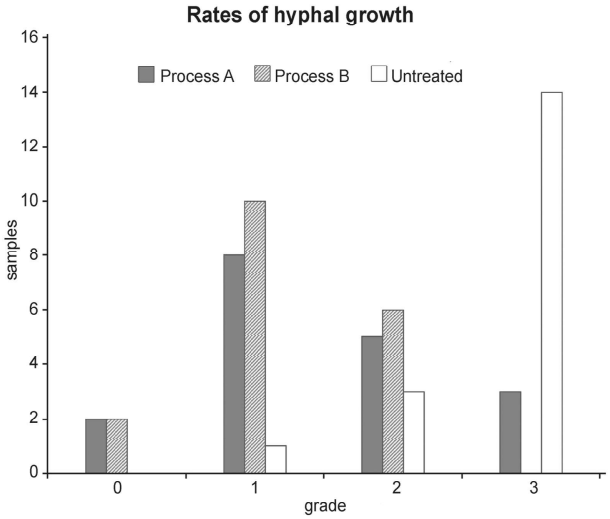

Fig. 4. Rates of hyphae growth over 18 days based on radial microscopy sections. Grade 0 = no growth and 3 = very abundant growth; Grey bars: furfurylated wood, process A; striped bars: furfurylated wood, process B; white bars: untreated wood.

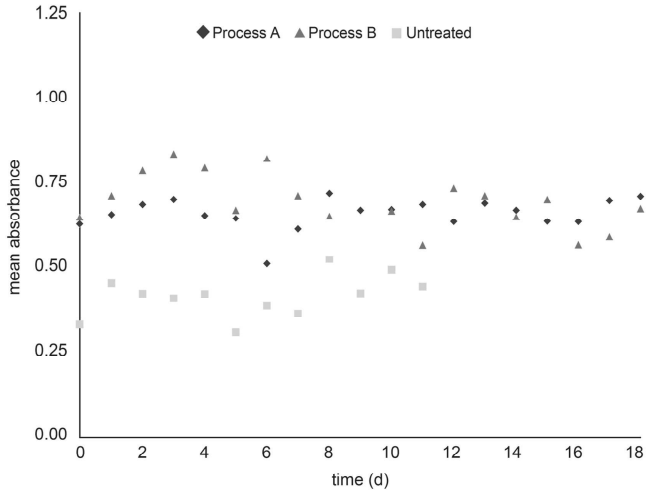

Fig. 5. Mean UV absorbance values at λ_{280nm} of untreated and furfurylated *P. radiata* before and during ascending stages of exposure to *Rhodonia placenta;* 11 and 18 days of the latter were analyzed, respectively; mean values based on 11,100 to 12,900 scanned measuring points. Rhombus – furfurylated wood, process A; triangles - furfurylated wood, process B; squares – untreated wood.

3.3. Cellular UMSP

Selected sample sections of untreated and furfurylated wood tissues of *P. radiata* incubated with *R. placenta* were scanned with monochromatic UV-light at λ_{280nm} wavelength. To ensure that the period of initial decay was included, harvest points until the first detectable ML + 2 days were monitored. In total, 18 days for the furfurylated samples and for the untreated samples a period of 11 days were chosen.

The development of the evaluated mean absorbance values (based on 11,100 to 12,900 scanned measuring points) over the decay period of cell wall regions with radially oriented CML of untreated and furfurylated (type A and B) samples are displayed in Fig. 5. Increased absorbance values compared to the uninoculated samples were recorded for untreated as well as for furfurylated samples during the first 4 days of the decay test. The analyzed areas in this study were particularly characterized by increased absorbance values compared to the

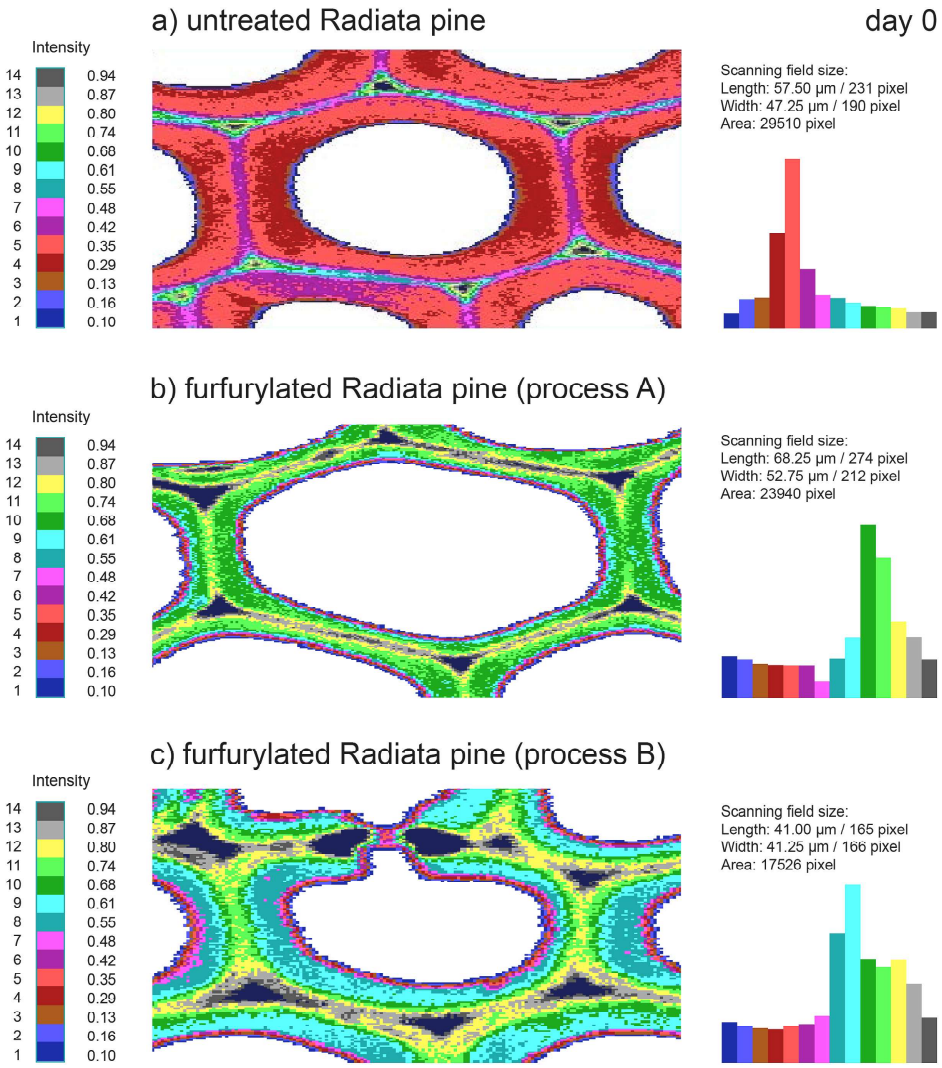

Fig. 6a. a-c. Representative area UV microscopic scanning profiles at λ_{280nm} of uninfected control samples of *Pinus radiata* (untreated and furfurylated). The colored pixels represent the absorbance intensities at λ_{280nm}; the corresponding histogram provides the statistical evaluation of the scanned areas; The highest absorbance values are measured in the area of the compound middle lamella (CML) and cell wall corners for untreated and furfurylated wood; The intense modification of the cell walls (6-1 b and c) is visualized by higher UV absorbance values; The untreated cell wall (6.1a) is characterized by absorbance vales from A_{280nm} 0.10 (S3) to A_{280nm} 0.42 (CML), the furfurylated samples (A, 6.1b) from A_{280nm} 0.42 (S3) to A_{280nm} 0.74 (CML) and (B, 6.1c) from A_{280nm} 0.42 (S3) to A_{280nm} 0.80 (CML).

uninoculated samples during the first days of decay. The absorbance values of the untreated samples stayed above the values of the uninoculated samples until day 4, 5 (type A) and 10 (type B). During the first 11 days, the highest measured absorbance values were 0.52 ($A_{280\ nm}$, day 8) for the untreated samples and for the furfurylated samples 0.72 ($A_{280\ nm}$, day 8, type A) and 0.8 ($A_{280\ nm}$, day 3, type B). The minimum absorbance values recorded during the same period were for the untreated samples 0.31 ($A_{280\ nm}$, day 5) and for the furfurylated samples 0.51 ($A_{280\ nm}$, day 6, type A) and 0.57 ($A_{280\ nm}$, day 11, type B). Common to all three variations was that the minimum mean absorbance value was lower than the reference value before decay. After 11 days, the mean absorbance values of furfurylated samples fluctuate between $A_{280\ nm}$ 0.57 and $A_{280\ nm}$ 0.73 with a decreasing amplitude until day 18. Compared to $W_{FA,B}$, $W_{FA,A}$ showed slightly lower values.

In Fig. 6.1a–c, representative two-dimensional UMSP profiles of undegraded samples are presented. The intensities of UV absorbance within the individual cell wall layers are displayed by the different color pixels. The highest absorbance intensities occurred in the area of the CML and the CC. The furfurylated profiles (Fig. 6.1b and c) showed significantly higher UV absorbances of the entire cell wall compared to untreated wood.

To illustrate the shift of absorbance values caused by initial decay activities, seen in this study, characteristic UV scans are presented in Fig. 6.2. After 5 days, local parts of the untreated and furfurylated wood cell walls (type A), especially within the thick S2 layer, showed a significant decrease in absorbance signals as well as irregularly distributed spots of higher absorbance values (Fig. 6.2a and b ↑). For both furfurylated sample variations, locally inhomogeneous absorbance pattern of the scanned cell wall layers compared to the undegraded samples can be seen (Fig. 6.2b and c ↑). However, type B had only a few minuscule spots of lower absorbance signals compared to type A and untreated wood. The tissue appeared relatively homogenous (Fig. 6.2 c).

Fig. 7 presents the development of the mean absorbance values of the scanned cells filled with polymerized FA. Distinct variations in polymerized FA absorbance signals of the scanned filled lumen were detected after decay. The mean absorbance values (based on 28,100 to 28,400 scanned measuring points) of type A and B vary between $A_{280\ nm}$ 0.88 and $A_{280\ nm}$ 1.23. Whereas the mean values of type A fell 5 times below the value of type An undegraded, the values of type B stayed above type B undegraded. Two representative 2D UMSP scanning profiles of tracheids filled with polymerized FA were selected to visualize the slight differences in the spectral behavior of infected samples from type A and B.

Figs. 8–1 shows a selection of the evaluated UV absorbance values as a function of distance from the Mlcc (0 µm) to the cell lumen. The most informative absorbance alterations in comparison to the respective uninfected sample were chosen to visualize lignin modification. The graph of the untreated and undegraded sample (day 0, reference) represents the natural (typical) lignin concentration of wood cell walls with the highest amount in the area of the MLcc, which decreased to the cell lumen (Figs. 8–1a). From the starting point Mlcc, the absorbance values at λ_{280nm} fluctuated more frequently in type B (A_{min}

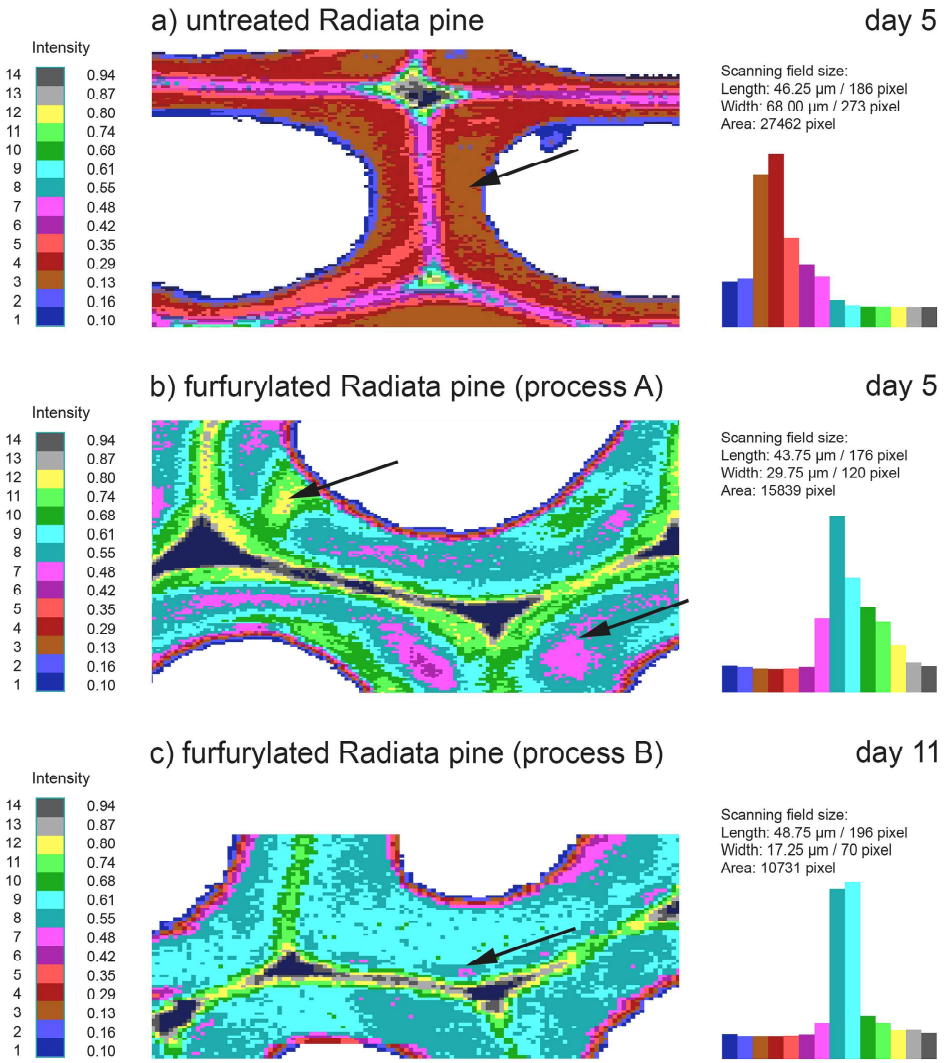

Fig. 6b. a-c. Representative area UV microscopic scanning profiles at λ_{280nm} of initial stages of decay in untreated and furfurylated *Pinus radiata* tracheid cell walls. The colored pixels represent the absorbance intensities at λ_{280nm}; the corresponding histograms provide the statistical evaluation of the scanned areas; The infected wood tissue shows local absorbance shifts to lower and higher absorbance intensities visualizing the degradation pattern. After 5 days of exposure to *R. placenta*: 6.2 a: the S2 layer is infected which is revealed by areas of lower intensities A_{280nm} 0.13 (↑); 6.2 b: The furfurylated cell wall (process A) revealed spots of higher (↑, yellow pixel A_{280nm} 0.80) and lower (↑, purple pixel A_{280nm} 0.48-0.42) absorbance intensities. 6.2 c: After 11 days, the furfurylated cell wall (process B) revealed spots of lower absorbance intensities close to the middle lamella A_{280nm} 0.48 (↑).

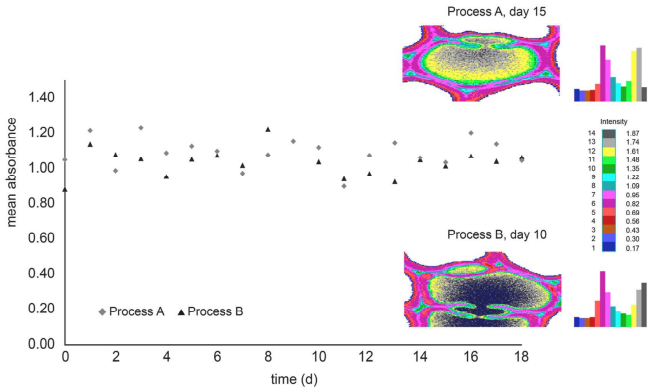

Fig. 7. Mean absorbance values at λ_{280nm} of polymerized FA deposits in the cell lumen of furfurylated *Pinus radiata* type A and B; two representative area UV-microscopic scanning profiles of exposure day 15 (type A) and day 10 (type B) are presented and statistically evaluated (histogram); Rhombus – furfurylated wood, process A; triangles - furfurylated wood, process B; squares – untreated wood.

1.03, A_{max} 1.60) than in type A (A_{min} 1.13, A_{max} 1.61) and untreated wood (A_{min} 0.84, A_{max} 1.05) throughout the analyzed time course of the experiment. The graph of the untreated sample at day 8 of incubation presents increased absorbance values throughout the whole course compared to the undegraded sample. In the local area of interest (1.25–3.0 µm), distinct absorbance changes were detected. The results indicated that initial lignin modification through brown rot degradation affected the entire cell wall.

Both, furfurylated samples of type A and B, were characterized by higher absorbance values (Figs. 8–1b,c) compared to the untreated sample in general. The undegraded sample of type A day 0 showed the typical UV absorbance profile of FA-modified wood cell walls, which is characterized by a distinct broad plateau close to the CML resulting from the FA modification process. Process type B day 0 is also characterized by a broad plateau. However, the graph proceeds unsteadily compared to type A, showing a shoulder around 2.5 µm with higher intensities that indicate an accumulation of poly(FA)-lignin complex caused by the modification process.

In contrast, the absorbance behavior of the degraded samples of the furfurylated wood performed differently. Whereas the absorbance values of type A remained beneath or rather close to the undegraded sample curve, the values of type B fluctuated. Two representative degradation curves are given in Figs. 8–1b,c. The graph of type A day 15 shows a significant slump of absorbance intensities around 2.0 µm compared to the undegraded sample. The spots characterized by lower absorbance values close to MLcc are depicted as purple colored pixel illustrated in Figs. 8–2b. At a distance of approx. 3.0 µm, the degradation curve of $W_{FA,B}$ day 6 shows a shoulder with higher intensities followed by a slow decrease in the absorbance values. At a distance of 2.25 µm, an absorbance peak at λ_{280nm} 1.21 for type B can be localized (not shown) that indicates an accumulation of modified lignin. The

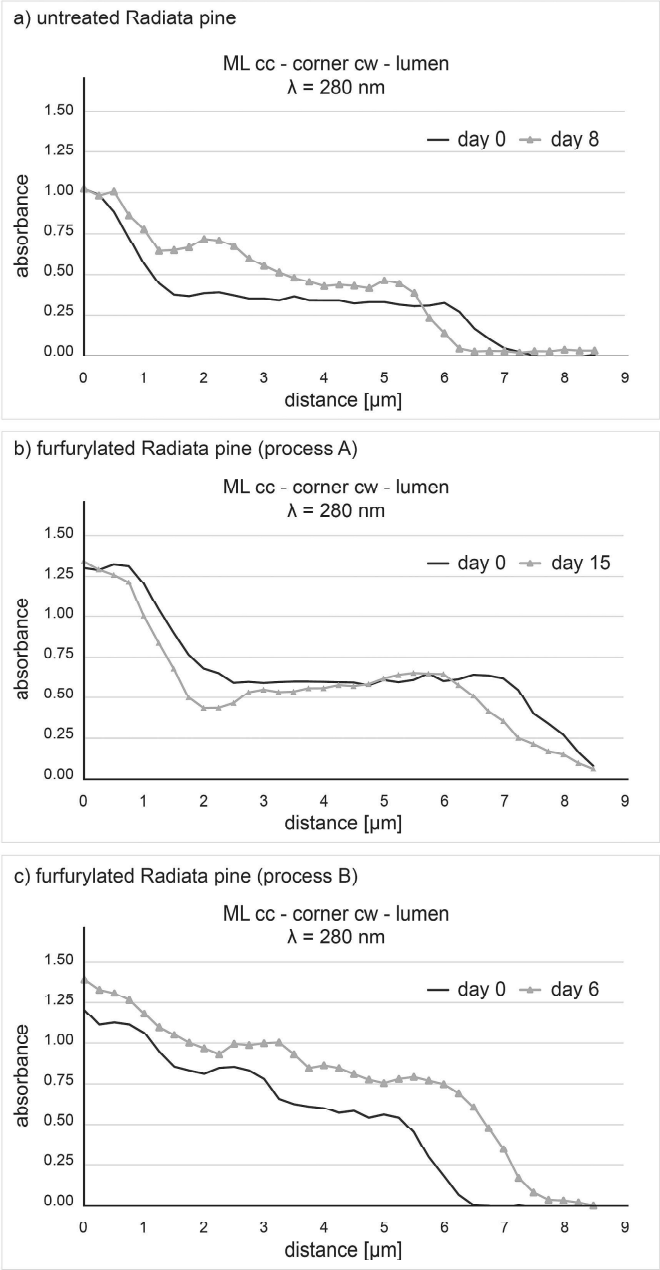

Fig. 8a. UV absorbance values at λ_{280nm} as a function of distance at the initial stages of decay in pine tracheid corner cell walls by *R. placenta*. 8-1 a: Line profile of undegraded and untreated *Pinus radiata*; after 8 days of exposure the absorbance values increased in the region of the primary and secondary wall. 8-1 b: Line profile of furfurylated *P. radiata*, type A; after 15 days of exposure, the absorbance values decreased especially in the region of MLcc. 8-1 c: Line profile of furfurylated *P. radiata*, type B; the evaluated UV absorbance values of the entire cell wall shifted to higher values (day 6).

presented results indicate that depolymerization of the modified lignin matrix and accumulation of modified lignin can be topochemically detected as well as the removal of polysaccharide components.

The following UMSP scanning profiles in Figs. 8–2 exemplify the described increase and decrease in absorbance intensities depending on the progress (state) of incubation. To optimize the image profiles, two different thresholds were applied, which are represented by the color scales. The two-dimensional image profiles of sound and degraded wood with the corresponding histogram clearly illustrate the shift of absorbance values regarding the progress of decay. The high spatial resolution of the UMSP is demonstrated by the three-dimensional image profiles. The "landscapes" of the scanned cells visualize the alterations in absorbance intensities across the individual cell wall layers. The results indicate that areas affected by initial degradation activities of *R. placenta* can be detected and visualized *in situ* by UMSP two- and three-dimensional images.

4. Discussion

Wood infected by brown rot fungi and the resulting structural modifications/alterations (Danninger et al., 1980; Eriksson et al., 1990; Goodell, 2003; Kim et al., 2019) lead to serious hazards of the wooden constructions (Zabel and Morell, 1992; Goodell, 2003). The onset of wood degradation by wood degrading fungi is initially (ML < 10%) not visible by LM (Carll and Highley, 1999). Therefore, it is of great interest to learn more about the non-enzymatic oxidative degradation by brown rot fungi in untreated and modified wood. DNA and gene expression studies, as presented in a review by Alfredsen et al. (2014), provided insights into fungal activity during the decay of modified wood. Information about the loss of strength and structural integrity during decay could be analyzed by high-energy multiple impact (HEMI) test (Brischke et al., 2006; Rapp et al., 2006; Ringman et al., 2017). However, degradation studies on the cell wall level *in situ* are rare (Irbe et al., 2006a,b; Fackler et al., 2010; Rehbein et al., 2011; Kim et al., 2015; Ehmcke et al., 2016; Goodell et al., 2017). In this study, structural and topochemical analyses of brown rot infected wood at the initial decay stage were performed by LM and UMSP to visualize non-enzymatic oxidative changes and lignin modification, within individual cell wall layers *in situ*. Mass loss and wood moisture content are measurable parameters that are of great importance when it comes to biodegradation and were taken into account in this study. Hereafter, the analyzed parameters mass loss, wood moisture content, fungal hyphae colonization and topochemical alterations within the individual cell wall layers during incipient brown rot degradation will be discussed.

4.1. Mass loss and moisture content

The results of ML analyses indicate that furfurylated wood is protected from decay for a prolonged period compared to untreated wood, which is in accordance with earlier results (Lande et al., 2004a; Venås, 2008; Esteves et al., 2011; Li et al., 2015; Ringman et al., 2017; Sejati et al., 2017). The significantly lower EMC of the furfurylated wood at standard climate conditions (20 °C, 65% RH) and throughout the course of the decay test compared to that of the untreated samples, corresponds to the findings of Lande et al. (2004a) and Venås (2008) and corroborates the stability of the FA treatment and its influence on the sorption properties (Hill, 2006).

The results in this study indicate that moisture conditions that allow for an onset of degradation in untreated and furfurylated woods were provided. For untreated wood, the minimum MC for softwood decay is commonly the fiber saturation range (FSR) of about 28–30% MC_{fs} or slightly above this range to provide free water that is necessary to start decay mechanisms (Schmidt, 2006). However, X-ray fluorescent microscopy studies on ion movement revealed that fungal decay could already start far below FSR at an ion dependent MC of about 16% (Zelinka et al., 2015). In a review of established theories on decay resistance of modified wood influenced by moisture exclusion and swelling reduction, a criterion of 25% MC was established below which decay does not occur (Thybring, 2013).

Throughout the decay test, the furfurylated samples had lower MC values compared to the untreated samples demonstrating the positive effect of wood modification with FA on hygroscopicity/sorption properties (Lande et al., 2004b; Moghaddam et al., 2016). The furfurylated sample of type A behaved differently compared to type B, indicating the influence of the WPGs as described by Ehmcke et al. (2017). The different furfurylation processes resulted in different WPGs characterized

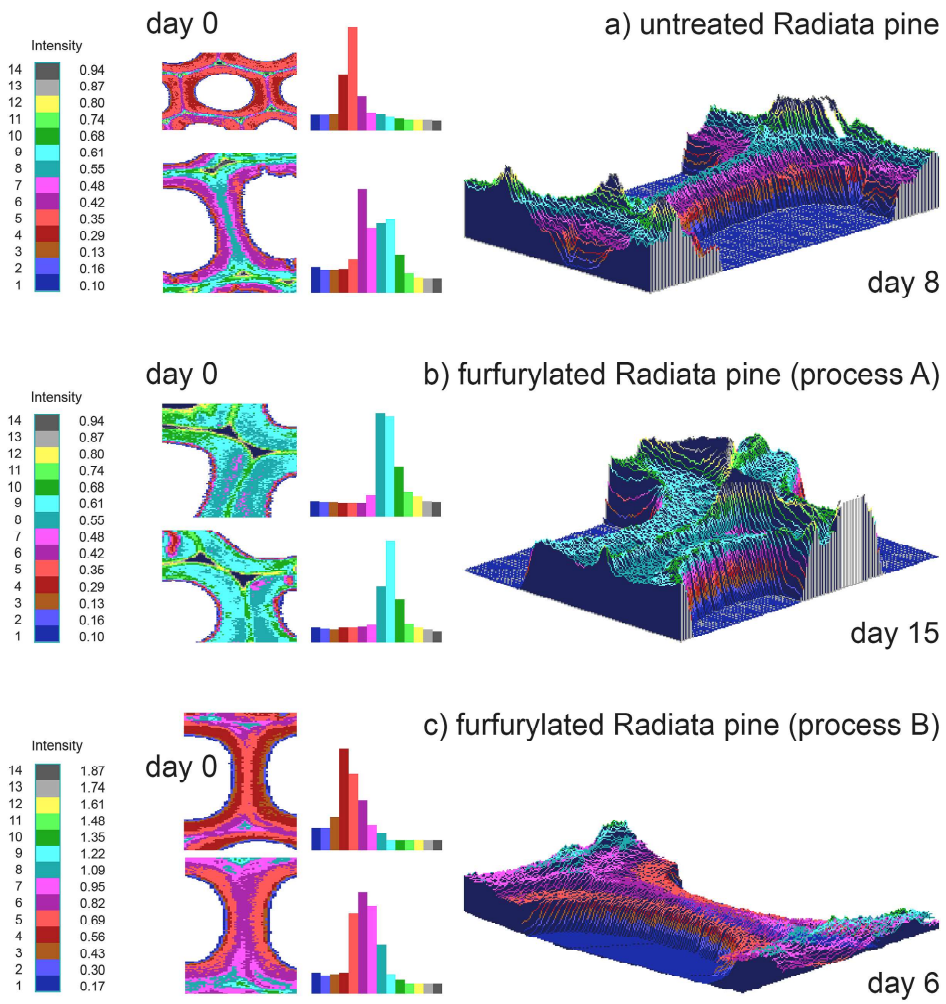

Fig. 8b. Representative UV microscopic scanning profiles (area and 3-D) at λ_{280nm} of early stages of decay in untreated (a) and furfurylated (b,c) *Radiata pine* cell walls by *R. placenta*. The data are evaluated from their corresponding histograms. The 3D image profiles intuitively visualize topochemical changes and cell wall modification at the initial stage of decay.

by various filled cell lumen and occluded micropores of the wood cell wall, where free water could be located. Earlier studies regarding sorption and dimension stability of furfurylated soft- and hardwood veneers by Moghaddam et al. (2016) revealed a reduced capillary liquid uptake and swelling. The different processes also resulted in an indirect impact on the sorption properties through a possible covalent bond formation to lignin molecules during the FA polymerization process of the samples, which must be considered.

Furthermore, the strong increase in MC of the samples, especially for the untreated samples, could be related to the fungal water production during decay. Smith and Shortle (1991) found, for example, MC in dry heartwood samples of *Pinus retinosa* increased to 1030% during decay by *R. placenta* for 7 days.

Flournoy et al. (1991) and Irbe et al. (2006a) reported the formation of "new pores" (2.1–9.9 nm) in cell walls of untreated *P. sylvestris* sapwood samples (50 × 25 × 15 mm) decayed by *R. placenta* after one month. It remained unclear, whether the formation of "new pores" during the performed decay test occurred and influenced the MC of the samples since it was postulated that the pore sizes and volume depend on the exposure time. Furthermore, the formation of micro capillary pathways through lignin modification discussed by Arantes et al. (2012) could also influence the moisture conditions in the samples.

4.2. Light microscopy

The incipient fungal hyphae colonization of untreated and furfurylated wood samples developed differently. No hyphal growth was found in the furfurylated sample sections after 24 h, which was however the case for untreated wood. The development and vast presence of hyphae in untreated wood was never seen in the furfurylated samples. The observed fungal colonization progress was shown to correspond to the moisture development of the untreated and furfurylated samples.

As seen in Figs. 3 and 4, the observed fungal colonization in type A and type B developed differently. Samples from type B preformed slightly better than from type A, which can be ascribed to i) the different solvents used in the furfurylation process, ii) the higher WPG level, iii) the filled lumen ratio and iv) the lower MC of type B (Fig. 2). LM and SEM image data provided by Ehmcke et al. (2017) indicated that the variability in filled cell lumens in the axial and radial directions of furfurylated radiata pine sapwood depended on the modification process and on the permeability as observed by Lande et al. (2010) and Zimmer et al. (2014) for Scots pine sapwood.

In contrast to studies by Rehbein et al. (2011), in this study the occurrence of hyphae was not restricted to the inner parts of the samples (Fig. 3). The analyzed radial and tangential sections of untreated and modified wood samples revealed hyphae growth over the entire sections. One reason for this divergence could be that the conclusion in the paper by Rehbein et al. (2011) referred to the evaluation of cross

sections. The cross sections still revealed intact tissue on the day of the first mass loss (Fig. 4). As other light microscopic studies showed (Irbe et al., 2006b, Rehbein et al., 2011), no structural cell wall attack was detected in the analyzed sections during the initial stages of wood decay. A mass loss of at least 10% was necessary for microscopic detection of cell wall damages (Carll and Highley, 1999).

The results of this study indicate that the presence and the intensity/amount of fungal hyphae in furfurylated wood are directly linked to the performance of the wood protection from decay. Furfurylated wood was protected from decay for a prolonged period compared to untreated wood, which corresponds to earlier results (Lande et al., 2004a; Venås, 2008; Esteves et al., 2011; Li et al., −2015; Ringman et al., 2017; Sejati et al., 2017). Furthermore, the observed fungal colonization by brown rot in FA-modified wood emphasizes the non-biocidal character as found for white rot (Pilgård et al., 2010c) and marine organisms (Westin et al., 2016).

4.3. Cellular UMSP

The highest absorbance intensities in the cell wall tissue were located in the area of the CML and the CC as previously described for untreated wood (Koch and Kleist, 2001; Koch and Grünwald, 2004), thermally modified wood (Mahnert et al., 2013) and furfurylated wood (Ehmcke et al., 2017). In general, the furfurylated scanning profiles showed significantly higher UV absorbances of the entire cell wall compared to untreated wood as previously described by Ehmcke et al. (2017). The reasons for the significantly higher absorbance values are condensing reactions of FA and lignin during the furfurylation process as previously proposed by Barsberg and Thygesen (2017) for hybrid poly(FA) lignin models. It is suggested that the absorbance differences between undegraded $W_{FA,B}$ and $W_{FA,A}$ are caused by the singularities in the furfurylation process itself (water/ethanol as solvent) and the thereby resulting variances of the cell wall modification as described by Ehmcke et al. (2017).

The present results confirm earlier findings by Ehmcke et al. (2016) that brown rot degradation of furfurylated wood can be topochemically analyzed by UMSP *in situ*. Increased absorbance values compared to the uninoculated samples were recorded for untreated as well as for furfurylated samples during the first 4 days of the decay test. These results are in accordance with previous results reported by Rehbein et al. (2011) and Irbe et al. (2006b) and can be basically explained by a relative increase in lignin in the degraded lignocellulosic cell wall matrix by brown rot. The detected inhomogeneous changes in the spectral behavior of the scanned cell wall layers originated from early fungal degradation processes. Both Irbe et al. (2006b) and Rehbein et al. (2011) have reported similar findings for untreated softwood. In this study, the suggested re-aggregation of modified lignin during brown rot degradation followed by an immediate filling of opened pores with repolymerised lignin as suggested by Goodell et al. (2017) can also be topochemically visualized. The removal of polysaccharide components previously shown by Arantes et al. (2009) and the partial depolymerization of the native lignin in combination with modifications in its side chains, could explain the increase in absorbance values seen in this study and previously shown by Irbe et al. (2006b).

The differences in the spectral behavior of furfurylated wood type A and type B during decay could be explained by the impact of solvents used in the different furfurylation processes and the difference in WPG. The results of the analyzed polymerized FA deposits in the cell lumen indicate that polymerized FA can be affected by brown rot *R. placenta*. Ehmcke et al. (2016) also found degradation-causing changes in absorbance values of polymerized FA deposits in the cell lumen. The changes in absorbance values are most likely explained by the attack of highly reactive hydroxyl radicals, produced in the non-enzymatic oxidative degradation (Goodell et al., 1997; Hammel et al., 2002; Arantes et al., 2012).

An established theory is that brown rot decay starts with lignin modification in the outermost part of the S2 layer of untreated (Fackler et al., 2010, Rehbein et al., 2011) and furfurylated wood (Ehmcke et al., 2017). However, findings by Kim et al. (2015) revealed that previous ideas concerning decomposition process of tracheids and fibers including secondary cell walls and CML/MLcc regions by brown rot fungus *R. placenta* need further detailing. Therefore, it was of great interest to generate specific information on alterations of this area (Fig. 1) during fungal exposure. Our findings support, for untreated wood, i) the perception that the brown rot degradation starts at the outermost part of the S2 layer, and ii) the degradation pattern Type 1 as described by Kim et al. (2015). The results of this study could be related to the suggested preferential degradation of middle lamella regions at incipient decay stages by *R. placenta* as described by Kim et al. (2015). Furthermore, our results support the findings by Kim et al. (2015) regarding disrupted lamellae of lignin aggregates and cellulose microfibril bundles in the outermost S2 layer of early stage decayed spruce tracheids.

The detected differences during the performed decay test of i) fungal colonization and hyphal growth, ii) spectral UV behavior and iii) varying degradation patterns strongly demonstrated the influence of the FA modification processes and the resulting WPG's. Furthermore, it has to be considered that the presented data do not preclude the possibility of further degradation pattern located in the wood tissue. This study provided insights into selected areas of about the size of one tracheid cell (100 μm × 100 μm) with a high geometrical resolution of 0.25 μm^2 per pixel.

5. Conclusions

The present paper provides a close monitoring over 18 days of incipient brown rot degradation by *R. placenta* in untreated and furfurylated wood. Samples of two different process conditions together with untreated wood samples were inoculated and topochemically investigated by UMSP and by LM. For the first time, UMSP area scans and selective line scans of an individual cell wall region provide detailed insights into non-enzymatic oxidative lignin modification at the initial decay stage of FA-modified radiata pine (*Pinus radiata*) visualizing non-enzymatic oxidative degradation *in situ*. The topochemical analyses indicate that early degradation patterns in the form of modified lignin do not only occur in the area of the outermost S2 layer, but also on local spots over the entire wood cell wall of untreated and FA-modified samples, underlining the need of improvement in the understanding of the onset of brown rot degradation. We have seen that the polymerized FA deposits in the cell lumen can be attacked by the highly reactive hydroxyl radicals, produced in the non-enzymatic oxidative degradation. These results also underline that furfurylated wood has a non-toxic mode of action, showing comparable degradation pattern to the untreated reference. High UV absorbance values of the entire cell wall compared to untreated wood confirms the previous findings that FA binds to the lignin matrix of the wood cell wall. Differences in the FA modification processes have distinct impact on the decay pattern affecting the moisture content, hyphal growth and UV absorbance intensities of the individual cell wall layers and FA deposits in the cell lumen. Information on how furfurylation could control the moisture content and if new pores are formed during decay in furfurylated wood is needed to increase our understanding of wood protection by FA modification.

Declaration of competing interest

The authors declare that they have no known competing financial interests or personal relationships that could have appeared to influence the work reported in this paper.

Acknowledgements

The authors extend their sincere thanks to the Research Council of Norway (RCN project 219294/O30, Wood-polymer composites for use in marine environments) for providing the test material, and Annica Pilgård gratefully acknowledges financial support from The Swedish Research Council Formas 942-2015-530. We also thank A. Vieler for laboratory work, UMSP preparations and sectioning, D. Paul and T. Potsch, Hamburg, for assistance in the UMSP preparation and analysis, and A. Khaloian Sarnaghi for excel formula writing. Furthermore, we thank A. Full and A. Wadenspanner for assistance in the light microscopy analysis, R. Rosin for image editing, A. Berger-James for proof reading and E. E. Thybring for discussion.

References

Alfredsen, G., Ringman, R., Pilgård, A., Fossdal, C.G., 2014. New insight regarding mode of action of brown rot decay of modified wood based on DNA and gene expression studies. Int. Wood Prod. J. 6 (1), 2008–2013. https://doi.org/10.1179/2042645314Y.0000000085.

Algeier, S.M., 2014. Biologischer Abbau von furfuryliertem Holz durch ausgewählte Basidiomyceten. M.Sc. Thesis. Technische Universität München, München, Germany.

Arantes, V., Qian, Y., Kelley, S.S., Milagres, A.M.F., Filley, T.R., Jellison, J., Goodell, B., 2009. Biomimetic oxidative treatment of spruce wood studied by pyrolysis-molecular beam mass spectrometry coupled with multivariate analysis and ^{13}C-labeled tetramethylammonium hydroxide thermochemolysis: implications for fungal degradation of wood. J. Biol. Inorg. Chem. 14 (8), 1253–1263. https://doi.org/10.1007/s00775-009-0569-6.

Arantes, V., Milagres, A.M., Filley, T.R., Goodell, B., 2011. Lignocellulosic polysaccharides and lignin degradation by wood decay fungi: the relevance of nonenzymatic Fenton-based reactions. J. Ind. Microbiol. Biotechnol. 38 (4), 541–555. https://doi.org/10.1007/s10295-010-0798-2.

Arantes, V., Jellison, J., Goodell, B., 2012. Peculiarities of brown-rot fungi and biochemical Fenton reaction with regard to their potential as a model for bioprocessing biomass. Appl. Microbiol. Biotechnol. 94 (2), 323–338. https://doi.org/10.1007/s00253-012-3954-y.

Bariska, M., Osuska, A., Bosshard, H.H., 1983. Änderung der mechanischen Eigenschaften von Holz nach Abbau durch Basidiomyceten. Holz Roh- Werkst 41 (6), 241–245. https://doi.org/10.1007/BF02608570.

Barsberg, S.T., Thygesen, L.G., 2017. A combined theoretical and FT-IR spectroscopy study of a hybrid poly(furfuryl alcohol) – lignin material: basic chemistry of a sustainable wood protection method. Chemistry 2, 10818–10827. https://doi.org/10.1002/slct.201702104.

Bravery, A.F., 1979. Screening Techniques for Potential Wood Preservative Chemicals. A Miniaturised Wood-Block Test for the Rapid Evaluation of Preservative Fungicides. IRG/Peebles. Reports No. 136. The International Research Group on Wood Preservation, Stockholm.

Brischke, C., Welzbacher, C.R., Rapp, A.O., 2006. Detection of fungal decay by high-energy multiple impact (HEMI) testing. Holzforschung 60, 217–222. https://doi.org/10.1515/HF.2006.036.

Bryne, L.E., Walinder, M.E.P., 2010. Ageing of modified wood. Part 1: wetting properties of acetylated, furfurylated, and thermally modified wood. Holzforschung 64, 295–304. https://doi.org/10.1515/HF.2010.040.

Carll, C.G., Highley, T.L., 1999. Decay of wood and wood-based products above ground in buildings. Journal of Testing and Evaluation, JTEVA 27 (2), 150–158.

CEN/TS 15083-1 2005, 2005. Durability of Wood and Wood-Based Products - Determination of the Natural Durability of Solid Wood against Wood- Destroying Fungi, Test Methods - Part 1: Basidiomycetes. pp. 18.

Curling, S.F., Clausen, C.A., Winandy, J.E., 2002. Relationships between mechanical properties, weight loss, and chemical composition of wood during incipient brown-rot decay. For. Prod. J. 52 (7/8), 34–39.

Danninger, E., Messner, K., Rohr, M., 1980. Degradation scheme of brown and white rot fungi on indigenous Austrian woods (beech, spruce). Holzforsch. Holzverwert. 32 (5), 126–130. https://eurekamag.com/research/000/852/000852865.php.

De Vetter, L., Depraetere, G., Janssen, C., Stevens, M., Van Acker, J., 2008. Methodology to assess both the efficacy and ecotoxicology of preservative-treated and modified wood. Ann. For. Sci. 65, 504. https://doi.org/10.1051/forest:2008030.

Donaldson, L.A., 2001. Lignification and lignin topochemistry—an ultrastructural view. Phytochemistry 57, 859–873. https://doi.org/10.1016/s0031-9422(01)00049-8.

Ehmcke, G., Pilgård, A., Koch, G., Richter, K., 2016. Improvement of a method for topochemical investigations of degraded furfurylated wood. Int. Wood Prod. J. 7 (2), 96–101. https://doi.org/10.1080/20426445.2016.1161866.

Ehmcke, G., Pilgård, A., Koch, G., Richter, K., 2017. Topochemical analyses of furfuryl alcohol-modified radiata pine (*Pinus radiata*) by UMSP, light microscopy and SEM. Holzforschung 71 (10), 821–831. https://doi.org/10.1515/hf-2016-0219.

EN 84, 1996. Wood Preservatives. Accelerated Ageing of Treated Wood Prior to Biological Testing, Leaching Procedure, vol. 7 European Committee for Standardization (CEN), Brussels, Belgium.

Eriksson, K.E.L., Blanchette, R.A., Ander, P., 1990. Microbial and Enzymatic Degradation of Wood and Wood Components, vol. 407 Springer, Berlin 978-3-642-46687-8.

Esteves, B., Nunes, L., Pereira, H., 2011. Properties of furfurylated wood (*Pinus pinaster*). Eur. J. Wood Prod. 69, 521–525. https://doi.org/10.1007/s00107-010-0480-4.

Fackler, K., Stevanic, J.S., Ters, T., Hinterstoisser, B., Schwanninger, M., Salmén, L., 2010. Localisation and characterisation of incipient brown-rot decay within spruce wood cell walls using FT-IR imaging microscopy. Enzym. Microb. Technol. 47 (6), 257–267. https://doi.org/10.1016/j.enzmictec.2010.07.009.

Fengel, D., Wegener, G., 1989. second ed. Wood - Chemistry, Ultrastructure, Reactions, vol. 613 Walter de Gruyter, Berlin 3-11-008481-3.

Fergus, B.J., Procter, A.R., Scott, J.A.N., Goring, D.A.I., 1969. The distribution of lignin in spruce wood as determined by ultraviolet microscopy. Wood Sci. Technol. 3 (2), 117–138. https://doi.org/10.1007/BF00639636.

Fukazawa, K., 1992. Ultraviolet microscopy. In: Lin, S.Y., Dence, C.W. (Eds.), Methods in Lignin Chemistry. Springer-Verlag, Berlin, pp. 110–121.

Flournoy, D.S., Kirk, T.K., Highley, T.L., 1991. Wood decay by brown-rot fungi: changes in pore structure and cell wall volume. Holzforschung 45, 383–388. https://doi.org/10.1515/hfsg.1991.45.5.383.

Goodell, B., Jellison, J., Liu, J., Daniel, G., Paszczynski, A., Fekete, F., Krishnamurthy, A., Jun, L., Xu, G., 1997. Low molecular weight chelators and phenolic compounds isolated from wood decay fungi and their role in the fungal biodegradation of wood. J. Biotechnol. 53 (2–3), 133–162. https://doi.org/10.1016/S0168-1656(97)01681-7.

Goodell, B., 2003. Brown rot fungal degradation of wood: our evolving view. In: In: Goodell, B., Nicholas, D., Schultz, T. (Eds.), Wood Deterioration and Preservation: Advances in Our Changing World, vol. 845. American Chemical Society, Washington D.C., pp. 97–118 6.

Goodell, B., Zhu, Y., Kim, S., Kafle, K., Eastwood, D., Daniel, G., Jellison, J., Yoshida, M., Groom, L., Pingali, S.V., O'Neill, H., 2017. Modification of the nanostructure of lignocellulose cell walls via a non-enzymatic lignocellulose deconstruction system in brown rot wood-decay fungi. Biotechnol. Biofuels 10, 179. https://doi.org/10.1186/s13068-017-0865-2.

Goldstein, I.S., 1955. The impregnation of wood to impart resistance to alkali and acid. For. Prod. J. 5 (4), 265–267.

Goldstein, I.S., 1960. Impregnating solutions and methods. GB Patent 846, 680.

Hammel, K.E., Kapisch, A.N., Jensen jr., K.A., Ryan, Z.C., 2002. Reactive oxygen species as agents of wood decay by fungi. Enzym. Microb. Technol. 30 (4), 445–453.

Hill, C., 2006. Wood Modification: Chemical, Thermal and Other Processes, vol. 239 John Wiley & Sons, Oxford, UK 978-0-470-02172-9.

Irbe, I., Andersons, B., Chirkova, J., Kallavus, U., Andersons, I., Faix, O., 2006a. On the changes of pinewood (*Pinus sylvestris* L.) Chemical composition and ultrastructure during the attack by brown-rot fungi *Postia placenta* and Coniophora puteana. Int. Biodeterior. Biodegrad. 57, 99–106. https://doi.org/10.1016/j.ibiod.2005.12.002.

Irbe, I., Noldt, G., Koch, G., Andersone, I., Andersons, B., 2006b. Application of scanning UV microspectrophotometry for the topochemical detection of lignin within individual cell walls of brown-rotted Scots pine (*Pinus sylvestris* L.) sapwood. Holzforschung 60 (6), 601–607. https://doi.org/10.1515/HF.2006.102.

Kim, J.H., Sutley, E.J., Martin, F., 2019. Review of modern wood fungal decay research for implementation into a building standard of practice. J. Mater. Civ. Eng. 31, 12. https://doi.org/10.1061/(ASCE)MT.1943-5533.0002998.

Karnovsky, M.J., 1965. A formaldehyde-glutaral fixative of high osmolality for use in electron microscopy. J. Cell Biol. 27 (2), 137A–138A.

Kim, J.S., Gao, J., Daniel, G., 2015. Ultrastructure and immunocytochemistry of degradation in spruce and ash sapwood by the brown rot fungus Postia placenta: characterization of incipient stages of decay and variation in decay process. Int. Biodeterior. Biodegrad. 103, 161–178. https://doi.org/10.1016/j.ibiod.2015.05.005.

Koch, G., Grünwald, C., 2004. Application of UV microspectrophotometry for the topochemical detection of lignin and phenolic extractives in wood fibre cell walls. In: Schmitt, U., Ander, P., Barnett, J.R., Emons, A.M.C., Jeronimidis, G., Saranpää, P., Tschegg, S. (Eds.), Wood Fibre Cell Walls: Methods to Study Their Formation, Structure and Properties. Swedish University of Agricultural Sciences, Uppsala, pp. 119–130.

Koch, G., Kleist, G., 2001. Application of scanning UV microspectrophotometry to localise lignins and phenolic extractives in plant cell walls. Holzforschung 55 (6), 563–567. https://doi.org/10.1515/HF.2001.091.

Koch, G., Schmitt, U., 2013. Topochemical and electron microscopic analyses on the lignification of individual cell wall layers during wood formation and secondary changes. In: Fromm, J., Robinson, D.G. (Eds.), Cellular Aspects of Wood Formation, Plant Cell Monographs 20. Springer-Verlag, Berlin Heidelberg, pp. 41–69.

Lande, S., Eikenes, M., Westin, M., 2004a. Chemistry and ecotoxicology of furfurylated wood. Scand. J. For. Res. 19 (5), 14–21. https://doi.org/10.1080/02827580410017816.

Lande, S., Høibø, O., Larnøy, E., 2010. Variation in treatability of Scots pine (*Pinus sylvestris*) by the chemical modification agent furfuryl alcohol dissolved in water. Wood Sci. Technol. 44, 105–118. https://doi.org/10.1007/s00226-009-0272-3. 2010.

Lande, S., Westin, M., Schneider, M., 2004b. Properties of furfurylated wood. Scand. J. For. Res. 19 (5), 22–30. https://doi.org/10.1080/0282758041001915.

Lande, S., Westin, M., Schneider, M.H., 2004c. Eco-efficient wood protection: furfurylated wood as alternative to traditional wood preservation. Manag. Environ. Qual. Int. J. 15 (5), 529–540. https://doi.org/10.1108/14777830410553979.

Li, W., Wang, H., Ren, D., Yu, Y.S., Yu, Y., 2015. Wood modification with furfuryl alcohol catalysed by a new composite acidic catalyst. Wood Sci. Technol. 49, 845–856.

Mahnert, K.-C., Adamopoulos, S., Koch, G., Militz, H., 2013. Topochemistry of heat-treated and N-methylol melamine modified wood of Koto (*Pterygota macrocarpa* K. Schum.) and Limba (*Terminalia superba* Engl. et Diels). Holzforschung 67 (2), 137–146. https://doi.org/10.1515/hf-2012-0017.

Martinez, A.T., Rencoret, J., Nieto, L., Jiménez-Barbero, J., Gutiérrez, A., Del Río, J.C., 2011. Selective lignin and polysaccharide removal in natural fungal decay of wood as evidenced by in situ structural analyses. Environ. Microbiol. 13 (1), 96–107. https://

doi.org/10.1111/j.1462-2920.2010.02312.x.
Martinez, D., Challacombe, J., Morgenstern, I., Hibbett, D., Schmoll, M., Kubicek, C.P., Ferreira, P., Ruiz-Duenas, F.J., Martinez, A.T., Kersten, P., et al., 2009. Genome, transcriptome, and secretome analysis of wood decay fungus *Postia placenta* supports unique mechanisms of lignocellulose conversion. Proc. Natl. Acad. Sci. U. S. A. 106, 1954–1959. https://doi.org/10.1073/pnas.0809575106.
Moghaddam, M., Wålinder, M.E.P., Claesson, P.M., Swerin, A., 2016. Wettability and swelling of acetylated and furfurylated wood analyzed by multicycle Wilhelmy plate method. Holzforschung 70, 69–77. https://doi.org/10.1515/hf-2014-0196.
Musha, Y., Goring, D.A.I., 1975. Distribution of syringyl and guaiacyl moieties in hardwoods as indicated by ultraviolet microscopy. Wood Sci. Technol. 9 (1), 45–58. https://doi.org/10.1007/BF00351914.
Nordstierna, L., Lande, S., Westin, M., Karlsson, O., Furó, I., 2008. Towards novel wood-based materials: chemical bonds between lignin-like model molecules and poly(furfuryl alcohol) studied by NMR. Holzforschung 62, 709–713. https://doi.org/10.1515/HF.2008.110.
Pfriem, A., Dietrich, T., Buchelt, B., 2012. Furfuryl alcohol impregnation for improved plasticization and fixation during the densification of wood. Holzforschung 66, 215–218. https://doi.org/10.1515/HF.2011.134.
Pilgård, A., De Vetter, L., Van Acker, J., Westin, M., 2010a. Toxic hazard of leachates from furfurylated wood: comparison between two different aquatic organisms. Environ. Toxicol. Chem. 29 (5), 1067–1071. https://doi.org/10.1002/etc.132.
Pilgård, A., Treu, A., Van Zeeland, A.N.T., Gosselink, R.J.A., Westin, M., 2010b. Toxic hazard and chemical analysis of leachates from furfurylated wood. Environ. Toxicol. Chem. 29 (9), 1918–1924. https://doi.org/10.1002/etc.244.
Pilgård, A., Alfredsen, G., Hiletala, A., 2010c. Quantification of fungal colonization in modified wood: *quantitative* real-time PCR as a tool for studies on *Trametes versicolor*. Holzforschung 64, 645–651. https://doi.org/10.1515/hf.2010.074.
Rapp, A.O., Brischke, C., Welzbacher, C.R., 2006. Interrelationship between the severity of heat treatments and sieve fractions after impact ball milling: a mechanical test for quality control of thermally modified wood. Holzforschung 60, 64–70. https://doi.org/10.1515/HF.2006.012.
Rehbein, M., Koch, G., 2011. Topochemical investigation of early stages of lignin modification within individual cell wall layers of Scots pine (*Pinus sylvestris* L.) sapwood infected by the brown-rot fungus *Antrodia vaillantii (DC.: Fr.) Ryv*. Int. Biodeterior. Biodegrad. 65 (7), 913–920. https://doi.org/10.1016/j.ibiod.2011.04.009.
Ringman, R., Pilgård, A., Brischke, C., Windeisen, E., Richter, K., 2017. Incipient brown rot decay in modified wood: patterns of mass loss, structural integrity, moisture and acetyl content in high resolution. Int. Wood Prod. J. 8 (3), 172–182. https://doi.org/10.1080/20426445.2017.1344382.
Saka, S., Whiting, K., Fukazawa, K., Goring, D.A.I., 1982. Comparative studies on lignin distribution by UV microscopy and bromination combined with EDXA. Wood Sci. Technol. 16 (4), 269–277. https://doi.org/10.1007/BF00353151.
Schmidt, O., 2006. Wood and Tree Fungi. Biology, Damage, Protection and Use. Springer, Berlin 3-540-32138-1.
Schneider, M.H., 1995. New cell wall and cell lumen wood polymer composites. Wood Sci. Technol. 29, 121–127. https://doi.org/10.1007/BF00229341.
Schneider, M.H., Philips, J.G., Lande, S., 2000. Physical and mechanical properties of wood polymer composites. J. Forest Eng. 11, 83–89.
Schultze-Dewitz, G., 1966. Relations between elasticity and static and impact bending strength of pinewood after exposure to basidiomycetes. Holz Roh- Werkst 24 (10), 506–512. https://doi.org/10.1007/BF02612884.
Schwarze, F.W.M.R., 2007. Wood decay under the microscope. Fungal biology reviews 21, 133–170. https://doi.org/10.1016/j.fbr.2007.09.001.
Scott, J.A.N., Procter, A.R., Fergus, B.J., Goring, D.A.I., 1969. The application of ultraviolet microscopy to the distribution of lignin in wood: description and validity of the technique. Wood Sci. Technol. 3 (1), 73–92. https://doi.org/10.1007/BF00349985.
Sejati, P.S., Imbert, A., Gérardin-Charbonnier, C., Dumarçay, S., Fredon, E., Masson, E., Nandika, D., Priadi, T., Gérardin, P., 2017. Tartaric acid catalyzed furfurylation of beech wood. Wood Sci. Technol. 51, 379–394. https://doi.org/10.1007/s00226-016-0871-8.
Smith, K.T., Shortle, W.C., 1991. Decay fungi increase the moisture content of dried wood. Int. Biodeterior. Biodegrad. 8, 138–146.
Spurr, A.R., 1969. A low viscosity epoxy resin embedding medium for electron microscopy. J. Ultra. Res. 26 (1–2), 31–43. https://doi.org/10.1016/S0022-5320(69)90033-1.
Stamm, A.J., 1977. Dimensional stabilization of wood with furfuryl alcohol resin. In: In: Goldstein, I. (Ed.), Wood Technology: Chemical Aspects, vol. 43. American Chemical Society, Washington D.C., pp. 141–149 9.
Thybring, E.E., 2013. The decay resistance of modified wood influenced by moisture exclusion and swelling reduction. Int. Biodeterior. Biodegrad. 82, 87–95. https://doi.org/10.1016/j.ibiod.2013.02.004.
Thybring, E.E., 2017. Water relations in untreated and modified wood under brown-rot and white-rot decay. Int. Biodeterior. Biodegrad. 118, 134–142. https://doi.org/10.1016/j.ibiod.2017.01.034.
Thygesen, L.G., Barsberg, S., Venås, T.M., 2010. The fluorescence characteristics of furfurylated wood studied by fluorescence spectroscopy and confocal laser scanning microscopy. Wood Sci. Technol. 44 (1), 51–65. https://doi.org/10.1007/s00226-009-0255-4.
Uppal, S.K., Gupta, R., Dhillon, R.S., 2008. Potential of sugarcane bagasse for production of furfural and its derivatives. Sugar Tech 10, 298–301. https://doi.org/10.1007/s12355-008-0053-6.
Van Eetvelde, G., De Geyter, S., Marchal, P., Stevens, M., 1998. Aquatic Toxicity Research of Structural Materials. IRG/WP/98-50114, 1–10. The International Research Group on Wood Preservation, Maastricht.
Venås, T.M., 2008. A Study of Mechanisms Related to the Fungal Decay Protection Rendered by Wood Furfurylation. PhD thesis. University of Copenhagen, Copenhagen.
Venås, T.M., Rinnan, Å., 2008. Determination of weight percent gain in solid wood modified with in situ cured furfuryl alcohol by near-infrared reflectance spectroscopy. Chemometr. Intell. Lab. 92, 125–130. https://doi.org/10.1016/j.chemolab.2008.02.002.
Winandy, J.E., Morrell, J.J., 1993. Relationship between incipient decay, strength, and chemical composition of Douglas-fir heartwood. Wood and Fibre Science 25 (3), 278–288.
Witomski, P., Olek, W., Bonarski, J.T., 2016. Changes in strength of Scots pine wood (Pinus sylvestris L.) decayed by brown rot (Coniophora puteana) and white rot (Trametes versicolor). Construct. Build. Mater. 102 (1), 162–166. https://doi.org/10.1016/j.conbuildmat.2015.10.109. online at.
Westin, M., P Larsson Brelid, P., Nilsson, T., Rapp, A.O., Dickerson, J.P., Lande, S., Cragg, S., 2016. Marine Borer Resistance of Acetylated and Furfurylated Wood – Results from up to 16 Years of Field Exposure. IRG/WP/16-40756, 1–9. The International Research Group on Wood Preservation, Lisbon, Portugal.
Yelle, D.J., Ralph, J., Lu, F., Hammel, K.E., 2008. Evidence for cleavage of lignin by a brown rot basidiomycete. Environ. Microbiol. 10 (7), 1844–1849. https://doi.org/10.1111/j.1462-2920.2008.01605.x.
Yelle, D.J., Wei, D., Ralph, J., Hammel, K.E., 2011. Multidimensional NMR analysis reveals truncated lignin structures in wood decayed by the brown rot basidiomycete *Postia placenta*. Environ. Microbiol. 13 (4), 1091–1100. https://doi.org/10.1111/j.1462-2920.2010.02417.x.
Zabel, R.A., Morell, J.J., 1992. Wood Microbiology: Decay and its Prevention. Academic Press, San Diego, California 0127752102.
Zelinka, S.L., Gleber, S.-C., Vogt, S., Rodriguez Lopez, G.M., Jakes, J., 2015. Threshold for ion movements in wood cell walls below fiber saturation observed by X-ray fluorescence microscopy (XFM). Holzforschung 69, 441–448. https://doi.org/10.1515/hf-2014-0138.
Zimmer, K.P., Høibø, O., Vestøl, G.I., Larnøy, E., 2014. Variation of treatability of Scots pine sapwood: a survey of 25 different northern European locations. Wood Sci. Technol. 48, 435–447. https://doi.org/10.1007/s00226-014-0660-1.